The Role of Small GTPases in Mammalian Cytokinesis

A thesis submitted to the

FACULTY OF BIOMEDICAL AND LIFE SCIENCES

For the degree of

DOCTOR OF PHILOSOPHY

By

Xinzi Yu

Division of Biochemistry and Molecular Biology
Institute of Biomedical and Life Sciences
University of Glasgow

February 2007

ProQuest LLC.
789 East Eisenhower Parkway
P.O. Box 1346
Ann Arbor, MI 48106 – 1346

Abstract

Cytokinesis is the final physical separation of two daughter cells, which occurs at the end of mitosis. Emerging evidence has placed membrane trafficking at the heart of mammalian cytokinesis, as it is clear that the control of membrane traffic into the cleavage furrow created by the ingressed acto-myosin contractile ring is vital for the expansion of surface area and proper separation. These findings also indicated that both the secretory and endocytic recycling pathways could be the potential internal membrane stores contributing to this process. Small GTPases are known to play crucial roles in the regulation of intracellular membrane traffic. Recent studies from diverse model systems highlighted roles for two GTPases Rab11 and Arf6 in *Drosophila* cellularisation, *Caenorabditis elegans* and mammalian cytokinesis. These proteins are both involved in endosomal recycling, and disruption of them by expressing mutants and RNAi results in severe cytokinesis defects. In a previous study, our group have identified Arfophilin2/Rab11-FIP4 as a dual Rab11/Arf binding protein. Immunofluorescence data revealed that FIP4 strikingly localises to the cleavage furrow and the midbody in mammalian cells during cell division. With this information in mind, it is proposed that the interaction of Rab11/Arf6 with Rab11-FIP3/4 may serve to regulate delivery of recycling endosomes (RE) to the furrow/midbody during cytokinesis in mammalian cells.

In this thesis, studies were carried out to investigate the function of Rab11 and Arf6 in mitosis. Firstly, the localisation of Rab11 and Arf6 throughout mitosis was examined. Both of the proteins were concentrated at the furrow/midbody region similar to Rab11-FIP4. Using GTP-deficient mutants and RNAi approaches, it was shown that Rab11 and Arf6 are both required for mammalian cytokinesis. Furthermore, time-lapse microscopy revealed that these two proteins both function in the late stage of cytokinesis, possibly midbody abscission but not furrow ingression.

Many Rab proteins have overlapping endosomal distributions, and therefore the second part of this study examined whether other endosomal Rabs also localise to the dividing site and contribute to membrane delivery to the furrow/midbody. Although none of the Rabs investigated showed characteristic distribution at the cleavage site, interference with one of the Rab GTPases, Rab4, did result in a minor defect in cytokinesis, implicating a role in this process.

Finally, preliminary study of regulation mechanism of FIP3 and FIP4 in mitosis was carried out. Bioinformatics and immunofluorescence experiments implicated that the FIPs

may be regulated by cell-cycle dependent kinases. Hence the possibility of FIP3 and FIP4 being phosphorylated by mitotic kinases, such as Aurora B and Polo-like kinase (Plk) was examined. This will provide more leads to elucidate FIP3 and FIP4's function in cell division and better our understanding of the membrane trafficking pathway during cytokinesis.

Table of Contents

List of Tables

List of Figures

List of Accompanying Material

A copy of DVD of cell division movies

Acknowledgement

A journey is easier when travelling together. Interdependence is certainly more valuable than independence. During my PhD, many people have kindly given me help and support, and I am glad now I have the opportunity to express my appreciation.

First of all, I would like to thank my supervisor Gwyn Gould, who helped me in countless ways in the past three years in his cool and groovy style. Thanks for being a great boss -- "always lightening the DOWNs and focusing the Ups"! This project is never possible without his advice, encouragement and support. I am also grateful for all his support and invaluable comments during the preparation of this thesis.

I greatly appreciate the Wellcome Trust offering me the studentship. Thanks Professors Dave Barry, Bill Cushley and Richard Cogdell for giving me the opportunity to study in the best small country.

Many thanks go to all the members in Lab 241, past and present. Thanks to Declan, for being a good friend and brighten the lab work with tons of fun! It is such a nice environment to work in, and I really enjoyed it! Of course, the pub lunches and lab nights out certainly made my PhD life more colourful! Thanks Dr. Luke Chamberlain and Dr. Nia Bryant for reading the thesis draft and kind advice! Thanks Fiona for always offering helps generously, especially the protein purification. Thanks Veronica for being a very good and warm friend and a lot of relaxing coffee time!

I would like to thank all the members in the cytokinesis team. I am grateful that I had the opportunity to work on such an interesting project! Thanks Giles for starting the project and leaving us so many leads to follow. I will never forget Andy, "the dude", who has given me tons of help to start my PhD. He is also a very good teacher of English slang and good buddy to hang out in the pubs. Johanne has been the most supportive and considerate bench mate in the past three years. It is such a pleasure to work with her, who is always showing interest and keeps positive! Louise is the newest "buddy" in this gang. You can tell how gifted and diligent she is simply by her groovy real time cell movies!

I also want to say thanks to my PhD committee, Miles Houslay, Pam Scott and Steven Yarwood. They monitored my work progress and made a lot of efforts in reading and providing me with valuable comments on regular stages of my study.

During my visit in the "mile high city", Denver, our "friend lab" has been a fantastic host. Thanks to Rytis, Glen and Eric for great hospitality! Glen gave me great help of the real time movies. He is also a fantastic tour guide of the trips to the Rocky Mountain and baseball game.

Big thanks to Alex for being a thoughtful friend and flatmate, and all the constructive advice on my project and valuable comments for this thesis. Thanks Margaret, Phil and Dominique for all the fun of Wednesday dinner and Texas hold'em games. Of course, I cannot forget our two adorable cats, Cleo and Patsy.

Thanks to my Chinese friends, Szushien, Danmei, Wangbo, Yinan, Zhenbo and Shelley who I practised and improved my cooking skills with. They make me feel less homesick. I also would like to thank my best friends Yi and Tutu, who are always there for me.

Craig and Jako should definitely take the credits for their great taste and choice of DVDs and B-movies, which gave me excellent education of western culture. The most unforgettable is "you know which" -- "Buck Rogers". Thanks Joan and Broham for constant nice meals, generosity and always being kind to me. Thanks Alan, Lorraine and C. Johnson for sharing millions of fun experience together.

Special thanks go to my ever-understanding Graham, my beloved boyfriend, the most enthusiastic and creative person who "can make anything happen", for giving me help, support, encouragement and coming up with lots of great ideas all the way through my PhD. I could not do this by myself. Although music and science is complete different field, Graham has been taking interest of my "monster cells" project and greatly helpful with image and video editing of this thesis. I cannot leave out all the fun we have together, capoeira, snowboarding, Darkwater gigs and the fab travelling in the "Sunshine State"! Really looking forward to trying more exciting stuff together after I survive "the longest day in my life"!

Last but not the least, I can never thank enough my mum and dad, who have been making efforts to give me the best education possible since I was born. Mum has always being hundred percent caring, encouraging and teaching me to keep a positive outlook. Dad is my strongest support through every single step I made, by always giving me the most invaluable advice when I need it, inspiring me trying new things and giving me full trust! Without their infinite love, patient and support this piece of work would never happen. To my parents I dedicate this thesis.

最后，我最应该感谢的是我的父母，他们的恩情我永远也回报不完。自从我一出生他们就尽最大的努力让我受到良好的教育。妈妈总是给我无微不至的关怀，并鼓励我保持积极的心态。爸爸是我迈出的每一步背后最强的支持。他总是在我最需要的时候给我最珍贵的建议，鼓励我努力尝试新东西并给我百分之百的信任！没有父母亲无私的爱，耐心和支持就不会有这本论文。我把我的论文献给我的父母！

Publications

Yu, X., R. Prekeris, and G.W. Gould. 2007. Role of endosomal Rab GTPases in cytokinesis. *Eur J Cell Biol*. 86:25-35.

Fielding, A.B., E. Schonteich, J. Matheson, G. Wilson, **X. Yu**, G.R. Hickson, S. Srivastava, S.A. Baldwin, R. Prekeris, and G.W. Gould. 2005. Rab11-FIP3 and FIP4 interact with Arf6 and the exocyst to control membrane traffic in cytokinesis. *Embo J.* 24:3389-99.

Wilson, G.M., A.B. Fielding, G.C. Simon, **X. Yu**, P.D. Andrews, R.S. Hames, A.M. Frey, A.A. Peden, G.W. Gould, and R. Prekeris. 2005. The FIP3-Rab11 protein complex regulates recycling endosome targeting to the cleavage furrow during late cytokinesis. *Mol Biol Cell*. 16:849-60.

Author's Declaration

I declare that the work described in this thesis has been carried out by myself unless otherwise cited or acknowledged. It is entirely of my own composition and has not, in whole or in part, been submitted for any other degree.

Xinzi Yu

February 2007

Abbreviations

ADP	Adenosine Diphosphate
ATP	Adenosine Triphosphate
Arf	ADP-ribosylation factors
Arl	Arf-like Protein
BFA	Brefeldin A
BLAST	Basic Local Alignment Search Tool
bp	base pair
cDNA	complementary DNA
COPI	Coat Protein I
DAPI	4-6-diamidino-2-phenylindole
DMEM	Dulbecco's Modified Eagle's Medium
DMSO	Dimethyl Sulphoxide
DNA	Deoxyribonucleic Acid
dNTP	deoxyribonucleic nucleotide 5'-triphosphates
DTT	Dithiothreitol
ECL	Enhanced Chemiluminescence
EDTA	Ethylenediaminetetraacetic Acid
EE	Early Endosome
EEA1	Early Endosome Antigen 1

EGFP	Enhanced Green Fluorescent Protein
Eferin	EF-hands-containing Rab11-interacting protein
EGTA	ethyleneglycol-bis(2-aminoethyl) N,N,N', N', -tetraacetic acid)
ER	Endoplasmic Reticulum
FCS	Fetal Calf Serum
FITC	Fluorescein Isothiocyanate
GAP	GTPase Activating Protein
GAPDH	Glyceraldehyde 3-Phosphate Dehydrogenase
GDF	GDI Displacement Factor
GDI	GDP Dissociation Inhibitor
GDP	Guanosine Diphosphate
GEF	Guanine-nucleotide Exchange Factor
GFP	Green Fluorescent Protein
GST	Glutathione S-transferase
GTP	Guanosine 5'-triphosphate
GTPase	Guanosine 5'-triphosphatase
h	hour
HA	Hemagglutinin
HeLa	Henrietta Lacks
HEPES	4-(2-hydroxyethyl)-1-piperazine-ethane-sulphonic acid

HRP	Horseradish Peroxidase
INCENP	Inner Centromere Protein
IPTG	Isopropyl β-D-thiogalactoside
kDa	kilo Dalton
LB	Luria-Bertani Broth
LE	Late endosome
min	minute
MKLP1	Mitotic kinesin like protein 1
MKLP2	Mitotic kinesin like protein 2
MOI	Multiplicity of Infection
mRNA	messenger RNA
miRNA	micro interference RNA
MT	Microtubule
MTOC	Microtubule Organising Centre
Nuf	Nuclear-fallout
PBS	Phosphate Buffered Saline
PBST	Phosphate Buffered Saline Tween
PM	Plasma Membrane
PLK	Polo-like kinase
PMSF	Phenylmethylsulfonyl fluoride

Rab11-FIP	Rab11 Family Interacting Proteins
RE	Recycling Endosome
REP	Rab Escort Protein
Rid	Rho-inhibitory domain
RILP	Rab-interacting Lysosomal Protein
RNA	Ribonucleic Acid
RNAi	RNA interference
ROCK	Rho Kinase
rpm	Revolutions per minute
RT-PCR	Reverse transcription polymerase chain reaction
SDS	Sodium Dodecyl Sulphate
SDS-PAGE	Sodium Dodecyl Sulphate Polyacrylamide Gel Electrophoresis
siRNA	small interfering RNA
SNAP25	Synaptosomal-Associated Protein of 25 kDa
SNARE	Soluble N-ethylmaleimide-sensitive Factor Attachment Protein Receptor
TEMED	Tetramethylethylenediamine
Tf	Transferrin
TfR	Transferrin Receptor
TGN	Trans Golgi network

VAMP	Vesicle-associated Membrane Protein
v/v	volume/volume ratio
w/v	weight/volume ratio

1 Introduction

1.1 Cytokinesis

1.1.1 Mitosis and cytokinesis

Cell division is an essential and fundamental process for the propagation of all living organisms. It consists of two major steps, mitosis and cytokinesis. Mitosis is the process by which a cell separates its duplicated genome into two identical halves. It is generally followed immediately by cytokinesis, which physically separates the cytoplasm and cell membrane of the mother cell into two daughter cells. The process of mitosis is complex and tightly regulated. The sequence of the events is divided into phases, corresponding to the completion of one set of activities and the start of the next. These stages are prophase, prometaphase, metaphase, anaphase and telophase.

Prophase is the first stage of cell division, Figure 1.1 panel A. At the onset of prophase, chromatins condense into highly ordered chromosomes. Since the genetic material has already been duplicated earlier in S phase, each chromosome has two sister chromatids, bound together at the centromere by the protein cohesin. The two centrosomes located outside the nucleus sprout microtubules by polymerizing free-floating tubulin protein. By repulsive interaction of these microtubules with each other, the centrosomes push themselves to opposite ends of the cell. The microtubule network starts to form the mitotic spindle at the same time.

Prometaphase follows prophase, during this period the nuclear envelope breaks down and microtubules radiating from the two centrosomes located at the opposite poles of the cells invade the nuclear space as the nuclear membrane dissolves. Kinetochores form at the centromeres of the chromosomes, with one for each chromatid. The kinetochore provides the pulling force necessary to separate the chromosome's two chromatids later.

At metaphase, condensed chromosomes align in the middle of the cell before being separated into each of the two daughter cell halves as shown in Figure 1.1, panel B. Microtubules formed in prophase have already attached themselves to kinetochores in metaphase. The centromeres of the chromosomes align themselves on the metaphase plate. One of the cell cycle checkpoints occurs during metaphase, which is only after all chromosomes have become aligned at the metaphase plate. When every kinetochore is properly attached to a bundle of microtubules, the cell enters anaphase.

Anaphase is the stage when chromosomes separate in a eukaryotic cell, as shown in Figure 1.1, panel C-E. Each chromatid moves to opposite mitotic spindle poles, which are near the microtubule organising centers. Anaphase can be divided into early and late anaphase. During early anaphase the chromatids separate and move towards the spindle poles, and this is achieved by shortening of the spindle microtubules with forces mainly exerted at the kinetochores. When the chromatids are fully separated the late anaphase begins, which involves the polar microtubules elongating and sliding relative to each other to drive the spindle poles further apart.

Following anaphase is telophase, Figure 1.1, panel F, in which non-kinetochore microtubules continue to grow and further elongate the cell. A new nuclear envelope using fragments of the parent cell's nuclear membrane, forms around each set of separated sister chromosomes. Both sets of chromosomes, now surrounded by new nuclear membrane, unfold back into chromatin.

In animal cell cytokinesis, a cleavage furrow develops where the metaphase plate used to be. An acto-myosin ring assembles at the position of the furrow, which constricts and pinches off the separated nuclei. In plant cells, vesicles derived from the Golgi apparatus move to the middle of the cell along microtubules scaffold called the phragmoplast. This structure directs packets of cell wall material, which coalesce into a disk-shaped structure called a cell plate. The cell plate eventually develops into a proper cell wall, separating the two nuclei (Figure 1.2). Each daughter cell has a complete copy of the genome of its parent cell, and mitosis is complete, see section 1.1.2.

1.1.2 Cytokinesis in plant and animal cells

Plant cell division is mediated by a specialized structure, the phragmoplast, an array of microtubules, actin filaments and associated molecules acting as a framework for the future cell wall, Figure 1.2, panel B. The phragmoplast can be divided topographically into two areas, the midline and the distal regions at both sides of the midline. The midline includes the central plane where some of the plus-ends of the anti-parallel sets of microtubules interweave to each other. It has been well established that Golgi-derived vesicles are the primary source of membrane in plant cytokinesis (Otegui and Stachelin, 2004). These vesicles are transported to the phragmoplast midline, where they fuse with each other and the cell-plate domains. Further observation showed that vesicles are tethered by linkers prior to fusion, and these linkers could be the exocyst complex (Otegui and Staehelin, 2004).

In contrast, cytokinesis in animal cells is dependent on a pronounced acto-myosin contractile ring that drives the PM invagination from the cortex, Figure 1.1, panel E. The acto-myosin ring assembles when the cell enters metaphase at the midpoint between two mitotic spindle poles. Its ingression compresses the spindle midzone and leads to formation of a condensed microtubules bridge structure called the midbody Figure 1.2, panel A, which consists of central spindle microtubules and proteins found there, details see 1.1.3.3. The most spectacular model of membrane expansion during cytokinesis is the *Drosophila* embryonic cellularisation. In *Drosophila* embryo, the first thirteen mitotic cycles occur in a syncytium containing 6000 nuclei. During the tenth cycle, these nuclei migrate to the actin-rich cortex, where they induce so-called pseudo-furrows around each mitotic apparatus at the metaphase of subsequent cycles. The metaphase furrows ingress only partially between the many mitotic apparatus as each segregates its associated nuclei during cycle 10 to 13. During the fourteenth cycle, cellularisation takes place and the furrows start to ingress fully between each nucleus, Figure 1.2, panel C. This model provides an excellent system for studying membrane trafficking because of the dramatic increased surface within a few tens of minutes and additional membrane materials are required largely to accommodate this morphology change (Lecuit and Wieschaus, 2000).

1.1.3 The process of animal cytokinesis

In this study, the main focus is mammalian cell cytokinesis, hence a detailed introduction of this process will be given as follows. Cytokinesis is a highly dynamic and complex process, for simplicity, it can be broken down into a series of sub-processes based on timing and cell morphology.

1.1.3.1 Positioning of the cleavage furrow

The first step of cytokinesis is the establishment of the cleavage site, which divides the spindle at the midpoint between the microtubule asters. Temporal and spatial machineries are both required for regulation of this process.

In animal cells, cytokinesis occurs promptly after anaphase onset. Several studies have related cyclin-dependent kinase 1 (Cdk1) to the transition from mitosis to cytokinesis (Shuster and Burgess, 1999). Inactivation of Cdk1 is crucial for the initiation of cytokinesis in cultured rat cells. Studies in sea urchin suggest that the phosphorylation of myosin regulatory light chain (MLC) of myosin II may also contribute to the timing of cytokinesis

(Shuster and Burgess, 1999; Yamakita et al., 1994), which controls the assembly of the contractile ring.

Spatially, two structures have been implicated in the initiation of cleavage furrow: astors, the radial arrays of centrosome-nucleated microtubules; and the central spindle, which forms between the separating chromatin in anaphase and consists of non-kinetochore spindle microtubules released from the spindle poles. Therefore, two models, "astral stimulation" and "central spindle", were suggested to induce the furrow initiation. The "astral stimulation" model supports the notion that astral microtubules are uniquely capable of inducing cleavage plane by delivering a "furrow-inducing signal" to the equatorial cortex. While the "central spindle" model proposes that the array of antiparallel non-kinetochore microtubules determines and initiates the cleavage furrow.

Evidence supporting both models has been discovered. In grasshopper spermatocytes, it is found that the spindle microtubules can self-assemble into organized bundles that promote furrowing even after asters and chromosomes are removed (Alsop and Zhang, 2003). This evidence suggests asters are not necessary for furrow positioning in grasshopper spermatocytes division. However, two other studies showed opposite results, which revealed that the central spindle is dispensable for cytokinesis. First, drug-induced monopolar spindles, which lack central spindle microtubules in mammalian PtK1 cells, are able to initiate and complete cytokinesis (Canman et al., 2003). The other line of evidence is that *C. elegans spd-1* mutant embryos lacking a central spindle can nevertheless complete the first embryonic division, though cytokinesis fails in subsequent cell divisions (Verbrugghe and White, 2004). A suggestion to integrate the two models together is that the astral microtubules deliver a furrow signal and then the central spindle may stabilise and propagate furrow ingression. Different cell types may adapt the general mechanism to meet specific requirements. In extreme situations, one of the two structures, astral array or the central spindle, is sufficient to induce furrowing.

1.1.3.2 The assembly and constriction of the contractile ring

Following the positioning of the cleavage furrow, an acto-myosin contractile ring assembles at the belt of the cell cortex where the furrow is placed. In this structure, actin is associated with the molecular motor myosin II (Fujiwara et al., 1978) and sliding of actin filaments by bipolar filaments of myosin II is critical for the progression of cytokinesis. The force-generating ability of myosin II is regulated by phosphorylation of myosin II, especially its light chains (Satterwhite et al., 1992). The phosphorylation level of myosin

increased rapidly upon initiation of cytokinesis (Yamakita et al., 1994). In addition, overexpression of an MRLC mutant that cannot be phosphorylated causes cytokinesis defects (Komatsu et al., 2000), supporting its function in assembly of the contractile ring.

RhoA, a small Rho GTPase, has been shown to positively regulate acto-myosin contractility. The Rho family of small GTPases consists of RhoA, Rac and Cdc42 whose role in human cells are well established in regulating actin dynamics. In interphase fibroblasts, activation of RhoA increases the level of polymeric actin and induces the formation of stress fibres. The similarity between stress fibres and contractile ring implicates that RhoA may use a similar mechanism to induce these structures. In cytokinesis, RhoA defines a narrow zone at the site where the contractile ring forms, and indirectly regulates myosin II phosphorylation via ROCK, A Rho kinase. ROCK is also strongly concentrated at the cleavage furrow and uses myosin light chain as a phosphorylation substrate. RhoA appears to inhibit myosin phosphatase, hence promotes the MRLC phosphorylation by blocking its dephosphorylation (Amano et al., 1996; Kosako et al., 1999). In *Drosophila*, RNAi of *Rok*, the homologue of ROCK affected furrowing, which was delayed and slowed, even distorted (Hickson et al., 2006).

Although the contraction of acto-myosin ring is an important contribution to furrowing, this is not the only force that drives ingression of the cleavage furrow. Numerous studies have shown that as the contractile ring advances, additional membrane material is required to accommodate the increased surface area for the formation of two daughter cells. Interestingly, research from both sea urchin embryos and *Xenopus* eggs have shown that the membrane insertion does not happen randomly across the cell surface but occurs specifically at the cleavage furrow (Shuster and Burgess, 2002). Live cell imaging of Golgi movement during *Drosophila* cellularisation revealed that Golgi move towards and closely associate with the advancing furrow, and inhibition of a Golgi associated protein, Lava Lamp, blocks furrowing (Sisson et al., 2000). More striking studies from scanning electron microscopy and live cell microscopy of *Xenopus* embryos demonstrated large clusters of exocytic fusion pores near the base of the invaginating furrow (Danilchik et al., 2003). These findings implicate a requirement of membrane addition to the furrow as the contractile ring contracts and this process is controlled to take place at the furrow site where specific lipids and proteins may be needed. This will be discussed in detail in 1.2.2.

1.1.3.3 Midbody formation

The constriction of the acto-myosin ring squeezes the antiparallel microtubules derived from the central spindle microtubules into a dense bundle. This creates a narrow band of cytoplasm and cytoskeleton that connects the two prospective daughter cells, which is called the midbody. The region where these microtubules overlap is the electron dense central "Flemming body" (Flemming, 1891).

The two main constituents of the midbody are the tightly packed residual central spindle microtubules and the proteins found there. Taking advantage of multidimensional protein identification technology (MudPIT), Skop and co-workers performed an analysis of the midbody proteome with midbodies purified from Chinese hamster ovary (CHO) cells (Skop et al., 2004). This elegant study identified 160 proteins that potentially play a role in cytokinesis localised at the midbody, and they fall into five groups. The largest class is the proteins involved in secretory or membrane trafficking (33%); 29% are actin-associated proteins; 11% are protein kinases; and another 11% are microtubule-associated proteins. The remaining 16% of the midbody proteins fall into a variety of different groups, which are difficult to classify. These molecules are not innocent bystanders: while they actively participate in various steps, including midbody formation and stabilisation, actin-ring disassembly and membrane fusion events. Indeed, 36% of them have previously been shown to participate in cytokinesis in one or more experimental systems.

1.1.3.4 Midbody stabilisation

The two new daughter cells are now connected by an intercellular midbody bridge that derived from a central spindle. The midbody is generally stable for 2-3 h, and then is severed in the final physical separation. A recent study found that a stable midbody bridge is essential for successful cytokinesis, and is thought to provide a scaffold that facilitates progression through the final abscission (Matuliene and Kuriyama, 2002).

One protein that has been proved to be a core component of the midbody is the Mitotic-Kinesin-Like-Protein 1, MKLP1/CHO1. Homologues of MKLP1 are called ZEN-4 and Pavarottin (Pav) in *C. elegans* and *Drosophila* respectively. These proteins belong to a family of proteins containing a kinesin motor domain and appear to have plus-end-directed microtubule motility (Nislow et al., 1992). MKLP1 is enriched at the midbody during cytokinesis, and is specifically important for the formation and maintenance of a stable midbody bridge between dividing cells. Expression of the ATP binding defective mutant or

depletion of CHO1, an isoform of MKLP1, inhibits the formation of the dense midbody matrix (Matuliene and Kuriyama, 2002). In these cells, the midbodies show abnormal morphology. Time-lapse microscopy showed that cells regress from the un-stabilised midbodies and form binucleate cells. Genetic studies in both *Drosophila* and *C. elegans* also support this notion (Adams et al., 2001b; Raich et al., 1998). ZEN-4, the *C. elegans* MKLP1 homologue, promotes central spindle assembly in conjuction with a Rho family GTPase-activating protein (GAP), CYK-4 (Jantsch-Plunger et al., 2000). ZEN-4 and CYK-4 form a complex called centralspindlin, and its counterparts composed of MKLP1 and MgcRacGAP in human cell has also been discovered (Mishima et al., 2002).

Another protein complex that localises to the central spindle and functionally participates in cytokinesis consists of Aurora B, INCENP and survivin. Biochemical interactions between these three proteins have been demonstrated in variety of organisms (Adams et al., 2000; Kaitna et al., 2000). The Aurora B complex is responsible for phosphorylation of Histone H3 that is required for chromosome segregation (Adams et al., 2001b). Interestingly, analysis of *C. elegans* embryos revealed ZEN-4 phosphorylation and localisation to the central spindle requires Aurora B (AIR-2) activity (Severson et al., 2000). These observations raise the possibility that the centralspindlin complex may need to be phosphorylated by the Aurora B complex, and the phosphorylation may promote the interaction of the complex with microtubules and promote microtubule cross-linking.

1.1.3.5 Disassembly of the contractile ring

After the midbody has formed and stabilised, the acto-myosin ring needs to be disassembled before the completion of cytokinesis. Two events have been shown to be involved in this process, externalization of phosphatidylethanolamine (PE) at the cleavage furrow and down-regulation of the Rho GTPase. Emoto and coworkers have shown that PE, which resides on the inner leaflet of the PM relocalises to the cell surface of the cleavage furrow just before midbody formation (Emoto et al., 1996). Treatments that sustain PE on the outer leaflet inhibit the completion of cytokinesis and lead to the formation of daughter cells connected by long cytoplasmic bridges. Interestingly, constituents of the contractile ring, including actin and myosin, remained in these bridges. This suggests that completion of cytokinesis is blocked because the contractile ring cannot be disassembled. Therefore, the current hypothesis is that redistribution of PE across the lipid bilayer is a signal that promotes actin disassembly.

RhoA has also been suggested to play an essential role in the contractile ring assembly and constriction as described in 1.1.3.2. Studies indicated that the down-regulation of Rho activity at the furrow/midbody is important for disassembly of the contractile ring and completion of cytokinesis (Jantsch-Plunger et al., 2000). This decreased activity is favoured by MgcRacGAP, a Rho-family GAP, which localises to the central spindle. The homologues of MgcRacGAP in *C. elegans* and *Drosophila*, CYK-4 and RacGAP50C, are also required for successful cytokinesis in these two model systems. Although MgcRacGAP has GAP activity towards all three members of the Rho family, only depletion of RhoA, not Rac or Cdc42, results in the same cytokinesis defects as disruption of CYK-4 and RacGAP50C in *C.elegans* and *Drosophila* (Jantsch-Plunger et al., 2000; Somers and Saint, 2003). Furthermore, in mammalian cells, MgcRacGAP colocalise with RhoA but not Rac or Cdc42 at the cleavage furrow and midbody, which further support the idea that GAP activity for RhoA provided by MgcRacGAP is important for the completion of cytokinesis.

1.1.3.6 Midbody abscission

To complete cytokinesis, the intercellular bridge between the two new daughter cells has to be sealed to remove the physical obstacle. This process is not a simple midbody break but an active, regulated process controlled by certain mechanisms.

Similar to the process of furrow ingression, the final abscission of the midbody in animal cells also requires membrane delivery and fusion events. It is generally believed that division may occur in the midbody bridge with a process similar to plant cell division. Membrane vesicles are delivered along microtubules to the midbody where they accumulate and fuse with each other and eventually seal off the intercellular canal, thus dividing the cell into two (Figure 1.3, panel A). This is supported by several lines of evidence: Skop and colleagues have shown that brefeldin A (BFA), a fungal metabolite which ER-Golgi and Golgi-Golgi trafficking inhibits the closure of the midbody in *C. elegans* (Skop et al., 2001). Low et al. have shown that two members of the SNARE membrane fusion machinery, syntaxin 2 and endobrevin/VAMP 8 localise to the midbody and expression of mutant forms of these proteins led to increased cytokinesis failure. By using time-lapse microscopy they showed that this failure in cytokinesis occurs specifically at the final abscission stage, as cleavage furrow ingression and all other parts of cytokinesis proceed normally up until this stage. (Low et al., 2003). Two possible models have been suggested of the manner that the intercellular bridge is sealed by membrane insertion as shown in Figure 1.3, Panel B (Finger and White, 2002). The first model

suggests a large vesicle, which probably formed by fusion of many small vesicles moves to the furrow and fuses with the PM cortex and seals the canal (Panel B, top). The second model proposes that smaller vesicles travel to the furrow region individually and fuse with the PM, gradually closing the gap between two daughter cells (Panel B, bottom). Both models highlighted the requirement of membrane trafficking to the midbody for the completion of cytokinesis.

Surprisingly, the centrosome has been related to cytokinesis completion. Live cell imaging of GFP-tagged centrosomes showed that the mother centriole moved into the intercellular bridge late in cytokinesis. As soon as this centriole leaves the midbody, cytokinesis starts, suggesting that the centrosome probably acts to check the timing of cytokinesis (Piel et al., 2001). The relation between centrosomes and completion was reinforced by the observation that a centrosome protein Centriolin is involved in completion of cytokinesis. This protein has been indicated localise to the midbody and depletion by RNAi led to multinucleate cells (Gromley et al., 2004).

1.1.4 Key regulators of cytokinesis

1.1.4.1 MKLP1 and other Kinesins involved in cytokinesis

Kinesins are a large family of proteins that contain a conserved motor domain, which binds to microtubules and couple ATP hydrolysis to generate force that allows the movement of kinesins along microtubules (Hirokawa, 1998). Most kinesins are microtubule plus-end-directed motors that move away from the microtubule organizing centre (MTOC). Kinesins have been implicated in a broad range of roles in cellular events, including intracellular migration of organelles and vesicles, mitotic spindle formation and chromosome segregation (Allan and Schroer, 1999; Hirokawa, 1998)

As briefly described in 1.1.3.4, Mitotic Kinesin-Like Protein 1, MKLP1/CHO1 is a plus-end-directed motor that crosslinks microtubules in antiparallel bundles via two microtubule binding domains and undoubtedly plays a major role in cytokinesis. MKLP1 and its *Drosophila* homologue Pavarotti and *C. elegans* homologue ZEN-4 all localise to the central spindle when the cell enters mitosis. Analysis of CHO1, a splice-variant form of MKLP1 reveals that mutations in CHO1 cause its failure to localise to the midzone. As a result, disorganisation of midbody matrix and furrow regression were observed (Matuliene and Kuriyama, 2002), suggesting its essential role in stabilising and maintaining the midbody. Pavarotti, is required for formation and maintenance of the central spindle during

cytokinesis. In a study of kinesins in *Drosophila* using RNAi, Pavarotti was the only one shown to be essential for cytokinesis as its depletion led to failure of central spindle formation and caused arrest of anaphase to cytokinesis (Goshima and Vale, 2003). In *C. elegans*, embryos lacking function of MKLP1 homologues ZEN-4, by using RNAi and temperature-sensitive mutation do not form central spindle, and furrow regression was observed (Raich et al., 1998; Severson et al., 2000).

Another plus-end-directed kinesin involved in cytokinesis is the Rab6-binding kinesin, Rab6-KIFL (also named as Rabkinesin6 or MKLP2). It shares a conserved motor domain, which is able to bind to microtubules and moves along it through ATP hydrolysis. Rab6-KIFL was initially identified as a binding partner of Rab6, a small GTPase implicated in anterograde traffic from Golgi to the ER, hence Rab6-KIFL was also thought to act in this process (Echard et al., 1998). However, it was subsequently discovered that Rab6-KIFL accumulates in the central spindle and becomes highly concentrated in the midbody during telophase and cytokinesis (Hill et al., 2000). As with MKLP1, Rab6-KIFL is also required for central spindle assembly, and interruption of this protein leads to defects of cytokinesis. Microinjection of antibodies against this protein resulted in increased binucleate cells and indicates an up-regulated protein level during cell division. More recently, RNAi analysis showed knock-down of this protein also affects cytokinesis (Neef et al., 2003). Because of its role in cytokinesis, Neef and co-workers suggested reclassifying Rab6-KIFL as a mitotic kinesin and therefore re-named it as Mitotic Kinesin-Like Protein 2 (MKLP2). Further investigation showed that MKLP2 can interact and be phosphorylated by PLK1, and the phosphorylation is important for correct localisation of both these proteins to the central spindle (Neef et al., 2003). It was also discovered that MKLP2 can interact with Aurora B and the interaction is important to localise Aurora B from the centrosomes to the central spindle (Gruneberg et al., 2004). It is not clear whether Rab6-KIFL's function in cytokinesis involves this interaction with Rab6. As described in 1.2.2.1, membrane trafficking, likely derived from Golgi is required for cytokinesis. Hence, Rab6 might function in secretory vesicles delivery to the cleavage furrow/midbody facilitated by KIFL via the microtubules network.

1.1.4.2 Septins

Septins are filamentous GTPases originally identified as genes important for yeast cell division. They form a ring of 10 nm filaments adjacent to the PM at the mother-bud neck prior to cytokinesis (Field and Kellogg, 1999). Mutations of septin genes resulted in abnormally elongated buds and the failure of cytokinesis completion. In yeast, they have

been implicated in a wide variety of functions, such as signalling, mediating diffusion barriers (Barral et al., 2000), spindle body orientation (Kusch et al., 2002) and cell-cycle checkpoint (Castillon et al., 2003).

There are 12 septin genes named *SEPT1-12*, ranging from 40-70 kDa, several of which contain alternative splicing in yeast. Two of them, *SEPT2* and *SEPT9* have been shown to be involved in cell division (Surka et al., 2002). Interference of *SEPT9* by RNAi or microinjection of antibody against it induces binucleate cells, an index of cytokinesis failure. This phenotype is reminiscent of the defects caused by disruption of *SEPT2*, which also results in increased binucleate cells and daughter cells connected by midbody bridges for a long time after furrow ingression completion (Surka et al., 2002). Interestingly, although these two septins are both involved in cytokinesis, they indicate distinct localisations. SEPT2 predominantly localises to the contractile ring, while SEPT9 is enriched at the central spindle region. As mentioned before, three mammalian septin homologs, Nedd5, H5 and MSF have also been implicated in cytokinesis (Kinoshita et al., 1997; Surka et al., 2002; Xie et al., 1999). Disruption any of these proteins leads to formation of an unstable intercellular bridge, and the appearance of binucleate cells. Emerging evidence has suggested roles for septins in regulation of membrane traffic in dividing cells. In yeast, exocyst subunits colocalise with septin, and disruption of exocyst components caused similar defective cell separation (Wang et al., 2002). In neurons, the exocyst subunit Sec6 colocalises with SEPT7 in growth cones and synapse assembly sites, where extensive membrane remodelling is required. SEPT5 was shown to bind syntaxin 1 and 2 directly (Beites et al., 1999). These raise the possibility that septins may function with exocyst and SNAREs to facilitate vesicle docking and fusion in cytokinesis.

1.1.4.3 Exocyst

The exocyst is an evolutionary conserved eight-subunit complex involved in vesicle tethering to specific sites on the PM in preparation for exocytosis. It was first identified in *Sacchaomyces cerevisiae*, where it is required for exocytosis. The eight components are Sec3p, Sec5p, Sec6p, Sec8p, Sec10p, Sec15p, Exo70p and Exo84p (TerBush et al., 1996). All the 8 subunits are hydrophilic and form a 19.5S complex that peripherally associates with the PM. The mammalian homologues of all eight yeast exocyst proteins were identified by Hsu and coworkers, and were thought to be involved in directing vesicles to the correct sites of fusion (Hsu et al., 1998).

Recent reports showed that several small GTPases functionally associate with the exocyst, including members of the Rab (Guo et al., 1999a), Rho (Adamo et al., 1999; Robinson et al., 1999) and Ral (Moskalenko et al., 2002) families. The yeast Rab protein Sec4 was the first GTPase found to interact with the exocyst component Sec15. Sec15 interacts with Sec4-GTP present on vesicles, and this interaction seems to trigger further interaction between Sec15 and other exocyst proteins, which finally leads to docking and fusion of secretory vesicles at specific sites. The interaction of Sec3p with GTP-Cdc42p and GTP-Rho1p in yeast is essential for the establishment and maintenance of the cell polarity by directing exocytosis at the buds (Guo et al., 2001).

Interestingly, in yeast the exocyst complex localise to regions where the cell surface expands, such as the bud tip during the cell cycle, and the neck that connects the mother and daughter cell. In mammalian cells, Sec15 colocalises with Rab11 on the recycling endosome compartment and binds to Rab11 in a GTP dependent manner, but not to Rab4, Rab6 and Rab7 (Novick and Guo, 2002). More recently, another exocyst component Sec10 has been found to associate with Arf6 and facilitate Arf6 mediated membrane remodelling and cell spreading (Prigent et al., 2003). Rab11 and Arf6 are both involved in endosomal trafficking suggesting that exocyst components may facilitate to tether vesicles regulated by Rab11 and Arf6 to the PM.

1.1.4.4 SNAREs

Membrane material delivered to the furrow/midbody region need to fuse with the PM and with each other to promote the completion of cytokinesis. Vesicle fusion is driven by a family of proteins known as SNAREs (Soluble NSF Attachment Protein Receptor), which have been established as central in most intracellular membrane fusion events (Rothman, 1994). SNAREs are divided into t-SNAREs and v-SNAREs according to their locations on target or vesicle membranes. On the basis of homology and domain structure, they are categorized into three groups, syntaxin, VAMP and SNAP25 subfamilies. Most SNAREs are found in specific cellular compartments, and it is believed that each type of transport vesicle has distinct v-SNAREs (VAMP) whose cytoplasmic domain can pair up with unique cognate t-SNAREs (syntaxins and SNAP25) on proper target membranes, with the subsequent formation of a four-helix bundle to drive membrane fusion.

Numerous studies have established that SNAREs have a fundamental role for membrane fusion events during cytokinesis in a range of organisms. In plant cytokinesis, the membrane fusion of secretory vesicles at the phragmoplast requires a plant-specific

syntaxin named KNOLLE, which is expressed during M phase only and localises to the plane of division. Its mutants cause accumulation of un-fused vesicles in the cell plate (Lauber et al., 1997). In sea urchin embryos, microinjection of antibodies against syntaxin 1 or *Botulinum neurotoxin C1* blocks the terminal step of cytokinesis (Schiavo et al., 1995; Walch-Solimena et al., 1995). In *Drosophila*, female germ line mutants for *syntaxin 1* do not undergo cellularisation after the syncytial blastoderm stage, when a massive increase in membrane surface area is required (Burgess et al., 1997). More recently, syntaxin2 and endobrevin/VAMP-8 have been shown to localise to the midbody during cytokinesis in NRK cells. Time-lapse microscopy further indicated that cells expressing syntaxin2D and VAMP-8 truncations remained in the midbody stage for a while, after which regression occurred and led to binucleated cells (Low et al., 2003).

1.1.4.5 Aurora kinase

Phosphorylation is an important reversible post-translational modification of proteins, which regulates a multitude of cellular events. Aurora kinases have recently emerged as essential regulators of cell cycle processes. Human Aurora A-C are a family of serine-threonine kinases ranging in size from 309 to 403 amino acid residues. Aurora A has been localized at both centrosomes and spindle microtubules (Bischoff et al., 1998; Kimura et al., 1997), and has been implicated in spindle assembly and as a drug target in diverse solid tumours (Dutertre et al., 2002; Kufer et al., 2002). Aurora B is a chromosome passenger, localising on centromeres from prophase through to metaphase, and then aligns at the spindle midzone and cortex at the site of furrow ingression (Adams et al., 2001a; Bischoff et al., 1998). Aurora B plays an essential role in chromosome segregation and cytokinesis by forming a complex with INCENP and survivin (Honda et al., 2003). Aurora C is expressed primarily in testis and some tumour cell lines, where it has been localised to spindle poles (Kimura et al., 1999; Tseng et al., 1998), and it has also been shown to be involved in spermatogenesis (Adams et al., 2000).

Aurora B has been found to orchestrate many aspects of cytokinesis by forming a complex with INCENP and survivin. Myosin II, a central constituent of the dividing force generating the acto-myosin ring, has been identified as a substrate of Aurora B (Murata-Hori et al., 2000). Inhibition of Aurora B function causes the mislocalisation of myosin II and furrow ingression defects (Straight et al., 2003). The Aurora B complex is required for the phosphorylation and stable recruitment of MKLP1/ZEN4, which functions to stabilise and bundle overlapping antiparallel microtubules at the central spindle in both *C. elegans* and mammalian cells (Kaitna et al., 2000; Mishima et al., 2002; Severson et al., 2000).

Aurora B also phosphorylates MgcRacGAP, which forms the centralspindlin complex with MKLP1 and is conserved both in human and worms (Mishima et al., 2002). Interestingly, phosphorylation of MgcRacGAP by Aurora B increased its GAP activity specifically towards RhoA, rather than the other two members of Rho family, Cdc42 or Rac (Minoshima et al., 2003).

1.1.4.6 Polo-like kinase

The family of Polo-like kinase is the human homolog of the founding member *Polo* in *Drosophila*. The original identification of *Polo* in *Drosophila* showed it is a serine-threonine kinase that is required for mitosis. Later, identification of Plk (*human*), *Cdc5* (*S. cerevisiae*) and *Plo1* (*S. pombe*) by mutational analysis also implicates an essential role of Plk in mitosis in these organisms.

So far, four mammalian Plks have been identified, and they share a highly conserved protein kinase domain at the N-terminus. Besides, Plk also contain Polo box domain, which is crucial for its subcellular distribution in mitosis and substrate specificity interaction. In human cells, Plk1 has been implicated in a broad range of processes from start to completion of mitosis, including mitotic entry, spindle formation and cytokinesis. Plk1 phosphorylate multiple proteins that regulate cytokinesis, such as MKLP1/CHO1, MKLP2 (Liu et al., 2004; Neef et al., 2003). Phosphorylation of these molecules are required for Plk1 localisation to the central spindle, and interference of the Plk1 substrates MKLP1, MKLP2 and NudC all results in defects in cytokinesis (Adams et al., 1998; Litvak et al., 2004; Neef et al., 2003). Removal of the Plk1 phosphorylation sites in MKLP1 or MKLP2 prevent final abscission, suggesting the Plk1 mediated phosphorylation plays a role in late stage of cytokinesis (Liu et al., 2004; Neef et al., 2003).

1.2 Membrane trafficking in cytokinesis

1.2.1 Intracellular membrane trafficking pathway

Eukaryotic cells have developed elaborate mechanisms for constitutive and regulated modes of secretion, as well as internalisation of various nutrients and substances, see Figure 1.4. Briefly, the secretory pathway allows cells to direct newly synthesised proteins, carbohydrates and lipids out towards the cell surface, while the endocytic system is responsible for the uptake of material from the extracellular environment and recycling

some of them back to the PM after sorting according to requirements. Although these two trafficking pathways act in the opposite direction, they are intricately linked. They are composed of distinct membrane organelles, and each of them has distinct biochemical composition and serves different functions.

The secretory system includes the endoplasmic reticulum (ER), the Golgi complex and the trans-Golgi network (TGN). This pathway starts with the ER, which consists of many interconnecting membrane tubules and cisternae. It acts like a quality control centre for the nascent synthesized polypeptides, since only correctly folded proteins progress into the secretory pathway (Ellgaard and Helenius, 2001). The Golgi apparatus is the place that proteins and lipids are modified, packed and sorted to the PM or retained in the ER/Golgi system.

The endosomal system consists of early/sorting endosomes (EE), recycling endosomes (RE), late endosomes (LE) and lysosomes. These compartments have distinct properties and may be distinguished morphologically (Sonnichsen et al., 2000). Many decisions are made within the endosomal system to determine the destination of the internalised receptors, ligands and lipids. These cargos normally have several destinations: the LE and lysosomes for degradation, the Golgi complex or recycling back to the PM. The endocytic trafficking pathways are regulated by multiple proteins with the Rab proteins emerging as key players, see section 1.3.3.

1.2.2 Membrane trafficking in animal cytokinesis

Recently, accumulating evidence has suggested an essential role of membrane trafficking in cytokinesis of mammalian cells. It is obvious that additional membrane material is acquired to accommodate the increased surface when a single cell divides into two. Using membrane surface marking techniques, it has been discovered that the additional membrane inserted during cytokinesis is not derived from expansion of pre-existing surface membrane but instead from internal stores (Bluemink and de Laat, 1973; Finger and White, 2002; Glotzer, 2001).

The first suggestion that membrane insertion is important for completion of cytokinesis was proposed by the fact that inhibition of syntaxins in *C. elegans* and sea urchin embryos caused cytokinesis defects (Conner and Wessel, 1999; Jantsch-Plunger and Glotzer, 1999). Inhibition of Rab11, a small GTPase required for vesicle trafficking through the recycling endosome, caused furrow regression in *C. elegans* blastomeres (Skop et al., 2001).

Moreover, a *rab11* transheterozygote also impaired cellularisation in *Drosophila* (Riggs et al., 2003). Striking studies from scanning electron microscopy and live cell microscopy of *Xenopus* embryos demonstrated large clusters of exocytic fusion pores near the base of the invaginating furrow (Danilchik et al., 2003). In this study, the extracellular surface of the PM was labelled with fluorescein isothiocyanate soybean agglutinin before cleavage. Addition of new, unlabelled membrane was seen accumulating at the furrow surface once furrowing starts. Another study of *C. elegans* cytokinesis an accumulation of membrane was observed by using membrane probe FM-1-43, and this was believed to seal the cytoplasmic bridge between dividing embryonic blastomeres (Skop et al., 2001).

Membrane trafficking required during cytokinesis may contribute to several aspects for this process. First, ingression of the cleavage furrow involves creating new membrane surface area, thus additional membrane must be provided for the expansion. Second, membrane delivery and vesicle fusion are required to seal off the intercellular canal between two daughter cells. Finally, membrane traffic may be necessary for insertion of specific proteins or lipids required for the cytokinetic machinery. Two models regarding the possible origins of the additional membrane required for cytokinesis have been suggested. The first model proposes that the vesicles targeted to the cleavage furrow derive from the secretory system, while the second model proposes that the membrane material are delivered by the endocytic system and likely sorted through the RE (Strickland and Burgess, 2004). Important evidence supporting both hypothesis have been shown, which will be discussed in detail in 1.2.2.1 and 1.2.2.2.

1.2.2.1 The secretory pathway

Microinjection of antibodies against Golgi-associated protein, Lava Lamp, lead to severe defects in Golgi distribution and furrow formation failure in *Drosophila* (Lecuit and Wieschaus, 2000). Further evidence implicating the secretory pathway as an important source of membrane during cell division is that BFA inhibits *C. elegans* embryo cytokinesis (Skop et al., 2001) and *Drosophila* cellularisation (Sisson et al., 2000). However, BFA does not interfere with cytokinesis during the cleavage of early sea urchin embryos, suggesting that different model systems may use different mechanisms during oogenesis. Further support for a role for the Golgi during cytokinesis comes from the study of Nir2, a Golgi-associated protein that travels to the cleavage furrow after it is phosphorylated by Cdk1 and Plk1 and dissociates from the Golgi (Litvak et al., 2004).

What remains to be determined is whether vesicles are derived directly from the Golgi or if they are first sorted through the recycling endosome. Indeed, the state of the Golgi during cell division is the subject of a long running debate (Barr, 2004). Briefly it centres around two models, one suggesting that the Golgi is absorbed into the ER during cell division, whilst the other suggested the Golgi fragments into smaller parts but remains separate from the ER. Interestingly, a recent report suggest that rather than the Golgi being required to provide membrane for cytokinesis, it is actually the dispersal of the Golgi that is important for mitosis/cytokinesis (Altan-Bonnet et al., 2003). It was argued that proteins resident in the Golgi during interphase are required elsewhere to carry out their functions in cytokinesis (Sisson et al., 2000). Therefore in order to function in cytokinesis the Golgi must first disassemble. These reports suggest that ultimately the Golgi is required for cytokinesis as a source of certain protein components, so that at the time of cytokinesis it is actually the lack of a normal interphase-type Golgi that is important for cell division.

1.2.2.2 Endocytic recycling pathway

Considering that cytokinesis requires the insertion of additional membrane material, it was surprising to discover that endocytosis-based membrane trafficking is also important for this process. As mentioned in 1.2.1, membrane trafficking within the endocytic pathway proceeds via a series of compartments, including EE, RE and LE. Recent studies have highlighted RE function in cytokinesis, and this organelle has a number of features that make it suitable in this role. First, the primary destination of the RE-derived vesicles is the PM, where new membrane is required in cytokinesis. Second, the RE sorts different types of proteins, and thus may facilitate selective delivery of specific proteins to the PM needed for cytokinesis. Third, the RE associates with microtubules and localises close to the microtubule-organising centre (MTOC), which actively regulates the mitotic spindle dynamics and contractile ring positioning. Therefore, membrane vesicles derived from endocytosis and sorted via the RE are suggested to be the second membrane origin for cytokinesis.

There is an increasing body of evidence supporting a role for endosomes in membrane delivery. Feng and co-workers clearly showed that endocytosis occurs specifically at the furrow from early to late stages in zebrafish embryos (Feng et al., 2002). In addition, they also showed that clathrin-coated pits, caveolin and dynamin II localise to the cleavage furrow, and that inhibition of these molecules led to a cytokinesis failure. Dynamin has also been shown to localise to the cleavage furrows and is necessary for cytokinesis completion in *C.elegans* (Thompson et al., 2002). In *Drosophila*, a clathrin-associated

protein α-adaptin were observed to localise to the advancing edge of the furrows (Dornan et al., 1997). A recent study of Rab5, a crucial regulator of EE trafficking, indicated that microinjection of a construct encoding a dominant negative Rab5, leads to failure of cellularisation (Pelissier et al., 2003). In *C.elegans*, interference of Rab11, which predominantly resides in RE and controls trafficking through this organelle, by RNAi inhibits the completion of cytokinesis and led to furrow regression (Skop et al., 2001). A study of *Drosophila* embryo cellularisation also demonstrates that Rab11 is essential for this event. Mutants of Rab11 and RE associated protein Nuf led to similar defects in both membrane addition and actin remodelling. In these embryos, the recruitment of both membrane and actin fails during the early stages of furrow formation and ingression (Riggs et al., 2003).

1.3 Rab and Arf GTPases

1.3.1 The Rab GTPase family

Rab/Ypt/Sec4 proteins exist in all eukaryotes investigated and form the largest branch of the Ras GTPase superfamily (Stenmark and Olkkonen, 2001). There are around 70 Rabs in humans as estimated from the sequenced genome (Zerial and McBride, 2001), of which ten subfamilies have been defined based on distinct specific sequence motifs. Rabs have been found in all eukaryotes studied, including 11 members in *Saccharomyces cerevisiae*, 29 members in *C.elegans* and 26 members in *Drosophila melanogaster*. This conservation and increased complexity throughout evolution reflects an essential cellular function of these molecules and more complicated intracellular trafficking events in higher eukaryotes.

Like all other Ras-like GTPase, Rabs undergo an intricate cycle between GDP-bound and GTP-bound forms to control their functions. Figure1.5, panel A shows that this cycle is basically regulated by four groups of regulators: Rab GDP-dissociation inhibitor (GDI), Rab Escort Protein (REP), GDP/GTP exchange factor (GEF) and GTPase-activating protein (GAP). In the GDP-bound inactive form, 10-50% of any given Rab protein is present in cytosol. GDI and REP together prevent Rabs binding to indiscriminate membranes and keep them unable to associate with effectors. The Rabs are presented to the geranylgeranyl transferase by REP, and the addition of one or two highly hydrophobic geranylgeranyl groups to a cysteine motif at the very carboxyl terminus is responsible for its reversible interaction with membranes (Anant et al., 1998). GDI binds to the prenylated Rabs in the GDP form (Garrett et al., 1994; Shapiro and Pfeffer, 1995), masking their

isoprenyl anchor and maintaining the Rab proteins in the cytosol (Goody et al., 2005). The attachment of Rab proteins to the appropriate donor membrane requires the function of a GDI displacement factor (GDF) (Pfeffer and Aivazian, 2004). Once dissociated from GDI, the Rabs are available for GEF catalysed GTP binding. GTP-Rabs are then free to interact with their downstream effectors, which fulfil their various roles in membrane trafficking. After completing their cellular function, the Rabs are inactivated via GTP hydrolysis regulated by GAP, and extracted from the membrane by GDI and recycled back to the cytosol.

Rab GTPases control discrete membrane trafficking events throughout the entire secretory/endocytic system. Individual Rab proteins localise to distinct intracellular vesicular compartments as shown in Figure1.5, panel B, suggesting that each Rab has a well-defined functional role. Such diverse localisations may be due to protein structural feature of this family. Rabs differ most in their carboxyl terminal regions, which have been implicated in subcellular targeting (Chavrier and Goud, 1999), whereas regions involved in guanine-nucleotide binding (switch I and switch II) are most highly conserved. Among the Rabs, Rab1, Rab2 and Rab6 localise to the Golgi and act at the level of the ER and Golgi along the biosynthetic/secretory pathway (Chavrier et al., 1990). Rab4 and Rab5 play roles in early steps of the endocytic process and endosome-endosome fusion (Gonzalez and Scheller, 1999; Martinez and Goud, 1998). Rab8 resides on TGN and regulates the targeting of trans-Golgi vesicles to the PM. Rab11 has been implicated in recycling of transferrin receptors (TfR) through the RE (Ren et al., 1998) and membrane transport from the TGN to the PM (Chen et al., 1998).

1.3.2 Rab effectors

It is believed that the key to Rab function is the recruitment of specific effectors that bind exclusively to their GTP-bound forms, and influence endocytic pathways at the level of budding, cytoskeletal transport and fusion. Each Rab assembles a multitude of effectors into a "Rab domain", thus coordinating numerous events through different effector functions (Zerial and McBride, 2001). The first Rab effector, Rabphillin 3A, was characterized in 1993 (Kishida et al., 1993). Since then, a large number of Rab effectors have been identified, for example, over 20 proteins were identified as interacting proteins of Rab5-GTP, suggesting a great complexity of functions of this GTPase (Christoforidis et al., 1999). The identified Rab effectors are a fairly heterogeneous group of proteins and serve diverse functions. Rabphilin-3A interacts with an actin-binding protein α-actinin and may induce the local organization of the actin cytoskeleton to regulate fusion of synaptic

vesicles with the PM. The role of Rabphilin 3A may be to link vesicles and the target membrane to the cytoskeleton at docking sites (Kato et al., 1996). In some cases, a motor protein can directly interact with Rab proteins. Rabkinesin-6, a Rab6 effector which contains a kinesin-like ATPase motor domain and a Rab-binding domain, has been suggested to facilitate vesicle transport to their proper destination by associating with the cytoskeleton (Echard et al., 1998). Rabs can regulate vesicle targeting by recruiting docking complexes. In yeast, the GTP-Sec4p interacts with Sec15p, a component of exocyst (Guo et al., 1999b), leading to the assembly of the exocyst and binding to Sec3p, which marks the exocytic sites at the PM. It is also reported that Rabs can influence vesicle fusion, via their effects on SNARE family members. A good example is the interaction of the Rab5 effector EEA1 with Syntaxin-13, which is required for homotypic EE fusion (McBride et al., 1999). One group of Rab effectors that have been recently identified are the Rab11 Family Interacting Proteins (Rab11-FIP family). These proteins interact with Rab11 through a conserved Rab11 Binding Domain (RBD) at the C-terminus (Hales et al., 2001; Prekeris et al., 2001) (see section 1.3.5).

1.3.3 Endosomal Rabs

Endocytic vesicles transit diverse pathways to deliver and retrieve cargo from organelles. Twelve Rab proteins have been localised to the endocytic pathway of mammalian cells, among which four are epithelial specific. So far, eight of these endocytic Rabs have been functionally characterised.

Figure 1.5 B is a schematic illustrating the present view of Rab-regulated endocytic pathways. In the first step of internalization, ligands are sequestered into clathrin-coated pits at the PM. Rab5 activity is important for this step and also for the subsequent homotypic fusion between the vesicles and the fusion of vesicles with the EE (McLauchlan et al., 1998). Rab21 has also been shown to predominantly localise to the early endocytic pathway and to regulate endocytosis and degradation of transferrin and epidermal growth factor (EGF) (Simpson et al., 2004). It was discovered lately that Rab21 has a function in regulating cell adhesion and motility via influencing on the endo/exocytic traffic of integrins (Pellinen et al., 2006). After entering EE, ligands can exit this compartment via several different pathways. A direct pathway for recycling receptors from EE back to the PM is mediated by Rab4 (Daro et al., 1996), which regulates the direct return of recycling cargo to the PM from the EE. Interestingly, Rab5 and Rab4 share common effectors (Mohrmann and van der Sluijs, 1999). Disruption of these Rabs leads to morphological

changes and trafficking defects of the EE (Chavrier et al., 1997). Hence, Rab5 and Rab4 act together to control influx into and efflux out of EE respectively.

In contrast to the EE to PM trafficking route regulated by Rab4, a slower recycling pathway, traversed by transferrin receptors and recycling membrane lipids, leads to the PM from EE via compartments called recycling endosomes (RE). The RE constitutes a distinct endocytic compartment characterized by a discrete protein composition and function (Daro et al., 1996; Sheff et al., 1999); Rab11 is the main resident and regulator of the trafficking through the RE. This compartment constitutes a slowly recycling pathway to the PM, and is also implicated in exocytic membrane transport from the Golgi (Chen et al., 1998; Urbe et al., 1993). Disruption of Rab11 by expressing its GTP deficient mutant Rab11 (S25N) causes accumulation of transferrin and transferrin receptor in the EE.

Rab7 regulates trafficking routes between EE and LE, which mediate transport of molecules destined for degradation. Rab7 also acts downstream of LE to control transport from LE to lysosomes in conjuction with its effector RILP (Cantalupo et al., 2001). Trafficking between the TGN and LE is marked by cation-independent mannose 6-phosphate receptor and furin, and is regulated by Rab9 (Lombardi et al., 1993).

1.3.4 Rab11 subfamily

Rab11 was first isolated from bovine brain membranes in 1988 (Kikuchi et al., 1988), and the human homologue of Rab11 was characterized by Drivas and co-workers in 1991 (Drivas et al., 1991). The mammalian Rab11 family consists of three members Rab11a, Rab11b and Rab25. Among these proteins, Rab11a has been the most extensively studied, with well established roles in regulating trafficking from the RE to TGN and PM (Ren et al., 1998; Ullrich et al., 1996). Rab11a and b are highly homologous (89% identity), and differences in protein sequence are only found at the C-terminal hypervariable region, which normally associates with its specific target membrane (Schlierf et al., 2000).

As briefly mentioned in 1.3.1, Rab11a mainly localises to the pericentriolar RE, where it partially co-localises with the TfR and regulates membrane trafficking through these compartments (Ullrich et al., 1996). Besides it is also involved in TGN and secretory vesicle trafficking in PC12 cells (Urbe et al., 1993), translocation of secretory vesicles in gastric parietal cells and glands (Calhoun et al., 1998), the recycling of the IgA receptor in MDCK cells (Wang et al., 2000), and phagocytosis and membrane extension in macrophages (Cox et al., 2000). Intriguingly, as described in 1.2.2, Rab11 has been shown

to play an essential role in *Drosophila* cellularisation, strongly suggesting that Rab11 regulated membrane trafficking plays a role in animal cytokinesis, which is a major lead this study follows. A study of Rab11b revealed it localises to a pericentriolar recycling compartment and is involved in regulating internalised Tf recycling back to the PM. Expression of GTP form (Q70L) and GDP from (S25N) of Rab11b both strongly interferes Tf trafficking (Schlierf et al., 2000).

Rab25 is expressed exclusively in epithelial cells and it localises to an apical pericentriolar endosomal compartment in MDCK cells. Disruption of Rab25 inhibits basolatral to apical transcytosis (Goldenring et al., 1993). Interestingly, Rab25 mRNA level selectively increased in epithelial ovarian cancers and its overexpression increases cell proliferation and inhibits apoptosis and anoikis (Cheng et al., 2004),.

1.3.5 Rab11 effectors

The complex localisations profiles and functional diversity of Rab11 is probably due to its association with multiple downstream effectors. The first Rab11 binding protein (Rab11BP) or rabphilin 11 was isolated from bovine brain and interacted with GTP-bound form of Rab11a. This protein localises to pericentriolar recycling compartments in MDCK and HeLa cells, and is involved in Tf recycling and membrane turnover events (Mammoto et al., 1999). The second Rab11 effector identified, Myosin Vb, interacts with all the members of the Rab11 family and overexpression of its truncation mutant lacking a motor domain retards trafficking through the PM recycling systems (Lapierre et al., 2001).

More recently, a family of Rab11 interacting proteins has been identified: the Rab11-FIPs (Rab11 Family Interacting Proteins). These include Rab11-FIP1, FIP2, FIP3, FIP4, pp75/Rip11 and RCP (Hales et al., 2001; Lindsay et al., 2002). Their binding to Rab11 is dependent on a C-terminal amphipathic α-helical motif known as the Rab11-binding domain (RBD), which is present in neither Rab11BP/Rabphilin nor Myosin Vb (Prekeris et al., 2001). This family can be further classified into three sub-groups. Class I, Rip11, FIP2 and RCP, which contain a C2 domain; Class II, FIP3 and FIP4 which have EF-hand domains and a proline rich region; Class III, with a solo member FIP1, which lacks any other conserved domain (Prekeris, 2003). Rab11-FIP1, FIP2 and pp75/Rip11 colocalise with Rab11 in the RE in both non-polarized HeLa cells and polarized MDCK cells. Another member, RCP, localises to EE and overexpression of its mutant strongly perturbs recycling through this compartment (Lindsay et al., 2002). Some members of the FIP family can also bind to other Rabs besides Rab11, such as Rab4 or Rab25, see Table 1.1.

Interestingly, Rab11-FIP3 and FIP4 are identical to Arfophilin and Arfophilin2, which were originally identified as Arf5 effectors in a yeast two-hybrid screen (Hickson et al., 2003; Shin et al., 1999). It was subsequently shown that they are also able to interact with Arf6, which bring a focus of integrating signals from Rab and Arf pathways in trafficking events (Fielding et al., 2005). These two FIP proteins were found to localise to the cleavage furrow during cytokinesis, which is distinct of other Rab11 binding proteins. Considering Rab11 play a crucial role in *Drosophila* cellularisation, it is intriguing to suggest that FIP3 and FIP4 might mediate this function of Rab11, which will be discussed in detail in section 1.4.

Rab11-FIPs	Rab binding	Arf binding	Localisation	Function
Rip11	Rab11	No	RE	Endosomal Recycling
RCP	Rab11 and 4	No	EE	Endosomal Recycling
Rab11-FIP1	Rab11	No	RE	Endosomal Recycling
Rab11-FIP2	Rab11	No	RE	Endosomal Recycling
Rab11-FIP3	Rab11 and 25	Arf5 and 6	RE and cleavage furrow	?
Rab11-FIP4	Rab11	Arf5 and 6	RE, focal adhesion and cleavage furrow	?

Table 1.1 Rab11-FIP family binding specificity and localisation

1.3.6 The ADP-ribosylation factor (Arf) family

ADP-Ribosylation Factors (Arfs) are another family of small guanine-nucleotide binding proteins belonging to the Ras superfamily (Verbrugghe and White, 2004). The human Arf family consists of three different groups of proteins: the Arfs, Arf-like (Arls), and SARs (Kahn et al., 2006).

The Arfs were originally purified from rabbit liver and bovine brain membranes as cofactors required for stimulation of cholera toxin-catalyzed ADP-ribosylation of Gs *in vitro* (Kahn and Gilman, 1984). Six mammalian Arf have been identified. The combination

of protein sequence comparison and structure lead to further classification of the six mammalian Arfs into three classes: Class I includes Arf1, Arf2 and Arf3; Class II Arf4 and Arf5; Class III has only one member, Arf6. Phylogenetic analyses indicate that these three classes of Arf diverged early, as there are representatives of each of the three classes in *Drosophila* and *C. elegans* (Kahn et al., 2006). In 1991, cloning of an essential gene in *Drosophila* that encoded a protein sharing homology with Arfs (50-60% identity), but lacks activity as cholera toxin cofactor and unable to activate PLD led to the name of Arf-like protein (Tamkun et al., 1991). Arl2 is the best-characterized Arl protein, and it regulates the folding of β-tubulin. Recent data also showed that Arl1 and Arf-related protein 1 (ArfRP1) localise to the TGN and regulate the teathering of endosome-derived transport vesicles (Burd et al., 2004). SAR protein was named following its identification as a secretion-associated and Ras-related protein. Two mammalian SAR proteins were characterised, sharing about 90% identity (Kuge et al., 1994). SAR proteins function through the recruitment of coat proteins or complexes to initiate vesicle budding similar to Arfs, though they only share <30% identity with Arfs and Arl.

As GTPases, the Arfs function as molecular switches by cycling between a GTP-bound active and GDP-inactive form. The exchange of GDP for GTP on Arfs allows them to associate with membranes, where they carry out their functions. *In vivo*, this cycle is massively accelerated by the presence of two families of Arf regulators, the Guanine-nucleotide Exchange Factors (GEFs) and the GTPase Activating Proteins (GAPs). The GEFs function by catalyzing the exchange of GDP for GTP, therefore activating the Arfs (Jackson and Casanova, 2000). The GAPs catalyse the intrinsic GTPase activity of the Arfs to return the GTP-bound form back to the inactive GDP bound form (Moss and Vaughan, 1998).

Among the mammalian Arfs, Arf1 has been the most extensively studied. It localises to the Golgi complex in its GTP-bound, myristoylated form (Liang and Kornfeld, 1997) and is involved in vesicle budding by recruiting numerous coat protein complexes including coat protein I (COPI) as well as the clathrin adaptors AP-1, AP-3 and AP-4 (Boman and Kahn, 1995; Donaldson and Jackson, 2000). The biological functions of Class II Arfs remain unclear. The only member of Class III Arf, Arf6, is the most divergent member of Arf family with only 64-69% identity to the other Arfs. Both its cellular localisation and function are distinct from the Class I and Class II Arfs as described in 1.3.6.

1.3.7 Arf6

Arf6 is the most divergent member of the Arf family. It has different distribution and function compared to other members. There are homologues of mammalian Arf6 in almost all eukaryotes including *Xenopus*, *Drosophila*, *C. elegans* and *S. cerevisiae*. A signature dipeptide sequence (Gln-Ser) adjacent to the Switch I domain allowed homologues of Arf6 to be identified. So far, three Arf6-specific GEF have been identified, ARNO, EFA6 and Arf-GEP100. In contrast to other Arf GEFs, these Arf6 GEFs generally are not inhibited by BFA (Donaldson, 2003).

As described in 1.3.6, class I Arfs mainly localise to TGN and are involved in vesicle formation at this site. In contrast, most Arf6 is present at the PM and to some extent on endosomal compartments where it regulates the flow of trafficking into and out of the cell and actin cytoskeleton dynamics at the PM (Donaldson, 2003). The pI of Arf6 is in the range of 8.5-9.5, while other Arfs range from 6.0-7.0, which might explain why a large amount of Arf6-GDP is also retained on the membrane. It is believed that this positive charge together with N-terminal myristation is responsible for targeting Arf6 to the PM. The ability of Arf6 to modulate cortical actin remodelling and to mediate cell shape changes and migration has also been well recognized.

In HeLa and other types of epithelial cells, Arf6 localises to a distinct endosomal compartment that contains membrane proteins endocytosed into cells independently of AP-2 and clathrin (Radhakrishna and Donaldson, 1997). This Arf6 regulated endosomal pathway is distinct from the classical, transferrin-containing endosomal system and the trafficking route followed by a number of PM proteins including major histocompatibility complex class I protein (MHCI) (Radhakrishna and Donaldson, 1997) and integrins (Brown et al., 2001). A current model of Arf6 action suggests that it cycles between the PM pool and an intracellular pool that can be referred to as the "Arf6 endosome". From this endosome, a proportion of Arf6 and cargo returns directly to the surface, while the remainder merges with the EE from where it is trafficked back to the surface by a route that has not yet been fully identified (Donaldson, 2002). This could be directly from the EE to the cell surface or, or may firstly cycle via the RE and then return to the cell surface (Chavrier and Goud, 1999). In this way it may exert its effects on both the vesicle trafficking/recycling system and the actin cytoskeleton underlying the PM. In addition, Arf6 also plays role in Fc-mediated phagocytosis (Zhang et al., 1998), GLUT 4 translocation (Millar et al., 1999) and exocytosis (Caumont et al., 1998).

The effect of Arf6 on cell shape and cell migration is mediated through its regulation of cortical actin. Arf6 was first observed to stimulate generation of protrusions (Radhakrishna et al., 1996). More studies subsequently showed that its ability to stimulate actin polymerization at discrete site on the PM is also required for cell spreading (Song et al., 1998), wound healing (Santy et al., 2001), cell migration (Palacios et al., 2001) and Rac-induced ruffling (Radhakrishna et al., 1999). It is interesting that Rac-mediated membrane ruffling requires non-Rho family GTPase, Arf6 activity, suggesting a crosstalk between two GTPases families (Radhakrishna et al., 1999). Arf6 can also regulate cortical actin cytoskeleton by affecting membrane lipid composition. In mammalian cells, Arf6 localises with PIP5-kinase, and activates PIP5 to generate phosphatidylinositol 4, 5-bisphosphate (PIP_2). PIP_2 recruits and influences the activity of several actin-binding proteins, which mediate the cortical actin network (Yin and Janmey, 2003).

Recently, it was reported that Arf6 redistributes in mitotic cells (Schweitzer and D'Souza-Schorey, 2002), concentrating adjacent to the cleavage furrow. Interestingly, overexpression of constitutively activated Arf6, (Q67L) revealed its marked localisation at the edge of the cleavage furrow and midbody site throughout the late stage of mitosis. High-level expression of Arf6 (Q67L) mutant results in severe cytokinetic defects, whereas low-level expression of these mutants did not show significant effects. This suggests the existence of alternative mechanisms underlying membrane traffic to the furrow site during cytokinesis. Because actin accumulation and phospholipid metabolism at the furrow site remains normal in cells expressing the mutants, it is believed that Arf6 may act during cytokinesis via machinery distinct from those operative in interphase cells.

1.4 Dual Rab and Arf interaction proteins: Rab11-FIP3 and Rab11-FIP4

1.4.1 Rab11 and Arf interacting proteins

Both Arfophilin (Rab11-FIP3) and Arfophilin 2 (Rab11-FIP4) were originally identified by their interaction with GTP-Arf5 in yeast-two-hybrid screens. Using constitutive activated Arf5 (Arf5 Q67L), Shin and colleagues identified Arfophilin as an 82.4 kDa novel Arf5 interacting protein (Shin et al., 1999). This finding is particularly interesting because class II Arfs were assumed to play only supplementary roles to the more abundant class I Arfs. Subsequent experiments by the same researchers revealed that Arfophilin also interacts with Arf6 in a glutathione S-transferase (GST) pulldown assay (Shin 2001). More recently,

two laboratories showed that Arfophilin can bind to Rab11-GTP and was named as Eferin and Rab11-FIP3 (Hales et al., 2001; Prekeris et al., 2001).

Similarly, our group identified a homolog of Arfophilin, termed Arfophilin 2 (Rab11-FIP4), also from a yeast-two-hybrid assay by using GTP-Arf5 as bait. Arfophilin 2 migrates on SDS gels at approximately 62 kDa and exhibits most homology with Arfophilin in the 300 amino acids at the C-terminus (63% identity, 79% homology), as indicated in Figure 1.6. The same study showed that it can also bind to Rab11 in a GTP dependent manner (Hickson et al., 2003). For clarity, these proteins will be addressed as FIP3 and FIP4 throughout this thesis. During the course of this study, using recombinant bacterially expressed proteins our group showed that FIP3 and FIP4 exhibit preferential binding to the three GTPases with which they interact: FIP3 has the binding preference Rab11>Arf6>>Arf5. In contrast, FIP4 interacts Arf6>>Rab11=Arf5. Intriguingly, both FIP3 and FIP4 bind to Rab11 and Arf6 at distinct sites, suggesting the FIPs may interact with the two GTPases simultaneously and may form a tenary complex *in vivo* (Fielding et al., 2005). Both FIP3 and FIP4 contain a Rab11 binding domain (RBD) identified by Prekeris (Prekeris et al., 2001). The RBD is a 20-amino acid motif located at the extreme C-terminus of the FIP proteins, which mediates the interaction between Rab11 and FIP3 or FIP4. Point mutations of a crucial amino acid in this region, FIP3 (I737L) and FIP4 (D538A) impair the abilities of the FIPs to bind to Rab11. In contrast, these mutants do not affect their interaction with Arf6, further supporting the idea that the binding sites in FIPs for Rab11 and Arf6 are distinct.

Binding of Arf5 and Arf6 to FIP3 is dependent on two different sequences on the Arf proteins; amino acids 2-17 in the case of Arf5 and amino acids 37-80 in the case of Arf6; these sequences are not homologous to each other. Both the Arfs interact within the same region of the FIP3 C-terminal domain, amino acids 612-756, and they may be two distinct binding sites within this region for binding to Arf5 and Arf6 separately (Shin and Exton, 2001). The domains involved in FIP4 binding to the Arf proteins remain unknown.

1.4.2 Subcellular localisation

Studies from our group of FIP4's localisation suggest several potential roles for this protein in membrane trafficking. During interphase, FIP4 was shown to localise to a perinuclear compartment, which partially overlapped with TfR and CI-MPR. In contrast, its overlap with early endosome markers such as EEA1 or RME1 was limited. In the perinuclear region, FIP4 also colocalises extensively with its binding partner Rab11

(Hickson et al., 2003), suggesting that FIP4 associates with RE but not EE, and may act as an effector of Rab11 in this compartment. A BFA-sensitive pool of FIP4 was also identified, which is similar to FIP3. Similarly, FIP3 colocalises with Arf5 to intracellular membranes, particularly the Golgi and possibly endosomes, suggesting a function in vesicle trafficking at these sites. Unpublished immunofluorescence results also showed that FIP4 partially overlaps with Arf6 at a peri-centrosomal area and focal adhesion, which might imply a role of FIP4 in cell ruffling or migration by interplaying with Arf6 (Fielding, 2005).

Interestingly, both FIP3 and FIP4 redistribute to the centrosomes shown by localisation with γ-tubulin in metaphase. Subsequently, they become strikingly concentrated at the furrow and decorate the ends of the midbody bridge during cytokinesis (Hickson et al., 2003). These localisations have only been seen in the case of FIP3 and FIP4 but not any other Rab11 interacting proteins. This observation implies that FIP3 and FIP4 redistribution in cytokinesis may be regulated by the mitotic machinery and are involved in this process (see 1.4.4).

1.4.3 Homology with Nuclear Fall Out (Nuf)

Interestingly, bioinformatics analysis reveals that FIP3 and FIP4 share high homology with the C-terminal ~300 amino acids of Nuf in regions predicted to form coiled-coils, whereas the N-termius is more divergent. As shown in Figure1.6, alignment of protein sequences of FIP3 (Arfo1), FIP4 (Arfo2) and Nuf revealed that they share greatest homology in their C-terminus. The residues shown in italics at the extreme C-terminus indicate the minimal RBD necessary to bind Rab11 (Prekeris et al., 2001). Over-expression of GFP-Nuf in mammalian interphase cells shows the same localisation with FIP4, and alters the morphology of endosomes similar to FIP4, suggesting that Nuf and FIP4 are functionally related (Hickson et al., 2003).

Previous reports demonstrated that Nuf physically associates with Rab11 and that they colocalise extensively at the centrosomes and subsequently at the cleavage furrow during *Drosophila* embryo cellularisation (Riggs et al., 2003). This colocalisation is mutual, as disruption of either Nuf or Rab11 led to mis-localisation of the other protein. The association of Nuf and Rab11 is essential for cellularisation, similar defects in actin and membrane recruitment at the furrow site and furrow formation were observed in both Rab11-deficient and *nuf*-derived embryos.

1.4.4 Potential cellular functions

Bioinformatics analysis of FIP3 and FIP4 revealed that they are hydrophilic with no potential signal sequences or transmembrane domains. Neither of the FIPs possesses the sec7 domains characteristic of Arf guanine nucleotide exchange factors, nor do they have the characteristics of Arf GTP activating proteins, suggesting that they are unlikely to be direct regulators of the Arf GTPase cycle.

Cellular localisations of these proteins provide clues to their functions. Both FIP3 and FIP4 partially colocalise with Rab11 on the RE and Arf5 on the TGN, suggesting they may have a role at these trafficking steps. One possibility is that they function as coordinators responsible for the crosstalk between these compartments. The most intriguing hypothesis comes from the localisation of FIP3 and FIP4 to centrosomes and furrow/midbody during cell division. This characteristic distribution is reminiscent of other molecules that have been shown to be important for cytokinesis, suggesting a role of these two proteins in cell division. Interesting, FIP4 is most abundant in testis, a tissue with a high degree of cell division. This idea is further supported by the fact that FIP3 and FIP4 share high homology with Nuf, Figure 1.6, which is required for *Drosophila* embryo cellularisation and associates with Rab11. In addition, FIPs interact and colocalise with Rab11. Disruption of Rab11 in both *Drosophila* and *C. elegans* leads to a cytokinesis failure. Overall, the homology, association with Rab11 and similar localisation of Nuf and FIPs all point to the hypothesis that they may be functional mitosis counterparts in flies and mammalian cells. This prompted us to investigate the functions of FIPs and their interaction partners in the process of mammalian cytokinesis.

1.5 Summary and Aims

To summarise, cytokinesis is the final step of mitosis, and is an important process for all organisms. Recent research has shown that cytokinesis is not simply a ripping apart of the two daughter cells, but a sophisticated process co-ordinating a variety of events such as membrane trafficking, cytoskeleton remodelling and vesicle fusion.

This study mainly focused on the roles of the GTPases, Rab and Arf, in mammalian cytokinesis. Because both Rab and Arf proteins have been established as key regulators of intracellular trafficking, this study will better our understanding of membrane trafficking events regulated by Rab and Arf in this process and further our understanding of the trafficking mechanisms that underlie cytokinesis. The main aims of this study are, first, to

determine the localisation of Rab and Arf GTPases throughout mitosis in mammalian cells. Second, to discover the potential function of these GTPases in cytokinesis. Third, to investigate the function of interaction among Rab, Arf and FIP3/4 in mammalian cytokinesis.

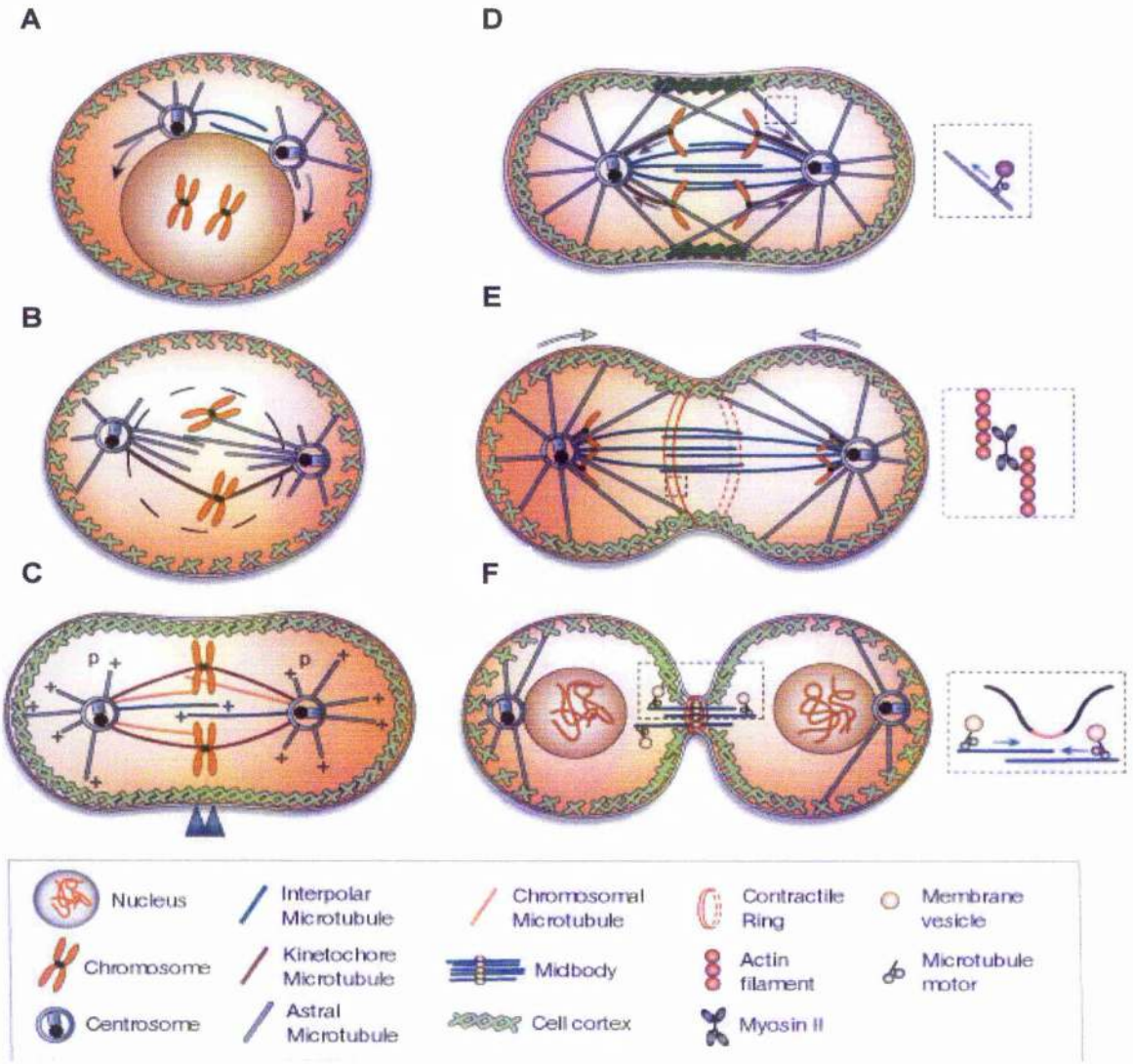

Figure 1.1 Mammalian cell division

(A) During prometaphase, the DNA condenses and two centrosomes start to migrate in opposite directions. **(B)** Condensed chromosomes are attached to the mitotic spindle microtubules and align at the midzone of the mitotic spindle in metaphase. **(C-E)** In anaphase, the cell starts to elongate and the furrowing site is positioned where the double blue arrows indicate. Cytoskeleton remodelling occurs at the cleavage furrow site and the acto-myosin ring is assembled at the midzone. The contractile ring then begins to contract, which leads to furrow ingression. **(F)** During telophase/cytokinesis, the acto-myosin ring finishes constricting which leads to formation of the midbody. The new nuclear envelope is developed and the condensed chromosomes return to loose DNA state. These schematic pictures are from Scholey, et al., 2003.

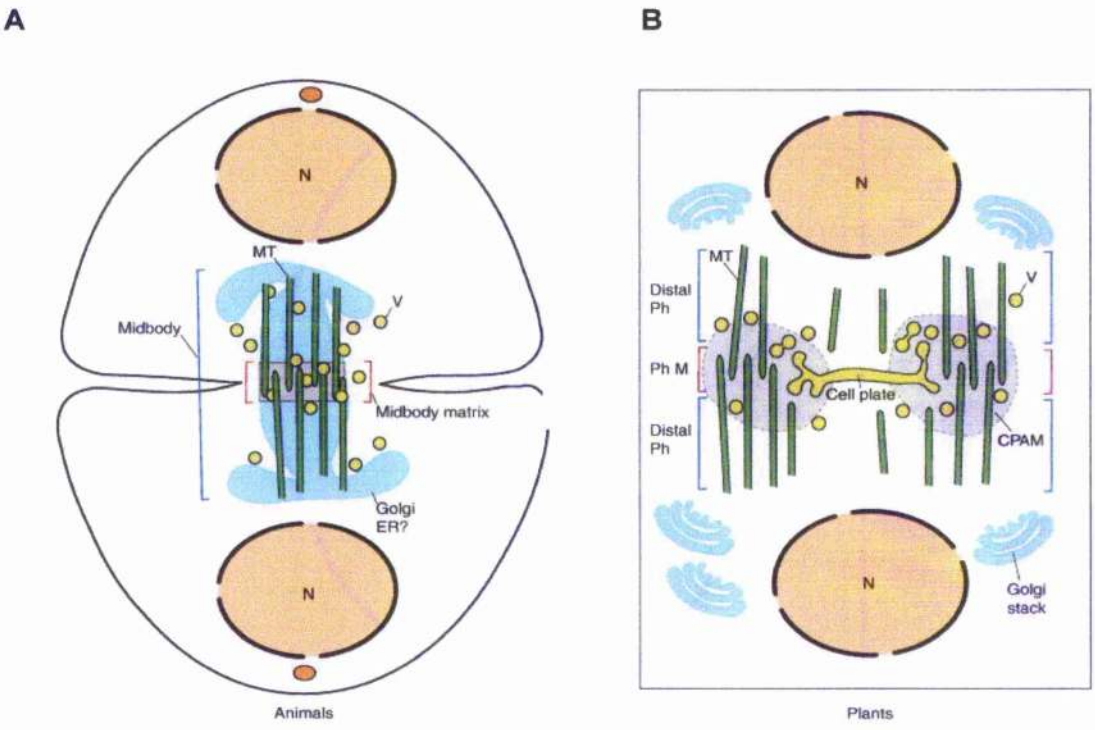

Figure 1.2 Animal and plant cell cytokinesis

Comparison of animal and plant cytokinesis: **(A)** Cytokinesis in animal cells. The spindle midzone is condensed into a narrow canal consisting of antiparallel microtubules (MT) and associated proteins. Membrane derived from Golgi may contribute to the midbody abscission. RE membrane vesicles (V) travelling along microtubules may also facilitate sealing of the intercellular canal. **(B)** Cytokinesis in somatic plant cells. A specialized structure called the phragmoplast is formed at the site of the future cell wall. The phragmoplast is divided into midline (Ph M), where the opposing microtubules interdigitate and distal phragmoplast (Distal Ph), located at the two sides of the midline. Golgi-derived membrane vesicles are the primary origin for membrane required during phragmoplast formation. A filamentous cell-plate assembly matrix (CPAM) accumulates at the midline. **(C)** Cellularisation of *Drosophila* syncytial blastoderm. Following migration of nuclei to the surface, furrow ingression occurs around each nucleus. Membrane trafficking is required for furrow formation and ingression. A and B are cited from Otegui et al., 2005; C is cited from Finger. F. and White. J., 2002.

A

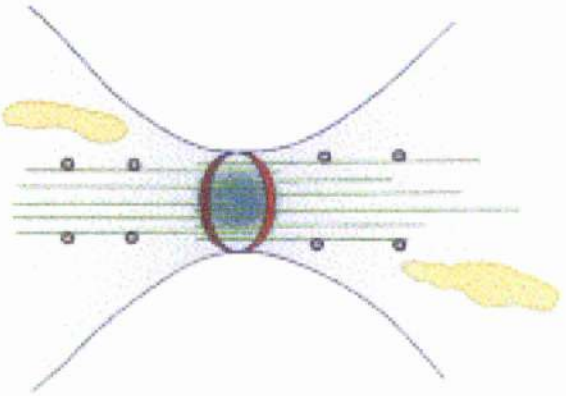

B

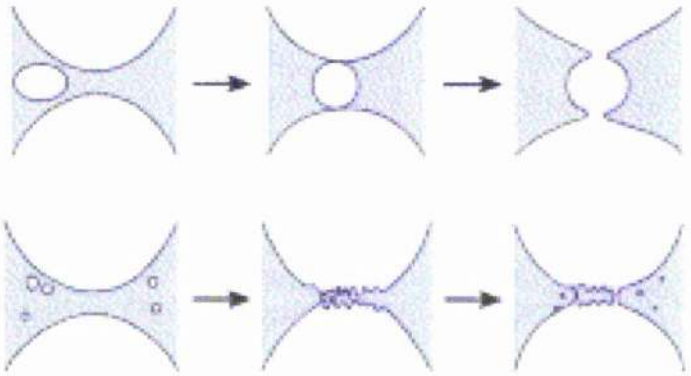

Figure 1.3 Midbody abscission in animal cells

(A) The cytoplasmic intercellular bridge of a dividing animal cell. The contractile ring (red) and the central spindle microtubules (green) must disassemble and the intercellular canal must be sealed, which requires membrane insertion. The inserted membrane may be Golgi or RE derived vesicles transported along the midzone microtubules or in the form of larger vesicles (yellow). **(B)** Two proposed models describing vesicles targeting to the midbody. Top panels: A large vesicle, which probably formed by fusion of many small vesicles moves to the furrow and fuses with the PM and seals the intercellular canal. Bottom panels: Smaller vesicles travel to the furrow region individually and fuse, gradually constricting the canal. The cartoons are cited from Finger. F. and White J., 2002.

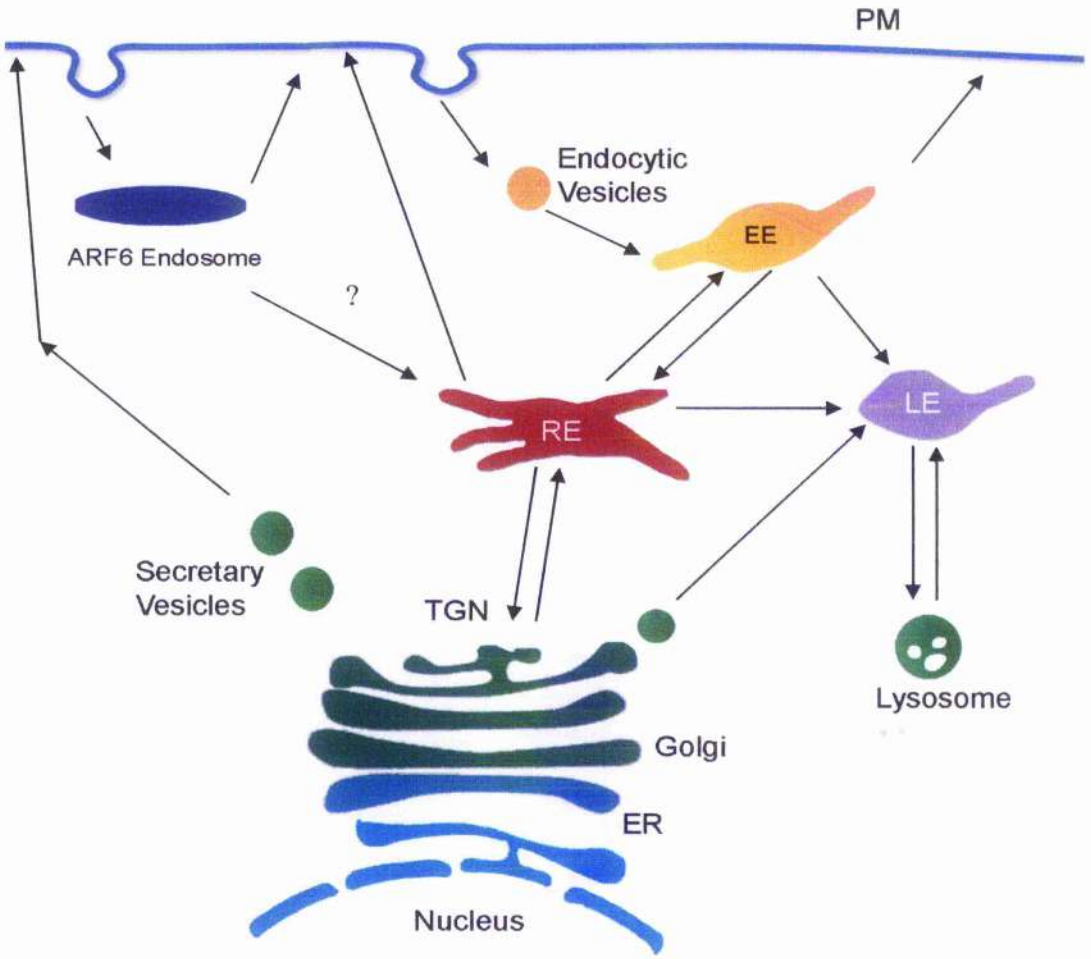

Figure 1.4 Schematic of intracellular membrane-trafficking pathways

The secretory and endocytic pathways are shown in this figure. The secretory pathway allows newly synthesized proteins or lipids to travel from the ER to the Golgi, and then to the PM as the arrows indicate. The endocytic pathway includes early endosomes (EE), recycling endosomes (RE) and late endosomes (LE). Cargoes internalized from the extracellular environment enter the endocytic pathway from the PM to the EE (yellow) first; after sorting, the cargoes can be delivered to the RE (red) and then cycled back to the PM. Alternatively they can be transported to the LE (purple) and lysosome (green) for degradation. ARF6 regulated endosomes (dark blue) (see 1.3.7) are distinct from the classic endocytic routes, but they may crosstalk with EE and RE. Crosstalk between the secretory and endocytic pathway occurs between individual compartments as the arrows indicate.

A

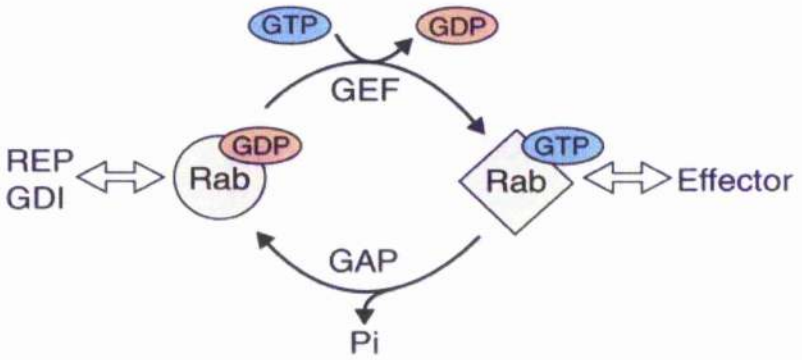

B

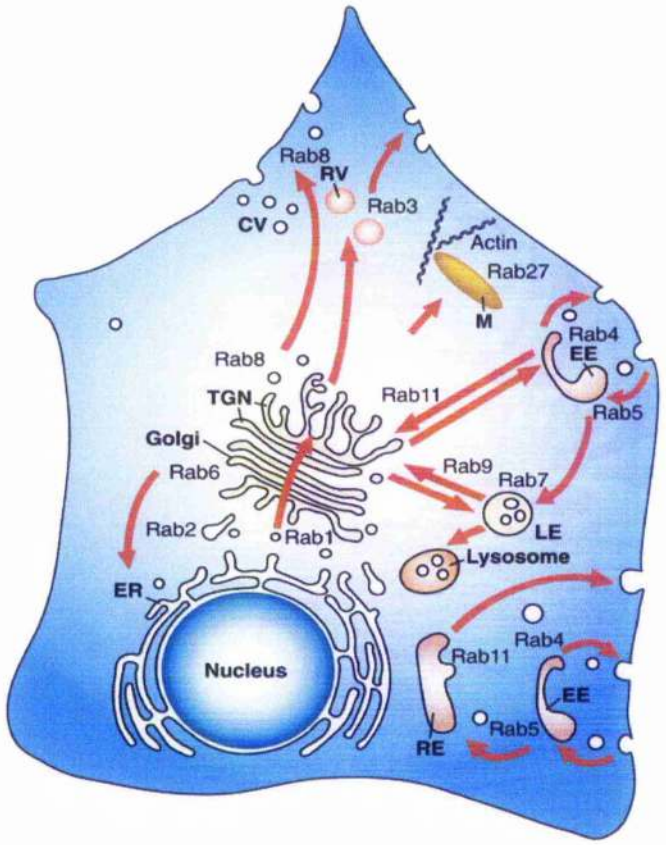

Figure 1.5 Rabs: GTPase cycle and intracellular distribution and functions

(A) The Rab GTPase switches between GDP and GTP bound forms. Conversion from GDP-bound Rab to GTP is catalyzed by GDP/GTP exchange factor (GEF), while GTP hydrolysis is favoured by GTPase-activating protein (GAP). The GTP-Rab can recruit specific effectors and carry out cellular functions. The GDP-Rab is associated with Rab escort protein (REP) and GDP dissociation inhibitor (GDI). **(B)** Intracellular localisation of Rab proteins in non-polarised cells. Individual Rabs decorate distinct membrane compartments and regulate intracellular trafficking through them. Both schematic pictures are cited from Stenmark and Olkkonen, 2001.

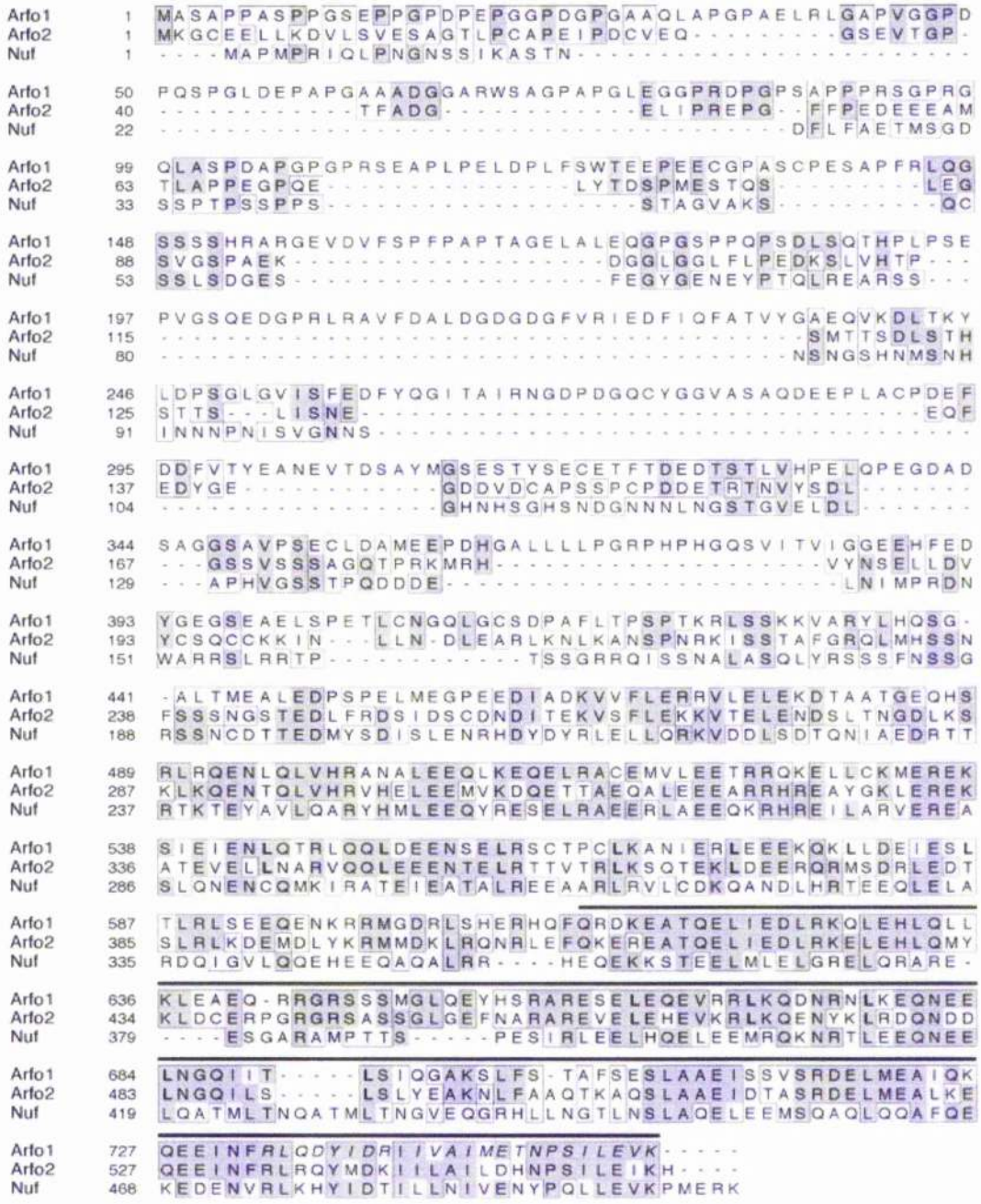

Figure 1.6 A ClustalW alignment of protein sequences of FIP3 (Arfo1), FIP4 (Arfo2) and Nuf

The three proteins share high homology at the C-terminus, while exhibiting more variance at the N-terminus. Shaded boxes highlight the residues identical in at least two proteins, and open boxes mark the homologous residues. The part with bold line is the ARF binding domain reported previously (Shin 1999). The minimal Rab11 binding domain (RBD) is in italic font (Prekeris, 2001). 26% of the whole sequence is identical across three proteins, while 63% identity was discovered between the FIP3 (Arfo1) and FIP4 (Arfo2) proteins. The alignment is cited from Hickson et al., 2003.

2 Materials and Methods

2.1 Materials

All materials used in this study were of a high quality and were obtained from the following suppliers:

Abgene (Abgene ABgene House, Epsom, UK)

Thin wall PCR tubes (0.2 ml)

Amersham Pharmacia Biotech (Little Chalfont, Buckinghamshire, UK)

Horseradish peroxidase (HRP)-conjugated donkey anti-rabbit IgG antibody

Horseradish peroxidase (HRP)-conjugated sheep anti-mouse IgG antibody

ECL Western blotting detection reagents

Glutathione sepharose 4B

Ambion (Austin, USA)

Nuclease-free water

Silencer siRNA Construction Kit

Bio-Rad Laboratories Ltd. (Hemel Hempstead, Hertfordshire, UK)

N, N, N', N' – tetramethylethylenediamine (TEMED)

Dharmacon (Lafayette, Colorado, USA)

All siRNA duplexes (except Arf6 and FIP4)

Eppendorf (Barkhausenweg, Hamburg, Germany)

Cellocate coverslips

Microloader tips

Femtotips

Fisher Scientific Ltd. (Loughborough, Leicestershire, UK)

Ammonium persulphate

Calcium chloride ($CaCl_2$)

Diaminoethane tetra-acetic acid, Disodium salt (EDTA)

Disodium hydrogen orthophosphate (Na_2HPO_4)

Glycerol

Glycine

N-2-hydroxyethylpiperazine-N'-2-ethanesulphonic acid (HEPES)

Hydrochloric acid (HCl)

Isopropanol

Magnesium Sulfate ($MgSO_4$)

Methanol

Potassium chloride (KCl)

Invitrogen (Paisley, Scotland, UK)

Dulbecco's modified Eagle's medium (without sodium pyruvate, with 4500mg/L glucose) (DMEM)

Dulbecco's modified Eagle's medium (without sodium pyruvate, with 4500mg/L glucose, with 25mM Hepes)

Opti-MEM

Foetal bovine serum (FBS)

10000U/ml penicillin, 10000U/ml streptomycin

Trypsin/EDTA solution

Lipofectamine 2000

Agarose

Sf-900 II Serum-Free Insect Cell Culture Media

Spodoptera frugiperda insect cells

Molecular Probes (Oregon, USA)

Alexa^{488}-conjugated donkey anti-mouse IgG secondary antibody

Alexa^{488}-conjugated donkey anti-rabbit IgG secondary antibody

Alexa^{488}-conjugated donkey anti-sheep IgG secondary antibody

Alexa^{594}-conjugated donkey anti-mouse IgG secondary antibody

Alexa^{594}-conjugated donkey anti-rabbit IgG secondary antibody

Alexa^{594}-conjugated donkey anti-sheep IgG secondary antibody

Alexa^{594}-conjugated donkey anti-rat IgG secondary antibody

Texas-Red-Transferrin

DAPI (4',6-Diamidino-2-phenylindole)

MWG-Biotech (Anzingerstr, Ebersberg, Germany)

oligonucleotide primers for siRNA of Arf6 and FIP4

New England Biolabs (UK) Ltd (Hitchin, Hertfordshire, UK)

Pre-stained protein marker, broad range (8-175 kDa)

Pierce (Rockford, Illinois, USA)

Slide-a-lyzer^{TM} dialysis cassettes

Promega (Southampton, UK)

All restriction enzymes

AMV reverse transcriptase

Pfu polymerase

Taq polymerase

Deoxynucleotide triphosphates (dNTPs)

Qiagen (Crawley, West Sussex, UK)

QIAprep™ spin miniprep kit

QIAprep™ spin maxiprep kit

Qiagen OneStep RT PCR kit

Roche (Mannheim Germany)

Complete EDTA-free protease inhibitor cocktail

Schleicher & Schuell (Dassel, Germany)

Nitrocellulose membrane (pore size: 0.45 μM)

Shandon (Pittsburgh, PA, USA)

Immu-mount™ mounting medium

Stratagene (La Jolla, CA, USA)

Pfu Turbo™ polymerase

Yorkshire Bioscience Ltd (Heslington, York, UK)

All oligonucleotide primers for RT-PCR

All remaining chemicals were supplied by Sigma Chemical Company Ltd, Poole, Dorset, UK.

***Escherichia coli* strains**

DH5α	F⁻ ϕ80d*lac*Z ΔM15 Δ (*lac*ZYA-*arg*F) U169 *rec*A1 *end*A1 *hsd*R17(r_{k-}, m_{k+}) *pho*A *sup*E44 λ⁻ *thi*-1 *gyr*A96 *rel*A1

DH10 Bac™	F⁻ *mcr*A (*mrr-hsd*RMS-*mcr*BC) ϕ80lacZΔM15 Δ*lac*X74 *rec*A1 *end*A1 *ara*D139 Δ(*ara, leu*)7697 *gal*U *gal*K λ⁻ *rps*L *nup*G /pMON14272 / pMON7124

Both strains were purchased from Invitrogen (Paisley, Scotland, UK).

Antigen	Source	Species	Dilution for Western Blot	Dilution for Immuno-fluorescence
Arf6	Gift, J.Donaldson	Rabbit	1:1000	1:200
Arf5	Home made, anti peptide	Sheep	1:500	1:200
FIP4	Home made (Characterised Hickson *et al*, 2003)	Sheep	1:500	1:200
Rab11	Zymed	Rabbit	0.4 μg/ml	1 μg/ml
Rab4	Abcam	Rabbit	0.2 μg/ml	1 μg/ml
Rab5	Santa-Cruz	Rabbit	0.2 μg/ml	1 μg/ml
Rab7	Abcam	Rabbit	0.5 μg/ml	N/A
Rab8	Abcam	Mouse	0.25 μg/ml	N/A
Rab9	Abcam	Mouse	0.2 μg/ml	N/A
Rab21	Abnova	Mouse	1 μg/ml	N/A
HA	Santa-Cruz	Mouse	0.2 μg/ml	1 μg/ml
c-myc	Santa-Cruz	Rabbit	0.2 μg/ml	1 μg/ml

Antigen	Source	Species	Dilution for Western Blot	Dilution for Immuno-fluorescence
Aurora B	Abcam	Rabbit	0.9 μg/ml	4.5 μg/ml
GAPDH	Ambion	Mouse	1:5000	N/A
α-tubulin	Sigma	Mouse	1:2000	1:3000

Table 2.1 Primary antibodies used for this study

Name	Plasmid	Insert gene
pEGFP-Rab11	pEGFP-N1	*Rab11*
pEGFP-Rab11 S25N	pEGFP-N1	*Rab11-S25N*
pcDNA-Rab4-c-myc	pcDNA3.1	*Rab4*
pcDNA-Rab4-S22N-c-myc	pcDNA3.1	*Rab4-S22N*
pcDNA-Rab5-c-myc	pcDNA3.1	*Rab5*
pcDNA-Rab5-S34N-c-myc	pcDNA3.1	*Rab5 S34N*
pEGFP-Rab7	pEGFP	*Rab7*
pEGFP-Rab9	pEGFP	*Rab9*
pEGFP-Rab21	pEGFP-C1	*Rab21*
pEGFP-Rab21-T33N	pEGFP-C1	*Rab21-T33N*
pEGFP-Rab22a	pEGFP	*Rab22a*
pEGFP-Rab22a-S19N	pEGFP	*Rab22a-S19N*
pcDNA-Arf6	pcDNA	*Arf6*
pcDNA-AFR6-T27N	pcDNA	*Arf6-T27N*
pcDNA-Arf6-Q67L	pcDNA	*Arf6-Q67L*
pEGFP-FIP3	pEGFP-N1	*FIP3*
pEGFP-FIP4	pEGFP-C2	*FIP4*
pFastBac-FIP4	pFastBac HT	*FIP4*

Table 2.2 Constructs used in this study

pEGFP-Rab11/Rab11-S25N: Rab11a/Rab11a S25N previously constructed in the lab were released from pGBT9 (CLONTECH) with Eco RI and Bam HI and cloned into pEGFP-N1 (BD Biosciences) with the same sites.

pcDNA-Rab4/Rab4-S22N: cDNA encoding Rab4a/Rab4a-S22N with a myc tag on the N-terminus were released from a pNot-Not plasmid (Gould lab) with Eco RV and then cloned into pcDNA3.1 (Invitrogen) with the same sites.

pcDNA-Rab5/Rab5-S34N: cDNA encoding Rab5/Rab5-S34N with a myc tag were released from pNot-Not with Eco RV and then cloned into pcDNA3.1 (Invitrogen) with the same sites.

pEGFP-Rab7 and pEGFP-Rab9: These constructs are kindly given by Dr. M. Seaman. (Addenbrooks Hospital, Cambridge, UK).

pEGFP-Rab21/Rab21-S33N: These constructs are as described in Simpson et al., 2004, and they are kindly given by Prof. Arwyn Jones (University College Wales, Cardiff, UK). Full-length Rab21 was generated by RT-PCR and cloned into the pEGFP-C1 vector using Bgl II and Hind III. Rab21 T33N was created by using the QuickChange PCR method and then cloned into the pEGFP-C1 (BD Biosciences).

pEGFP-Rab22a/Rab22a-S19N: These plasmids are kindly given by Dr. V. Olkkonen. (National Public Health Institute, Helsinki, Finland). Rab22a cDNA was amplified by PCR and subcloned into pEGFP-C1 (BD Biosciences) with Bam HI site. The Rab22a S19N mutant was obtained by site directed mutagenesis (QuickChange kit from Stratagene), and also cloned into pEGFP-C1 (BD Biosciences) with Bam HI.

pEGFP-FIP3: cDNA encoding full-length FIP3 was cloned into pEGFP-N1 (BD Biosciences) with Bam HI sites.

pEGFP-FIP4: The full-length FIP4 digested with Bam HI and Sal I from pPCRII (Invitrogen) was cloned in frame into the Bgl II and Sal I sites of pEGFP-C2 (BD Biosciences).

pFastBac-FIP4: cDNA encoding full-length FIP4 was cloned into pFastBac HT (Invitrogen) plasmid with Bam HI and Eco RI. The 6-His tag is present on the upstream of the inserted gene.

Gene	Target	Positions in Target Gene	Source
Rab11a	AATGTCAGACAGACGCGAAAA	539-559	Synthesized by using Silencer siRNA Construction Kit (Ambion)
Rab11b	AAGCACCTGACCTATGAGAAC	283-303	
Arf6	GCACCGCATTATCAATGACCG	309-329	
Arf5	TGCAGGAGGACGAGCTGCGGG	305-325	
FIP3	AAGGCAGTGAGGCGGAGCTGT	1183-1203	
FIP4-436	AACCGGCAAAAGTCCTTGAAG	436-456	
FIP4-1067	AAGTCATTGAGCAGGTTGATT	1067-1087	
FIP4-1654	AACAGCTTGTCCATCATGCGC	1654-1674	
Aurora B	CGCGGCACTTCACAATTGAT	266-286	Obtained from Dharmacon
Plk1	AAGCTCTTGGCAAAGCGCCC	1301-1321	
GAPDH	TGGTTTACATGTTCCAATA	230-248	

Table 2.3 Targets of RNAi duplexes used for this study

Gene	Forward Primer	Reverse Primer
Rab4a	ATGTCGCAGACGGCCATGTCC	GTACAAAACCCTCTTCTACA
Rab4b	GAAGACTGTGAAGCTACAG	CTGCCGAAGCTGGCGGA
Rab5a	TATCACAAATGAGGA	TGGCAGAATTTGCTCCTGG
Rab5b	CGTTATTGCCCTGGCAGGGA	GTTCTGCTGGGACTGTTCATG
Rab5c	CAGCTGCTGGGAACAAGATC	GAATTCCACGGCTCTCTTGC
Rab7	CTGACCAAGGAGGTGATGG	CTGGCCTGGATGAGAAACTC
Rab8a	CATCCGGAACTGGATTCGC	CTCTTCTGCTGCTCCGGTGTG
Rab8b	CCGAACAATCACGACAGCG	GGTCCACCTGCTCCTGCT
Rab9a	TACCCAGCTCTTCCATACA	GACTGTGTCTGTCTGAATCA
Rab9b	CCTGCTCTTAAAGGTCATTC	GGAGCCACTGTTCAAGTCA
Rab21	ACGGAAAATGTTGGGAAATG	TAGAGCCATTGCCTTTTGCT
Rab22a	CCAGTACCAAAATGAGCTAC	TTACCGCCAGATGGCAGGTT
Rab22b	GCCTTGTGGAAATGAACTTC	AGCATCCTTCAGGGGAACC

Table 2.4 PCR primers used in this study. All the sequences are given from 5' to 3'

General solutions

DNA loading buffer	40% (w/v) sucrose, 0.25% bromophenol blue
Immunofluorescence buffer	PBS plus 0.2% fish skin gelatin and 0.1% donkey or goat serum (according to the species in which the secondary antibody were raised in); freshly made and filtered through a Nalgene 0.2 μm vacuum type filter.
Lysis buffer	50 mM Hepes, 100 mM KCl, 5 mM NaCl, 1 mM $MgCl_2$, 0.5 mM EGTA, 1 mM EDTA, Complete™ EDTA-free Protease Inhibitor Tablets (Roche), 0.1% Triton-X, 100 1mM, DTT
PBST	PBS plus 0.1% (v/v) Tween-20
Phosphate buffered saline	136 mM NaCl, 10 mM NaH_2PO_4, 2.5 mM KCl, 1.8 mM KH_2PO_4, pH 7.4
SDS-PAGE electrode buffer	25 mM Tris, 190 mM glycine, 0.1% (w/v) SDS
SDS-PAGE sample buffer	93 mM Tris-Cl pH 6.8, 1 mM sodium EDTA, 10% (w/v) glycerol, 2% (w/v) SDS, 0.002% (w/v) bromophenol blue 20mM dithiothrietol
SOC media	0.5% Yeast extract, 2.0% tryptone, 20 mM glucose 10 mM NaCl, 2.5 mM KCl, 10 mM MgCl2, 20 mM MgSO4
Terrific broth	12 g bacto-tryptone, 24 g bacto-yeast extract, 4 ml

	Glycerol, 2.31 g KH_2PO_4, 12.54 g K_2HPO_4, dH_2O to make 1 L
TAE	40 mM Tris-Acetate, 1 mM EDTA

2.2 Methods

2.2.1 Molecular Biology

2.2.1.1 DNA restriction digestion

Approximately 1 μg DNA was used to check the presence or orientation of insert and 2 μg DNA was used for subcloning restriction digestion. Digestion was normally carried out in a 20 μl volume containing 2 μl 10x enzyme buffer, 0.5-1 μl appropriate restriction endonuclease and 100x BSA according to enzyme instructions. Sterile water was used to make up the total volume to 20 μl. The mix was incubated at 37 °C for 2 h followed by addition of DNA loading buffer and analysis by agarose gel electrophoresis.

2.2.1.2 Agarose gel electrophoresis

0.32 g agarose (Sigma) was dissolved in 400 ml TAE buffer and melted in a microwave oven to make 0.8% agarose gel. 30-50 ml melted agarose was transferred to a 50 ml tube and cooled down to 50-60 °C by sitting on ice for several minutes before 10 μl ethidium bromide was added. The agarose gel was then poured into a horizontal gel cartridge with an appropriate comb inserted. The gel was allowed to set for about 30 min at room temperature. When it was ready the cartridge was transferred into a gel running tank with the comb position at the negative charge end. Then the comb was gently removed and DNA samples mixed with loading buffer (30% (v/v) glycerol, 0.25% bromophenol blue) were applied to the wells. 1 kb or 100 bp DNA ladders (Promega) were loaded to the first lane to compare the size of DNA fragments of the samples. Electrophoresis was carried out at 80 volts for 40-50 min.

2.2.1.3 Gel extraction and purification of DNA

A clean sharp blade was used to cut the DNA band precisely from agarose gel under the UV light. This step should be performed as quickly as possible to minimize DNA damage caused by UV irradiation. The sliced gel then was transferred into a fresh tube and extraction was carried out using QIAGEN gel extraction kit. The manufacturer's protocol of the kit was followed. Briefly, the gel slice was dissolved in 600 μl QC buffer at 37 °C until the agarose gel was completely dissolved. The solution then was applied to a QIAspin column and centrifuged in a microfuge at 14,000 xg for 1 min. The column then was

washed twice with 750 µl PE buffer containing ethanol and spun at full speed. The flow-through was discarded and the column was spun for a further 30 sec to ensure complete removal of PE buffer. The column was transferred to a sterile 1.5 ml microcentrifuge tube. 50 µl buffer EB buffer, pre-warmed to 50 °C, was added to the centre of the column and incubated at room temperature for 1 min. The column was spun at 14,000 xg for 1 min and the eluted DNA was collected in the microcentrifuge tube.

2.2.1.4 DNA ligations

Plasmid DNA and insertion DNA fragments cut with appropriate enzymes were mixed at a mole ratio of 1:8. The mix also includes 1 µl 10x ligation buffer, 1 µl T4 DNA ligase (Promega). Sterile water was added to make the total volume up to 10 µl. The mix was incubated at 16 °C overnight. 5 µl of overnight ligation mixture was then used for transformation into *Escherichia. coli* DH5α or XL1-blue.

2.2.1.5 Preparation of competent *Escherichia coli*

A single colony from a freshly streaked agar plate of the appropriate strain was used to inoculate 5 ml of 2YT. This culture was grown at 37 °C with shaking at 250 rpm overnight. The culture was then used to inoculate 500 ml of 2YT the next morning, and grown at 37 °C with shaking at 250 rpm until the optical density (OD) at 600 nm reached 0.6. The culture was spun down at 4000 xg for 10 min in a Beckman bench top centrifuge and resuspended in 50 ml ice cold $CaCl_2$ on ice for 30 min. Following this incubation, the cells were again pelleted at 4000 xg and resuspended in ice cold $CaCl_2$. 15 % (w/v) glycerol was added to the resuspended cells. Aliquots were then frozen in liquid nitrogen and stored at -80 °C until needed.

2.2.1.6 Transformation of *Escherichia coli*

Competent *E.coli* cells DH5α were thawed on ice, which are chemical competent cells routinely made in the lab. For each transformation, 5 µl of ligation mixture or 1 µl (50ng) purified DNA plasmids were added to 100 µl competent cells. The DNA and competent cells was mixed gently and left on ice for 30 min. The cells were then heat shocked in a water bath of 42 °C for 90 sec followed by sitting on ice for 2 min. After this, 500 µl of SOC medium was added to each tube and incubated at 37 °C for 1-2 hrs. The cells then were spun down at 14,000 xg for 30 sec and 500 µl medium was removed. The cells were

resuspended in the remaining 100 µl medium and plated evenly on a 2x YT agar plate containing appropriate antibiotics. The plate was incubated inverted at 37 °C overnight.

2.2.1.7 Small scale DNA preparation from *Escherichia coli*

5 ml 2x YT containing appropriate antibiotics in a 15 ml plastic tube was inoculated with a bacterial colony from 2x YT agar plates or frozen glycerol stocks. The bacteria were grown at 37 °C with shaking at 250 rpm overnight. DNA purification was carried out using a QIAGEN Miniprep kit according to the manufacturers protocol. Briefly, the bacteria from 1.5 ml overnight culture were harvested by centrifugation for 2 min at 14,000 xg in a microfuge. The supernatant was discarded and 250 µl P1 buffer containing RNase was added and the pellet was resuspended by pipetting up and down several times. 250 µl P2 buffer then was added to the tube to lyse the cells by gently inverting the tube 4-6 times. 350 µl buffer N3 was added to the tube and again mixed by inverting several times. The tube then was centrifuged at 14,000 xg in a microfuge for 10 min. The supernatant was carefully removed and applied to a Qiagen miniprep spin column and spun at full speed for 1 min. The flow-though was discarded and 750 µl buffer PE (with ethanol added) was added to wash the column twice. The column was spun again and the flow-through was discarded. The column was spun again for a further 1 min to ensure the wash buffer was completely removed. 50 µl of buffer EB was pipetted to the centre of the column and incubated for 1 min. The solution containing DNA was then collected by centrifugation of 1 min in a fresh 1.5 ml tube.

2.2.1.8 Total RNA preparation from mammalian cells

HeLa cells were grown to 80-90% confluency, the media was aspirated and the cells were rinsed once with PBS. For isolation of RNA used for checking the mRNA level of distinct Rab isoforms the cells were grown in 6-well plates. siRNA was transfected into the cells (2.2.3.3) and left for 48 or 72 h before harvest. Then the cells were trypsinzed and collected in a 15 ml centrifuge tube (Corning) by centrifuge at 4,000 xg in a Beckman bench top centrifuge for 3 min. Total RNA was extracted using Qiagen RNeasy Mini Kit using the manufacturer protocol. 600 µl buffer RLT containing 10 µl/ml β-mercaptoethanol was added to the cell pellet, and the sample was homogenized for 30 sec using a rotor-stator homogenizer. The whole sample was added to an RNeasy mini spin column and centrifuged at 8000 xg for 15 sec. 700 µl of buffer RW1 was added onto the RNeasy column and centrifuged at 8,000 xg for 15 sec to wash the column. The RNeasy

column was transferred into a fresh tube, and 500 µl buffer RPE was added to the column and spin at 8000 xg for 15 sec. This step was repeated once with centrifugation at 10000 xg for 2 min to dry the RNeasy membrane. The RNeasy column then was centrifuged for further 1 min to eliminate remaining RPE buffer. The RNeasy column was transferred to a fresh 1.5 ml tube. 30-50 µl of 70 °C pre-warmed RNase-free water was added onto the centre of the column membrane, and the column was spun for 1 min at 8000 xg to elute the RNA.

2.2.1.9 Reverse Transcription Amplification of DNA by Polymerase Chain Reaction (PCR)

The RT-PCR was carried out in thin walled PCR tubes (Abgene) and a BioRad gradient thermocycler. RNA extracted from mammalian cells as described in 1.2.1.7 was used as template to amplify DNA fragments. Reverse transcription and PCR are performed sequentially by using QIAGEN OneStep RT-PCR Kit. All oligonucleotide primers were ordered from Yorkshire Bioscience Ltd and highly purified salt free (HPSF). Stocks of oligonucleotides were made at 100 µM in TE buffer (10 mM Tris-HCl, pH 8.0, 1 mM EDTA). They were then diluted in nuclear-free water (Ambion) to bring concentration to 25 µM before use for PCR.

Reactions were set up on ice typically as follows:

5x QIAGEN OneStep RT-PCR Buffer	10.0 µl
dNTP Mix (containing 10 mM of each dNTP)	2.0 µl
Primer Forward (25 mM)	1.2 µl
Primer Reverse (25 mM)	1.2 µl
QIAGEN OneStep RT-PCR Enzyme Mix	2.0 µl
Template RNA	1.0 µg
RNase-free water	Variable
Total volume	50.0 µl

The tubes were then vortexed gently and spun quickly in a microfuge before thermal cycling was initiated. Typical cycling conditions were as follows:

50 °C	30 min	
95 °C	15 min	
94 °C	15 sec	→ x 35
45 ~ 55 °C	30 sec	
72 °C	1 min/kb	
72 °C	10 min	
4 °C	pause	

After the PCR cycling, 10 µl of the reaction mixture was analysed by agarose gel electrophoresis (2.2.1.2).

2.2.2 Biochemical Methods

2.2.2.1 SDS-PAGE

Sodium dodecyl suphate Polyacrylamide Gel Electrophresis (SDS-PAGE) was carried out according to standard protocols. The Bio-Rad mini-PROTEAN II gel apparatus and either 10 or 15 well combs were used.

A resolving gel was prepared using 30% acrylamide/bisacrylamide, 1.5 M Tris-HCl (pH 8.8) (to a final concentration of 375 mM), 10% (w/v) SDS (to a final concentration of 0.1%), polymerised with 10% (w/v) ammonium persulphate and TEMED. 4 ml of the resolving gel was poured into the gel apparatus and allowed to set at room temperature with 0.5 ml isoproponal overlaid at the top. The stacking gel was prepared using 30% acrylamide/bisacrylamide, 1 M Tris-HCl (pH 6.8) (to a final concentration of 125 mM), 10% (w/v) SDS, and was polymerised with 10% (w/v) ammonium persulphate and TEMED (to a final concentration of 0.05%). The stacking gel was then applied on the top of the resolving gel with a comb inserted at the top and allowed to polymerise at room temperature.

The protein samples were resuspended in 2x SDS-PAGE sample buffer and were boiled for 5 min in water bath. The samples were then loaded to the wells in the stacking gel, adjacent to broad-range (8-173 kDa) pre-stained molecular weight markers. Gels were

electrophoresed in SDS-PAGE running buffer (25 mM Tris, 190 mM glycine and 0.1% (w/v) SDS) at 80 V to allow protein samples to focus in the stacking gel. The voltage was increased to 120 V when the dye front reach the boarder between the stacking and resolving gel and protein samples then were allowed to separate in the resolving gel.

2.2.2.2 Immunoblotting

Transfer buffer (25 mM Tris, 190 mM glycine, 20% (v/v) Methanol) was prepared, and transfer of proteins from SDS-PAGE to nitrocellulose membrane was performed at 70 mA overnight. Before incubation with antibody, the nitrocellulose membrane was first stained with ponceau to ensure efficient transfer of the proteins. The ponceau staining was then washed away using PBST (PBS, 0.1% Tween-20 (v/v)). The membrane then was incubated in 5 % (v/v) skimmed milk in PBST buffer at room temperature with shaking for 30 min to block the non-specific sites. The primary antibody were diluted at concentration 1:1000 in dried skimmed milk in PBST buffer and the nitrocellose membrane was heat-sealed in a polythene bag together with the primary antibody solution, and incubated with shaking at room temperature for 1 h. Following the incubation, the nitrocellose membrane was washed with PBST buffer for 5 times, 5 min per wash. High salt PBST with 0.5 M NaCl was used if the antibody gave high background. Dried skimmed milk in PBST buffer containing appropriate secondary antibody (HRP-linked IgG) at dilution 1:1000 were applied to the nitrocellose membrane and incubated with shaking for 1 h. The same washes were then carried out as above. Equal volumes of Amersham "Detection Regent I" and "Detection Regent II" were mixed and applied to the membrane in the dark for 1 min. The blot then was quickly dried and wrapped with cling film to be fixed in a light tight cassette. In the dark room, the blot was exposed to Kodak film for appropriate exposure times, and the films were developed using a X-OMAT automatic processor.

2.2.2.3 Purification of recombinant protein by using baculovirus

Generally 2 x 10^7 *Spodoptera frugiperda* (Sf9) cells from a log phase culture were plated in a 150 cm^2 flask with 30 ml SFM 900 II media. For purification of one protein 30 flasks of Sf9 cells were prepared. The cells were incubated for 1 h to allow them to attach to the flask, and they were infected with a P2 stock (titer about 10^7) at MOI = 10. The cells then were incubated at 27 °C for 72-96 h. During this period, infected cells showed morphological infection signs, their size of total volume and nuclei both increased, and intercellular granules formed. At this point, cells were harvested by pipetting the media over the loosely attached monolayer. The cell suspension was transferred to 50 ml conical

tubes and spun down at 600 xg for 5 min at 4 °C. The pellet was washed once in ice-cold PBS and spun down again. 1 ml His-lysis buffer (50 mM NaH_2PO_4, 300 mM NaCl, 10mM imidazole, pH 8.0) per flask was used to lyse the cells. After incubation on ice for 15 min, the lysate then was French Pressed twice at 1000 psi and centrifuge at 30,000 xg for 30 min. Meanwhile, the Ni-NTA agorose (Qiagen) was washed 3 times in His-washing buffer (50 mM NaH_2PO_4, 300 mM NaCl, 20 mM imidazole, pH 8.0). 50 µl Ni-NTA agarose per ml cell lysate was added and rotated at 4 °C with gentle rotation overnight. The agarose then was washed four times with 20 bed volumes of His washing buffer. His-tagged protein was eluted with elution buffer (PBS containing 10% glycerol, 250 mM imidazole).

2.2.3 Cell Culture

2.2.3.1 Culture and transfection of HeLa cells

HeLa cells were cultured in 75 cm^2 or 150 cm^2 flasks (Corning) with Dulbecco's Modified Eagle Medium supplemented with 10% Fetal Calf Serum (Invitrogen Life Technologies), 1% glutamine and 100 U/ml penicillin and 100 U/ml streptomycin. HeLa cells were transfected using Lipofectamine 2000. Briefly, cells were seeded in 12-well plate 24 h before transfection. The next day, 1 h before transfection the medium was replaced with 1 ml fresh complete media. At the time of transfection, appropriate amount of DNA plasmids (1.6 to 2 µg) and Lipofectamine 2000 reagent (4 µl) were mixed with 50 µl serum free media Optimem in separate tubes. 5 min after Lipofectamine 2000 was mixed with Optimem, the two tubes containing DNA-Optimem and Lipofectmine 2000-Optimem were combined together and mix gently. The mix was incubated at the room temperature (25 °C) for 20 min to allow the DNA/Lipofectmine 2000 complex to form. After this, 100 µl mix of DNA/Lipofectamine 2000/Optimem total was applied to each well. Cells were incubated at 37 °C with 5% CO_2 for 24, 48 or 72 h before further analysis.

2.2.3.2 siRNA synthesis

siRNA targets of Arf5 and Arf6 were selected according to Silencer siRNA Construction Kit Instruction and Ambion (www.ambion.com/techlib/misc/siRNA finder.html) and Qiagen (www.qiagen.com) website. In addition, the choosen sequences have been blasted against the nr database for 'short and almost complete matches'. Only sequences that meet the requirement of both websites and have no homology of more than 15 nt to any unrelated gene were used for further experiments. After using these criteria siRNA targets chosen for the genes are:

The sense and antisense siRNA oligonucleotide templates were then ordered (MWG), and used to synthesize siRNA duplexes with the Silencer siRNA Construction Kit. The manufacturers protocol was followed. Briefly, first each siRNA oligonucleotides template was hybridised to a T7 promoter primer by setting up the reaction:

T7 promoter primer	2 μl
DNA hybrization buffer	6 μl
sense/antisense siRNA oligo template	2 μl

The reaction were performed at 70 °C for 5 min and then kept at room temperature for 5 min. The hybridized templates from last step were then mixed with reagents as follows and the oligonucleotide templates were transcribed into RNA by being filled in with Klenow DNA polymerase:

10x Klenow reaction buffer	2 μl
10x dNTP mix	2 μl
Nuclease-free H_2O	4 μl
Exo-Klenow	2 μl

All the reagents were gently mixed by pipetting and spun down quickly. The mix then was incubated at 37 °C for 30 min. The transcribed ssRNA templates were then used to synthesize dsRNA by the following method:

Sense/antisense siRNA template from last step	2 μl
Nuclease-free water	4 μl
2x NTP Mix	10 μl
10x T7 reaction buffer	2 μl
T7 enzyme mix	2 μl

Again, all reagents above are gently mixed and kept at 37 °C for 2 h.

After this, the sense and antisense transcription reactions were combined and incubated at 37 °C overnight to maximize the yield of RNA and facilitate hybridization of the sense and antisende strands of the siRNA.

RNase and DNase were added to the synthesized siRNA to eliminate remaining ssRNA and DNA.

Digestion Buffer	6 µl
Nuclease-free water	48.5 µl
RNase	3 µl
DNase	2.5 µl

After 2 h incubation at 37 °C, the mixture was cleaned using the RNA clean column provided by the kit. The concentrations of final eluted siRNA were determined by A_{260} with a spectrophotometer.

All of the other siRNA duplexes were designed and produced by Dharmacon as siGENOME Smartpool and they were used for transfection directly.

2.2.3.3 Transfection of siRNA into HeLa cells

DharmaFect I transfection reagent (Dharmacon Inc.) was used to deliver siRNA duplex to HeLa cells and the standard protocol supplied with the products was followed. Briefly, before transfection, siRNA duplexes were adjusted to a concentration of 2 µM with siRNA buffer. In the case of 12-well plate, 50 µl of 2 µM siRNA with 50 µl serum-free DMEM were mixed. In another fresh tube, 2 µl DharmaFect 1 was diluted in 98 µl DMEM, and incubated at room temperature for 5 min. After the incubation, the two tubes were combined together and mixed thoroughly. After 20 min incubation at room temperature, supply 800 µl complete media to the tube to make the final volume 1 ml and the final concentration of siRNA 100 nM. The 1 ml mix was added to cells in each well of 12-well plate, rocked back and forward gently. Cells were then incubated at 37 °C for appropriate time before further analysis.

In the case of Rab11, RNAi targeted both isoforms Rab11a and Rab11b have been tested. Rab11a antibody only detects Rab11a protein and showed good reduction of this protein 3.2.3.3. Unfortunately, the Rabbit and Chicken antibodies against Rab11b used in previous

reports did not work in my hand (Schlierf et al., 2000). Hence it is not clear whether Rab11b protein is depleted by the RNAi treatment. Binucleate cells were observed only in cells treated with Rab11a siRNA, but not Rab11b siRNA. Therefore, experiments carried out with Rab11 RNAi in subsequent chapters only refer to Rab11a.

2.2.3.4 Adenovirus amplification and purification

For each adenovirus amplification thirty 150 cm^2 flasks of HEK293 cells were grown to approximately 50% confluency. 50 ml virus stock was diluted into 100 ml growth media (DMEM containing 5% FBS), and 5 ml of them was applied to each flask. The flasks were rocked gently for several min and incubated at 37 °C until cells float off, normally 2-4 days. The cells then were spun down at 600 xg for 5 min. The media were kept as virus stock for infection next round, and the cell pellet was resuspended in 10 ml PBS and an equal volume of ARKeloneP was added, mixed thoroughly and allowed to stand for 10 min until the layers separated. The mix was then centrifuged at 600 xg for 5 min. The top layer that contains virus was then taken and purified by $CsCl_2$ gradient. The "$CsCl_2$ 1.4" was prepared by dissolving 53 g $CsCl_2$ in 87 ml of 10 mM Tris-HCl pH 7.9. While the "$CsCl_2$ 1.2" was made by dissolving 26.8 g $CsCl_2$ in 92 ml of 10 mM Tris-HCl pH 7.9. Before use, both were filtered in a sterile hood with 0.2 μm filter. To carry out the $CsCl_2$ gradient, 1.5 ml "$CsCl_2$ 1.2" was added to Beckman 14 x 95 mm tubes, and 3 ml of "$CsCl_2$ 1.4" was carefully added to the bottom of the "$CsCl_2$ 1.2". The PBS containing virus was placed gently on the top. The tube was spun in a SW40 swing-out rotor at 90,000 xg for 90 min at 8 °C. After the centrifugation, a fine white virus ring formed between the two $CsCl_2$ layers. This was aspirated by using a syringe. The purified virus solution was then dialyzed against 1 L TE overnight. The dialyzed virus was then further placed on the same $CsCl_2$ gradient for a second time. The final purified virus was then dialyzed, aliquoted and stored at -80 °C.

2.2.3.5 Adenovirus infection of HeLa cells

HeLa cells were seeded on 13 mm coverslips in 12-well plate the day before infection. The next day, the growth media was removed and 1 ml serum-free DMEM was added to each well. Adenovirus was added to the cells at dilution from 1:100 to 1:500. The virus was left 5 h to allow efficient infection in serum-free medium before appropriate amount FBS was added to each well to bring the final concentration to 10%. The infected cells were left for 24, 48 or 72 h before further analysis was performed.

2.2.3.6 Microinjection of antibody into HeLa cells

HeLa cells were seeded on grid collocates coverslips in a 10 cm dish the day before injection. The antibody was prepared with PBS at concentration ranging 0.25-0.5 mg/ml and centrifuged in a microfuge at 10,000 xg for 10 min to pellet protein aggregates. Before injection, the normal culture media was replaced with microinjection media (DMEM containing 10% FBS and 10 mM Hepes). The 10 cm dish then was placed on an Axiovert 135 (Zeiss) microscope stage fitted with an Eppendorf Microinjection 5171 and Transjector 5246 system. The antibody was loaded to Femtotips using a slim Micro Loader tip. All the cells observed with microscope in chosen area on cellocate were injected with the antibody solution at the conditions of injection pressure of 150, compensatory pressure of 40 and injection time ranging from 0.2-0.5s. The injected area was marked and cells were returned to 37 °C to recover and grow before further analysis.

2.2.3.7 Fluorescent transferrin internalization

HeLa cells were incubated for 2 h with serum-free media, and Texas-red transferrin (25 μg/ml) was added for 30 min. The cells were then washed extensively in cold PBS before fixation. For the transferrin chase experiment, the cells were kept with complete growth media containing 1 mg/ml iron-saturated transferrin for 30 min chase time. The cells were then washed in cold PBS and fixed as described above.

2.2.3.8 Culture and transfection of Sf9 cells

Spodoptera frugiperda Sf9 insect cells were used as the host for the baculovirus transfer vector. Sf900 II Serum-Free Medium (SFM) (Invitrogen), a protein-free medium optimized for the growth and maintenance of Sf9 cell was used for culture. The cells were kept in an incubator at 27 °C. To amplify cells, a 150 cm^2 flask was vigorously shaken and transferred to a sterile tube. The cells were spun down and resuspended in 20 ml SFM. The 20 ml SFM was split evenly into five 150 cm^2 flasks.

To transfect a bacmid encoding gene of interest into insect cells, CellFECTIN reagent was used. In a 6-well tissue culture plate, 9 x 10^5 Sf9 cells were plated each well in 2 ml of Sf900 II SFM and incubated at 27 °C for 1 h to allow the cells to attach. In two separate tubes, the transfection reagents were prepared. In tube A, for each tranfection, 2 μg bacmid DNA was diluted into 100 μl Sf-900 II SFM without antibiotics. In tube B, for each transfection, 5 μl CellFECTIN reagent was diluted into 100 μl Sf-900 II SFM without

antibiotics. The two tubes were combined and incubated at room temperature for 15 min to allow the lipid/DNA complex to form. Meanwhile, Sf9 cells were washed once with 2 ml of Sf-900 II SFM. 0.8 ml Sf-900 II SFM was added to each tube containing lipid/DNA complexes and 1 ml lipid/DNA complexes were added to each well of the cells and the cells were incubated at 27 °C for 5 h. After the incubation, the transfection mixture was removed and 2 ml Sf-900 II SFM was added to each well and incubated at 27 °C for 72 h before harvesting the virus from the cell culture medium.

2.2.4 Immunofluorescence and Microscopy

2.2.4.1 Immunofluorescence staining of cells

HeLa cells were plated in 12-well plates containing 13 mm diameter glass coverslips at 60-70% confluence 24 h before immunofluorescence staining. The next day growth media was removed and cells on cover slips were gently washed once with PBS. The cells then were fixed with 2 ml fresh made 4% paraformaldehdye for each coverslip and incubated at room temperature for 10 min. The coverslips were then washed 3 times with PBS and then 2 ml of 30 mM NH_4Cl was added for 5 min. Coversilps were again washed 3 times with PBS before 0.1% Triton (in PBS) was added to permeabilize the cells for 10 min. Again cells were washed 3 times in PBS, and 3 times in blocking buffer (PBS plus 0.2% Fish Skin Gelatin (Sigma), 0.1% Donkey Serum (Sigma). Blocking buffer was freshly prepared and passed through a 0.2 μM filter. Primary antibody was diluted at concentration of 1:200 in blocking buffer, followed by centrifugation in a microfuge at 14,000 xg for 10 min. The solution of primary antibody was then applied to the cover slips. After 1 h incubation at room temperature, the cells were washed again 3 times in blocking buffer followed by 3 times in PBS. "Alexa Fluor Dyes" secondary antibodies 488 (green), 594 (red) and 647 (blue) were used. The secondary antibodies were diluted in blocking buffer at 1:200. 150 μl secondary antibody solution was applied to each coverslip and incubated for 1 h in dark. After this the coverslips were again washed 3 times in blocking buffer and 3 times with PBS. If actin staining was required then phalloidin was diluted in PBS and added to coverslips for 30 min. A 1:20 dilution of Molcular Probes 488, 594 or 647 nm phalloidin stock was used as appropriate. Cells were then washed again 3 times with PBS. If nuclear staining was required, then DAPI, diluted in PBS to a final concentration of 1 μg/ml was added and incubated for 2 min, before a final 3 washes with PBS. Coverslips were then mounted onto glass slides using a drop of "Immunomount" and then left overnight in the dark to dry. The exposure of coverslips to light was minimised throughout the whole procedure to help prevent fading of fluorescence.

2.2.4.2 Confocal microscopy

Mounted coverslips were observed using 40x oil or 63x oil immersion objective on a Zeiss confocal microscope (Carl Zeiss, Germany) equipped with Zeiss LSM5 Pascal instrument. Argon laser was used to excite 488nm Alexa-Fluor dyes (Molecular Probe) and GFP fusion proteins, while helium neon lasers were used to excite 594nm Alexa-Fluor dyes. Zeiss Pascal software was used to collect images. Images were saved as mdb files which can be exported as TIFF format and edited using Photoshop (Adobe).

2.2.4.3 DeltaVision microscopy

3D image sets were aquired using a MicroMax cooled CCD camera (5MHz, Roper Scientific, USA) on a DelatVision Restoration Microscope (Applied Precision, LLC, WA, USA), equipped with a 100W Mercury Arc lamp, 6-position interchangeable excitation filter wheel, Olympus 1x71 inverted microscope stand and Olympus Plan-Apo 60x Oil, 1.42NA, 0.10 mm WD objective. Optical sections were recorded every 0.2 μm. 3D data sets were collected and deconvolved using SoftWorx software. TIFF files were generated from original single optical sections and imported to Adobe Photoshop for editing.

2.2.4.4 Video-microscopy

For time-lapse analysis, HeLa cells were seeded in 6-well plate with 22 mm glass coverslips the day before experiment. The next day, cells were transfected with either siRNA or DNA plasmids of interest. Video-microscopy was carried out 24-48 h post-transfection. Before imaging, the treated cells were transferred to pre-warmed DMEM with 20% FCS and 20 mM HEPES. Microscopy was performed on a partially motorized inverted Axiovert 135 (Zeiss) microscope with either phase illumination or fluorescence. The microscope was equipped with an environmental control chamber, which maintained the cells at 37 °C. 32x or 63x oil objectives were used for observation. The filters and shutters are driven by AxioVision 4.4 software (Zeiss) and images were recorded every 60 sec. Individual TIFF or AVI files were imported into Photoshop (Adobe) or iMovie (Apple) for further editing.

3 The Role of Rab11 and Arf6 GTPases in Mitosis

3.1 Introduction

3.1.1 Binucleate cell experiment

To evaluate cytokinesis defects, the binucleate cell assay was applied extensively in this chapter. Basically, this assay monitors production of binucleate cells, a typical defect in the process of cytokinesis. This phenotype occurs because the karyokinesis is not disrupted, DNA material separates and distributes into two halves of the cell and forms two intact new nuclei. If cytokinesis fails, the cytoplasm is not able to divide into two cells, which causes two nuclei to remain in one cell. Therefore, an efficient way to detect whether a protein is important for cytokinesis is to perturb its action in living cells, for example by depleting the protein by RNAi, or overexpressing a mutant form, or blocking the protein by microinjecting an antibody against it. After the appropriate period of time (for HeLa cells, 15-20 h per cell cycle) to allow this disruption to affect cells and cause a corresponding phenotype, the cells were processed for immunofluorescence analysis. If the protein in question is a crucial player in cytokinesis, the effect can be easily evaluated by quantification of cells containing two nuclei.

Although this approach has been used in many studies on cytokinesis and offered a relatively efficient and straightforward way to assess the defects, it also has several drawbacks. First, if a binucleate phenotype does occur, it is not possible to reveal at which precise stage of cytokinesis the cell has failed. Binucleate cells can form at the furrow ingression step, or at midbody formation after furrowing is complete, or even at the final abscission step of the midbody. To elucidate the timing of molecule function, real time microscopy needs to be performed. The second limitation is that the binucleate cell is not the only phenotype when a cytokinesis defect occurs. Other possibilities such as cytokinesis delay, abnormal furrow formation and midbody morphology or cell death may also be caused by cytokinesis failure. Again, real time video microscopy with quantification of various phenotypes is required to obtain more comprehensive results.

Despite these limitations, however, the binucleate experiment is a very efficient method to start investigation of a molecule's role in cytokinesis. Hence in this chapter, the binucleate experiment was applied combined with a range of other approaches to determine the function of Rab11 and Arf6 in cytokinesis.

3.1.2 RNA interference (RNAi)

RNA interference (RNAi) is the technique of using double-stranded RNA to target specific mRNAs for degradation, thereby silencing their expression. It has developed into one of the most exciting and powerful methods to analyse gene function in the past fifteen years. In this study, RNAi was used extensively to downregulate genes of interest in order to investigate their functions.

During the 1990's, the phenomenon of gene-specific silencing was described as "co-suppression" in plants (Napoli et al., 1990) and "quelling" in fungi (Romano and Macino, 1992). In 1995, Guo and Kemphues first reported that injection of either anti-sense or sense RNAs into *C. elegans* interfered with specific gene expression (Guo and Kemphues, 1995). Three years later, Fire, Mello and coworkers found that the injection of double-stranded (ds) RNA into worms induced even more potent sequence-specific gene silencing, and they coined the term "RNA interference" (RNAi) (Fire et al., 1998). More recently, the accumulating understanding of RNAi pathway discovered that exogenous dsRNA are processed into small interfering RNAs (siRNA) ranging from between 21 to 23 nt by endonucleolytic cleavage (Caplen et al., 2001; Elbashir et al., 2001).

Studies later revealed the RNAi mechanism is actually an evolutionarily conserved defence approach against invading viral genomes or clear aberrant transcription products. The RNAi pathway is triggered by dsRNA sharing sequence-specific homology to target mRNAs and includes several steps as follows. First, the dsRNA is cleaved to yield siRNAs by an enzyme known as Dicer in an RNase III-like manner. Dicer is a highly conserved family of RNase III enzymes that act to cleave the dsRNA dependent on ATP. Second, the siRNA generated from the dsRNA form the RNA-inducing silencing complex (RISC) with multiple proteins. Third, the RISC targets the corresponding mRNA for destruction.

Preliminary attempts to use RNAi in mammalian systems using long dsRNAs as triggers resulted in the induction of a non-specific Type I interferon response rather than sequence-specific silencing (Ui-Tei et al., 2000). The interferon response causes global changes in proteins expression, masking any sequence-specific effects and eventually leading to apoptosis. This phenomenon makes the application of the RNAi as an efficient method to study individual gene quite difficult. The discovery that siRNA can trigger gene specific silence without causing sequence-nonspecific responses enables synthetic RNA duplexes to be applied in culture cells efficiently (Caplen et al., 2001; Elbashir et al., 2001).

To perform efficient gene silencing using siRNA in the target mRNA, it is crucial to select the proper siRNA sequence. Although the rules that lead to effective siRNA-directed gene silencing remain undefined, it is known that different siRNAs targeting the same gene vary markedly in their effectiveness. The sequence itself is not the only determinant of the silencing effect, other factors may be accounted for include the secondary structure of the target mRNA and the binding of RNA interacting proteins. Elbashir and coworkers revealed that siRNA with 3' overhanging UU dinucleotides are the most effective, hence they suggested select sequence starting with "AA" dinucleotide in the target mRNA (Elbashir et al., 2001).

The discovery of RNAi has changed our understanding of how cells guard their genomes, and developed new strategies for investigating gene functions. With RNAi, the sequence of a gene can now be used to specifically inhibit its cellular function. Reverse genetic strategies moving from gene sequence to function have now taken on new importance.

3.1.3 GTP deficient mutants of small GTPases

In this chapter, GTP-binding deficient mutants were used to disturb the GTP cycle of GTPases in question to investigate their role during cytokinesis. All Ras-like small GTPases share a common domain, which consists of a six-stranded β sheet, comprising five parallel strands and one anti-parallel one, surrounded by five α helices. The elements responsible for guanine nucleotide and Mg^{2+} binding, as well as GTP hydrolysis, are located in five loops that connect the α helices and β strands. Crystallographic analysis of p21-Ras (Stroupe and Brunger, 2000) and yeast Rab sec4p (Milburn et al., 1990) shows that the GDP- and GTP-bound states adopt two different conformations, with the major nucleotide-induced differences in regions denoted switch I and switch II (Schlichting et al., 1990).

After this, several other studies showed that mutations equivalent to the activating Q61L mutation in p21-Ras inhibit both the intrinsic and the GAP-induced hydrolysis (Tisdale et al., 1992; Walworth et al., 1992). In contrast, mutants corresponding to the inhibitory S17N mutant of p21-ras have a preferential affinity for GDP (Ridley and Hall, 1992). For example, it was shown that mutations in Rab5 protein in this switch regions change states of their GTP/GDP binding. Rab5 Q67L predominantly locks Rab5 in GTP-bound form, while Rab5 S34N locks this protein in its GDP-bound state. These mutants dramatically change the morphology of early endosome and alter trafficking from the cell surface to the endosome (Stenmark et al., 1994). Comparable mutants of Rab11 were made later in this

study (Ullrich et al., 1996), and Rab11 Q70L preferentially binds to GTP and Rab11 S25N predominantly associates with GDP. Overexpression of Rab11 S25N showed disperse cytosolic staining, and caused marked inhibition of transferrin recycling. In contrast, overexpression of Rab11 Q70L constricts to the perinuclear area. Although it also inhibits transferrin (Tf) recycling, the effect was milder than Rab11 S25N (Ullrich et al., 1996).

3.1.4 Hypothesis and Aim

Rab11 and Arf6 GTPases have been established as essential regulators of endosomal membrane trafficking, and the endosomes have been suggested as one of the origins of membrane material required for cell division. Here, it was proposed that Rab11 and Arf6 controlled membrane trafficking might contribute to cytokinetic machinery, probably for the furrow ingression or final closure of the intercellular bridge. In this chapter, an investigation was performed to reveal the distribution of these two proteins throughout the cell cycle. If the immunofluorescence experiments show that Rab11 and Arf6 do localise to the furrow/midbody during cytokinesis, functional experiments, such as RNAi, microinjection of antibodies and overexpression of mutant proteins would be carried out to determine whether the localisation implicates their involvement in this process.

3.2 Results

3.2.1 Localisation of Rab11 during interphase and mitosis

As mentioned in section 1.3.4, the primary role of Rab11 is to regulate vesicle recycling between the pericentrosomal recycling endosomes, the PM and TGN (Ullrich et al., 1996). Interestingly, previous work from *C. elegans* embryos revealed that Rab11 is a key regulator in furrow formation during cytokinesis (Skop et al., 2001). Similarly, a *Rab11* transheterozygote exhibits cellularisation defects in *Drosophila* (Riggs et al., 2003). Such studies suggest that Rab11 may play a role in mammalian cytokinesis, however, the function of Rab11 in this model system of cell division remains to be investigated.

To this end, first we sought to look at the distribution of Rab11 throughout the mammalian cell cycle. HeLa cells were seeded on glass coverslips 24 h before being processed for immunofluorescence. Our experience has shown that after this period there are significant numbers of cells in mitosis for analysis. The cells were also stained for microtubules to identify various stages of the cell cycle. Figure 3.1 shows the distribution of Rab11 during varying stages including interphase, metaphase, anaphase, telophase and cytokinesis.

Consistent with previous reports (Ren et al., 1998; Ullrich et al., 1996), the bulk of the endogenous Rab11 was observed in a single discrete cluster at the perinuclear region with some dispersed dots throughout the cytoplasm (Figure 3.1, panel a-c). During metaphase (panel d-f), chromosome DNA has condensed and aligned at the central spindle, and Rab11 positive vesicles were observed enriched around centrosome/MTOC, as seen in the yellow area of MTOC (red) and Rab11 (green) (panel f). In anaphase, Rab11 vesicles started to move towards the central spindle with the centrosome pool still evident. By telophase, the actin-myosin ring has constricted and cleavage furrow largely progressed, and Rab11 was seen accumulated around the advancing furrow and some scattered on the PM (panel j-l). During cytokinesis (panel m-o), the midbody bridge has formed and elongated, two daughter cells prepare to separate, the majority of Rab11 has become strikingly concentrated at the furrow area and some vesicles can also be viewed in the bridge of the newly formed midbody. Colocalisation of Rab11 (green) and microtubules on the bunched midbody (red) was shown nicely in panel o.

The accumulation of Rab11 positive vesicles at the dividing furrow strongly suggested a possible role of Rab11 to mediate RE trafficking to the cleavage furrow/midbody to supply membrane material or proteins required for carrying out cytokinesis.

3.2.2 Colocalisation of Transferrin and Rab11 at the cleavage furrow and midbody

To test whether the Rab11 positive endosomes accumulated around the furrow/midbody during mitosis represents the real recycling endosome rather than a specialized endocytic pathway, a Transferrin (Tf) internalization experiment was carried out. HeLa cells were serum starved for 2 h before incubation with 25 μg/ml Texas-red Transferrin for 30 min and fixation for immunofluorescence. The internalized Texas-red labelled Tf reveals the classic RE compartments. These cells were also co-stained for endogenous Rab11. In Figure 3.2, the vast majority of Tf colocalised nicely with Rab11 throughout the cell cycle.

The fact that Rab11 positive vesicles concentrated around the cleavage furrow also contain Tf suggests that bona fide RE, rather than a special endocytic pathway regulated by Rab11, is involved in membrane delivery to the cleavage furrow/midbody during cytokinesis.

3.2.3 Rab11 is required for mammalian cytokinesis

3.2.3.1 Rab11-S25N Adenovirus binucleate experiments

As mentioned in section 3.1.3, Rab11-S25N refers to a point mutation in the Rab11 protein sequence in which the residue 25, asparagine, is substituted for serine. This amino acid is located in the loop 1 region of the protein, which together with loop 2 is the sequence that binds to GTP/GDP. Previous studies have shown that mutation of S25N attenuates Rab11 ability binding to GTP and maintains the protein in the GDP bound state. Therefore it is referred to as an "inactive" mutant. This mutant has been established to efficiently inhibit recycling endosome trafficking mediated by Rab11 (Ullrich et al., 1996). Therefore, to test whether Rab11 regulated RE trafficking is involved in cytokinesis, the GDP restricted form was used to disrupt Rab11 function.

HeLa cells were infected by adenovirus bearing myc tagged Rab11-S25N and incubated at 37 °C for 24 or 48 h before analysis. Cells on coverslips were then fixed and processed for immunofluorescence, while a parallel group of cells was used to make a cell lysate for examination of the protein expression. A virus with a vector containing GFP alone was used as a negative control. 10 μg equal amount of cell lysate from each time point as well as mock cells were loaded to an SDS-PAGE and an anti-c-myc antibody was used to blot the over-expressed protein. In Figure 3.3, panel A, the anti-c-myc antibody picked up a

specific band at 25 kDa, the c-myc-Rab11 S25N, whose expression level reached a maximum at 48 h. The cells were left up to 72 h post-infection.

To visualize whether Rab11-S25N has an effect in cytokinesis, immunofluorescence was carried out to examine binucleation of these cells. The treated cells were fixed and stained with anti-c-myc to reveal the expressing mutant protein and anti-αtubulin to verify various mitotic stages. DAPI was used to stain for DNA. The coverslips were then observed using a confocal microscope as described in 2.2.4.2. In Figure 3.3, panel B shows two cells expressing myc-Rab11 S25N (green) containing two nuclei, an indication of cytokinesis failure, while cells without Rab11 S25N expression only have single nucleus as in wild type cells. This result suggests that Rab11-S25N has no effect on nuclear division, but inhibits the physical separation of the cytoplasm into two prospective daughter cells.

To quantify the effects more precisely, the binucleate cells of each sample were counted. Figure 3.3, panel C shows the percentage of multi/binucleate cells, the blue bars show results obtained 24 h post-infection whereas the purple bars are results from cells 48 h post-infection. As shown, cells infected by virus but not expressing Rab11 S25N show a percentage of binucleate cells similar to that of uninfected cells. Conversely, 24 h post-infection, myc-Rab11 S25N expression raised the percentage of binucleate cell from 2.4% to 14.0%. The percentage is around 10.0% at 48 h post-infection (statistically significant $p<0.05$).

Although it has been established that Rab11 S25N caused a marked inhibition of transferrin recycling in mammalian cells in a previous report (Ullrich et al., 1996), it was important to confirm this in our hands. Therefore, a Tf internalization assay was carried out in cells infected with the Rab11 S25N virus. In Figure 3.3, panel D, a wild type cell in cytokinesis was stained for endogenous Rab11. Rab11 positive RE vesicles are enriched at the furrow/midbody and Texas-Tf colocalises with Rab11 on these vesicles. However, myc-Rab11 S25N (green) showed cytosolic distribution and lost the normal staining pattern enriched at centrosomes and furrow/midbody, and also abolished Tf accumulation at the same sites, which suggests that the typical RE trafficking to the furrow/midbody is blocked by Rab11 S25N.

3.2.3.2 Microinjection of Rab11 antibody

Microinjection of individual cells with a specific antibody is a common method to interfere with the function of the corresponding protein. Binding of the antibody to the protein of

interest might prevent it from interacting with its effectors and partners *in vivo*, and therefore perturb its cellular function.

To confirm the effects caused by Rab11 S25N, microinjection was chosen to disrupt Rab11 function. HeLa cells were plated on Cellocate, a special coverslips grids marked with numbers for easily locating cells, 24 h before injection to allow easy identification of injected cells. 0.5 mg/ml anti-Rab11 solution were prepared and loaded into a femtotip (Eppendorf). Individual cell clusters in carefully chosen grids on Cellocate were injected as described in 2.2.3.6. Cells were kept at 37 °C for 48 h before they were fixed and stained for DAPI and microtubules to visualize binucleate phenotypes.

In Figure 3.4, panel A, binucleate cells were observed in the injected area. Quantification of this experiment is shown in panel B, and the number of binucleate cells in the anti-Rab11 injection field was significantly increased compared to the control injected with pre-immune serum. Injection of antibody against Rab5, another GTPase involved in early endosome trafficking, had a slight effect on the percentage of binucleate cells, but this was not statistically significant.

Although the increase of binucleate cell fraction in the anti-Rab11 injection is not as dramatic as that observed in the virus experiment, this can be easily explained by the fact that delivery of antibody to cells by injection is more challenging and affected by more environmental factors than virus infection. Although the injection pressure and time had been optimized, the injection position and antibody uptake amount may vary in individual cells. Therefore, a smaller fraction of cells may take up the right amount of antibody and show the phenotype compared to the virus expression. Nonetheless the results support a role for Rab11 in cytokinesis.

3.2.3.3 RNAi of Rab11

To further establish the role of Rab11 in cytokinesis, an alternative approach, RNAi, was applied. The targets chosen, see

Table 2.3, were recommended by Rytis Prekeris (University of Colorado), as these sequences have been validated by his group.

siRNA duplexes against Rab11 were transfected into HeLa cells, respectively at a series of concentrations: 75 nM, 100 nM and 125 nM as recommended by the manufacturer. Cells

were incubated at 37 °C for 48 and 72 h before immunoblot analysis to determine the effect on Rab11 expression. In Figure 3.5, panel A, the Rab11 expression of the siRNA treated cells was greatly reduced compared to mock and scrambled siRNA transfected cells in a dose dependant manner. A house keeping gene GAPDH was also blotted (upper blot) to indicate equal amount of total protein that were loaded to each lane. The depletion of Rab11 was proven to be specific, as the expression of other three Rab GTPases, Rab4, Rab5 and Rab8 was not affected (Figure 3.5, panel B).

Cells knocked down with Rab11 induced an increase of binucleate cells. To describe the phenotype more precisely, quantification of binucleate cells observed in Rab11 siRNA treated cells is performed and shown in Figure 3.5, panel C. Consistent with the Rab11 S25N virus experiment result, the binucleate cells count dramatically increased under the siRNA treatment compared to controls, 15.5% of cells were observed to be binucleated. Scrambled siRNA and siRNA selective for Rab4 and Rab5 did not increase the number of binucleate cells. Collectively, the results of the virus, microinjection and siRNA experiments argue that Rab11 is integral for the completion of mammalian cytokinesis and strongly supports the notion that recycling endosomes may be intimately involved in the membrane traffic events at the growing furrow/midbody. To detect whether Rab11 is responsible for Arf6 and its binding protein FIP4's localisation to the midbody in cytokinesis, immunofluorescence of these two proteins were performed with Rab11 depleted cells. Results from this experiment revealed that RNAi against Rab11 did not influence FIP4 and Arf6's localisation to the midbody (data not shown).

However, a limit of all these three experiments is that they are not able to reveal which stage of cytokinesis Rab11 regulates. Binucleate cells may either arise from a failure of furrowing or by regressing from the furrow if the final abscission fails. To answer this question, time- lapse video microscopy was considered being carried out, which will be described and discussed in section 3.2.6.

3.2.4 Localisation of Arf6 in mitosis

To test the function of Arf6 in mammalian cell mitosis, first it was sought to localise this protein during cell division. During interphase, Arf6 is thought to cycle from the PM to its own "Arf6 endosome" (Radhakrishna and Donaldson, 1997). From here a part of it returns directly to the PM, while the remaining travel to the sorting and recycling endosomes before moving back to the cell surface, which suggest the possibility that "Arf6 endosome" could encounter with Rab11-containing recycling endosome at some point and collapse

into the latter. This idea is supported by previous observation from our group, which showed that Arf6 partially overlaps with FIP4 and transferrin receptor (TfR) at a perinuclear patch (Fielding, AB, data not shown).

A rabbit anti-Arf6 antibody kindly given by Dr. Donaldson (NIH) was used for immunofluorescence to visualize Arf6. α-tubulin and DNA were also co-stained to verify cells in different phases of mitosis. Figure 3.6 shows the endogenous Arf6 staining in all stages of mitosis. During interphase, Arf6 mainly localises to peripherally distributed vesicles and the PM (Figure 3.6, panel a-d). When condensed chromosomes aligned at the middle plate in metaphase, it starts travelling to the two poles and associates with microtubules and shows an evident distribution along the mitotic spindle (panel e-h). Interestingly, both Rab11 and FIP4 localise to the area of the two pole from metaphase, suggesting a spatially regulation of these three molecules during cell cycle. Yellow colour in panel h shows the colocalisation of Arf6 with microtubules, which is fairly similar to FIP4 distribution. In anaphase cells, Arf6 localised to the midzone of mitotic spindle and seem to decorate the midzone microtubules (panel i-l). With the constriction of the actin-myosin ring in telophase and cytokinesis, Arf6 was enriched at the growing furrow and at the two ends of the midbody bridge (panel m-o). In the merged images, colocalisation of Arf6 and microtubules at the midbody is clearly visible.

3.2.5 Arf6 plays a functional role in cytokinesis

3.2.5.1 Expression of Arf6 GTP deficient mutants results in cytokinesis failure

Studies by Schweitzer and D'Souza-Schorey showed that overexpression of the Arf6-GTP locked form (Q67L) led to a series of cytokinesis defects, suggesting a role of Arf6 in this event (Schweitzer and D'Souza-Schorey, 2002).

Like all GTPases, Arf6 also cycles between its GDP-bound and GTP-bound states. To confirm whether Arf6 function depends on Rab11 and FIP4 in cytokinesis, the GTP deficient mutants were over-expressed in HeLa cells using adenovirus. Arf6 T27N, an inactive GDP-locked form; Arf6 Q67L, an active GTP locked form and wild type Arf6 were applied for this study. This experiment was performed similarly to the Rab11 S25N virus experiment, only except that the Arf6 proteins expression can be visualize directly by a GFP tag. Adenovirus bearing these genes was applied to HeLa cells in serum-free media.

Serum was supplied to the cells 6 h after the virus was applied. 24-48 h post-infection, cells were fixed and stained to view the phenotype.

The expression of Arf6 WT, T27N and Q76L was confirmed by immunoblots of cell lysates with anti-GFP (Figure 3.7, panel A). In panel B, immunofluorescence images of infected cells revealed increased cytokinesis failure occurred in cells expressing Arf6 T27N, but not WT and Q67L expressing cells. It is noteworthy that, in the binucleate cells observed, the majority of GFP-Arf6 T27N localized to the plate between two nuclei, where the midbody was supposed to form. This observation implicates that the inactive Arf6 is still able to localize to the midbody position. However, the disruption of its intricate GTP cycle perturbed its cellular function, which consequently leads to increased percentage of binucleate cells as quantification indicated in panel C. In this experiment, Arf6 Q67L and WT expression only showed minor effect on cytokinesis compared to the defects caused by Arf6 T27N.

3.2.5.2 Active Arf6 recruits Rab11 and FIP4 to the furrow/midbody during cytokinesis

During this work it was constantly observed that although Rab11 S25N and siRNA depletion resulted in increased cytokinesis failure, these disruptions of Rab11 did not affect FIP4 localisation to the midbody. Considering the striking staining of Arf6 at the furrow and midbody region, as well as its binding affinity with FIPs, especially to FIP4 (Fielding et al., 2005), it is interesting to ask the question whether Arf6 localised FIP3 and/or FIP4 to the proper sites during mitosis.

To test this hypothesis, plasmids encoding HA tagged Arf6 WT, Q67L and T27N were transfected into HeLa cells with Lipofectamine 2000 either with GFP-FIP4 plasmid to view FIP4 or co-stained with endogenous Rab11.

The HA epitope was then used to identify cells expressing the Arf6 forms in question. The effect of Arf6 mutants on the distribution on Rab11 was first examined (Figure 3.8). In cells expressing Arf6 WT and Q67L, Rab11 (green) localised properly at the midbody region with a minor pool staining at the centrosome area. In contrast, Arf6 T27N expression caused an obvious reduction of Rab11 at the furrow/midbody.

Similarly, in Arf6 WT cells GFP-FIP4 shows normal localisation at the midbody in cytokinesis (Figure 3.9, panel a-c). Expression of the GTP restricted form Arf6 Q67L

increased the accumulation of FIP4 at furrow/midbody as shown in panel d-f, where GFP-FIP4 decorates the cleavage furrow and forming midbody strikingly. The same distribution was observed in the case of GFP-FIP3 (Fielding et al., 2005). In contrast, in cells expressing Arf6 T27N (panel i-k), GFP-FIP4 accumulation at the furrow/midbody sites was greatly attenuated. Instead, it was hardly observed at furrow/midbody but localises to small disperse intracellular vesicles and the centrosomes. These results clearly showed that localisation of Rab11 and FIP4 is dependent on active Arf6. GDP restricted Arf6 misplaced these two proteins from the dividing site. This suggests that one of the cellular functions of the interaction between Arf6 and FIP3/FIP4 could be to help these proteins localize to furrow/midbody during cytokinesis.

3.2.5.3 RNAi of Arf6

To confirm the results obtained from the virus experiment, another independent method was applied to deplete endogenous Arf6 protein. An efficient siRNA target against Arf6 gene published in a recent report (Sabe, 2003) was used in this study.

The siRNA duplex was transfected into HeLa cells seeded on glass coverslips by Lipofectamine 2000 (see section 2.2.3.3). Cells were incubated for 24 and 48 h before immunoblot and immunofluorescence analysis to examine protein expression and the binucleation phenotype. Figure 3.10, panel A shows that 24 h post-transfection, endogenous Arf6 was effectively reduced to less than 10% of that in control cells. To view the binucleation phenotype, a mouse anti-tubulin antibody was used to stain microtubules and DAPI to stain for DNA. Surprisingly, immunofluorescence results from 5 independent experiments showed that depletion of Arf6 did not affect cytokinesis (Figure 3.10, panel B). No obvious increase of binucleate cells was observed, and cells appeared to be perfectly normal.

Since it was shown that active Arf6 determines the proper localisation of Rab11 as well as Rab11-FIP4 to furrow/midbody, it is wondered where these two molecules would localise in the absence of Arf6. Therefore, Rab11 and FIP4 were stained in cells depleted with Arf6. In Figure 3.10, panel C, FIP4 staining can be seen clearly at the furrow/midbody area after the Arf6 siRNA treatment. The same observation was seen in the case of Rab11 (data not shown). These results suggest that Arf6's function may be dispensable in cytokinesis and could be taken over by another unknown molecule, possibly other Arf proteins, to correctly target Rab11 and FIP4 positive RE vesicles to the furrow.

3.2.6 Video microscopy: cytokinesis defects

3.2.6.1 Time lapse video microscopy of Rab11 RNAi cells

Although it has been shown that expression of the GDP-restricted form of Rab11 and depletion of Rab11 by RNAi both led to increased cell binucleation (section 3.2.3), it was not known how these abnormal cells formed. Do the cells furrow at all? Or do they regress after the cleavage furrow is complete? To determine which exact stage of cytokinesis Rab11 is required, mitosis progression after inhibition of Rab11 function by RNAi was analysed with time-lapse microscopy.

Cells grown on 22 mm glass coverslips were transfected with Rab11 siRNA as described in 2.2.3.3, and incubated for 36 h before observation. Cells then were placed in a 37 °C chamber with a stream of warm air. The cells were then observed with a Zeiss Axiovert 135 inverted microscope, and phase contrast images were taken every 60 sec. Wild type cells were also filmed as a control. To analyse the progression of cell furrowing and undergo cytokinesis more precisely, the videos were edited to begin at the start of anaphase onset and end at the midbody final abscission using Mac iMovie software. Selected still frames representing essential stages of cell division, were captured and are shown in Figure 3.11. The complete movies corresponding to the stills have been included on the DVD attached to this thesis.

Figure 3.11, panel A shows a typical dividing process of a wild type cell. As mentioned the anaphase onset was marked as time point of 0.00 (panel a). The cleavage furrow ingresses at the same time as actin ring restriction. This process was completed in less than 10 min (panel b-d). Immediately after furrowing, the residual central spindle microtubules are bundled and elongated as the midbody bridge forms with an evident dense protein matrix in the middle. The intercellular bridge extends and thins for roughly 3 h (Figure 3.11, panel A, panel e-k). About 3.5 h after anaphase onset, the midbody breaks from one side of the dense matrix in the midbody and the two daughter cells become completely separated (panel l).

In contrast, 40% of Rab11 siRNA treated cells observed could not complete cytokinesis as normal. In Figure 3.11, panel B, panel a-f, the cell elongated, furrowed and formed the midbody normally. However, from about 2.5 h after anaphase onset, the midbody started to shrink and two prospective daughter cells were pulled closer instead of elongating and detaching. By nearly 3 h (panel h), the midbody was hardly seen and two daughter cells

were positioned very close to each other. This situation lasted for about 2 h and a fusion of two cells occurred 5 h after anaphase onset (panel i). The two nuclei remained separated, therefore the fusion led to formation of a binucleate cell.

A limit of this approach is that it is impossible to determine how much Rab11 has been knocked down in the cells being examined. However, furrow regression occurred in 42.9% Rab11 siRNA treated cells compared with 0% in mock transfected cells, and such data strongly argues that Rab11 plays an essential role in the late stage of cytokinesis, most likely the final abscission of the midbody (n=14).

3.2.6.2 Time lapse video microscopy of Rab11 S25N virus infected cells

To confirm the time-lapse microscopy result from RNAi cells, the same method was used to test the cells infected with the GDP-restricted form c-myc tagged Rab11 S25N adenovirus.

In agreement with the RNAi result, in 7 of the 12 cells studied, the furrow regressed and the cells became multi-/binucleated. As shown in Movie 3.2, the cells rounded up, elongated and furrowed as normal. The midbody is hard to see because of difficulties in maintaining a constant clear focus plane during the whole filming process. But from the cell profile and movement it is clear that the daughter cells were connected by a midbody after the cytoplasm separated. The midbody remained for about 2 h; however the two daughter cells were never completely separated. On the contrary, they regressed back about 3.5 h after anaphase onset and formed binucleate cells. These results further back up the Rab11 RNAi data, and 58.3% cells examined by this approach exhibited such furrow regression after abscission failure.

3.2.6.3 Time-lapse video microscopy of Arf6 T27N virus infected cells

It has been hypothesized that Rab11/FIP4/Arf6 serves as a ternary complex to facilitate membrane delivery to the furrow/midbody in mitosis (Fielding et al., 2005). Disruption of Arf6 should therefore perturb the same step as Rab11. To this end, time-lapse imaging was carried out with cells expressing GFP-Arf6 T27N. This was chosen because Arf6 T27N expression increases the number of binucleate cells. In addition, the GFP tag facilitates the identification of appropriate cells to study.

15 cells expressing GFP-Arf6 T27N expression were observed, and 8 of them (53.33%) could not complete cytokinesis and became binucleated as shown in Figure 3.12. It shows a cell expressing Arf6 T27N, panel A represents the GFP and phase contrast merged frames, and panel B shows in phase contrast images. These data clearly depict that the furrow formed and advanced as in normal cells (panel a-d), and a midbody was formed, but did not elongate (panel e-f). Regression took place from about 3 h after anaphase onset (panel g-h) and formed a binucleate cell (panel i-l).

3.2.6.4 Time-lapse video microscopy of Rab11 and Arf6 knock-down cells

Since no increase of binucleate cells is observed from RNAi depletion of Arf6, it was possible that Rab11 compensated its function. Therefore, a double knockdown of Rab11 and Arf6 was carried out. Interestingly, the result exhibits a synergistic effect in the double knockdown, which induced about 20% of binucleate cells compared to the 15% caused by Rab11 and 3% caused by Arf6 (data not shown).

To explore the reason of the slight increase of binucleate cells, video microscopy was carried out to observe the formation of binucleate cells induced by this double knockdown. siRNA against Rab11 and Arf6 were co-transfected into HeLa cells and incubated 48 h to allow the proteins to be degraded before video microscopy. Interestingly, this experiment discovered that knockdown of both proteins consistently causes the furrow to regress rapidly after its formation with normal kinetics, as shown in Figure 3.13. Compared to Rab11 single knockdown, the cells regress relatively earlier. The midbody bridge is hardly formed under these conditions, and the furrow regressed very rapidly as soon as ingression finished. This result indicated the double knockdown of Rab11 and Arf6 causes defects at a step earlier than Rab11 or Arf6 alone, suggesting a synergic effect that may affect formation and stabilisation of the midbody apart from final abscission. In total 10 cells were filmed; 7 of them could not complete the abscission.

3.2.6.5 The fate of multi/binucleate cells

After the formation of binucleate cells, an interesting question arises: what is the fate of these binucleate cells? Will they keep dividing as normal cells, or will their second division also be defective? To answer these questions, time-lapse imaging was performed with these binucleate cells. The images series in Figure 3.14 show the process of a binucleate cell division. The cell rounded up and prepared to divide typically (panel a-f), however, it formed a triangular shape furrow instead of an ordinary cleavage furrow (panel

g-h) when cytokinesis initiated. The triangular furrow underwent ingression and met at the midpoint of the cell, which divided the cell into three prospective daughter cells and led to a trilobal shape cell (panel, i). Interestingly, after a while two of these three daughter cells fused back to one which leads to one bigger daughter cell and another smaller one (panel j-k). The two cells left were still connected (panel k-l). It is hard to see how many nuclei these contain but the total DNA copies in the cell should be more than 2 at this moment. The two cells struggled to separate for about 2 hours (panel l), but no separation was observed. Finally the smaller daughter cell underwent apoptosis first, then, the same situation arose in the larger cell. This phenotype has been observed generally in multi/binucleate cells after disruption of Rab11 or Arf6.

The results from this experiment showed that most of these multi/binucleate cells could survive and entered the next cell cycle, where they also can round up normally. However, during cytokinesis, an abnormal triangular furrow formed, which may be driven by multiple mitotic spindle poles and attempted to carry out division. However, after struggling for a while, the cell could not resolve the error caused by the multiple copies of genetic material and execute cell death, which could likely be apoptosis or necrosis. The fact that the multinucleate cells could survive interphase but then underwent apoptosis suggest that cytokinesis may also be a check point to get rid of abnormal individuals in a cell population, thus facilitating the maintenance of their genetic material.

3.3 Discussion

3.3.1 Localisation of Rab11, Arf6 and their binding partner FIP4 in mitosis

Membrane traffic to the furrow/midbody is essential for the progression of animal cell division. However, the source of the membranes and mechanisms regulating membrane material delivery to the dividing sites in cytokinesis remains unclear. To this end, in this chapter, first I studied the localisation of Rab11, a crucial maker of RE and key regulator mediating recycling of proteins and membranes to the PM in the cell cycle. Consistent with previous studies (Ullrich et al., 1996), the results showed that Rab11-labelled endosomes are perinuclear and localise closely with centrosomes. During prometaphase, these endosome vesicles retained their organized morphology tightly clustered around the centrosome/MTOCs, which is unique among endocytic organelles. MTOC is thought to induce furrow invagination primarily through stimulatory and inhibitory interactions between the plus ends of microtubules and the cortex (Glotzer, 2004). In addition, it has also been shown to play an important role in organising and positioning the centrosome and RE. Therefore it is intriguing to suggest that the centrosome/MTOC may influence the position of the Rab11-positive RE localisation during cell division. This may also facilitate centrosome/MTOC and Rab11 containing RE communication, and hence support the idea of coordination between furrowing initiation mediated by MTOC and membrane transport regulated by Rab11 to the cleavage furrow.

During telophase, Rab11 positive endosomes were observed concentrated around the advancing furrow, and in the midbody bridge later on in cytokinesis. An elegant study using zebrafish embryos has shown that exocytosis takes place in the proximity of the cleavage furrow (Danilchik et al., 2003). Therefore the accumulation of Rab11-positive endosomes in this area suggests that vesicles derived from RE may be one of the membrane sources required during cytokinesis. The presence of internalized Texas-red Tf on these vesicles close to the furrow/midbody argues that they represent bona fide RE, instead of a different pathway involved of Rab11.

Rab11 and Arf6 dual binding protein, FIP4 shares very similar localisation with Rab11 during mitosis (Wilson et al., 2005). During interphase, it partially colocalises with Rab11 containing RE (Hickson et al., 2003). It localises to the two centrosomes from prometaphase, and aligns along at the midzone in metaphase. Finally it becomes strikingly

concentrated at the two ends of the midbody bridge. The distribution of FIP4 suggests that a pool may be present on the Rab11-regulated RE from interphase, and the interaction between FIP4 and Rab11 may play a role of their colocalisation to the midbody during cytokinesis.

Arf6 has been implicated in diverse cellular events such as cell adhesion, migration, invasion through its effect on membrane recycling and actin modelling (Hashimoto et al., 2004; Radhakrishna and Donaldson, 1997; Schafer et al., 2000). It was found at the PM and peripheral vesicles during interphase, and Arf6 Q67L is enriched in the furrow/midbody during cytokinesis (Schweitzer and D'Souza-Schorey, 2002). To confirm this distribution as well as to localise endogenous Arf6 in mitosis, immunofluorescence was performed. Interestingly, despite its peripheral vesicle distribution, Arf6 starts to localise on vesicles around the centrosome area from metaphase and appears to be associated with microtubules, which is reminiscent of Rab11 and FIP4's localisation at this stage. In anaphase, a large amount of Arf6 was seen at the central spindle, and finally became concentrated at the midbody bridge during cytokinesis (Figure 3.6). The distribution of Arf6 suggests that in interphase, it may be present on an "Arf6 endosome" which is distinct of the Rab11-FIP4 containing endosome. During metaphase, the Arf6 endosome appears at the centrosome area and may merge with the Rab11 endosome at some extent probably via interaction of FIP4.

GTPases act by recruiting effectors that facilitate targeting and fusion of transport vesicles (Gonzalez, 2003). Given the binding ability of FIP4 to both Rab11 and Arf6 (Hickson et al., 2003) with their striking localisation to the furrow and midbody, it is proposed that the interactions among them may important for their characteristic localisation to the furrow/midbody. The fact that FIP4 and Arf6 localisation at the midbody were not affected in cells with down-regulated Rab11 suggests that Rab11 is not responsible for their localisation in cytokinesis. Interestingly, interference of Arf6 weakened or abolished Rab11 and FIP4's localisation to furrow/midbody and caused binucleate cells, strongly suggesting that Arf6 localisation to the midbody is required for Rab11 and FIP4 targeting to the same dividing site. High quality confocal images also revealed that Arf6 and FIP4 but not Rab11 have been found to decorate a very fine ring structure within the midbody, the midbody ring during late stage of cytokinesis, Figure 3.6. The ring structure has been suggested as a docking site of the delivery of secretory vesicle membrane, and number of proteins function in vesicle docking and fusion such as snapin, exocyst component and SNAREs are also been found in this specific ring structure (Gromley et al., 2005). A previous study in our lab has shown that FIP4 colocalises extensively with MKLP1 at the

midbody ring (Fielding. A, unpublished data). Arf6 has been discovered to interact with exocyst component Sec10p (Prigent et al., 2003), which raises the possibility that Arf6 tethers endosome vesicles to exocytosis sites marked by exocyst. Together with the dual interaction of FIP4 with Rab11 and Arf6, this suggests that FIP4 and Arf6 may reach the midbody and midbody ring to anchor Rab11-positive RE vesicles via their interaction.

3.3.2 Rab11 and Arf6 play vital roles during mammalian cell cytokinesis

Given the localisation of Rab11 and Arf6 to the cleavage furrow and the midbody bridge, it was sought to determine whether they play an active role in this cellular process. Therefore, Rab11's role was tested by overexpressing its GDP-locked inactive form in HeLa cells, this mutant led to a high frequency of binucleate cells. The nuclei in these abnormal cells appear to be intact, suggesting karyokinesis was not affected, but a blockage occurred during cytokinesis. This was the first study to show that Rab11 mediated membrane trafficking is an integral facet of mammalian cytokinesis, which complements previous studies carried out in both *Drosophila* and *C. elegans*, which have shown that Rab11 is essential for successful cellularisation and cytokinesis (Riggs et al., 2003; Skop et al., 2001). This result was supported by the data using depletion of Rab11 by siRNA and microinjection of antibody against Rab11, both of which increased cytokinesis failure.

Similar methods were also used to investigate Arf6's function. It was previously reported that Arf6 GTP restricted form (Q67L), induces aberrant phenotypes in cytokinesis, such as binucleated, visibly connected and closely positioned cells (Schweitzer and D'Souza-Schorey, 2002). In our hands, transfection of the Arf6 GDP-locked mutant increased the fraction of binucleate cells. It was also revealed that the defects caused by wild type Arf6 and its GTP-locked mutant were less severe, in which only an slight increase in binucleation percentage was observed. This result is somehow different with what has been shown in the Schweitzer paper, however, this can be explained by various expression level and expression timing of these mutants in distinct experiments, these may have caused different phenotypes. In addition, GTPases act based on their GTP cycles, overloading any form of the GTPase in question will affect the cycle and block corresponding GTPase function.

The RNAi method was also applied to knock down endogenous Arf6. Surprisingly, the depletion did not induce any obvious abnormality in cytokinesis, suggesting a

compensatory mechanism may take over in the absence of Arf6. Considering cytokinesis is such a vital event for cells, it is likely that cells may employ redundant machineries to ensure it completes successfully to maintain genetic stability. Using multidimensional protein identification technology (MudPIT), Skop. A and colleagues have identified 160 proteins that possibly function in cytokinesis from purified midbodies of CHO cells. Among these 160 candidates, 36% of them have been previously been shown to play roles in this process. Further analysis using RNAi was carried out to study homologous genes in *C. elegans*. In the 172 genes detected, 38 of them have previously been shown involved in *C. elegans* mitosis or meiosis. 16 of them specifically function in cytokinesis (Skop et al., 2004). The Arf6 RNAi results reported here are somewhat distinct from that of a similar study using siRNA against Arf6 but different target sequences were used (Schweitzer and D'Souza-Schorey, 2005). They reported that depletion of Arf6 caused an increased frequency of cells remaining "closely appositioned", which they interpreted as a defect in abscission. However, their data were collected from synchronised cells 6 h after entering mitosis, whereas the data shown here are not collected from synchronised cells. Regardless of this, both studies support an integral role of Arf6 in cytokinesis.

As the binucleate assay has its limits to detect minor defects and the precise stage of individual proteins acts, time-lapse microscopy was employed to test the role of Rab11 and Arf6 in more detail. Time-lapse video microscopy of Rab11 RNAi and Rab11 S25N expressing cells clearly revealed that disruption of Rab11 did not affect furrowing, but midbody abscission. The cells formed cleavage furrows and midbodies as normal, however, the two daughter cells connected by the midbody bridge fused back to one containing two individual nuclei, suggesting a blockage occurred during final abscission.

Interestingly, a striking phenotype was observed in cells depleted of both Rab11 and Arf6: complete rapid regression after furrow formation. This regression is earlier compared to the Rab11 single knockdown phenotype. In this case, the furrow ingresses with normal dynamics, but it regresses before a midbody bridge is formed, about an hour after onset of anaphase. This observation suggests that the co-depletion may have an effect on midbody formation and stabilisation, which has been reported to happen earlier than lack of membrane material for the abscission step (Severson et al., 2000). Considering GFP-Arf6 T27N, a GDP-locked mutant also caused furrow regression with the midbody hardly formed (Fig. 3.13), this suggests that Arf6 may have a function in midbody formation and stabilisation as well as membrane delivery for finishing cytokinesis. This idea is supported by the fact that Arf6 is involved in regulating cytoskeleton dynamics by associating with MT and cortical actins. Interestingly, it has been shown to increase the ability of Rac to

form PM ruffles (Radhakrishna et al., 1999). A recent study suggested that Rac activity needs to be down-regulated to diminish cortical stiffness and favour acto-myosin ring constriction regulated by RhoA and ROK in *Drosophila* S2 cells (D'Avino, et al., 2006). This brings a focus for the quick regression phenotype observed in this study. The interruption of Arf6 may affect Rac activity, hence might increase cortical stiffness and cause the acto-myosin to bounce back early before midbody formation. Therefore, it will be interesting to further investigate the connection of Arf6 and the Rac/Rho pathway during cytokinesis in future study.

However, it is puzzling the defects of midbody formation caused by Arf6 only occurred while over-expressing its GDP restrict mutant or by co-depletion with Rab11. An interpretation that fits in this situation might be that Arf6 functions to maintain the midbody as well as facilitate docking of Rab11/FIP4 containing vesicles. When Arf6 is knocked down, another unknown molecule, possibly another Arf protein, may take over its role. This molecule is probably delivered to the midbody by the Rab11-regulated vesicles. Hence, when Arf6 and Rab11 were both depleted the potential molecule that may compensate for Arf6's role fails to reach the furrow/midbody zone, hence causing early regression from the furrow. As for the defects caused by Arf6 T27N, the mutant may occupy the location at the midbody. Therefore, the active candidate cannot be correctly positioned, leading to furrow regression as shown in Figure 3.12.

3.3.3 A model of Rab11/FIP3/4/Arf6 ternary complex regulates membrane delivery to the furrow/midbody

The class II FIPs (Rab11-FIP3 and Rab11-FIP4) have been shown to be able to interact with both Rab11 and Arf5/6 proteins (Hickson et al., 2003; Shin et al., 2001). Previous studies from our group and this study showed that FIP3 and FIP4 localise to the centrosomes from metaphase and then to the furrow/midbody during cytokinesis, which is strikingly reminiscent with the distribution of its interaction partners. During the course of this study, our group showed that FIP3 is recruited to the RE by Rab11 and plays a role in cytokinesis. However, targeting of FIP3 to the midbody is independent of Rab11 (Wilson et al., 2005). Our further investigation showed that FIP4 and FIP3 interact with Rab11 and Arf6 at distinct sites. A point mutation of FIP3 (I737E) blocks the binding of FIP3 to Rab11, but not Arf6. Similarly, a corresponding mutation in FIP4 (D538A) also abrogates Rab11 interaction, while it still interacts with Arf6 (Fielding et al., 2005). Therefore Arf6 is proposed to facilitate the localisation of FIP3/FIP4 vesicles delivered to the midbody

site. In this study, by using Arf6 GTP deficient mutants, it is shown that the activity of Arf6 is required for both Rab11 and FIP3/4 localisation to the midbody. Interestingly, *in vitro* interaction assay using recombinant bacterially expressed proteins suggests that Rab11, Arf6 and FIP3/4 are able to form a ternary complex (Fielding et al., 2005), though the scenario *in vivo* still remains to be further elucidated. Time-lapse microscopy provided convincing results showing that interference of Rab11 and Arf6 leads to similar defects at the late stage of cytokinesis. Disruption of FIP3 by using RNAi and point mutant has indicated similar phenotype, however, RNAi study of FIP4 has not been successful and will be continued and discussed in Chapter 5.

Accordingly, these data may suggest that recruitment of FIP3/4 to the pericentrosome RE vesicles is dependent on Rab11. The "Arf6 endosome" that employs a distinct route with the classical endocytic pathway may fuse with the Rab11-containing endosome and encounter FIP3/4. The Rab11/FIP3/4/Arf6 then arrives at the furrow/midbody in a manner dependent upon Arf6 activity. The data of the immunofluorescence, binucleate assay and time-lapse microscopy experiments presented in this chapter firmly support the hypothesis that delivery of the Rab11/FIP3/4/Arf6 vesicle is essential for sealing the intercellular bridge between two daughter cells to complete cytokinesis.

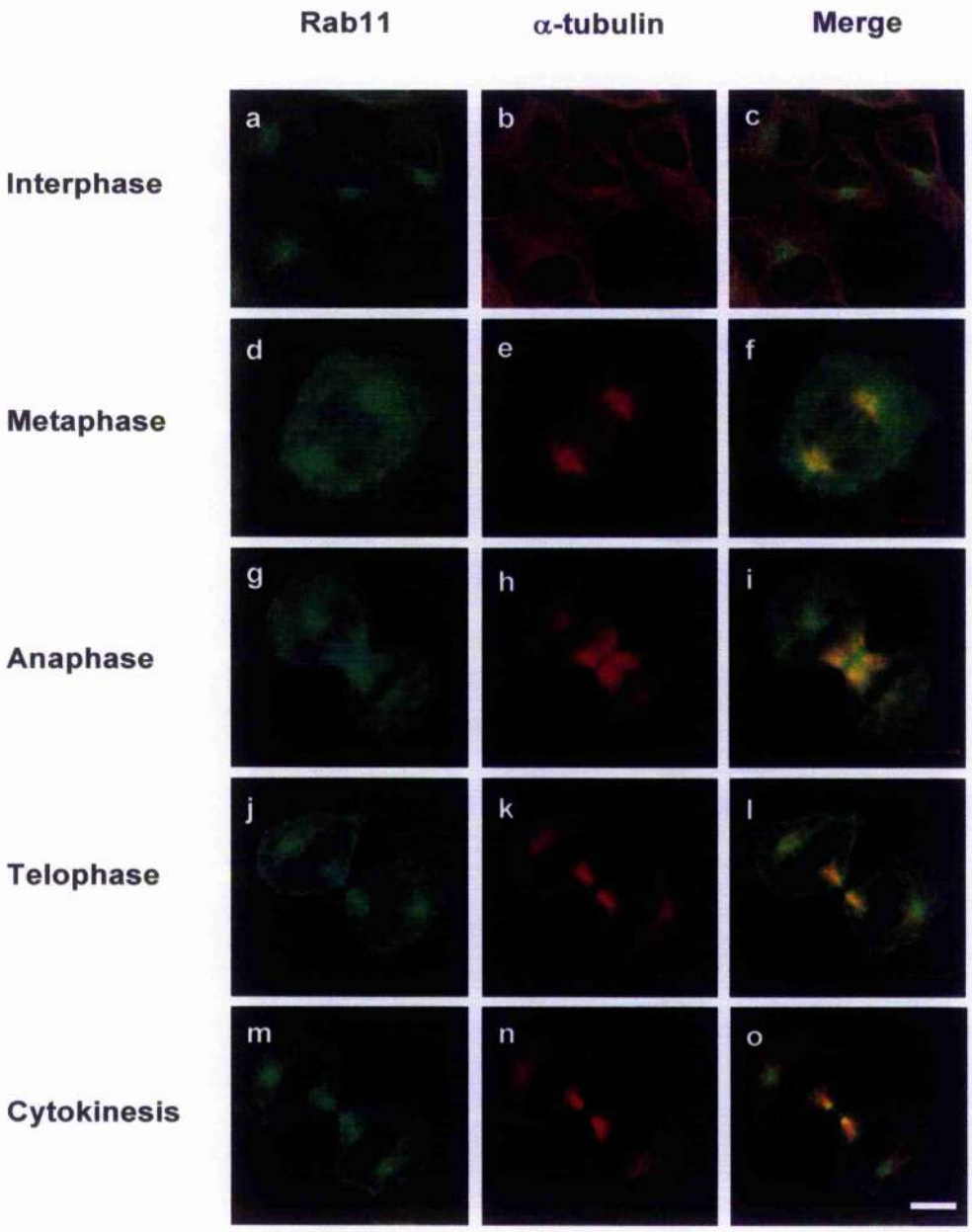

Figure 3.1 Subcellular localisation of endogenous Rab11 in HeLa cells during mitosis

HeLa cells grown on 13 mm glass coverslips were fixed in 4% paraformaldhyde and then pemeabilised with 0.1% Triton-X-100. Cells were then processed for immunofluorescence using primary anti-Rab11 antibody followed by Alexa-488 anti-rabbit secondary antibody (green). They were also stained with anti-αtubulin antibody followed by Alexa-594 anti-mouse (red). Images were collected with a Zeiss Pascal Microscope (see section 2.2.4.2). The 488 nm, 594 nm channels are shown individually and merged together. Data from a representative experiment are shown. Scale bars: 10 μm.

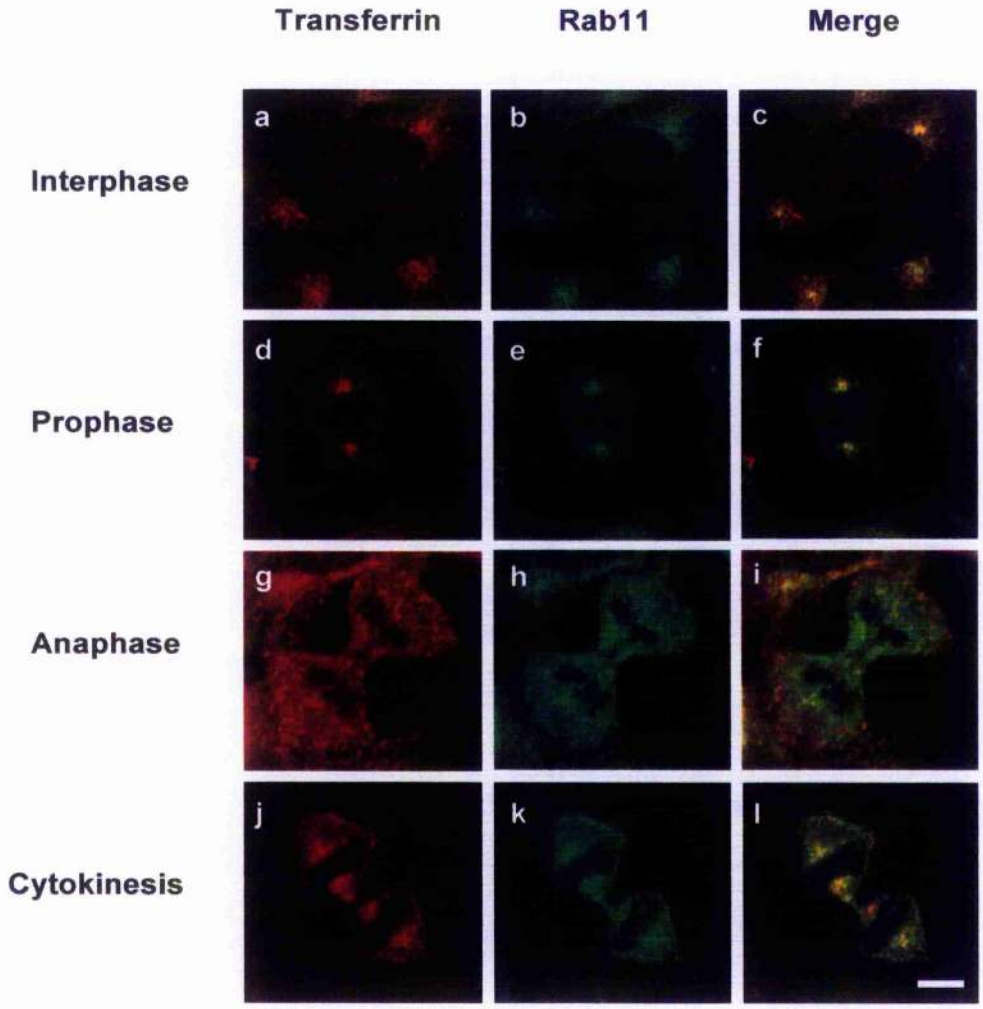

Figure 3.2 Colocalisation of Rab11 and Transferrin throughout mitosis

Serum starved HeLa cells were incubated with Texas-red Tf for 30 min and washed extensively. Cells were then fixed and stained with endogenous Rab11 using anti-Rab11 followed by an Alexa-488 conjugated secondary antibody. Cells at different stages of mitosis were observed, and representative images were shown above. Yellow areas shown in merged images (c, f, i, l) represent the degree of colocalisation of Rab11 (green) and Tf (red). Scale bar: 10 μm.

A

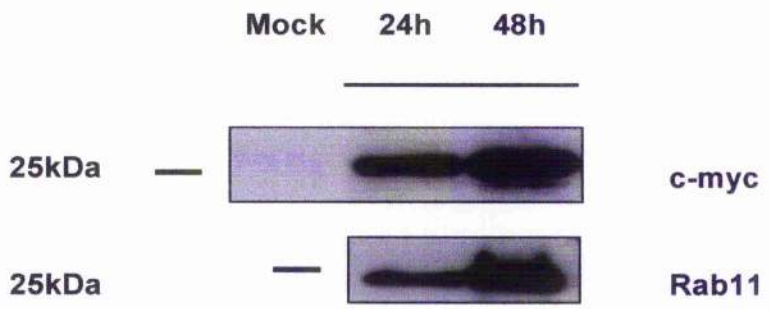
Mock
24h
48h
25kDa
c-myc
25kDa
Rab11

B

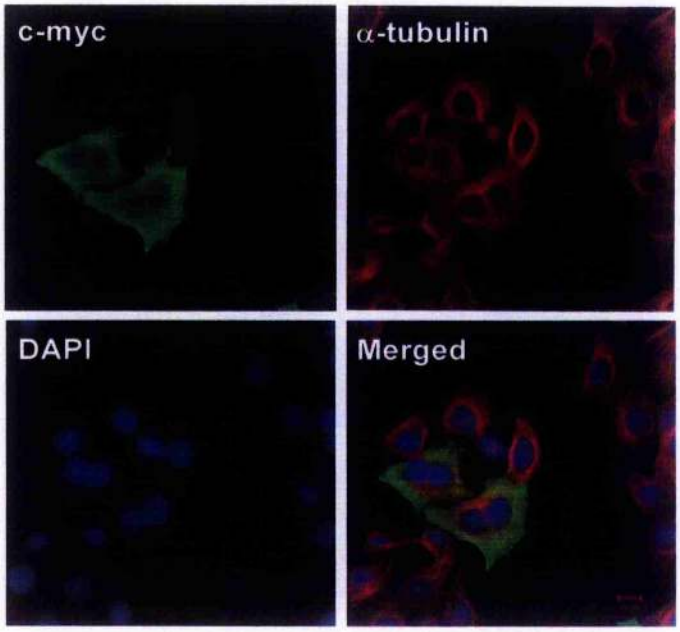
c-myc
α-tubulin
DAPI
Merged

C

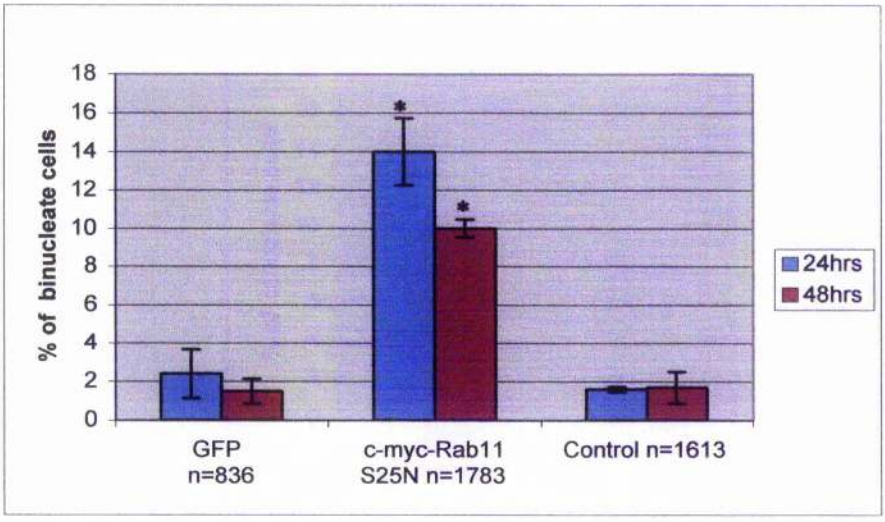
% of binucleate cells
18
16
14
12
10
8
6
4
2
0
*
*
24hrs
48hrs
GFP
n=836
c-myc-Rab11
S25N n=1783
Control n=1613

D

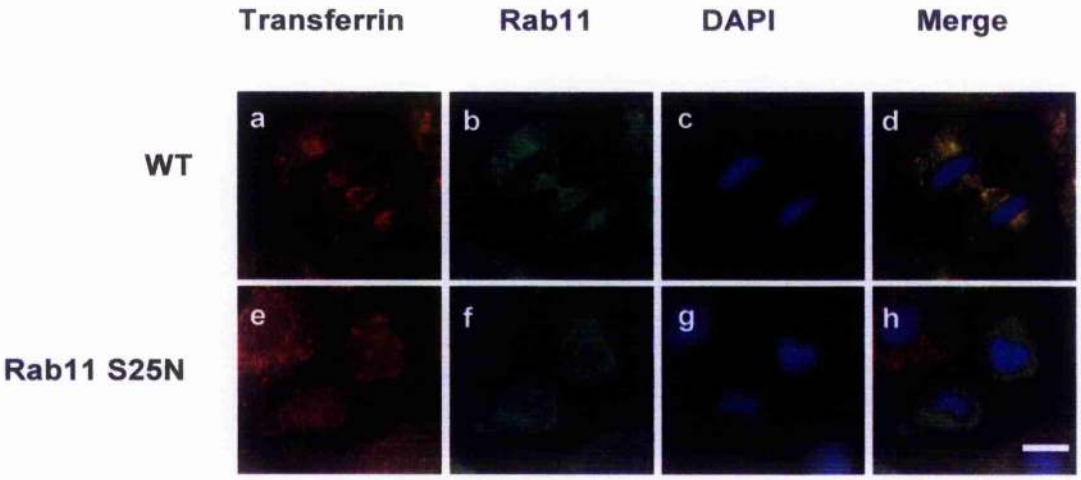

Figure 3.3 Rab11 S25N expression leads to cytokinesis defects

HeLa cells were infected with c-myc-Rab11 S25N adenovirus and left for 24 and 48 h before further analysis by immunoblot and immunofluorescence. Virus expressing GFP alone was used as a negative control. **(A)** A fraction of cells were used to make cell lysates for immunoblotting to examine the ectopic protein expression level. Blot of cells 24 and 48 h post-infection with anti-c-myc and anti-Rab11 antibodies are shown. **(B)** Cells were then fixed and stained with anti-αtubulin antibody recognized by an Alexa-594 fluorescence secondary antibody (red). c-myc-Rab11 S25N was detected by staining with a rabbit anti-c-myc antibody followed by Alexa-488 secondary antibody (green). DAPI was used to stain the nuclei. The confocal image shows a typical field of cells observed from the coverslips. 488 nm, 594 nm and DAPI channels were shown separately and merged. **(C)** The bar graph shows the percentage of cells containing double or multiple nuclei of cells expressing myc-Rab11 S25N, GFP alone as well as uninfected ones, which are the means ± SD. $^{*}p<0.01$ (t-test) compared to the GFP alone expression controls. Each bar is the average of 5 independent experiments in which more than 150 cells were quantified. Total cell counts were shown below the corresponding bar. **(D)** Panel a-d, wild-type cells that had internalized Texas-red Tf (red) after 30 min were co-stained with endogenous Rab11 (green). Panel e-h, cells that had internalized Texas-red Tf (red) were co-stained with c-myc (green) to detect expression of Rab11 S25N. Scale bar: 10 μm.

A

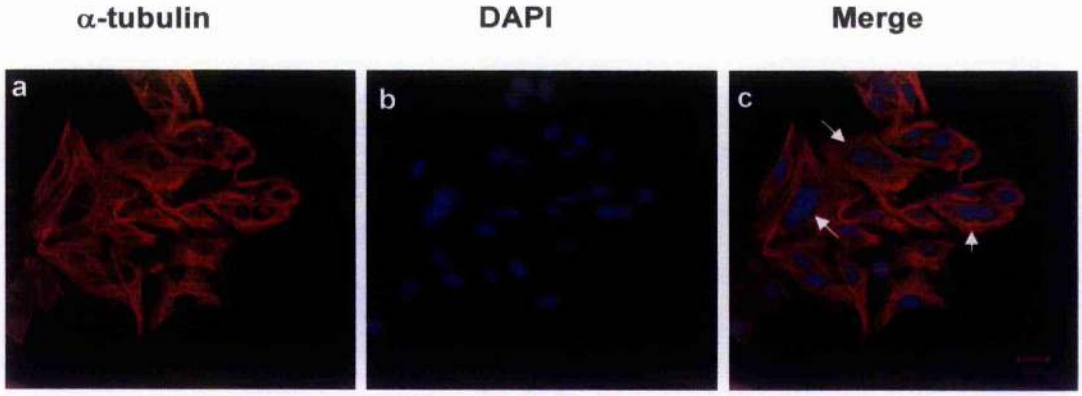

B

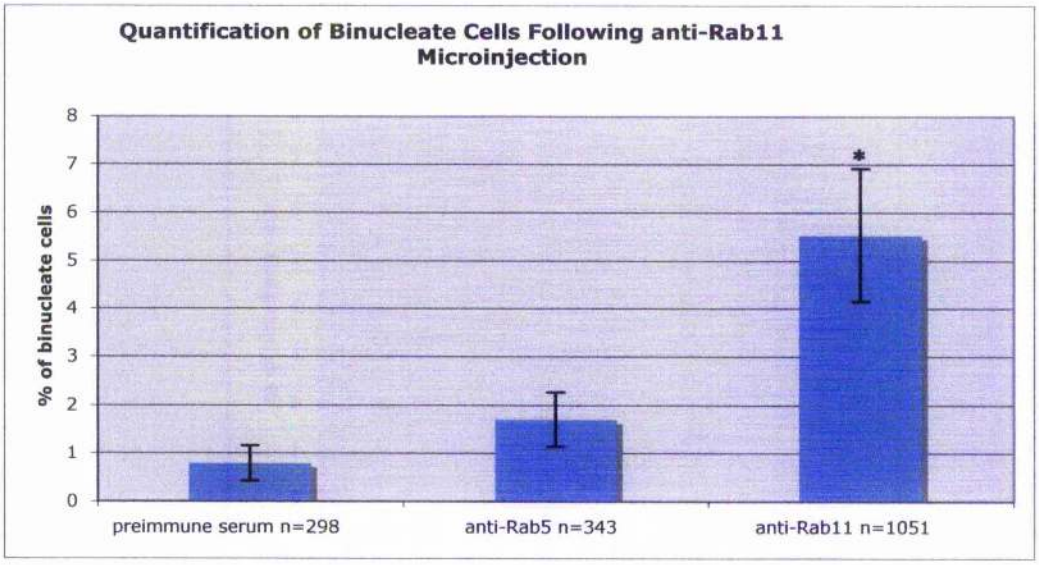

Figure 3.4 Microinjection of antibody against Rab11 inhibits cytokinesis

HeLa cells grown on Cellocate (Eppendorf) were injected with antibody against Rab11a and incubated at 37 °C for 48 h before being fixed and processed for immunofluorescence to observe binucleation. **(A)** Cells were then stained with anti-αtubulin (red) and DAPI (blue). Induced binucleate cells are indicated with white arrows in panel c. **(B)** The bar graph shows the percentage of binucleate cells in cells injected with anti-Rab11, anti-Rab5 and pre-immune serum. The bars are the means ± SD. *$p<0.05$ (t-test) compared to the preimmune serum injection control. Scale bar: 10 μm.

A

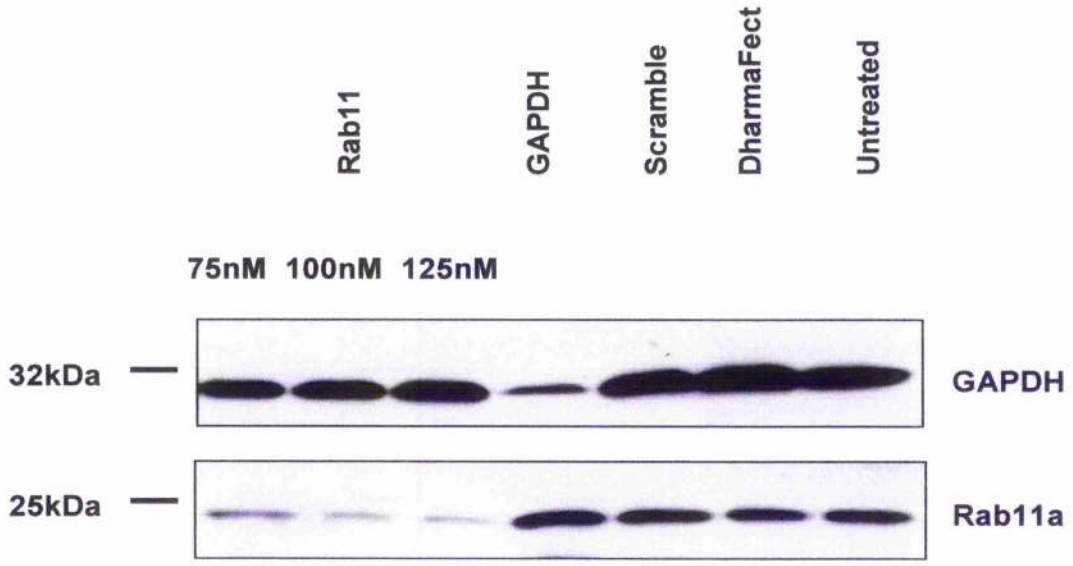
Rab11
GAPDH
Scramble
DharmaFect
Untreated
75nM 100nM 125nM
32kDa
GAPDH
25kDa
Rab11a

B

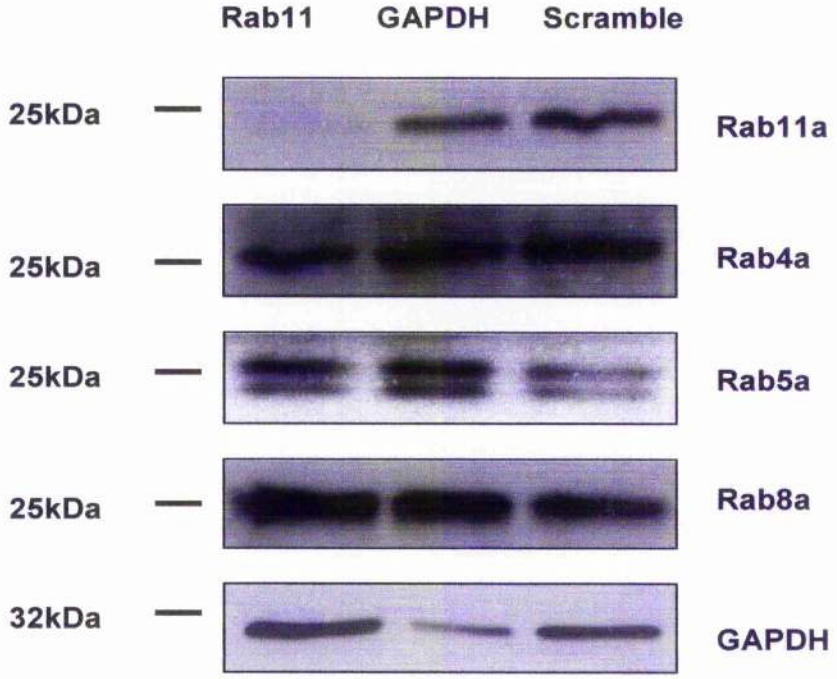
Rab11 GAPDH Scramble
25kDa
Rab11a
25kDa
Rab4a
25kDa
Rab5a
25kDa
Rab8a
32kDa
GAPDH

C

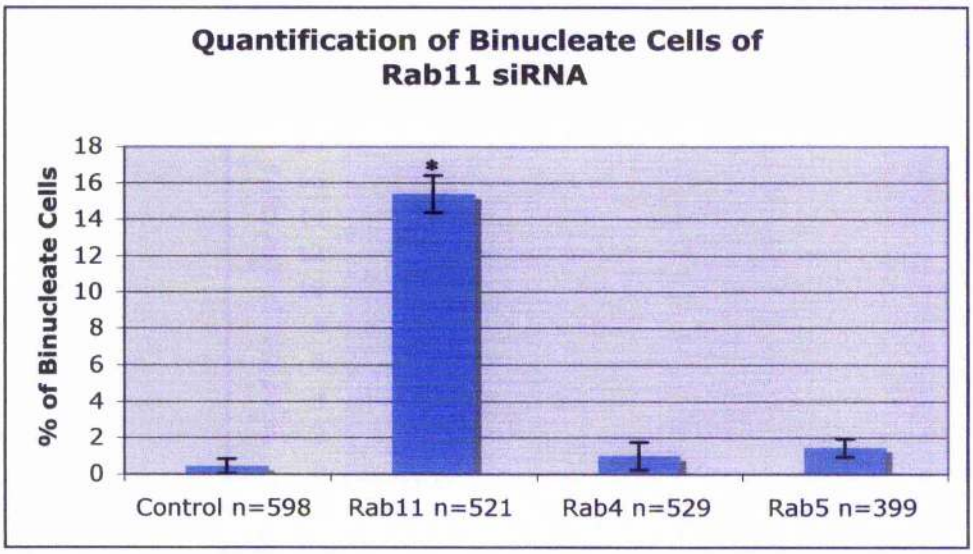

Figure 3.5 RNAi depletion of Rab11 inhibits cytokinesis

HeLa cells were treated with siRNA duplexes against Rab11 and incubated 48 and 72 h before analysis. **(A)** Immunoblots indicate that Rab11 was efficiently depleted compared to control cells 48 h post-transfection. GAPDH was used as a loading and positive control. **(B)** Immunoblots of other Rab GTPases protein level in Rab11 knock down cells 48 h post-transfection. 100 nM siRNA against Rab11 and other Rabs was transfected into HeLa cells and the depletion is selective because other Rabs expression is not affected. **(C)** Quantification of binucleate cells percentage in cells treated with Rab11, Rab4, Rab5 and scramble (Control) siRNA cells 48 h post-transfection. The bars are the means ± SD. $^{*}p<0.05$ (t-test) compared to the scramble siRNA control.

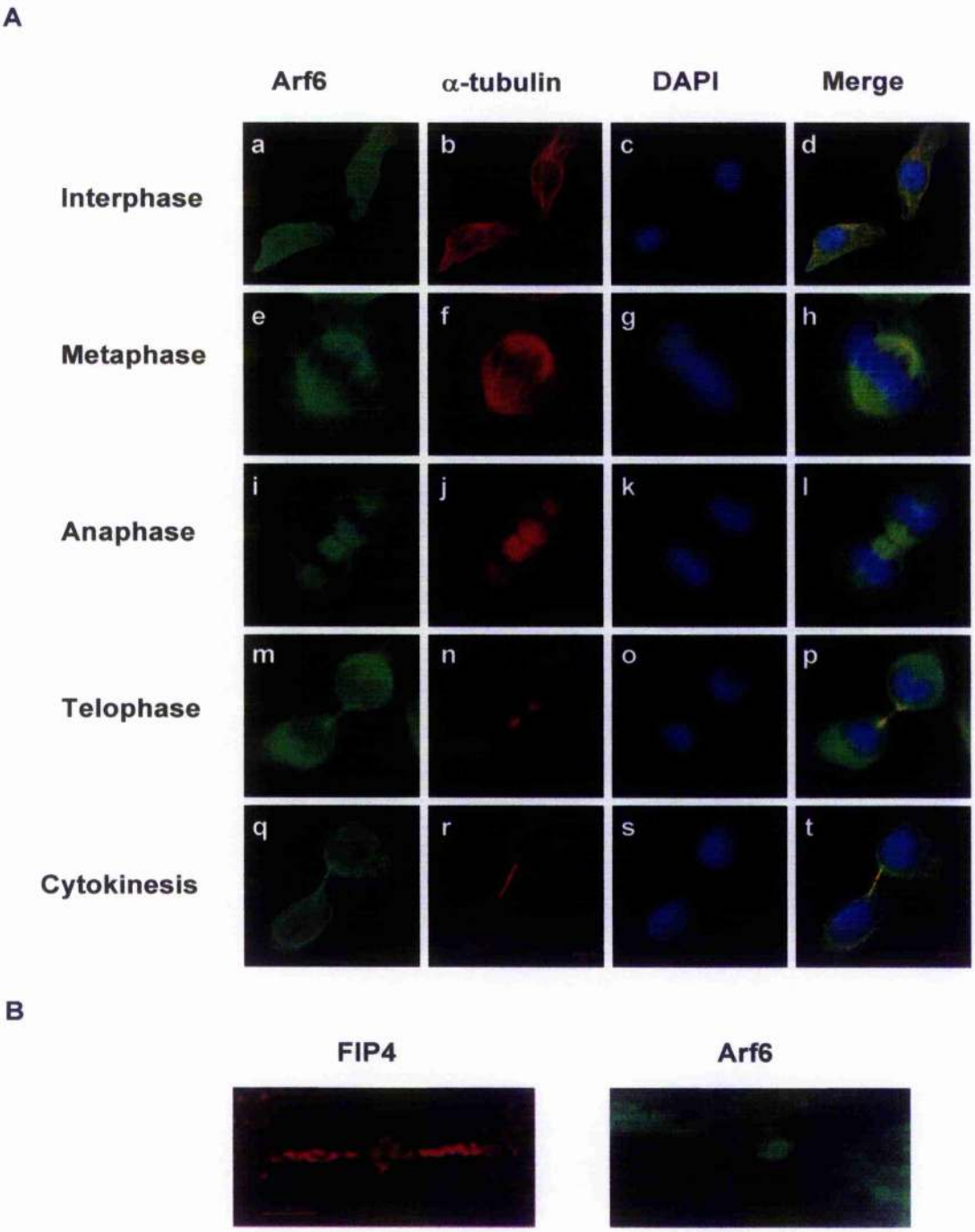

Figure 3.6 Subcellular localisation of Arf6 in HeLa cells during mitosis

(A) HeLa cells grown on 13mm coverslips were fixed and processed for immunofluorescence using a primary anti-Arf6 antibody followed by Alexa-488 fluorescent secondary antibody (green). The cells were also stained with α-tubulin followed by Alexa-594 (red). DAPI was used to stain for the DNA (Blue). Confocal images were collected of typical cells on various stages and merged images of three channels were shown on the right (d,h,l,p,t). **(B)** Cells in late cytokinesis processed as described in section A were observed with 100x objective. It was revealed that Arf6 (green) decorates a fine ring structure in the midbody bridge. FIP4 (red) has been found to localise to the same structure in a previous study (Fielding AB, unpublished data). Scale bar: 10 μm.

A

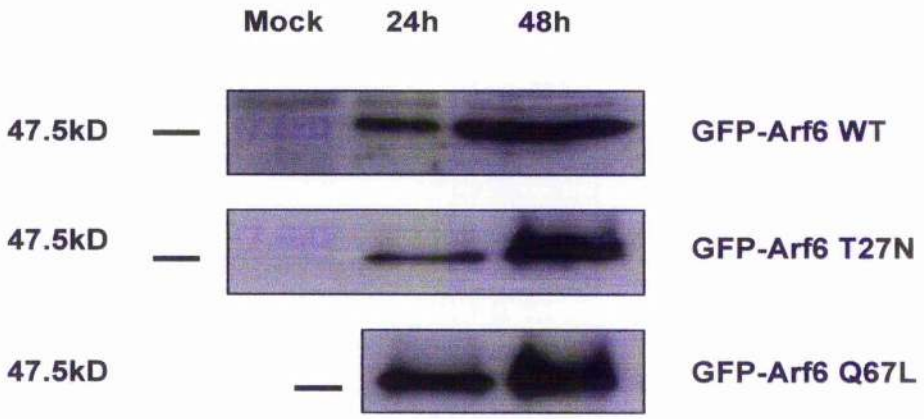
Mock
24h
48h
47.5kD
GFP-Arf6 WT
47.5kD
GFP-Arf6 T27N
47.5kD
GFP-Arf6 Q67L

B

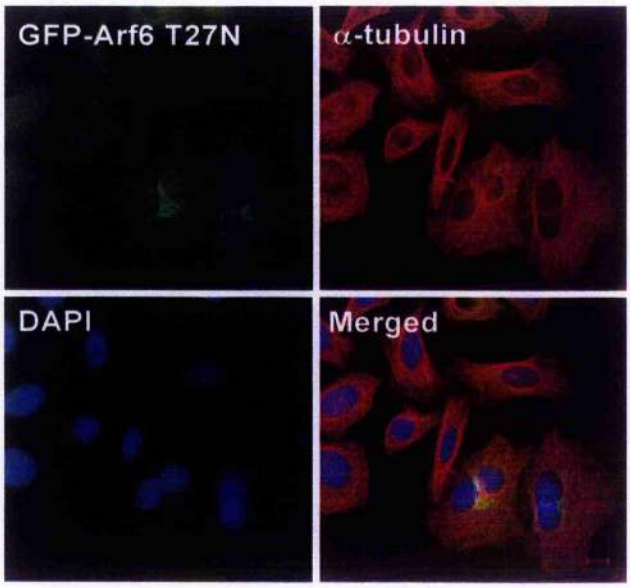
GFP-Arf6 T27N
α-tubulin
DAPI
Merged

C

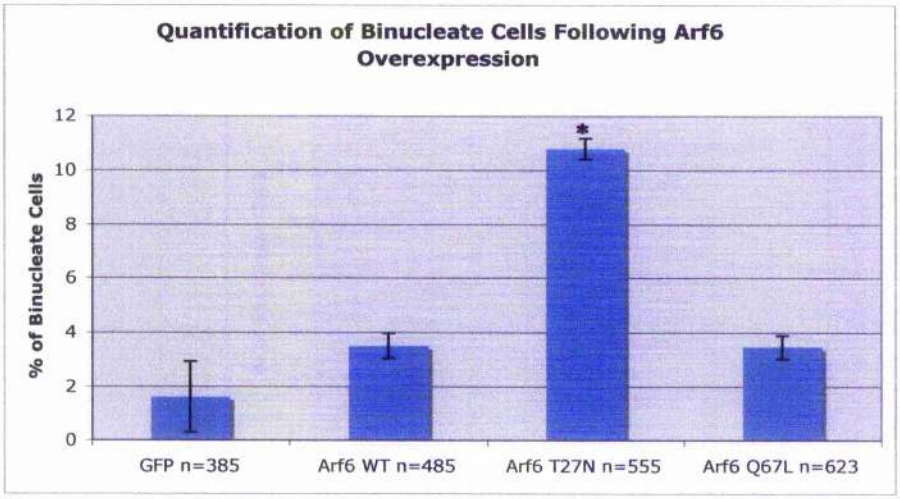
Quantification of Binucleate Cells Following Arf6 Overexpression
% of Binucleate Cells
0
2
4
6
8
10
12
*
GFP n=385
Arf6 WT n=485
Arf6 T27N n=555
Arf6 Q67L n=623

Figure 3.7 Overexpression of Arf6 T27N leads to cytokinesis defects

Cells were infected with GFP-Arf6 T27N, GFP-Arf6 Q67L or GFP-Arf6 WT adenoviruses and incubated for 24 and 48 h prior to analysis by immunoblotting and immunofluorescence. Virus only expressing GFP was used as a negative control. **(A)** A fraction of cells were used for Western blots and expression of GFP-Arf6 T27N, GFP-Arf6 Q67L and GFP-Arf6 wild type determined using anti-GFP antibody at 24 and 48 h. **(B)** Cells were fixed and stained for αtubulin (red), GFP (green) and DAPI (blue) 48 h post-infection. Images were taken on a Zeiss LSM Pascal microscope (see 2.2.4.2). 594 nm, 488 nm and DAPI channels are shown separately as well as merged. **(C)** The bar graph shows the percentage of cells with double nuclei expressing GFP, GFP-Arf6 WT, T27N, Q76L. Data represents the mean ± SD. $^{*}p<0.01$ (t-test) compared to the GFP alone expression control. The total numbers of cells quantified were shown under the corresponding bars. Each series is an average of 3 independent experiments. Scale bar: 10 μm.

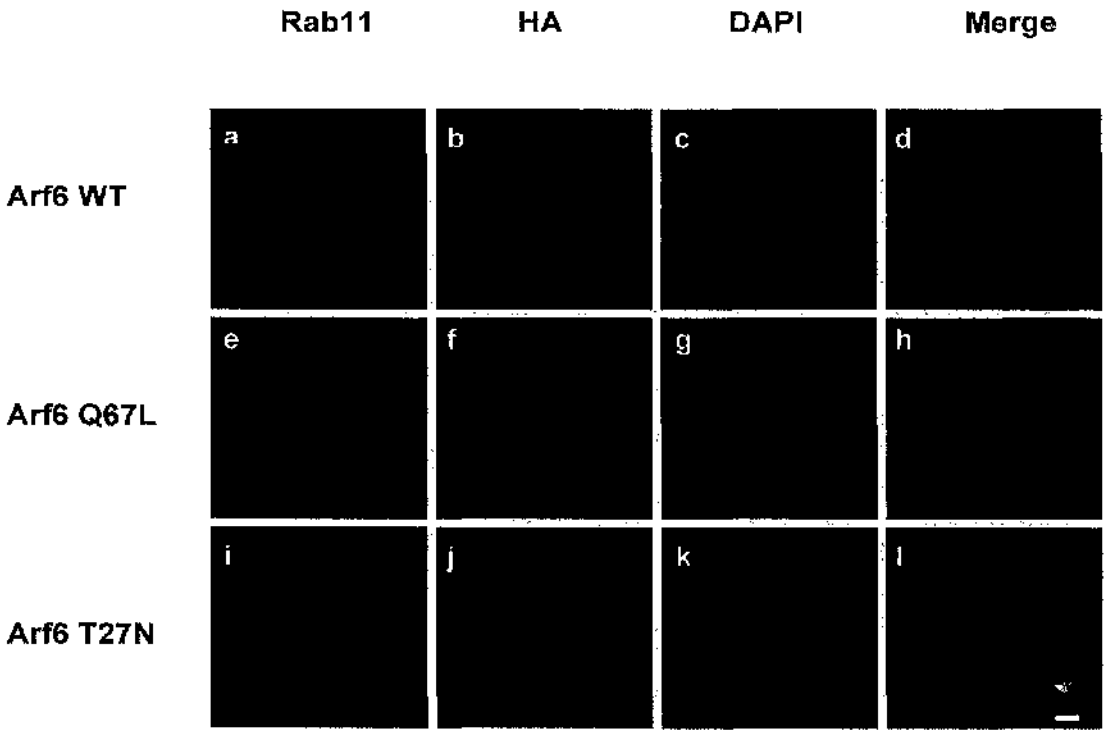

Figure 3.8 Arf6 T27N delocalises Rab11 from the midbody during cytokinesis

HeLa cells were transfected with wild type HA-Arf6, HA-Arf6 Q67L and T27N. Cells then were fixed and co-stained with anti-Rab11 and anti-HA antibody followed by Alexa-488 nm and Alexa-594 nm fluorescent secondary antibody respectively. DNA was stained with DAPI to identify cells undergoing cytokinesis and merged images were shown on the right column. Rab11 localisation to the furrow/midbody region appears normal in cells expressing wild type Arf6 (a-d) and Arf6 Q67L (e-h), however Arf6 T27N abolishes this distribution (i-l). Scale bar: 10 μm.

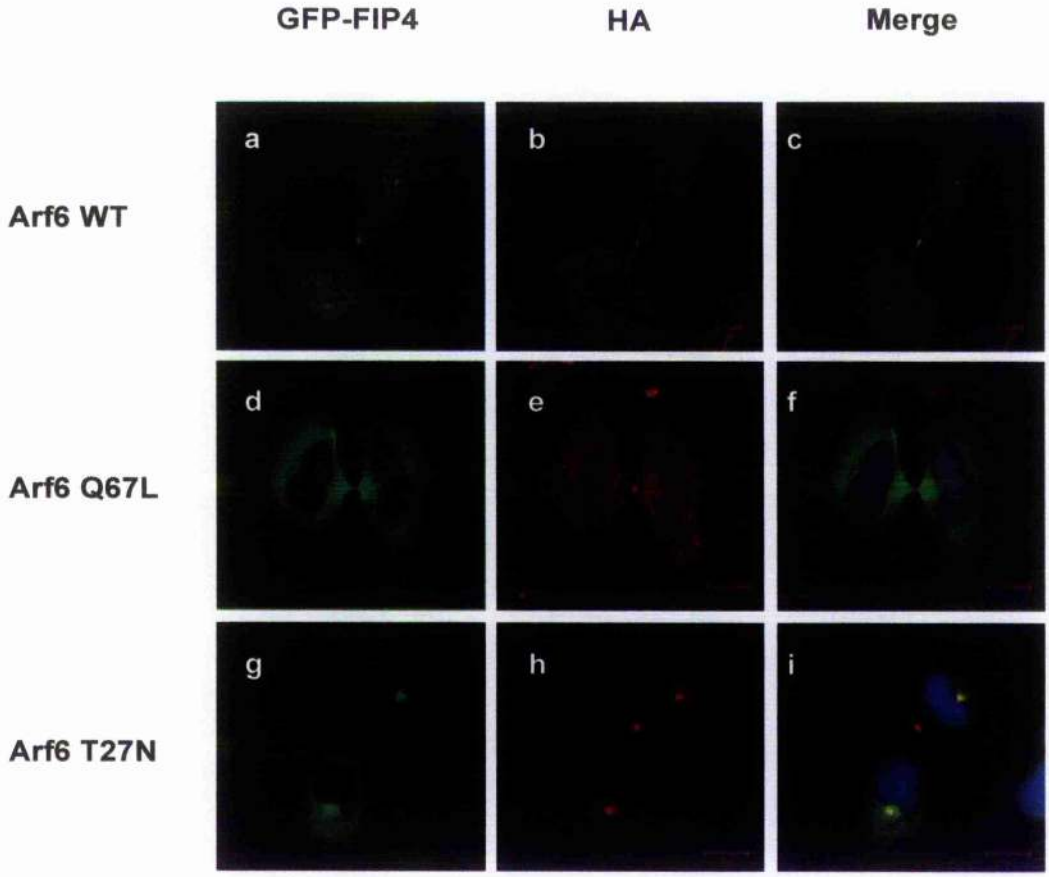

Figure 3.9 GFP-FIP4 is recruited to the midbody by active Arf6 Q67L but mislocalised by Arf6 T27N

HeLa cells were cotransfected with GFP-FIP4 and wild type HA-Arf6, HA-Arf6 Q67L and T27N. Cells then were stained with anti-HA antibody followed by Alexa-594 nm secondary antibody. Merged images were shown on the right column. GFP-FIP4 localises to the midbody in Arf6 WT expressing cells, and Arf6 Q67L accumulates to furrow/midbody in expressing cell (d-f). However, this localisation is blocked by the expression of Arf6 T27N (g-i). Scale bars: 10 μm.

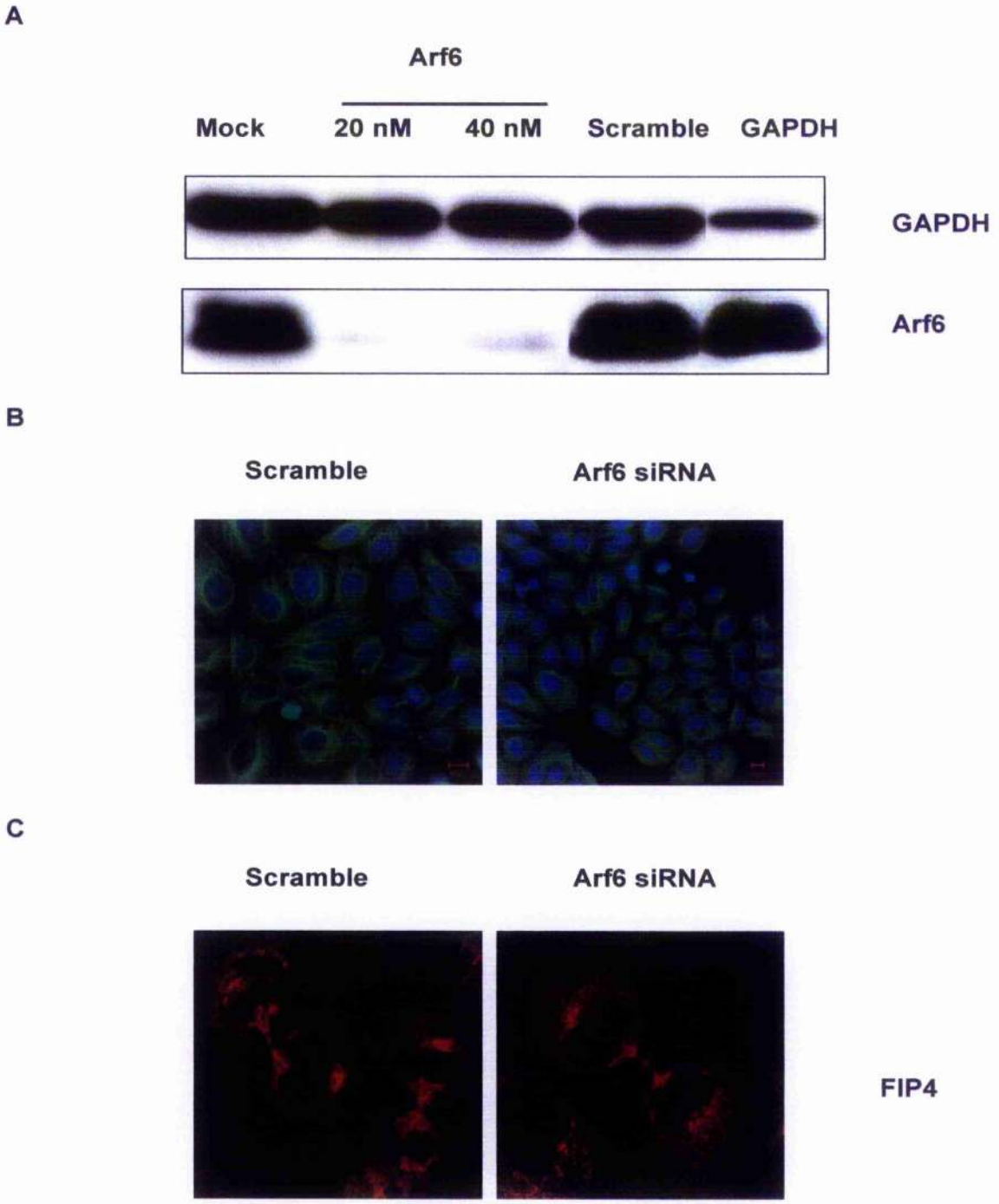

Figure 3.10 RNAi depletion of Arf6

HeLa cells were treated with siRNA duplexes against Arf6 and incubated for 24 and 48 h before analysis. **(A)** Immunoblots indicate that Arf6 was efficiently depleted compared to control cells after 24 h. GAPDH was used as a loading and positive control. **(B)** Cells transfected with Arf6 and scramble siRNA were stained with αtubulin (green) and DAPI (blue) to verify phenotype of binucleate cells. Immunofluorescence showed that no binucleate cells were observed in Arf6 knockdown cells. **(C)** Same treated cells were stained with endogenous FIP4 followed by Alexa-594 (red). As shown, FIP4's localisation to the midbody is not affected by Arf6 depletion. Scale bar: 10 μm.

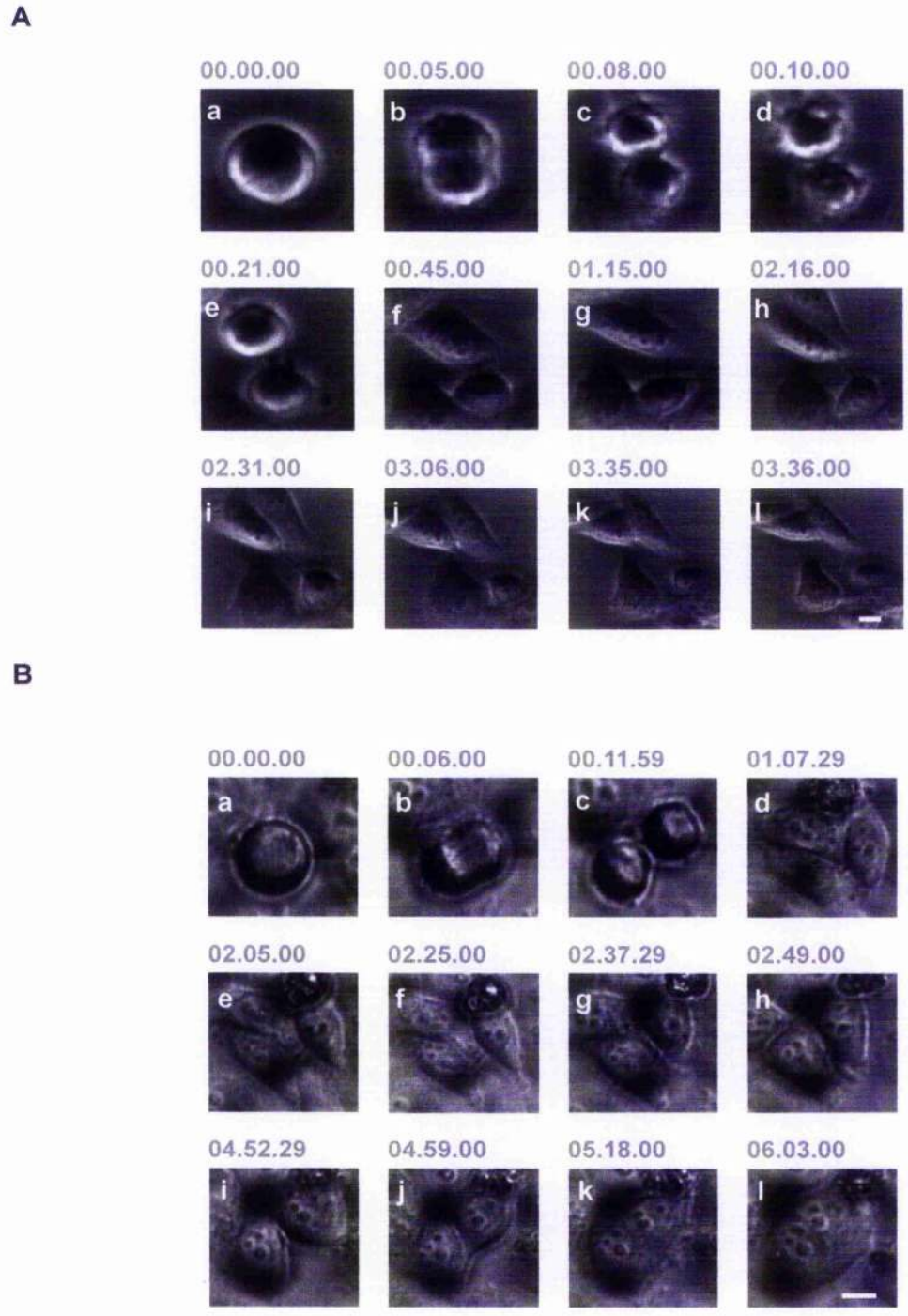

Figure 3.11 Time- lapse video microscopy of Rab11 siRNA treated cells

Wild type and cells treated with Rab11 siRNA were placed in a 37 °C chamber and phase contrast images were recorded of chosen dividing cells every 60 sec. The AVI movies were edited with Mac IMovie and selected still frames were shown here. **(A)** The wild type cell finished cytokinesis in about 3.5 h from anaphase onset. **(B)** An inhibition occurred during midbody abscission in Rab11 siRNA treated cells, which later regressed and formed binucleate cells. Real time movies corresponding to these still frames have been included in the DVD attached. Scale bar: 10 μm.

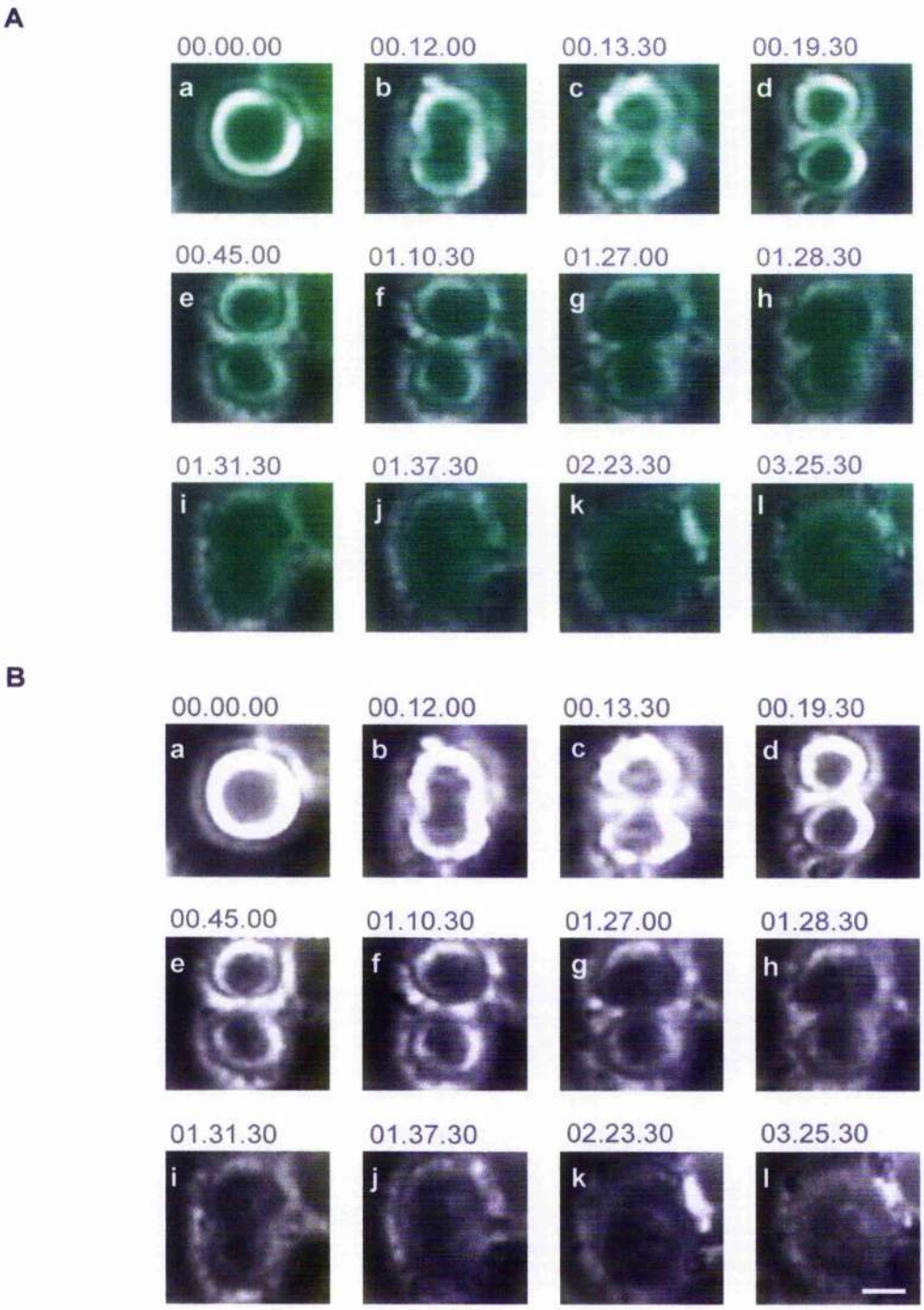

Figure 3.12 Time-lapse video microscopy of cells expressing GFP-Arf6 T27N

Cells infected with GFP-Arf6 T27N were placed in a 37 °C chamber 24 h post-infection. GFP and phase contrast images were recorded in chosen dividing cells every 60 sec. The AVI movies were edited with Mac iMovie and selected still frames are shown. **(A)** Merged images of GFP and phase contrast of a cell expressing GFP-Arf6 T27N showing it regressed after the furrow formed. **(B)** Only phase contrast selected still images to show the cell profile. Real time movies corresponding to these still frames are included in the DVD attached to this thesis. Scale bar: 10 μm.

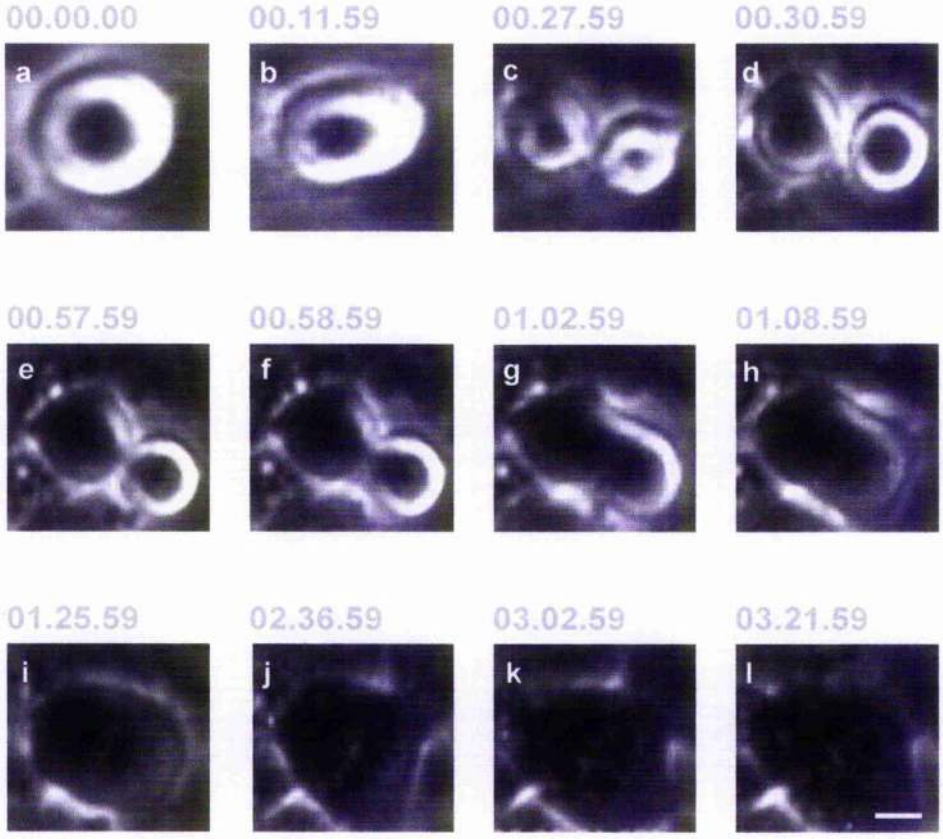

Figure 3.13 Time-lapse video microscopy of Rab11 and Arf6 co-depletion cells

Cells co-transfected with Rab11 and Arf6 siRNA were placed in a 37 °C chamber and phase contrast images were recorded of chosen dividing cells every 60 sec. The AVI movie then was edited with Mac IMovie and selected still frames are shown here. As seen, the Rab11 and Arf6 siRNA co-transfected cells exhibited a quick regression without midbody formation, which become a binucleate cell in the end. Real time movies corresponding to these still frames have been included in the DVD attached. Scale bar: 10 μm.

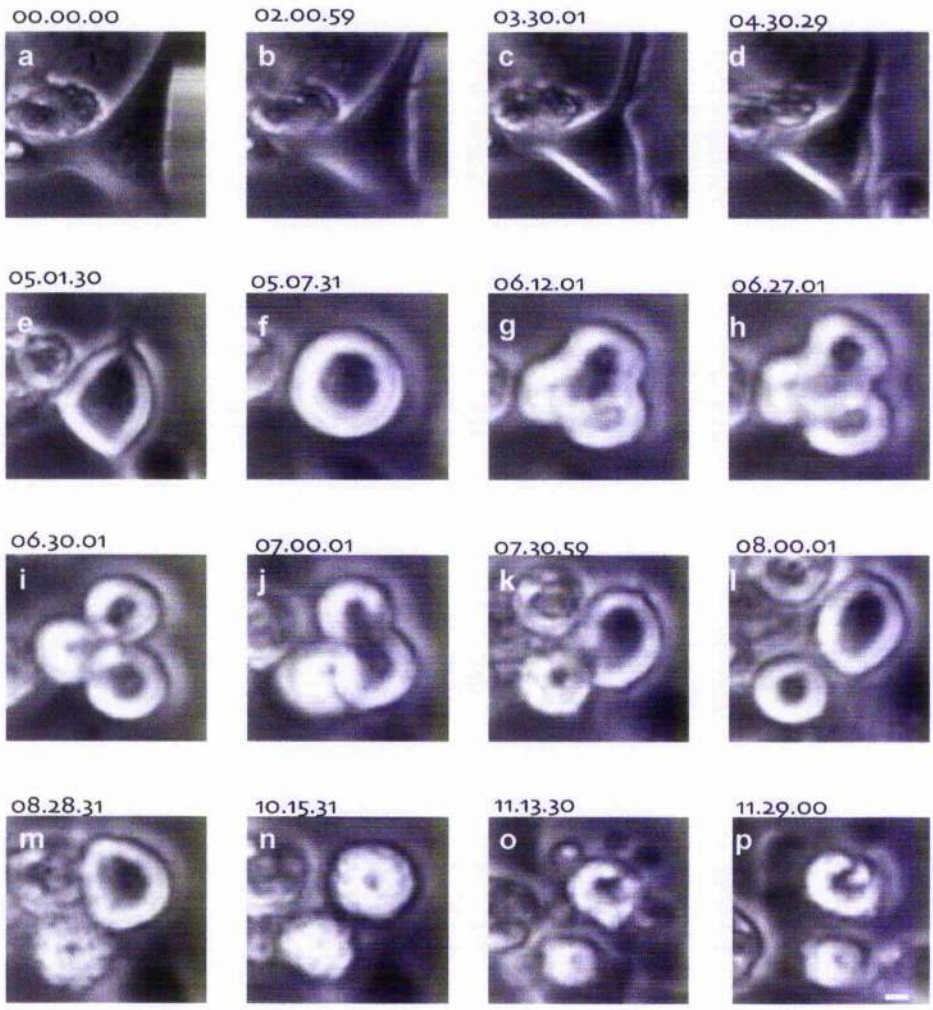

Figure 3.14 Time-lapse video microscopy of binucleate cell dividing

Cells treated with Rab11 siRNA were placed in a 37 °C chamber 48 h post-transfection. Phase contrast images were recorded of chosen binucleate cells every 60 sec. The AVI movies were edited with Mac iMovie and selected still frames were shown here. The binucleate cell could not undergo cytokinesis and execute cell death. Real time movies corresponding to these still frames have been included in the DVD attached. Scale bar: 10 μm.

4 Role of Endosomal Rabs in Cytokinesis

4.1 Introduction

4.1.1 Endocytic Rab proteins

As previously described in 1.3.1, Rab/Ypt/Sec4 proteins exist in all eukaryotes investigated and form the largest branch of the Ras GTPase superfamily (Lazar et al., 1997; Stenmark and Olkkonen, 2001). There are around 70 Rabs in humans as estimated from the sequenced genome (Zerial and McBride, 2001), of which ten subfamilies have been defined based on distinct specific sequence motifs. A number of Rabs are conserved from yeast to human. The conservation and increased complexity throughout evolution reflects an essential cellular function of these molecules in different organisms. In recent years, an increasing number of small GTPases of the Rab family have been identified and characterized that serve critical regulatory roles in vesicular transport. A strikingly high number of Rab GTPases have been localised to endosomal membrane compartments (Somsel Rodman and Wandinger-Ness, 2000).

Material internalized from the cell surface first enters the EE, where the dissociation of the ligands and receptors and sorting of the receptors take place. Rab4 and Rab5 are two Rab GTPases known to function in the early endosome pathway. Rab5 is required for the delivery of material from the PM to the EE as well as homotypic endosome fusion in this organelle, hence it controls the entry of material into the endocytic pathway (Bucci et al., 1992; McLauchlan et al., 1998). Rab4 is responsible for fast recycling from EE to PM (Sheff et al., 1999; van der Sluijs et al., 1992b). Interestingly, Rab4 has been shown phosphorylated on Ser-196 by $p34^{cdc2}$ kinase during mitosis (Bailly et al., 1991; van der Sluijs et al., 1992a). Phosphorylated Rab4 is GTP bound but cytosolic, hence this protein could be a target for regulation of endocytic transport during mitosis. Studies from our lab also indicated that depletion of Rab11 up-regulates Rab4 expression levels (Wilson et al., 2005) suggesting there may be a compensatory machinery between these two molecules.

Rab7 is involved in the transport from EE to LE as well as to lysosomes (Chavrier et al., 1990; Feng et al., 1995). It is worth noticing that this GTPase has been detected in the midbody bridge in a midbody protein screen study (Skop et al., 2004). Rab9 can be found in the LE as well as the TGN and functions in transport between these compartments (Benli et al., 1996; Lombardi et al., 1993). Rab21 largely colocalises with the EE and affects the dynamics and morphology of this organelle. Overexpression of its GDP restricted mutant, Rab21 T33N, affected effective delivery of EGF to late endosomes and

lysosomes for degradation. Its role seems to be confined to the endocytic pathway since no obvious effect of Rab21 overexpression on Golgi morphology was noted (Kauppi et al., 2002). Rab22a is associated with early and late endosomes and the TGN. Overexpression of GTP deficient mutants decreased endocytosis of a fluid phase marker and strongly affected the morphology of endosomes (Kauppi et al., 2002; Mesa et al., 2001). It has also been reported that perturbation of Rab22a affects traffic from endosomes to the Golgi apparatus, probably by promoting fusion among endosomes and impairing the proper segregation of membrane domains required for targeting to the TGN (Mesa et al., 2004). Rab22b is also termed Rab31, it has been suggested to play a role in anterograde exit from the TGN (Ng et al., 2007).

4.1.2 Hypothesis and Aim

Completion of cytokinesis requires Rab11-dependent membrane trafficking events to deliver new membrane to the dividing site for the midbody abscission. Many Rab proteins have overlapping distribution in endosomal trafficking pathways and the different Rab-controlled domains exchange membrane material dynamically. Therefore, it is proposed that other endosomal Rabs besides Rab11 may also contribute additional membrane material for the process of cytokinesis. In this chapter, the localisations of Rabs mainly involved in endocytic pathway in cell cycle were examined. Using RNAi and Rab GTP-deficient mutants, their functions in cell division was further investigated.

4.2 Results

4.2.1 Localisation of endosomal Rabs during cytokinesis

In Chapter 3, it has been shown that Rab11 mediated RE trafficking is a crucial facet of cytokinesis. Our studies also revealed that Rab11 positive vesicles are enriched at the furrow/midbody region to supply the required membrane for cytokinesis. Since Rab proteins are known key regulators of intracellular membrane trafficking and the whole pathway is tightly interconnected and orchestrated, we asked the question whether other endosomal Rabs are involved in this process by exchanging membrane material with Rab11 regulated RE. It was first sought to examine whether other endosomal Rabs exhibit similar localisation as Rab11.

To address this, the distribution of GFP-tagged Rabs that have been shown by other groups to faithfully report the localisation of endogenous proteins were examined (Miaczynska and Zerial, 2002; Weigert et al., 2004). In this regard, Rab4 and Rab5, the classic Rabs involving in early endosomal traffic have been examined; Rab21 and Rab22, Rab proteins suggested to communicate different domains within the secretory and endosomal pathways, and Rab7 and 9 which regulate traffic in the late endosomal pathway. We were also interested in Rab8, which has been reported to play a critical role in cytokinesis in *C. elegans* embryos (Skop et al. 2001).

To investigate the role of the selected endosomal Rabs in cytokinesis, first their subcellular localisation during this process was studied. Figure 4.1 shows the localisation of these endosomal Rab proteins during cytokinesis. In good agreement with previous studies, Rab11 concentrates strongly to the furrow/midbody of all cells undergoing cytokinesis. In contrast, no accumulation of any of the other Rabs in these regions was observed. Intriguingly, we consistently found that Rab4, 5, 7, 8 and 9 stained a perinuclear compartment facing away from the midbody region in dividing cells. Image analysis revealed that for these Rabs the image intensity of the GFP-signal between the two mitotic spindle poles was at least 2-fold lower than that observed outside the two poles (data not shown). This distribution was the opposite with that of Rab11, which consistently stained the furrow and midbody regions between the two mitotic poles, see Figure 3.1

However, the lack of localisation of a given Rab protein to the furrow/midbody does not necessarily preclude an important role for these Rabs in cytokinesis, since these Rabs may function to control traffic from a given compartment to Rab11 regulated vesicles then into

the furrow/midbody region. Hence, functional assays were carried out to determine the consequences of disrupting these endosomal Rab proteins. Two independent approaches, over-expression of GDP restricted mutants of Rabs or depletion by RNAi was used.

4.2.2 Function of endosomal Rabs during cytokinesis

4.2.2.1 Over-expression of Rab GDP restricted mutants

To determine whether disruption of the endosomal Rabs has an effect on cytokinesis, first we expressed GDP resticted mutants of these proteins. To facilitate this, plasmids expressing c-myc tagged Rab4 S22N, Rab5 S34N, Rab11 S25N, Rab21 T33N and Rab22 S19N were transfected into HeLa cells. 24 h post-transfection, cells expressing these mutants were fixed and stained with the c-myc tag antibody to reveal expression. The results were compared to data obtained upon over-expression of Rab11 S25N that has been previously shown to induce cytokinesis defects. Cells positive for the Rab mutants in question with two or more nuclei as an index of cytokinesis failure were quantified and shown in Figure 4.2, panel B. As shown, in all the Rab proteins screened in this experiment, only Rab11 S25N expression resulted in increased cytokinesis defects, with about 15% Rab11 S25N positive cells exhibiting a binucleate phenotype. In Figure 4.2, panel A, immunoblotting of cell lysate expressing the Rab4, 5 or 11 mutants revealed that their expression levels are at least higher than that of the endogenous Rab in all cases.

To ensure the over-expression of GDP restricted mutants does perturb the Rabs function in endocytic traffic, the distributions of internalized Texas Red-Tf in cells over-expressing Rab4 S22N, Rab5 S34N and Rab11 S25N were examined. As described in 2.2.3.7, HeLa cells were incubated with 25 μg/ml Texas Red-Tf for 30 min at 37 °C followed by extensive washing. Cells then were stained with c-myc followed by Alexa-488 to view expression of these mutants as well as internalized Tf distribution. Figure 4.2, panel C shows that all these mutants functioned as expected and interfered with endosomal traffic in manners similar to previous studies. Rab5 S34N expression significantly reduced Tf uptake into the cells, Rab4 S22N resulted in an increased peripheral dots distribution of the Tf containing vesicles, while Rab11 S25N expression caused tubularisation of the endosomal network (Bottger et al., 1996; Rybin et al., 1996; van der Sluijs et al., 1992b)

4.2.2.2 RNAi of endosomal Rabs

Since over-expression of Rab proteins may induce non-specific events, or may not reach the levels of expression sufficient to exert an effect in cytokinesis, an alternative approach to further screen the functions of the endosomal Rab proteins, as well as to extended the study to examine the role of more other members of the Rab family was applied.

Dharmacon siRNA SmartPools selective for the different Rabs were used. The SmartPool siRNA is a pool consists of 4 mixed siRNA duplexes targeting distinct sites of the mRNA, and guaranteed to cause more than 75% reduction of target gene at mRNA level. Since many of the Rabs exist as different isoforms, including Rab4 (a, b), Rab5 (a, b, c), Rab11 (a, b), Rab8 (a, b), and Rab9 (a, b), siRNA selective for the different isoforms were used in combination with the intention to knock-down all isoforms of the Rab in question. It was first sought to verify the selectivity of the SmartPool reagents. HeLa cells were transfected with SmartPool siRNA against individual isoform of each Rab protein and cells were lysed 48 h post-transfection for immunoblotting to analyse knockdown of expression of the corresponding protein. Figure 4.3 panel A shows the immunoblots of selective depletion of each isoform. Take Rab5a for example, Rab5a was effectively depleted in cells treated with corresponding siRNA, whereas the SmartPool designed to deplete cells of Rab5b or Rab5c did not decrease the Rab5a protein levels. Similar results were observed in cells depleted with Rab4a, Rab8a, Rab9a and Rab11a. However, because isoform-selective antibodies for the b and c isoforms were not available, similar analyses of these isoforms could not be undertaken.

Next all the siRNA against each isoform of these Rabs were combined and co-transfected them into HeLa cells. Figure 4.3 panel B shows representative immunoblots to show that the siRNAs employed were able to deplete cells of the specific Rab for which antibodies were available. The blots clearly demonstrate that effective depletion (>85%) was achieved for Rab4a, 5a, 8a, 9a and 11a. Again because of the lack of specific antibodies against the b and c isoform of all the Rabs, it was not possible to directly determine the depletion level of these isoforms.

In order to resolve this issue, RT-PCR was carried out to analyse all Rabs for which antibodies were not available, and observed essentially quantitative depletion of all mRNAs selectively using the specific SmartPools. HeLa cells were transfected with siRNA against appropriate isoforms and incubated for 48 h. mRNA was then extracted from the treated cells and quantified. Equal amount of total RNA from each experiment then was

added to RT-PCR as template. To further ensure equal addition of total RNA, a housekeeping gene, Glyceraldehyde 3-Phosphate Dehydrogenase (GAPDH), was amplified from these RNA templates as shown in Figure 4.4, panel A. The intensity of the GAPDH bands in each lane appeared to be approximately the same, suggesting that similar amount template RNA was applied to each RT-PCR experiment. To confirm that specific downregulation of Rab isoform expression had been achieved, Rab isoform expression was assessed by RT-PCR after transfection with isoform-specific siRNA (Figure 4.4, panel B). In all cases, siRNA transfection was found to specifically knockdown Rabs in an isoform-specific manner.

After confirming that all the isoforms are depleted by corresponding siRNA, the cytokinesis effects caused by the knock-down was analysed using binucleate cells as an index. Surprisingly, depletion of all these endosomal Rabs, with the exception of Rab11 (~15%), produced no significant increase in the percentage of binucleate cells as shown in Figure 4.3. The modest increase in the percentage of binucleate cells observed upon Rab8 or Rab21 depletion did not reach statistical significance. This experiment supports the essential function of Rab11 in cytokinesis shown by previous work from our lab (Wilson et al., 2005). This study extends the observation to show that of all the other endosomal Rabs studied here, only depletion of Rab11 led to cytokinesis failure.

However, as discussed in 3.3.2, Rab11 and Arf6 play vital roles during mammalian cell cytokinesis, yet cytokinesis seems to be a remarkably resilient process. Cells seem to have many "backup" mechanisms to ensure successful cytokinesis. Hence depletion of these endosomal Rabs may only have minor effect on the process, since other members of Rab family may compensate the function. Otherwise it can be accounted for that if there is little effect but cells still can struggle through and eventually achieve division, though a dividing rate could be affected. Hence binucleation is not the only or precise index to determine cytokinesis defects here. To detect subtle consequence on cytokinesis caused by depletion of these endosomal Rabs, time-lapse video microscopy was performed.

4.2.3 Measurement of dividing rate of cells depleted with Rab4 and Rab5

Considering Rab4 and Rab5 control the membrane traffic through the EE and have close crosstalk with Rab11, time-lapse experiments of cells depleted of Rab4 and Rab5 were carried out. They were chosen for detailed analysis also because endocytosis from the PM has been demonstrated to be involved in cytokinesis (Schweitzer and D'Souza-Schorey,

2005). In Chapter 3, it was shown that normal cells finish division in about 3.5 h after anaphase elongation commences, while knock-down of Rab11 induced furrow regression and finally led to cytokinesis failure. Since the depletion of Rab4 and Rab5 did not show any significant increase of binucleate cells, we used time-lapse videomicroscopy to detect subtle effects in these cells, such as a slower dividing rate.

Cells were co-transfected with siRNA of Rab4 a/b and Rab5 a/b/c and incubated for 48 h before video-microscopy as described in section 2.2.4.4. The process of cell division was recorded and each critical step was marked with time point to analyse the dividing kinetics. Surprisingly, no significant division effect was observed in cells depleted of Rab5. They furrowed normally and achieved abscission within 3.5 h since anaphase elongation onset as shown in Figure 4.6. Interestingly, delayed midbody abscission in cells treated with Rab4 siRNA was constantly seen (Figure 4.5). The furrow ingressed and the midbody formed at normal timing. However, instead of being ripped off as ordinary midbody within 1.5-2 h, the midbody of Rab4 depleted cells remained for more than 5 h. The midbody finally broke and two daughter cells separated, the delay of abscission is evident. About 40% (5 in 12) cells that have been examined exhibited this phenotype. Although the precise mechanism remains unclear, this observation implicates the Rab4 regulated early endosomal pathway might participate in cytokinesis events, likely at the midbody abscission stage, coordinating with Rab11 regulated pathway. Depletion of this molecule might block a specific pathway of traffic to the midbody body site, and insufficient membrane delivery may then lead to delay of the intercellular bridge abscission.

4.3 Discussion

4.3.1 Distribution of endosomal Rabs in cytokinesis

Membrane traffic has been recognised to be an integral part for the successful completion of cytokinesis. Prevailing models suggest that traffic of secretory vesicles into the midbody is crucial for completion of cytokinesis (Fielding et al., 2005; Gromley et al., 2005). Increasing evidence has shown that proteins involved in membrane traffic and fusion function in cytokinesis, including Rab11, Arf6, Rab11-FIP3/4, clathrin, dynamin and SNARE proteins. Recent work from our lab has suggested that membrane vesicles derived from RE and marked by the presence of a Rab11 effector protein, Rab11-FIP3, traffic into the furrow/midbody region of cells where they interact with components of the Exocyst complex and Arf6 during abscission.

As a first attempt to identify other Rab proteins involved in cytokinesis, the distributions of GFP-tagged endosomal Rabs in HeLa cells were examined Figure 4.1. Rab11 was observed in the furrow and midbody region of dividing cells consistent with previous studies. However, it is striking that all of the other Rabs appeared to be effectively excluded from this region. The majority of the staining of the other Rab proteins was present on a peri-nuclear compartment and punctuate vesicle structures facing away from the furrow or midbody. Such data may implicate that these structures may be spatially regulated with Rab11 positive vesicles focussed around the centrosomes and trafficking towards the furrow, while Rab4, 5, 7, 8 and 9 containing vesicles face away from the furrow.

This is of particular interest because endocytosis has been observed taking place at the two pole regions during telophase and cytokinesis in a recent study (Schweitzer et al., 2005). It was originally thought that endocytosis and endosomal trafficking do not occur during mitosis but instead resumes during the G1 phase (Berlin and Oliver, 1980; Warren et al., 1984). However in this report, the authors discovered that endocytosis was inhibited during early mitosis, and resumed in a distinct fashion during anaphase and early telophase by starting from the polar regions of the dividing cells. In addition, the ligands internalized from the polar region have been observed to migrate to the cleavage furrow, which shares a very similar pattern with Rab11 regulated vesicle distribution. After cells complete cleavage furrow ingression, endocytosis occurred at the cleavage furrow area.

Considering that the majority of endosomal Rabs are localised near the polar region, it is intriguing to suggest that other endocytic Rab proteins, especially Rab4 and Rab5 may be responsible for the endocytosis events at the polar region during telophase, while Rab11 is involved in bridging the traffic between the polar region and furrow/midbody since it has been observed at both sites. The concentration of Rab11 at the furrow/midbody strongly suggested its involvement in the endocytosis events at the final midbody abscission.

4.3.2 Effects of overexpression of endosomal Rabs GTP deficient mutants on cytokinesis

In order to investigate potential function of the endocytic endosomal Rab proteins on cytokinesis, two independent methods were used to perturb these Rabs function, the over-expression of dominant negative (GDP-restricted) mutants or gene silencing by RNAi (Figure 4.2 and Figure 4.3).

The over-expression levels of the GDP-restricted mutants of Rab4 and Rab5 are both higher than the endogenous proteins as shown in Figure 4.2. However, no increased binucleation percentage was observed in these cells, whereas Rab11 S25N exerts a significant effect on cytokinesis. The RE is at the crossroads of several transport routes and continuously exchanges membrane with EE, LE compartments, the PM and the TGN. The EE traffic regulated by Rab4 and Rab5 that has partial overlaps with Rab11 containing vesicles and exchange membrane frequently. Previous studies have shown that overexpression of Rab4 S22N and Rab5 S34N affects the morphology of Rab11 regulated RE (Stenmark et al., 1994; Mohrmann et al., 2002), therefore it is surprising to observe no cytokinesis defects by over-expressing dominant negative Rab4 and Rab5. However, the lack of binucleation is perhaps because the expression of these mutants did not reach the level sufficient to cause any obvious defects.

To overcome these limits, RNAi was applied as an alternative method to further investigate the functional role of these Rabs. Increased percentage of binucleation was observed in cells depleted of Rab11 in agreement with previous reports (Wilson et al., 2005). However, cells depleted with other endosomal Rabs still revealed no binucleation phenotype. Further analysis of the cytokinesis process by time-lapse video microscopy in these cells revealed that cells knocked down with Rab4a and b exhibited delayed abscission. The midbody formed as normal but lasted much longer, of a magnitude similar to the previously observed for Rab11. In contrast to Rab11-depleted cells, Rab4-depleted cells were eventually able to complete abscission. This delay was observed in greater than 40% of the

cells examined. In this regard, it is of interest that depletion of Rab11 has been reported to result in an up-regulation of Rab4 protein level (Wilson et al., 2005). Interestingly, cells depleted of Rab4, Rab5 or Rab11 exhibited no effect on furrowing. All cells furrowed normally, and with broadly similar kinetics. Such data argue that Rab4, 5 and 11 are not required for furrowing, but strongly suggests that both Rab11 and, to some degree, Rab4 are involved in midbody abscission. Rab4 has been shown to regulate traffic from early endosomes to the PM (Daro et al., 1996; Mohrmann et al., 2002; van der Sluijs et al., 1992b), whereas Rab11 controls recycling from RE to PM (Chen et al., 1998; Ren et al., 1998; Ullrich et al., 1996; Wilcke et al., 2000). Hence, our data support the notion that both of these trafficking routes are responsible for membrane supply in cytokinesis, with Rab11 regulated RE appearing to play a more significant role.

Interestingly, a recent study has reported that another Rab protein, Rab35 plays an essential role in both the stability of the midbody bridge and final abscission (Kouranti et al., 2006). Although the exact route controlled by Rab35 is not clear yet, this GTPase has been localised to the PM and endocytic compartments, and controls a fast endocytic recycling pathway. Interference of Rab35 by GDP-restricted mutant or RNAi led to a 3.5 fold increase of binucleation arising from destabilisation of the intercellular bridge. In addition, the time required for abscission was strongly increased in cells that did not become binucleated, which is reminiscent with the defect caused by Rab4 depletion. The study further showed that Rab35 is involved in correct localisation of two molecules essential for the post-furrowing steps of cytokinesis, phosphatidylinositol 4,5-bis phosphate lipid (PIP2) (Emoto and Umeda, 2001; Field et al., 2005), and SEPT2 (Spiliotis and Nelson, 2006; Kinoshita et al., 1997).

Collectively, a possible model controlling membrane trafficking during cytokinesis could be suggested. There may be multiple routes contributing to this process, orchestrated by Rab11, Rab35 and possibly Rab4. It is interesting that none of these Rab GTPases has an effect on furrow ingression, but appear to function in midbody bridge abscission. Rather, it appears that Rab11 and Rab35 are more significant for this process by leading to significant increase of multi-/binucleate cells. Although cells depleted of Rab4 finally struggled to break the bridge, the process has been largely delayed. Hence, it is likely that these GTPases mediating endocytic traffic play a functional role at a late stage, by either controlling membrane vesicles trafficking for the abscission, or by delivering important cargoes to the dividing site. The fact that only these few specific Rab proteins are responsible for the membrane delivery for abscission, whereas interference of Rabs mediated in other traffic routes did not cause obvious effect implies that the endosomes

supplied for cytokinesis may act as a ready source and do not exchange material with other membrane compartments. Therefore, disruption of other trafficking routes has little effect on membrane trafficking in cytokinesis.

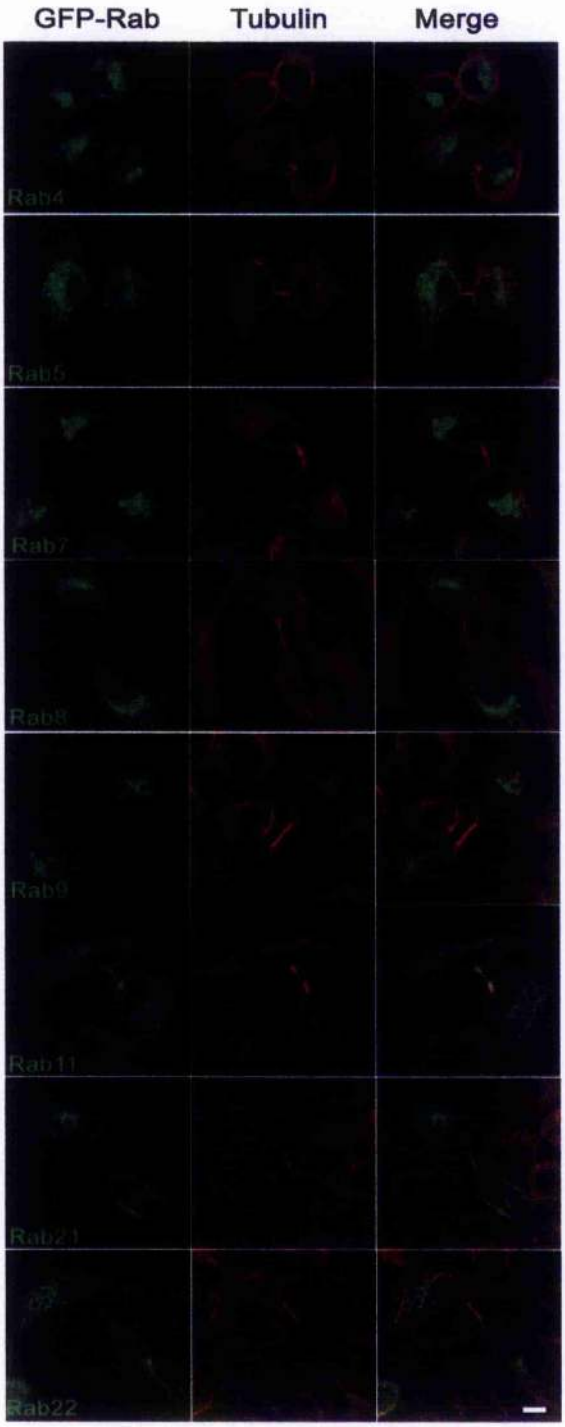

Figure 4.1 Subcellular localisation of GFP endosomal Rabs during cytokinesis

Cells were transfected with DNA plasmids encoding GFP-Rabs as indicated. 24 h post-transfection, cells were fixed in 4% paraformaldhyde and stained with anti-α-tubulin antibody followed by Alexa-594 fluorescent secondary antibody. Shown are representative images of cells in cytokinesis, with the distribution of GFP-Rabs as indicated (green), and tubulin (red). Only Rab11 containing vesicles were observed localised at the furrow/midbody region. The other GFP-Rabs distribute on compartments facing away from the midbody. Scale bar: 10 μm.

A

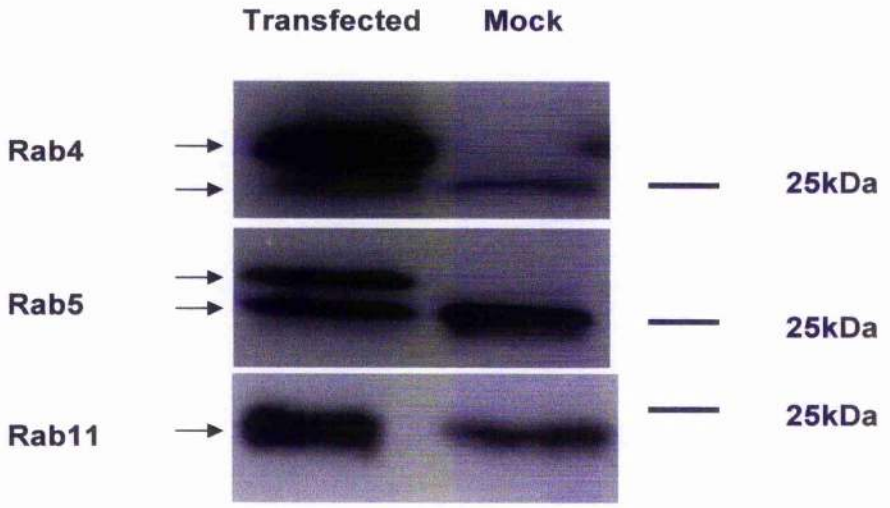
Transfected
Mock
Rab4
Rab5
Rab11
25kDa
25kDa
25kDa

B

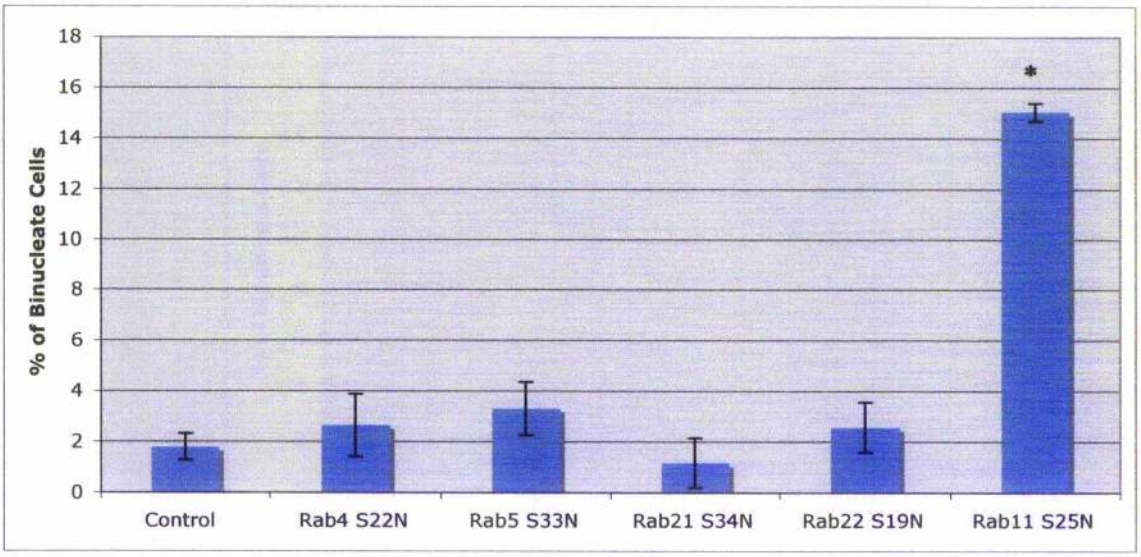
% of Binucleate Cells
18
16
14
12
10
8
6
4
2
0
*
Control
Rab4 S22N
Rab5 S33N
Rab21 S34N
Rab22 S19N
Rab11 S25N

C

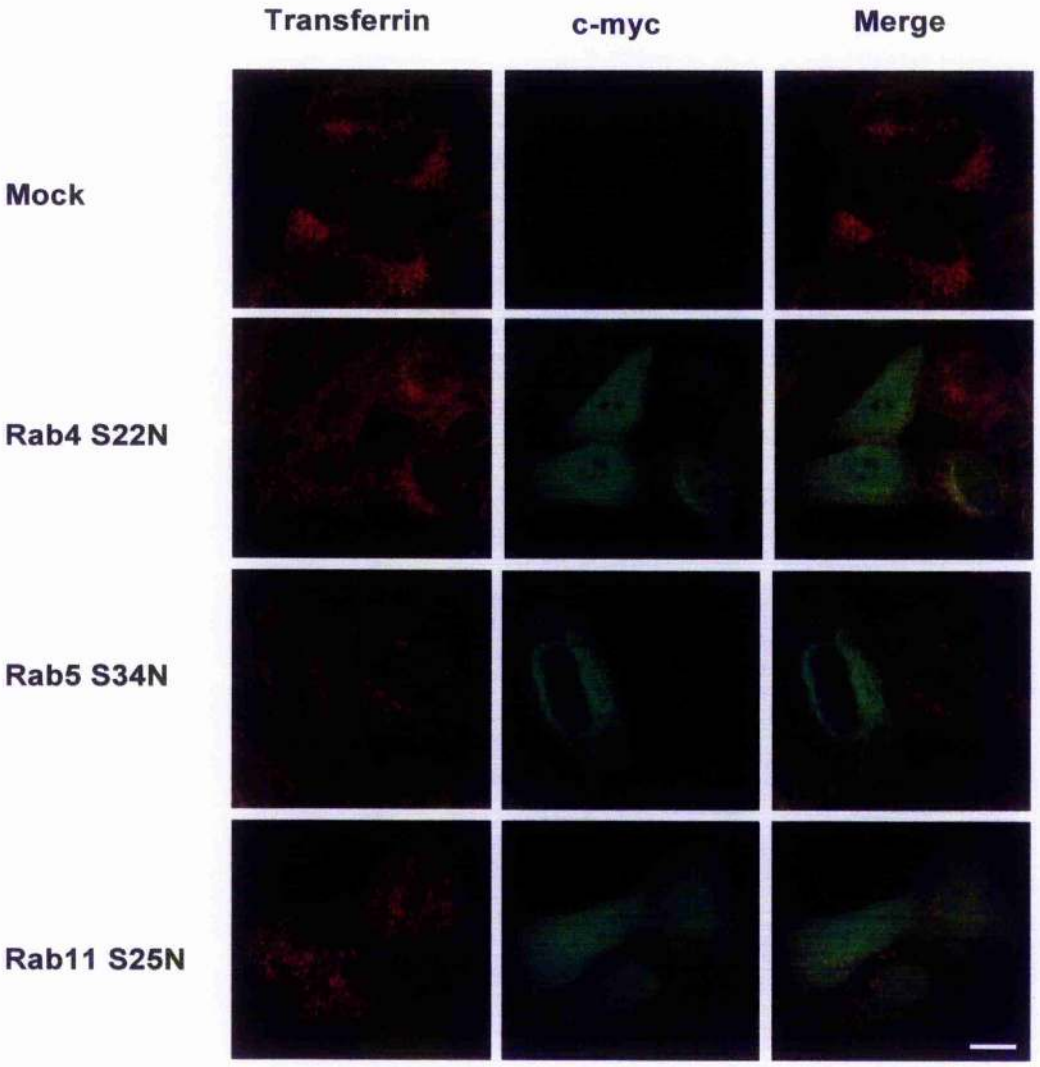

Figure 4.2 Overexpression of GDP restricted mutants of endosomal Rabs does not cause cytokinesis defects

HeLa cells were transfected with plasmids encoding c-myc tagged Rab4 S22N, Rab5 S34N, Rab11 S25N, Rab21 S33N and Rab22 S19N and analysed as indicated in the figure. **(A)** 48 h post-transfection, cells were lysed and analysed for expression of corresponding Rab proteins as indicated. Because of the lack of the antibodies that can detect Rab21 and Rab22 on immunoblots, they are not shown here. Only blots of Rab4, Rab5 and Rab11 are shown. The arrows on the right indicate tagged mutant and endogenous proteins, upper arrows (mutant proteins), lower arrows (endogenous proteins). There is only one arrow in the Rab11 blot, because the mutant and endogenous proteins are very close to each other. **(B)** Cells were also fixed and stained for expression of the Rab mutants in question (epitope-tag antibodies), tubulin and DAPI to allow quantification of the numbers of cells expressing the mutant Rab, which exhibited a binuclear phenotype. Shown are the data from three independent experiments, presented as a mean and S.D. Over-expression of Rab11 S25N resulted in a statistically significant increase in the percentage of binucleate cells, $^{*}p<0.01$ (t-test) compared to the mock transfect control. **(C)** Cells transfected with Rab4 S22N, Rab5 S34N and Rab11 S25N were incubated with 2.5 μg/ml Texas-red Tf for 30 min at 37°C followed by extensive washing and then processed for immuno-fluorescence. Shown are representative images of staining with c-myc tag to view the Rab GDP mutants (green) and Texas-red Tf (red). Scale bar: 10 μm.

A

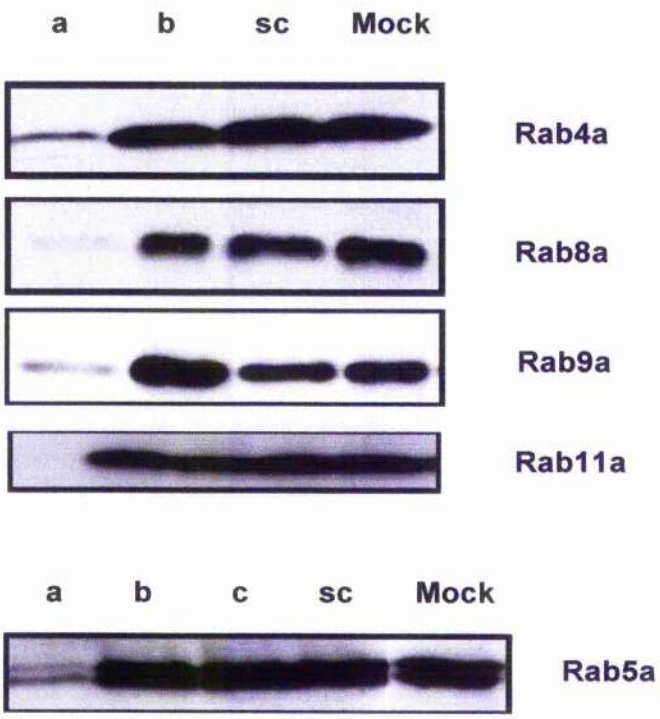
a
b
sc
Mock
Rab4a
Rab8a
Rab9a
Rab11a
a
b
c
sc
Mock
Rab5a

B

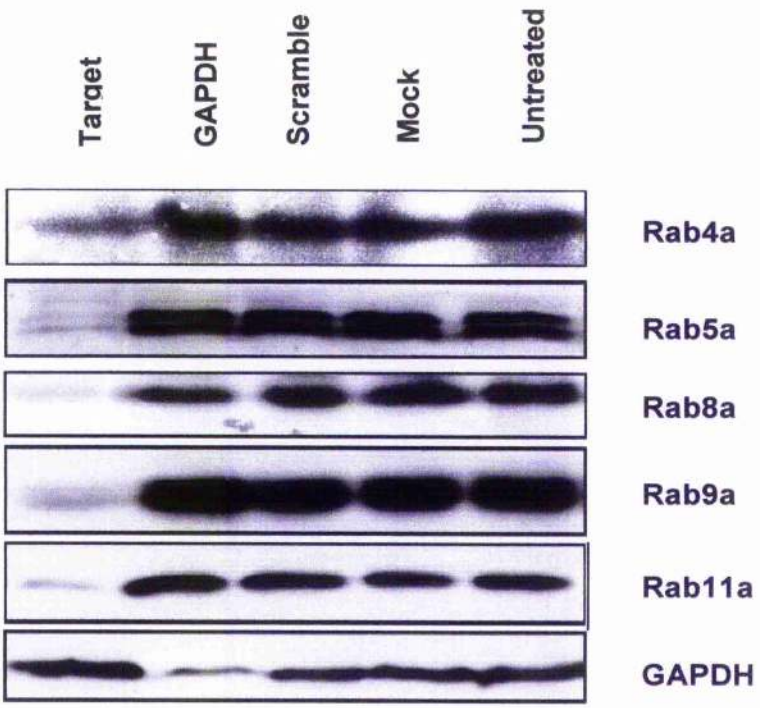
Target
GAPDH
Scramble
Mock
Untreated
Rab4a
Rab5a
Rab8a
Rab9a
Rab11a
GAPDH

C

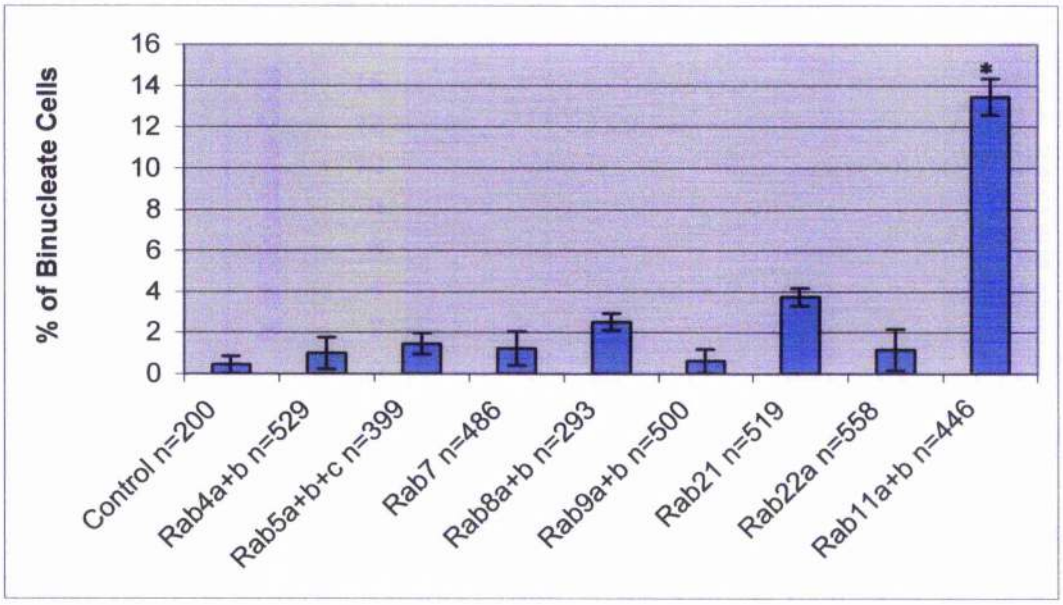

Figure 4.3 RNAi of endosomal Rabs did not result in significant increase of binucleate cells

(A) HeLa cells were transfected with siRNA targeting individual isoforms of the Rab protein in question. 48 or 72 h post-transfection (the experiment shown was from 48 h, but similar data was observed after 72 h) cells were lysed and blotted with isoform-selective antibody indicated on the right. Above the figure 'a' 'b' and 'c' correspond to the isoform of the Rab species targeted by the SmartPool siRNA, 'sc' represents lysate from cells transfected with a scrambled control SmartPool, and 'mock' are cells treated with Dharmafect I transfect reagent in the absence of any siRNA. Note that the Rab4a, Rab5a, Rab8a, Rab9a and Rab11a isoforms are selectively depleted by the corresponding SmartPool, and not affected by the 'b' or 'c' selective SmartPool. The immunoblots of Rab21 and Rab22 are not shown here because of the lack of antibodies that detect these Rabs. **(B)** As Panel A except cells were treated with the 'a' isoform SmartPool ('Target'), GAPDH SmartPool ('GAPDH'), a scrambled control ('Sc'), Dharmafect reagent alone ('mock') or untreated ('Mock'). Again, these controls reveal the selective knockdown of the indicated Rab. **(C)** 48 h (not shown) or 72 h (shown) after transfection, cells were fixed and stained for tubulin and DAPI to allow quantification of the numbers of cells exhibiting a binuclear phenotype. Knockdown of Rab11 results in a significant increase in binuclear cells, $^{*}p<0.01$ (t-test) compared to the scramble siRNA control, whereas all other Rab knockdowns did not lead to a statistically significant increase in the appearance of binuclear cells. The number of cells counted in all experiments is shown. In this case, 'Control' refers to cells treated with Dharmafect reagent alone.

A

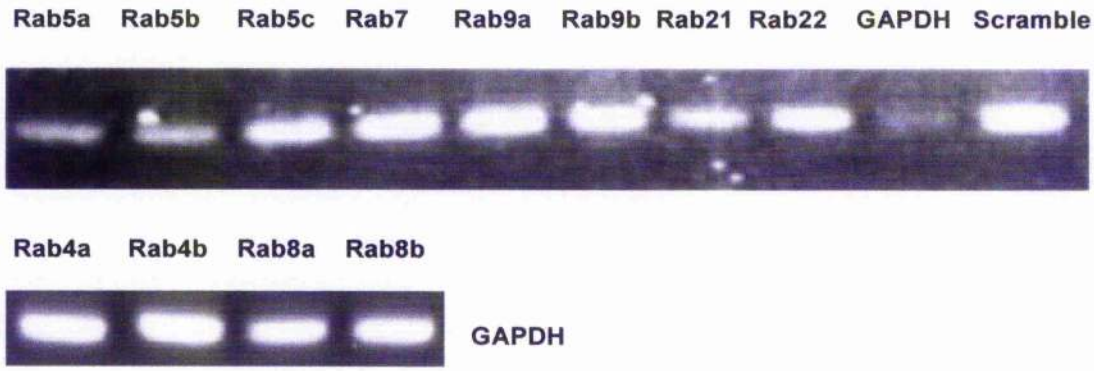
Rab5a Rab5b Rab5c Rab7 Rab9a Rab9b Rab21 Rab22 GAPDH Scramble
Rab4a Rab4b Rab8a Rab8b
GAPDH

B

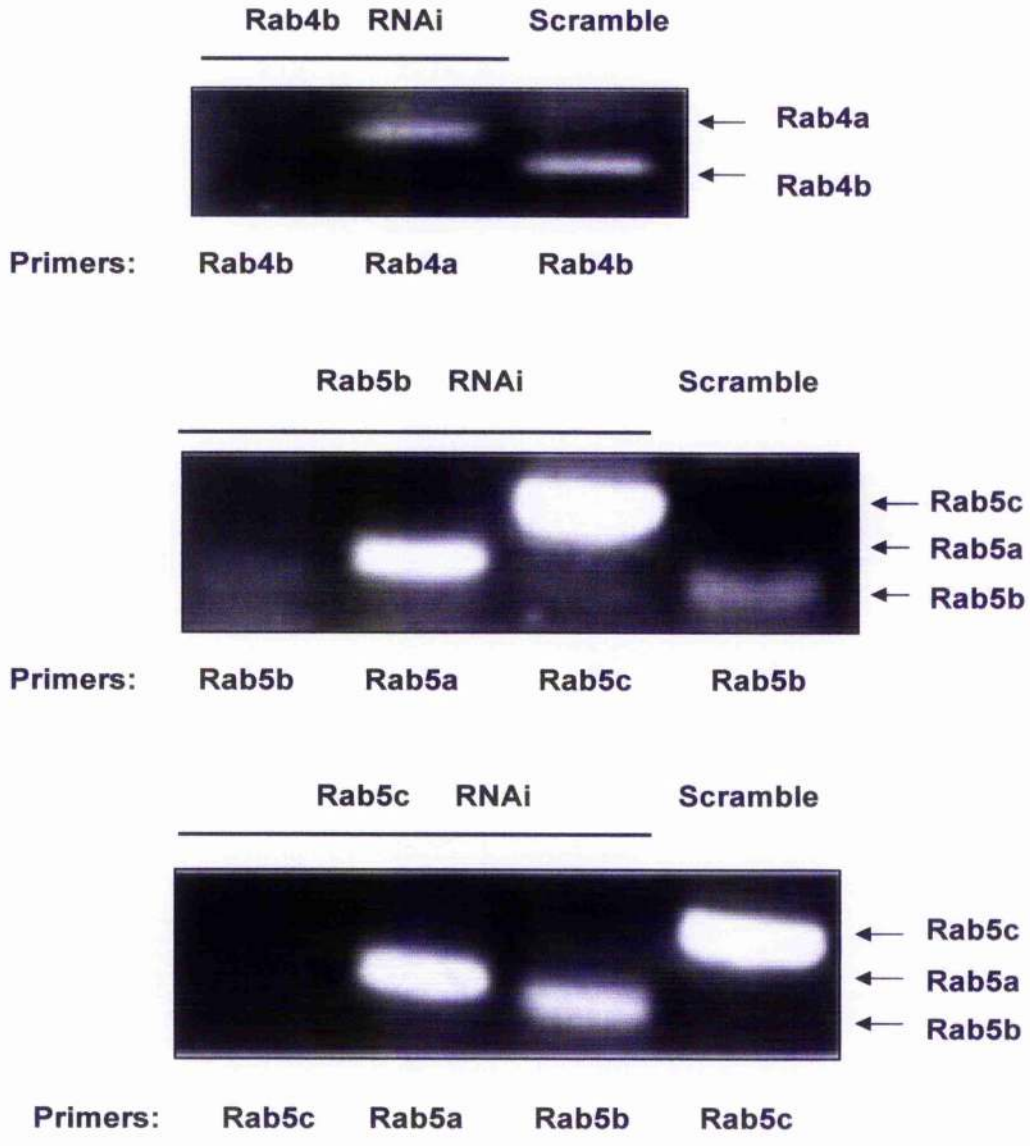
Rab4b RNAi Scramble
Rab4a
Rab4b
Primers: Rab4b Rab4a Rab4b
Rab5b RNAi Scramble
Rab5c
Rab5a
Rab5b
Primers: Rab5b Rab5a Rab5c Rab5b
Rab5c RNAi Scramble
Rab5c
Rab5a
Rab5b
Primers: Rab5c Rab5a Rab5b Rab5c

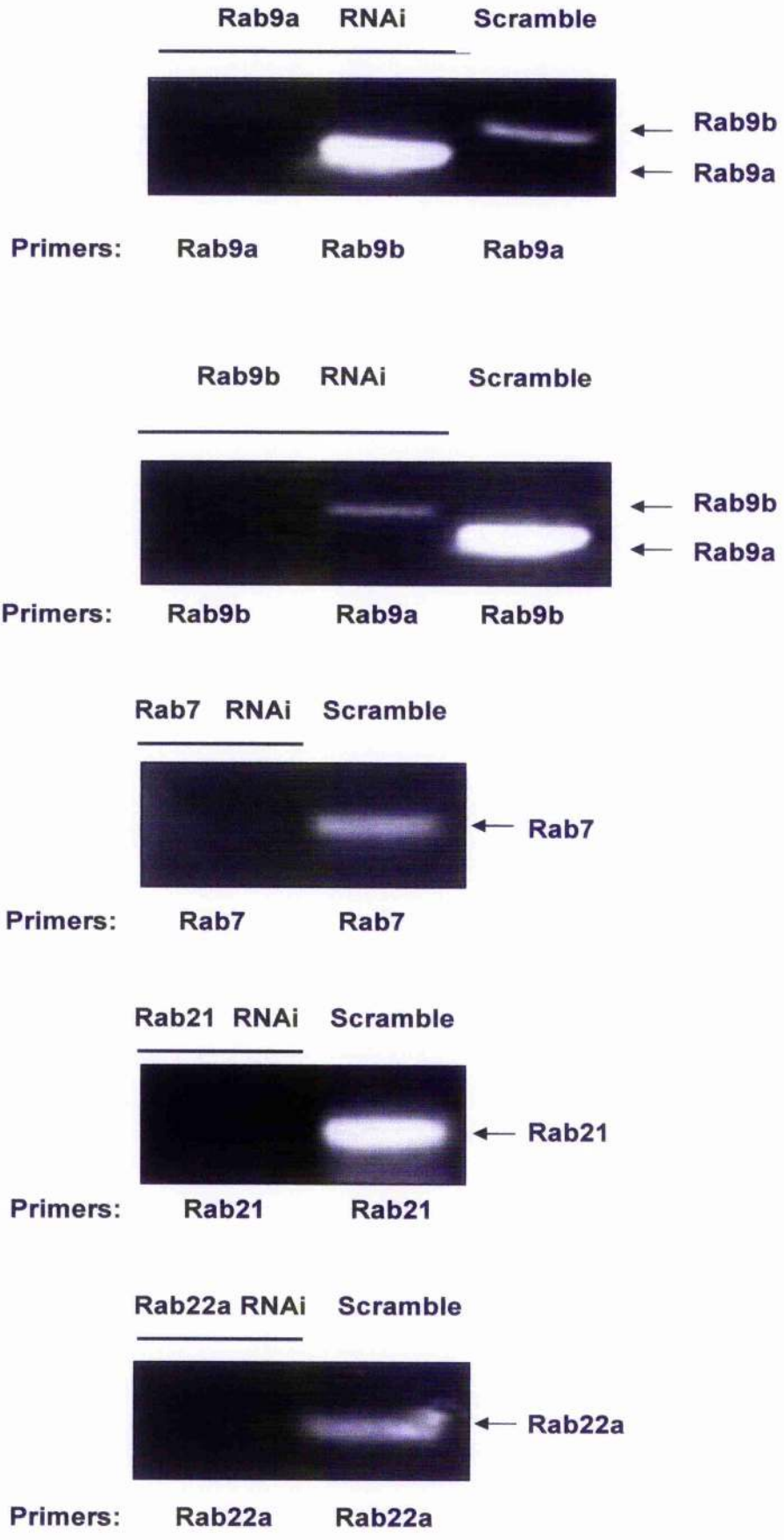
Rab9a RNAi Scramble
Rab9b
Rab9a
Primers: Rab9a Rab9b Rab9a
Rab9b RNAi Scramble
Rab9b
Rab9a
Primers: Rab9b Rab9a Rab9b
Rab7 RNAi Scramble
Rab7
Primers: Rab7 Rab7
Rab21 RNAi Scramble
Rab21
Primers: Rab21 Rab21
Rab22a RNAi Scramble
Rab22a
Primers: Rab22a Rab22a

Figure 4.4 RT-PCR of endosomal Rabs

(A) HeLa cells were transfected with siRNA SmartPool to deplete cells of the specific Rab isoforms indicated (above each panel). Cells treated with scrambled siRNA SmartPool were employed as control. 48 h post-transfection mRNA was isolated, and RT-PCR was carried out using GAPDH selective primers as indicated on the right of the figures. **(B)** As panel A, except that RT-PCR was performed using Rab isoform selective primers, as indicated at the bottom of the figures. The identity of the PCR products is shown on the right. These data show that the SmartPool in question specifically depleted the expected Rab isoforms at the RNA level.

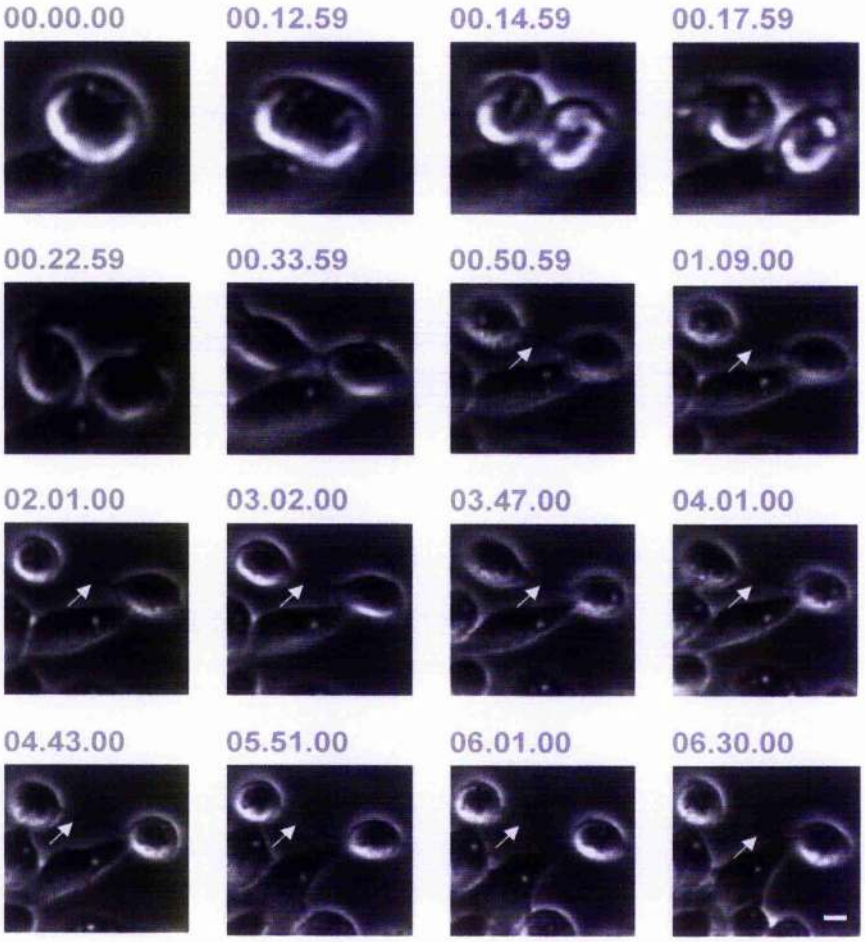

Figure 4.5 Time-lapse microscopy of Rab4 siRNA treated cells

HeLa cells were co-transfected with siRNA targeted for Rab4a and 4b. 48 h post-transfection, cell division process were analysed by time-lapse video microscopy as described. Shown are representative still images, repeated on at least ten cells, with the time of the collection set of the images. The cells exhibited phenotype with long-lasting midbodies (indicated by white arrows) at the time points shown. Furrowing kinetics are not affected and broadly identical to normal conditions. The movies corresponding to these stills are presented in the DVD attached to this thesis. Scale bar: 10 μm.

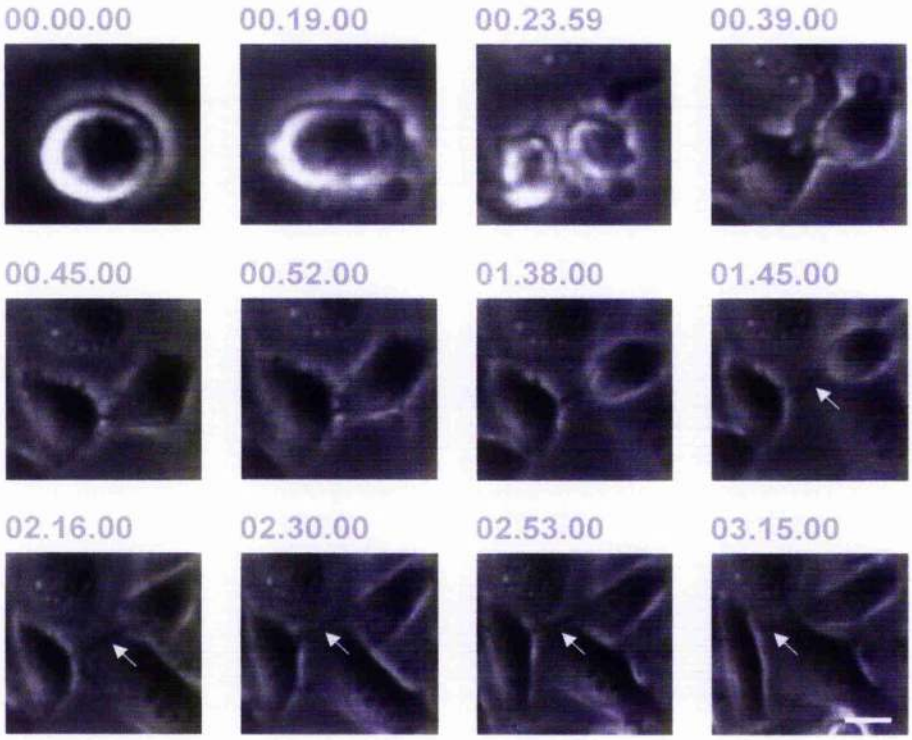

Figure 4.6 Time-lapse microscopy of Rab5 siRNA treated cells

HeLa cells were co-transfected with siRNA targeted for Rab5a, 5b and 5c. 48 h post-transfection, cell division process were analysed by time-lapse video-microscopy as described. Shown are representative images, repeated on at least ten cells, with the time of the collection set of the image. The cells appear to divide in a dynamic as normal cells. Furrow and midbody (white arrows indicated) formed normally, and no defects were detected in the whole process. The movies corresponding to these stills are presented in the DVD attached to this thesis. Scale bar: 10 μm.

5 Functional studies of FIP3 and FIP4 in mitosis

5.1 Introduction

In this chapter studies were carried out to investigate the role of FIP3 and FIP4, the binding partners of Rab11 and Arf6, during mitosis. Both of Rab11 and Arf6 strikingly colocalise with the two FIPs at the midbody during this process. Since both bind to Rab11 and Arf6, FIP3 and FIP4 have been suggested to couple signals mediated by these two GTPases and facilitate their activities in membrane trafficking during cytokinesis. Although previous investigation has addressed the role of FIP3 and FIP4, especially FIP3 in cell division (Wilson 2003), there are still many questions remaining to be answered. Why are there two Class II FIPs in mammalian cells? It was shown that FIP3 depletion results in severe cytokinesis defects similar to Rab11 interference. However, knockdown of FIP4 was not successful. What is the consequence of FIP4 disruption? Will it cause the same phenotype of FIP3 depletion? Hence in the following study FIP4's function will be investigated by using RNAi and fluorescence microscopy methods.

Cell cycle is tightly regulated by several groups of protein kinases, such as Cdk, Plk, Aurora kinase and Citron kinase, and their activities are known to underlie both early and late cytokinetic events. The rapid change in spatial localisation of FIP3 and FIP4 during mitosis implicates that there may be an acute mode of regulation of the FIPs to regulate their distribution. A strong candidate for this acute modification is phosphorylation. It is interesting to notice that their closely related protein, Nuf, is dynamically phosphorylated in a cell cycle-dependent manner in *Drosophila* (Rothwell et al., 1998). In addition, the FIPs localise to the central spindle in anaphase and telophase and to the midbody in cytokinesis, which overlap with certain kinases, such as Aurora B and Plk1. Such observations raise the possibility that the FIPs might be regulated by phosphorylation in a cell cycle-dependent fashion. Aurora B is responsible for phosphorylation of many cytokinesis essential regulators, such as myosin II (Straight et al., 2003), the centralspindlin complex (Mishima et al., 2002) and INCENP. Plk1 regulates functions of a number of molecules such as MKLP1 (Adams et al., 1998), Nir2 (Litvak et al., 2004) and Rho1 (Yoshida et al., 2006) in mitosis. With this information in mind, some preliminary research of FIP3/4 phosphorylation was carried out in this chapter.

5.1.1 Baculovirus Expression System

Baculovirus are the most prominent virus known to infect the insect population. They have double-stranded circular, super coiled DNA in a rod-shaped capsid. So far more than 500

baculovirus have been identified based on the host origin. The two most common used virus in foreign gene expression are *Autographa califomica* multiple nuclear polyhedrosis virus (AcMNPV) and *Bombyx mori* (silkworm) nuclear polyhedrosis virus (BmNPV).

Wild-type baculovirus exhibit both lytic and occluded life cycles, and the important difference between these two cycles is the induction of polyhedrin production at the beginning of the very late phase. In the baculoviruses expression system, the naturally occurring polyhedrin gene in the wild-type virus genome is replaced with the recombinant gene of interest. This expression is generally controlled by a polyhedrin or a p10 promoter. In the late phase of infection, the virions are assembled and budded recombinant virions are released. During the very late phase of infection, the inserted heterologous genes are placed under the transcriptional control of the strong AcNPV polyhedrin promotor. Thus, the recombinant protein is expressed in place of the naturally occurring polyhedrin protein. Baculovirus are propagated in insect hosts that post-translational modify peptides in a manner similar to that of mammalian cells. The most widely used cell line for baculovirus expression system is Sf9, a clonal isolate of the *Spodoptera frugiperda* cell line IPLB-Sf21-AE. It was originally established from ovarian tissue of the fall armyworm (Vaughn et al., 1977). The other common used cell line is Sf21, also from *Spodoptera frugiperda*. It is suggested that different insect cell lines might support varying levels of expression and differential glycosylation with the same recombinant protein.

Sf9 cells and Bac-to-Bac Baculovirus Expression system were chosen in this study. The Bac-to-Bac Baculovirus Expression system takes advantage of the site-specific transposition properties of the Tn7 transposon to simplify and enhance the process of generating recombinant bacmid DNA. The first essential component of this system is a pFastBac vector into which the foreign gene is cloned. Depending on the pFastBac vector selected, the gene of interest is under control of the *Autographa califomica* multiple nuclear polyhedrosis virus (AcMNPV) polyhedrin (PH) or the p10 promoter for high-level expression in insect cells. This expression cassette is flanked by a left and right arm of Tn7. After the gene of interest is inserted into the pFastBac vector, which was transformed into a DH10Bac *E. coli* strain containing a baculovirus shuttle vector (bacmid) and a helper plasmid to allow a recombination occur between the pFastBac and the bacmid through the mini-att Tn7 transpon. Once the transposition is completed, the high molecular weight recombinant bacmid DNA is prepared from the DH10Bac *E. coli* cells and transfected into insect cells to produce a recombinant baculovirus stock. After further amplication and titering of the original virus stock, the high-titre stock is used to infect insect cells for large-scale expression of the recombinant protein.

5.1.2 Hypothesis and Aim

FIP3 and FIP4 are concentrated at the cleavage furrow and midbody during cytokinesis. Their binding partners, Rab11 and Arf6, have been shown to be essential at the closure of the midbody bridge during cytokinesis. FIP3 has been indicated to play a role in cytokinesis associated with Rab11, however, FIP4's function still requires to be further elucidated. As FIP3 and FIP4 share high homology, it is interesting to reveal more about FIP4 role in cytokinesis and analyse functional differences between FIP3 and FIP4. Therefore, in this chapter FIP4's function was investigated by using RNAi and fluorescence microscopy methods. A study of regulation machinery of FIP3 and FIP4 in cytokinesis has also been carried out in this study. It is proposed FIP3 and FIP4 might be regulated by cell cycle regulated kinases, based on the fact that Nuf, their *Drosophila* homologue is a highly phosphorylated protein in mitosis and FIP3/FIP4 colocalise with certain kinases. Two essential cell cycle regulated kinases, Aurora B and Plk1 have been tested in this chapter. Furthermore, in order to carry out phosphorylation studies in the future full-length proteins of FIP3 and FIP4 were produced using baculovirus system.

5.2 Results

5.2.1 RNAi of FIP4

It has been clearly shown that both Rab11 and Arf6 play integral roles in mammalian cytokinesis. Their interaction partner, FIP4 is hypothesised to couple Rab11 and Arf6 function during this process, most possibly as a tethering factor to facilitate membrane delivery and docking. However, as direct experimental evidence showing that FIP4 is required in cytokinesis is still lacking, the precise function of FIP4 during mitosis remains to be further elucidated. The initial difficulty in the design of these experiments was finding an efficient method to perturb FIP4 function. In the case of Rab11 and Arf6 GTPases, GTP-deficient mutants turned out to be a powerful tool to study their roles. Since no such mutants were available for FIP4, the approach to investigate FIP4's action is relatively limited.

In order to study FIP4 function directly, RNAi with Dharmacon SmartPool was attempted. The cells were seeded on glass coverslips at about 50-60% confluence 24 h before the experiment. The next day, total concentration 75 nM, 100 nM and 125 nM of siRNA against FIP4 were delivered into the cells by using DharmaFect-1 transfection reagent. SmartPool siRNA targeting GAPDH was applied to the cells as a positive and loading control. Cells were harvested and processed for immunoblotting as well as immunofluorescent experiments 48 and 72 h post-transfection. Figure 5.1 shows a representative blot of cell lysates harvested at 72 h post-transfection. The lower panel indicates that GAPDH was efficiently reduced on the protein level. However, no decrease of FIP4 protein was achieved with any condition compared to the controls.

To rule out the possibility that the siRNA concentrations used were not high enough to cause a knockdown effect on FIP4 or the expression analysis was not carried out at the right point, the concentration of the SmartPool was raised up to 150 nM, and the incubation time was also increased up to 96 h. Considering siRNA duplexes may be degraded over a long period of incubation time, a second transfection was performed 48 h after the first transfection. Unfortunately, these optimizations did not make much difference (data not shown). The treatment of the SmartPool siRNA had no obvious effect on FIP4 protein expression. This is not the first time to attempt to knock down FIP4. Before this study, attempts to deplete FIP4 were also carried out using various targets as shown in

Table 2.3 by one of my colleagues (Andrew Fielding, unpublished data).

5.2.2 Video microscopy of GFP-FIP4

Due to the difficulty of depleting FIP4 by using RNAi, an alternative approach was applied to investigate its role in mitosis. A plasmid encoding GFP tagged FIP4 was over-expressed in HeLa cells. 48 h post-transfection, cells were fixed and immunostained with anti-tubulin antibody and DAPI to view the effect. As shown in Figure 5.2, panel a-c, in agreement with previous reports, GFP-FIP4 shows tight perinuclear localisation in interphase and concentrates at the midbody during cytokinesis (Hickson et al., 2003; Wilson et al., 2005). If FIP4 does play a role during cytokinesis, its overexpression might influence the functions of Rab11 and Arf6 by affecting the interaction relationship between itself and Rab11 and Arf6. For instance, overexpressed FIP4 might sequester Rab11 and Arf6 more than in the normal situation, thus blocking their cellular function. Immunofluorescence was first carried out to view whether overexpression of GFP-FIP4 causes cytokinesis defects. However, the results revealed no effect on binucleation. Cells at different stages undergoing mitosis with GFP-FIP4 expression were shown in Figure 5.2, GFP tagged appears similar localisation as endogenous FIP4.

To observe these cells in more details and reveal any subtle defect, time-lapse video microscopy was performed as described in 2.2.4.4. 36 h post-transfection, cells transfected with GFP-FIP4 were observed with a Zeiss AxioVert 200 fluorescent microscope. Images were taken every 90 sec as shown in the Movie 5.2 included on DVD. Surprisingly, in all the 5 cells observed, the cells rounded up normally, but none of them was able to initiate cytokinesis. In Movie 5.2, GFP-FIP4 appeared to aggregate in the cells and formed a bright spot structure. These cells remained rounded up for more than 7 h but did not proceed to cytokinesis implicating a blockage at the initiation of furrowing. To rule out this observation is due to phototoxicity produced by the fluorescent light, GFP-tubulin expressing cells were used as a positive control. As Movie 5.1 shows, a cell expressing GFP-tubulin was able to undergo mitosis as normal. The bipolar spindle decorated by GFP-tubulin expression carried on mitosis at the normal dynamics.

5.2.3 Preliminary studies of FIP3 and FIP4 phosphorylation

5.2.3.1 Colocalisation of FIP4 with Aurora B and Plk1

FIP3 and FIP4 have been shown to become highly concentrated at the central spindle and midbody during mitosis (Wilson et al., 2005), which is reminiscent of the distribution of two mitotic kinases, Aurora B and Plk1. To analyse their mitotic distribution dynamics in more detail, colocalisation of Aurora B and Plk1 with FIP3 and FIP4 was carried out.

HeLa cells seeded on 13 mm coverslips were fixed and processed for immunofluorescence. Endogenous Aurora B was stained with a rabbit anti-Aurora B followed by Alexa-488 secondary antibody and FIP4 was labelled with sheep anti-FIP4 antibody followed by Alexa-594. The coverslips then were observed by using a DeltaVision restoration microscope as described in 2.2.4.3. Figure 5.3 shows the images of individual channels as well as merged. Consistent with previous data, FIP4 show perinuclear localisation during interphase, while majority of Aurora B were present in the nuclei. FIP4 and Aurora B both aligned at the metaphase plane during metaphase and anaphase, and yellow colour showing high colocalisation was evident in Figure 5.3, panel h-l. In telophase and cytokinesis, these two molecules are strikingly concentrated at the two ends of the midbody bridge, panel p and t. The fact that FIP4 and Aurora B have distinct distributions in interphase and show extensively colocalisation from metaphase to cytokinesis suggests that they may have a function association in mitosis. FIP3 shows similar distribution pattern with FIP4, which also colocalises largely with Aurora B during mitosis (data not shown).

However, the image quality of Plk1 and FIP4 co-staining are not very good, probably because the Plk1 antibody used is not suitable for immunofluorescence. Hence more informative images are required to indicate their localisations in mitosis.

5.2.3.2 Depletion of Aurora B mislocalises FIP3 and FIP4 from the midbody during cytokinesis

To test whether there is a functional relation between Aurora B and FIP3/FIP4, RNAi was utilised to examine whether the depletion of Aurora B has an effect on the FIPs localisation in mitosis. siRNA duplex against Aurora B described in **Table 2.3** were synthesized by Dharmacon and transfected into to HeLa cells at a concentration of 100 nM. 48 and 72 h post-transfection, the cells were lysed and analysed for the knockdown of the protein. In Figure 5.4, panel A shows that Aurora B protein expression was efficiently decreased

compared to controls. Consistent with previous studies, a great increase in cytokinesis failure was observed by using binucleate cell counts as an index for cell division defects, and more than 50% cells became multi/binucleated in this experiment, panel B.

To evaluate the effect of Aurora B depletion on FIP3 and FIP4, plasmids encoding GFP-FIP3 and GFP-FIP4 were delivered into cells 24 h after transfection of Aurora B siRNA to view their localisations. 24 h post-transfection, cells were fixed and processed for immunofluorescence. Interestingly, in more than 70% cells, GFP-FIP3 and GFP-FIP4 lost their localisation to the midbody, as shown in Figure 5.5. The majority of them were sequestered at the two centrosomes, and almost no GFP fluorescence was observed at midbody/furrow region. In the cells in where FIP3 and FIP4 still remain at the midbody, the GFP signal was also largely attenuated. This experiment suggests that there is a association between Aurora B and FIP3 and FIP4, and the FIPs positioning to the midbody may be mediated by Aurora B function. A plausible hypothesis is that FIP3 and FIP4 maybe phosphorylated by Aurora B and the phosphorylation is required for their localisation to the midbody. When Aurora B is depleted, it fails to phosphorylate the FIPs, which led to their delocalisation in most of the cells (~70%). The remaining ~30% cells with proper distribution of FIP3 and FIP4 can be explained by residual Aurora B in the cells.

Similarly, siRNA against Plk1 was applied to HeLa cells with transfection of GFP-FIP3 and FIP4. Interestingly, this treatment has no effect on FIP3 and FIP4 localisation at the midbody compare to Aurora B (data not shown). Although this experiment has only been done once and further analysis needs to be carried out, it might implicate a specific mechanism mediated by Aurora B to regulate FIP3/4 localisation in cytokinesis.

5.2.3.3 Bioinformatics: potential phosphorylation consensus of Aurora B in FIP3 and FIP4

To seek more evidence of the phosphorylation hypothesis of FIP3 and FIP4, bioinformatics was applied. A novel group-based phosphorylation predicting and scoring method, GPS (Xue et al., 2005; Zhou et al., 2004), was used to predict the potential phosphorylation sites of FIP3 and FIP4. The GPS server is a comprehensive PK-specific prediction server, which could predict kinase-specific phosphorylation sites from protein primary sequences for 71 different protein kinase groups. Using MCAK as an example, the phosphorylation site predicted by GPS in MCAK was validated by experimentation, in which six out of seven predicted potential phosphorylation sites on MCAK were experimentally verified. This

server was also compared with the other two *in silico* phosphorylation sites prediction tools, ScanSite 2.0 and NetPhosK 1.0, which proved that the GPS server provides satisfying performance.

Protein sequences of Rab11-FIP3 (NP 055515) and FIP4 (NP 116321) in FASTA format were entered to the GPS server for prediction. Aurora B kinase was chosen to run the prediction. 4 of Aurora B phosphorylation consensus sites were discovered in the FIP3 sequence, see **Table 5.1.** The GPS scores of three of them are above the cut-off value 3.7, which represents 94.44% sensitivity and 97.14% specificity.

Gene	Position	Sequence	GPS score
FIP3	428	KRLSSKK	4.522
	647	GRSSSMG	4.696
	661	ARESELE	4.391
	713	AEISSVS	3.826
FIP4	304	RKISSTA	5.043

Table 5.1 Potential Aurora B consensus in FIP3 and FIP4

Interestingly, among these predicted sequences, S649 of FIP3, RRGRSSSMG, is embedded in a very nice consensus sequence for phosphorylation by metazoan Aurora B (K/R; K/R; X0-2; S), which is derived from a number of well-characterized substrates, such as histone H3, ICP-1/INCENP, MCAK, CYK-4/MgcRacGAP and CENP-A. The data shown here have given some preliminary evidence to support the idea of bridging the function of FIPs between mitotic kinases. If we prove that FIPs can be phosphorylated by Aurora B, this would be a starting point to identify their phosphorylation sites.

5.2.3.4 Production and purification of recombinant FIP3 and FIP4 from baculovirus

In order to investigate whether FIP3 and FIP4 are substrates of Aurora B kinase, *in vitro* phosphorylation assays were planned. To carry out these assays, the full-length proteins in question needed to be expressed and purified.

In previous studies, it was attempted to purify full length FIP4 using the pGEX-5X vector (Pharmacia) in BL21 cells with a GST tag at the N terminal (Fielding A, unpublished data). However, purification of the full-length product proved difficult, which resulted in a ladder of protein fragments of several different sizes when tested on a protein gel. A possible reason for this mixed population of fragments may be due to possible stalling of the bacterial translational machinery at various sites along the GST-FIP4 sequence. Some codons in human genes rarely appear in bacterial DNA and the bacteria contain few of these tRNAs. Therefore, when attempting to translate a human gene in bacteria, the process may be stalled due to the lack of the required tRNA. Another possibility is that purification of larger proteins using the tagged method is generally more difficult than smaller proteins.

To overcome this problem, it was decided to use Bac-to-Bac baculovirus expression system to create full-length FIP3 and FIP4. Full-length FIP3 and FIP4 cDNA sequences were cloned inserted into pFastBac™ HT plasmid with 6x His tag upstream of the gene inserted. The pFastBac vector with inserted gene of interest was transformed into a DH10Bac *E. coli* to allow recombination between the pFastBac with bacmid. The large molecular weight bacmids with recombinant gene in question were purified from DH10Bac *E. coli*. Transfection of bacmids into insect cells was then carried out as described in 2.2.3.8. 5 µl of bacmid DNA per well of 6-well plate was mixed with Cellfectin and serum-free Grace insect medium and applied into Sf9 insect cells. 5 h later, the transfection medium was replaced with fresh Sf900-II medium and the cells were incubated for 72 h to make the P1 stock. After the incubation, supernatant from each well was collected and transferred into a sterile tube. It was spun at 500 xg for 3 min to get rid of cell debris, and 2 % of FBS was added and stored in dark at 4 °C. Cells were lysed and processed for immunoblot to view the expression of protein in question. Anti-FIP3 and anti-FIP4 antibodies picked up bands at the right size from the transfected cells. Meanwhile a bacmid with no inserted gene was used as a negative control and neither of the antibodies detected any signal from the control (data not shown).

Because the titre of P1 stock is normally low and not enough for large-scale protein expression, it is necessary to amplify P2 stock from the initial P1 stock as described in 2.2.3.8. Sf9 cells were seeded at a density of 2x 10^6 cells/ml per with 15 ml Sf-900 II media in a 150 cm^2 flask. Each flask was inoculated with 300 µl of P1 stock and cultured at 27 °C for 48 or 72 h. At the end of this incubation the supernatant was removed and spun at 500 xg to clear any cell debris. This baculovirus P2 stock with higher titre was stored at 4 °C in dark and used for large-scale recombinant protein production.

In order to obtain the highest protein expression, it is necessary to optimise the multiplicity of infection (MOI) and the incubation time of infection. To this end, cells were seeded in a 12-well plate at a density of 6 x 10^6 per well, and allowed them to adhere for 1 h. Cells were then washed with Sf900-II medium once and 300 µl of the medium was added to each well. The titre of P2 stock was assumed to be 10^7 pfu/ml as there was not enough time to quantify the titre using the plaque assay before the end of these studies. Cells were infected at a series of MOIs, 1, 2, 5, 10 and 20 as recommended on the manufacturer's manual. The inoculate volume required was calculated using the formula as follows:

Inoculum required (ml) = MOI (pfu / cell) x number of cells / titre of viral stock (pfu/ml)

48 and 72 h post-infection, cells were harvested and analysed for protein expression by immunoblotting as shown in Figure 5.6. The cell lysates were probed with anti-FIP3 and anti-FIP4 antibodies. As the figure indicates, His-FIP3 did not express at 48 h, while His-FIP4 started to show expression from 48 h at MOI = 2. His-FIP3 expression initiates from 48 h, and reach the maximum expression at MOI = 5. His-FIP4 highest expression is obtained at 72 h with MOI = 20. Based on this result, it was decided to infect the Sf9 cells at an MOI of 5 for FIP3 and 20 for FIP4 and culture Sf9 cells for 72 h for the peak production of the recombinant proteins.

The large-scale protein expression then was attempted following the optimisation experiments. For each protein, thirty-five 150 cm^2 flasks of Sf9 cells were grown to a density of 6 x 10^7 cells/ml and each flask contained 30 ml Sf-900II media. The cells then were incubated with appropriate amount of virus and allowed to grow at 27 °C for 72 h. The cells then were resuspended in the media and spun down at 1000 xg. The cell pellets were washed twice with PBS and lysed in lysis buffer at a ratio of 4 ml buffer per 2 x 10^7 cell and broken by passing the French press at 950 psi. Insoluble material was removed by centrifugation at 30,000 xg in a JA 20 rotor for 30 min. The supernatant was then incubated with Ni-NTA agarose pre-equilibrated washing buffer containing 20 mM imidazole overnight at 4 °C. The next day, the cell lysate and Ni-NTA agarose mix was loaded to a column. The agarose then were washed 3 times with 2 ml wash buffer. Recombinant proteins were collected by 5 times elution with elution buffer. As shown in Figure 5.7, the 5 protein fractions were analysed by both immunoblot and 12 % SDS-PAGE gel followed by Coomassie blue staining. In Figure 5.7, panel A, anti-FIP3 antibody was used to blot FIP3, and a clean band of FIP3 at the appropriate size 82 kD was detected. Anti-FIP4 antibody also blots a specific band at the right size around 63 kD. The results indicated that the 6x His tagged FIP3 and FIP4 are clearly present in the elutions.

However, when the protein fractions were analysed by SDS-PAGE with Coomassie blue staining, it was discovered that multiple protein bands were present in the purification. By comparing with the gel of FIP3 and FIP4, it appears that the multiple bands of the two purifications have the same pattern. The specific main bands of FIP3 or FIP4 were not clearly shown on the corresponding purification. These results suggested that the His tagged FIP3 and FIP4 have been successfully eluted in the protein fractions, however, some non-specific insect cell proteins also came down with these elutions.

5.3 Discussion

In this chapter, experiments were carried out to further study the function and potential regulation mechanism of FIP3 and FIP4. To reveal FIP4's role and compare it with FIP3 in mitosis, RNAi was first attempted to see the direct consequence of it absence. Dharmacon SmartPool was used to knock down FIP4. Although several attempts have been performed with varied concentration of the siRNA from 50 nM to 150 nM; harvest time from 24 to 96 h; multiple transfections, no reduction of FIP4 expression was observed. Several reasons may be considered to affect the depletion performance. Firstly, the delivery of siRNA into the cells is the first essential step. In this experiment, siRNA against a house-keeping gene GAPDH was used as a positive control to ensure efficient transfection. Since GAPDH was depleted successfully, it ruled out the problem of the delivery method. Secondly, the SmartPool siRNA has been tested to eliminate 75% of the mRNA transcripts by the manufacturer, but no reduction of protein was observed in this experiment. The most likely reason would be that FIP4 has a long half-life. Longer periods of time may be required to reveal the protein decrease as well as cytokinesis effects. Thirdly, the siRNA duplexes used here may not be the most efficient ones. mRNA is likely to form secondary structure or may be modified by variety of factors, which could cause some regions not easy to access for the siRNA duplex. siRNA against different regions could be considered in future studies. Further studies have been carrying out by other colleagues in the lab.

The real time microscopy study of GFP-FIP4 showed an interesting phenotype that is different from what have been observed by interference its binding partner Rab11 and Arf6. Disruption of Rab11 or Arf6 by using RNAi or GTP deficient mutants resulted in cytokinesis defects. Treated cells underwent furrow ingression, however, a regression occurred after the ingression completed, suggesting a blockage at the late stage of cytokinesis. FIP4 interacts with Rab11 and Arf6 simultaneously and three of them all show concentrated localisation to the midbody during telophase and cytokinesis, it is proposed that they act as a trimeric complex to facilitate cytokinesis. Therefore, interference of FIP4 function is expected to induce similar consequences. To our surprise, the time-lapse microscopy showed that GFP-FIP4 did not lead to cell binucleation by inhibiting final abscission. Instead, it appears to cause cells arrest at G2/M boundary with cells rounding up without undergoing cytokinesis. This appears that FIP4 may actually have a different function in mitosis at the initiation of cell cycle in contrast to Rab11 and Arf6. However, it can not be ruled out that large amount GFP overexpression is likely to affect other pathways and lead to non-specific secondary effects. Interestingly, real time movies of

cells expressing GFP-FIP3 indicate different phenotype. It localises first to the centrosome in anaphase and then dramatically relocates to the furrow in late cytokinesis, suggesting these two proteins may play different role in mitosis. Because only a small population of cells with GFP-FIP4 expression were examined in this experiment (5 cells), it might not represent all the cases. In further studies, bigger size sample of cells needs to be observed to obtain more information.

Independent immunofluorescence experiments have previously shown that Aurora B and FIPs localised at the central spindle and midbody (Severson et al., 2000; Wilson et al., 2005). This prompted us to study whether FIPs can be phosphorylated by Aurora B. Interestingly, bioinformatics analysis showed that a sequence around S649 in FIP3, RRGRSSS, fit the criteria of a putative consensus sequence (K/R; K/R; X0-2; S/T) for phosphorylation by metazoan Aurora B kinase derived from some well-established substrates. Several other potential Aurora B sites in FIP3 and FIP4 are also predicted by using a comprehensive PK-specific prediction server, GPS. These data support the idea that FIPs may be regulated by Aurora B in mitosis. More detailed study of FIPs and Aurora B spatial distribution indicate that they have different distribution pattern during interphase. However, when the cell cycle is initiated, they all redistribute at the metaphase plate. In metaphase, the majority of Aurora B is detected along the metaphase plate, which is consistent with previous studies for its interaction with kinetochores and role in chromosome segregation. In this period although the majority of FIP4 is present on intracellular vesicles, but certain amount of it can be viewed on the metaphase plane (Figure 5.3, panel e-h). The colocalisation of these two proteins became more evident during anaphase at the metaphase plate, panel I. During telophase and cytokinesis, concentrated colocalisation of these two proteins was observed at the midbody. This distribution of FIP4 and Aurora B during mitosis suggested a good opportunity for these two proteins to meet *in vivo* and allow phosphorylation to occur. This idea is backed up by numerous previous studies of other Aurora B substrates. Aurora B shows colocalisation with many molecules that are its phosphorylation substrates. It partially colocalises with MKLP1/ZEN4 at the central spindle (Guse et al., 2005), and colocalises with mitotic centromere-associated kinesin (MCAK) at the centromere (Gorbsky, 2004).

The extensive colocalisation of Aurora B and FIP4 in mitosis prompted us to further study the functional relationship between the FIPs and Aurora B. Studies in this chapter showed that depletion of Aurora B siRNA delocalises FIP3 and FIP4 from the midbody. In the absence of Aurora B, more than 60% cells indicated no localisation of FIP3 and FIP4 at the midbody, which is almost 2-fold of the control cells. The majority of the GFP signals were

observed at the two mitotic spindle pole areas in these cells, which implicates an inhibition of these two molecules positioning to the right place. This is reminiscent of the situation when cells were treated with hesperadin, a small molecule inhibitor of Aurora kinase, which largely reduced the phosphorylated MKLP1 staining at midbody. MKLP1 has been shown phosphorylated at two sites by Aurora B kinase, in which the phosphorylation of S708 is important for successful completion of cytokinesis (Guse et al., 2005). The abnormal localisation of FIP3 and FIP4 in Aurora B depleted cells suggested that the FIPs localisation to the midbody might act in an Aurora B dependent manner. So it is reasoned the FIPs might be substrates of Aurora B, and the localisation of FIP3/FIP4 in this process may require phosphorylation modification mediated by Aurora B. However, it cannot be ruled out that the mislocalisation of FIP3/4 may due to a secondary effect induced by Aurora B. It is likely that depletion of Aurora B may affect its other substrates, which further cause indirect consequence on FIP3/4 localisation.

To verify whether Aurora B directly acts on FIP3/4, further experiments need to be carried out. It is worth checking whether endogenous FIP3 and FIP4 also are mislocalised from the midbody when Aurora B is disrupted. More importantly, *in vitro* phosphorylation studies need to be performed to test whether FIP3 and FIP4 can be phosphorylated.

In order to carry out the *in vitro* phosphorylation assay, production of full-length FIP3 and FIP4 proteins were tried using Bac-to-Bac baculovirus system. Figure 5.6 showed that FIP3 and FIP4 have been expressed successfully in Sf9 cells. Purification was then carried out. As shown in Figure 5.7, although proteins of interest were detected in elutions by immunoblotting, coomassie staining of SDS-PAGE indicated that there were contaminations with non-specific proteins from insect cells. In addition, the protein expression level is not high enough to identify the specific bands on the Comassie staining.

Several reasons are considered to explain these results. Firstly, the baculovirus has not been plaque purified and titered, hence the titres used in the large-scale expression are not accurate. Significant quantities of virus that does not express the protein of interest may, therefore have affected the expression of the recombinant proteins. Secondly, to get higher protein production, larger population of Sf9 cells are required. Culturing Sf9 cells in spinning culture instead of adhesion condition will be more efficient to grow the cells, which have been using in study following this thesis. Thirdly, many endogenous insect cells proteins may contain histidine, which interact with the Ni-NTA agarose. Although different concentrations of imidazole have been used for eluting the proteins of interest, non-specific proteins bands are still present in the protein fractions.

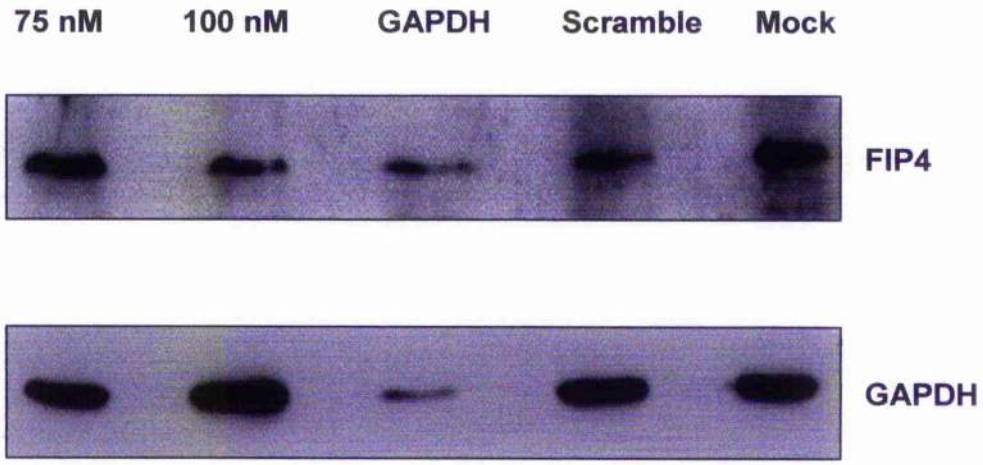

Figure 5.1 RNAi of FIP4

HeLa cells were transfected with SmartPool siRNA against FIP4 and incubated for 48, 72 or 96 h before analysis by immunoblot. Concentrations of siRNA applied were shown above the figures. The immunoblots shown here are representative blots from 72 h. The upper panel was blotted with sheep anti-FIP4 antibody raised in-house and the lower panel was blotted with mouse anti-GAPDH antibody. The lower panel indicates that positive control GAPDH was efficiently depleted. However, no obvious decrease on FIP4 protein level as shown in upper panel.

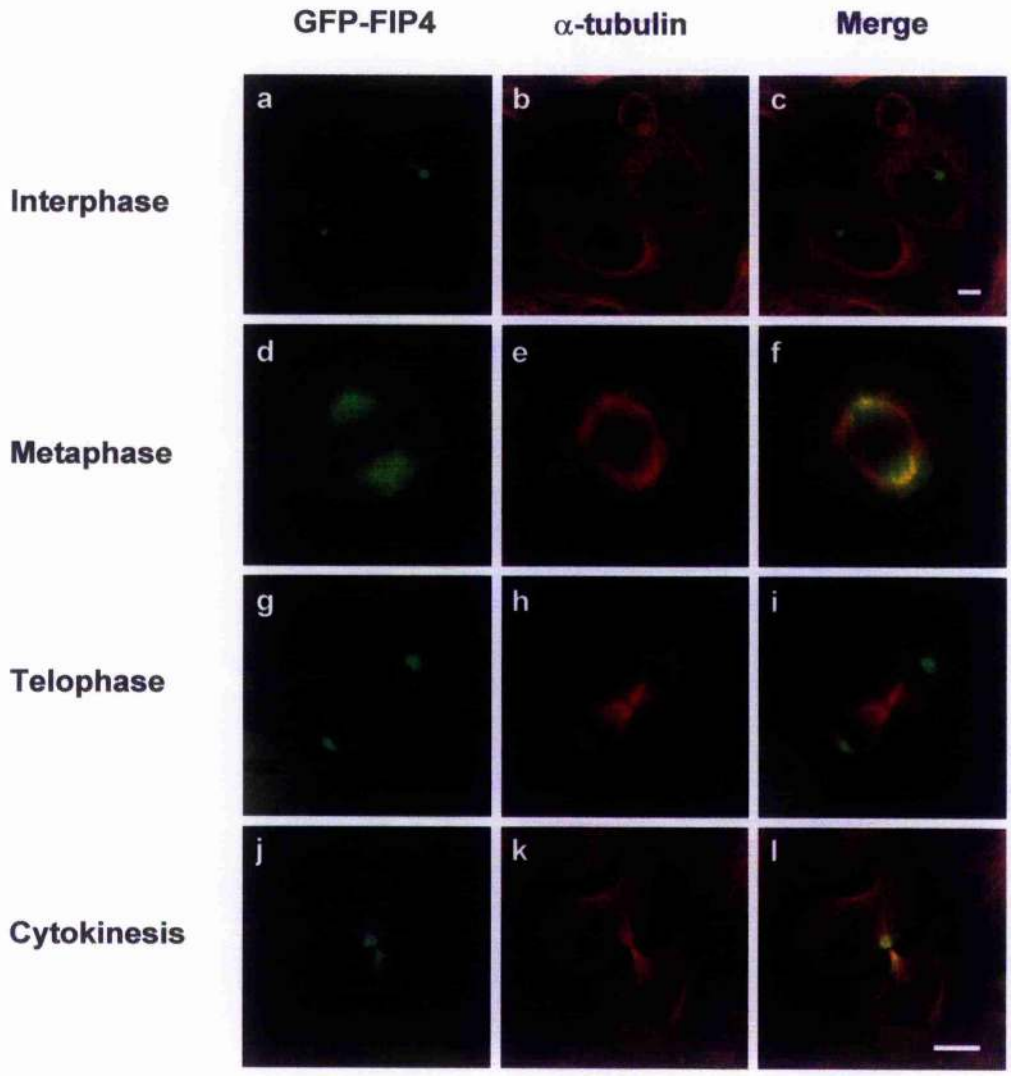

Figure 5.2 Subcellular localisation of GFP-FIP4 in HeLa cells during mitosis

HeLa cells grown on 13 mm glass coverslips were transfected with pEGFP-FIP4 using Lipofectamine 2000. The cells were incubated for 24 h before fixation in 4% paraformaldhyde and pemeabilised with 0.1% Triton-X-100. Immunofluorescence then was carried out using anti-αtubulin antibody followed by Alexa-594 anti-rabbit secondary antibody (red). Images were collected with a Zeiss Pascal Microscope as described in 2.2.4.2. The 488 nm, 594 nm channels are shown individually and merged together. Representative data are shown above. Scale bars: 10 μm.

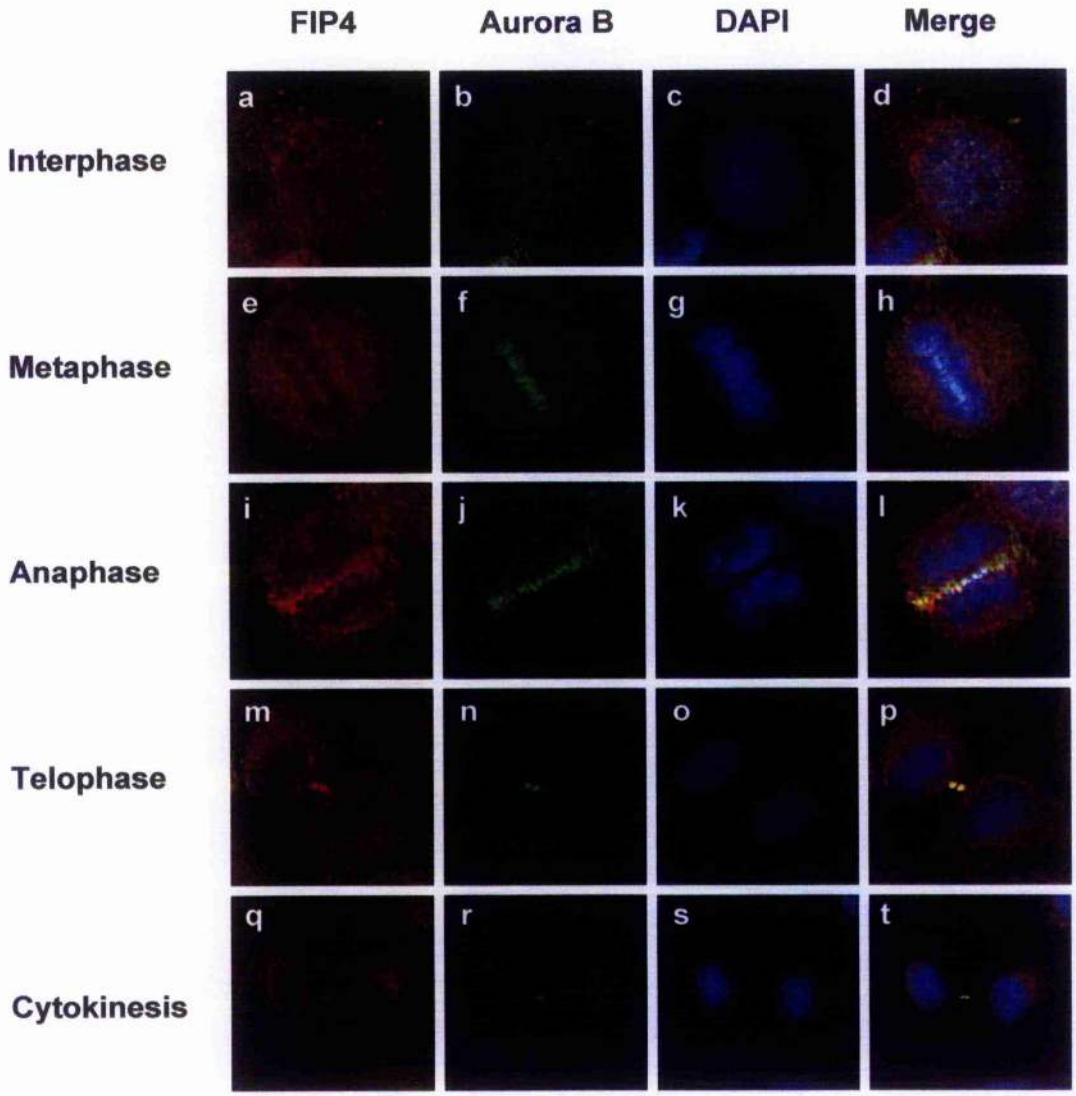

Figure 5.3 FIP4 and Aurora B colocalise during mitosis

HeLa cells grown on 13 mm glass coverslips were fixed in 4% paraformaldehyde and pemeabilised with 0.1% Triton-X-100. The cells then were stained using anti-FIP4 and anti-Aurora B antibodies followed by Alexa-594 (red) and 488 (green) fluorescent secondary antibodies. The DNA was also stained with DAPI, and Images of the cells at various stages of mitosis were collected using a Zeiss Pascal Microscope (described in section 2.2.4.2). The 488 nm, 594 nm channels are shown individually and merged together. Data shown are representative from at least 3 experiments.

A

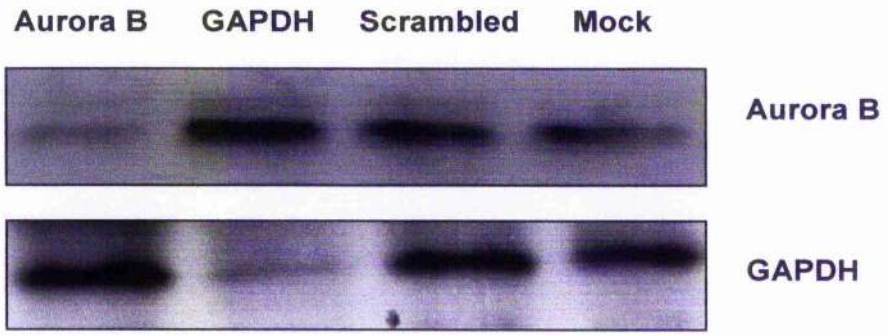

B

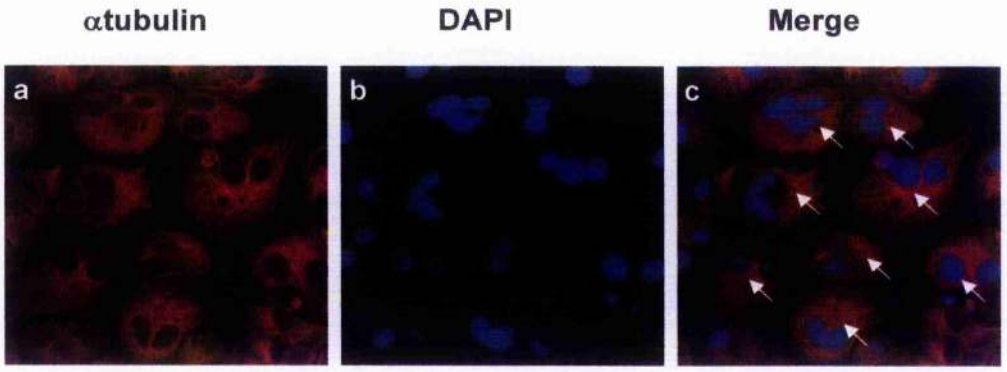

Figure 5.4 RNAi of Aurora B

HeLa cells were transfected with siRNA duplex against Aurora B and incubated for 72 h before analysis. **(A)** 5 μg cell lysates were loaded to each lane for immunoblot experiment. As indicated, Aurora B protein level was efficiently reduced compared to controls. GAPDH was used as a loading and positive control. **(B)** The cells seeded on coverslips with the same treatment as (A) were processed for immunofluorescence staining with anti-αtubulin followed by Alexa-594 (red). The DNA was stained with DAPI to verify multi/binucleate cells. Images were collected with Zeiss Pascal Microscope (described in section 2.2.4.2). The multi/binucleate cells were indicated with white arrows. Representative images are shown here.

A

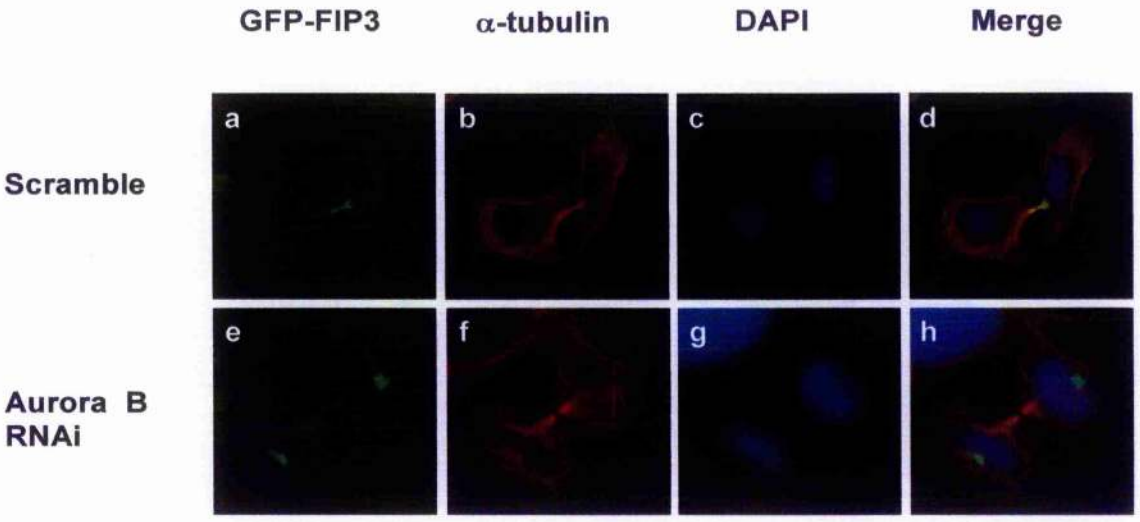
GFP-FIP3
α-tubulin
DAPI
Merge
Scramble
Aurora B RNAi
a
b
c
d
e
f
g
h

B

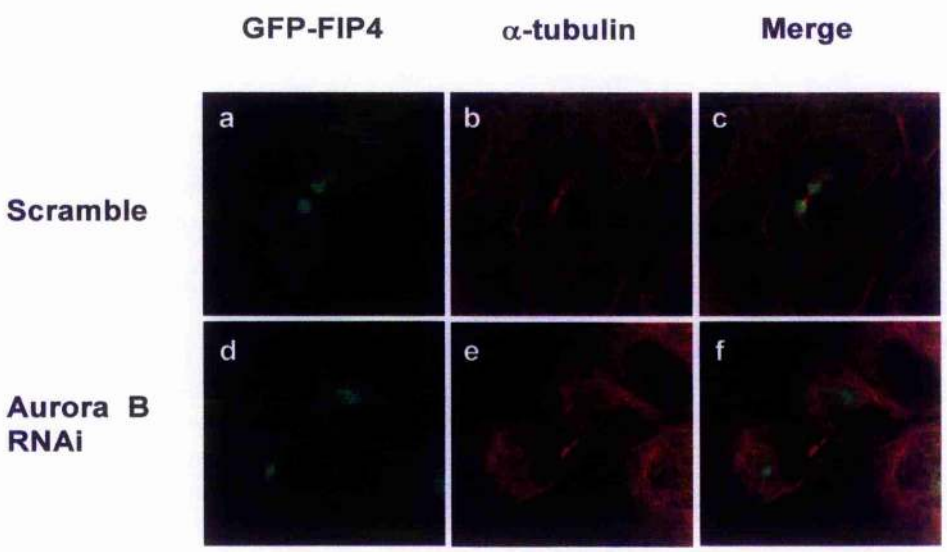
GFP-FIP4
α-tubulin
Merge
Scramble
Aurora B RNAi
a
b
c
d
e
f

C

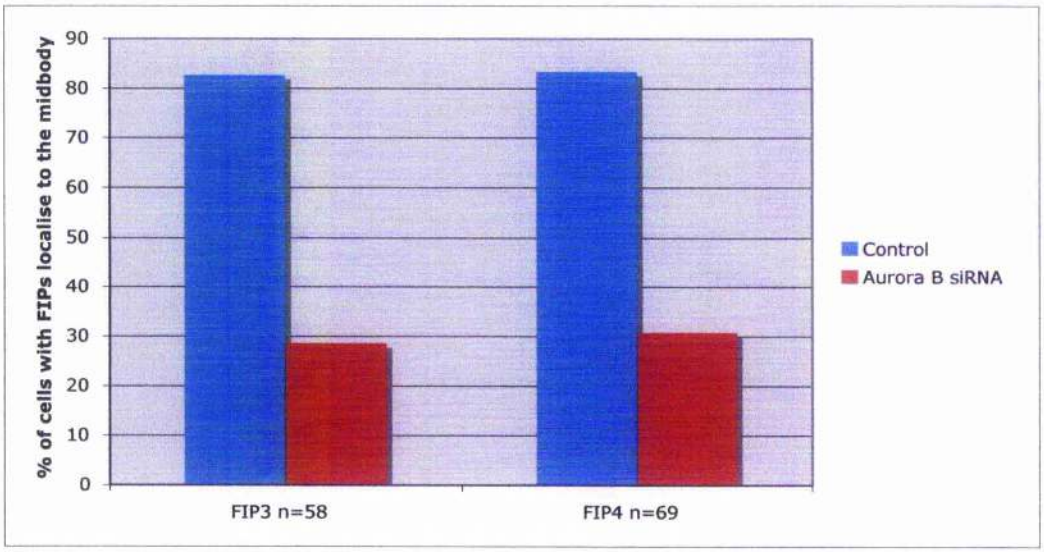

Figure 5.5 GFP-FIP3 and GFP-FIP4 mislocalise in cells depleted with Aurora B

(A, B) HeLa cells were transfected with scramble (panel A, a-d; panel B, a-c) or siRNA targeted for Aurora B (panel A, e-h; panel B, d-f). 24 h post-transfection, plasmids encoding GFP-FIP3 and GFP-FIP4 were transfected into the cells. Another 24 h later, the cells were fixed and processed for immunofluorescence. GFP-FIP3 and GFP-FIP4 were visualized by the GFP signal (green). The microtubules were stained with anti-αtubulin antibody followed by Alexa-594 (red) secondary antibody. Images of mitotic cells were collected using a Zeiss Pascal confocal microscope as described in section 2.5. Data shown are representative images. **(C)** The bar graph indicates the percentage of cells in which GFP-FIP3 and GFP-FIP4 localised at the midbody in the cells treated with either scramble or Aurora B siRNA from the same experiment. Total cells counts were shown below the corresponding bar.

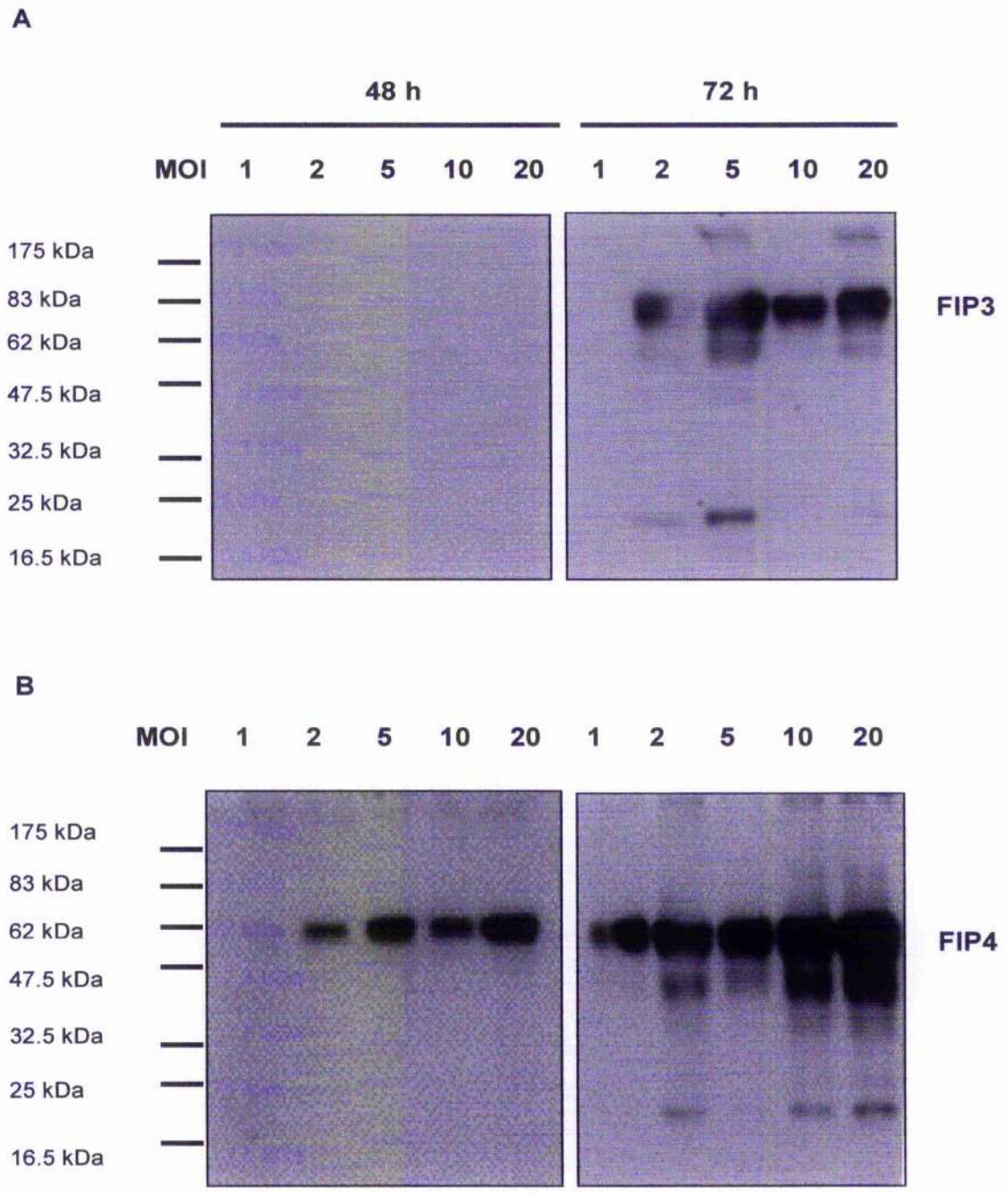

Figure 5.6 Optimisation of His-FIP3 and His-FIP4 expression with baculovirus

HeLa cells were seeded in 24-well plates at a density of 6 x 10^5 cell/ml with 300 μl of Sf- 900 II medium and allowed to settle down for 1 h. Then they were infected with P2 virus stock at a series of estimated MOI as indicated on the upper panel of the figures. The infected cells were incubated at 27°C for 48 h and 72 h to allow expression. After the indicated time, cells were washed twice with 300 μl PBS and lysed directly into 400 μl of 1 x SDS-PAGE sample buffer followed with boiling for 5 min. Immunoblot was carried out by using anti-FIP3 and anti-FIP4 antibodies to probe for the expressed recombinant proteins as shown.

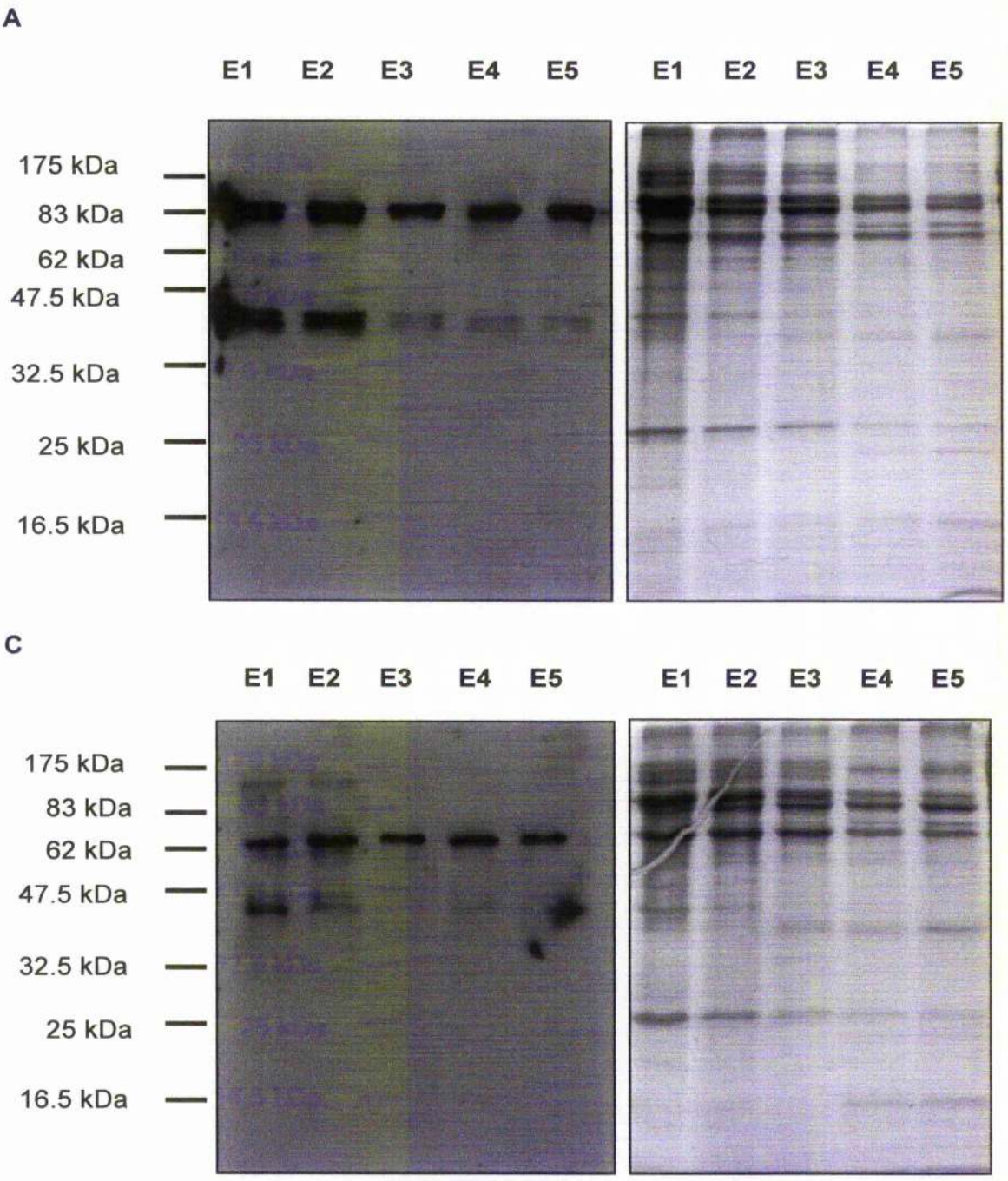

Figure 5.7 Purification of His-FIP3 and His-FIP4 proteins expressed by baculovirus

Each recombinant protein was expressed in 35 of 150 cm^2 flasks Sf9 insect cells. 72 h post-infection, the cells were washed once and lysed in lysis buffer as described in 2.2.2.4. After centrifugation, the supernatant was collected and incubated with Ni-NTA agarose overnight. The agarose was washed 3 times the next day, and proteins were eluted in 5 fractions. **(A)** 10 μl of elution 1-5 of His-FIP3 was loaded to each lane on SDS-PAGE and proceed for immunoblot with anti-FIP3 antibody on the left or coomassie blue staining on the right. **(B)** Same experiment as (A), except the loading protein is His-FIP4. The positions of the broad range markers are indicated.

6 Conclusion and future direction

Cytokinesis, an essential facet of mammalian cell division, is the process that physically cleaves two prospective daughter cells at the end of mitosis. It is highly regulated by a complex interplay of the mitotic spindle, the acto-myosin cytoskeleton and membrane fusion events. The work presented in this thesis sought to understand the molecular mechanisms underlying targeted deposition of new membrane during cytokinesis process by studying small GTPases, Rabs and Arf. These molecules are established critical regulators in intracellular membrane trafficking, which make them excellent candidates for membrane transport required in cytokinesis. In this study, the use of a diverse range of techniques such as RNAi, GTP deficient mutants of GTPases and microinjection have been applied to investigate the roles of Rab, Arf GTPases and their effectors in mammalian cytokinesis.

The study presented in this thesis is the first time to show that Rab11 plays an essential role in mammalian cytokinesis. It was previously known that Rab11 predominantly localises to the RE and regulate trafficking from this compartment during interphase. In this study, it was discovered that Rab11 positive RE relocate to centrosomes during anaphase and then the furrow/midbody during cytokinesis. Three independent methods, RNAi, Rab11 GTP-deficient mutant and microinjection of Rab11 antibody, have been used to disrupt function of Rab11 and all caused increased cell binucleation, a hallmark of cytokinesis defects. Together, these data strongly argue that Rab11's function is an integral facet of this process. Time-lapse microscopy further pinpointed the precise stage that Rab11 acts in the final abscission step, since its interference has no effect on furrow ingression. This work supports a essential role of Rab11 in mammalian cytokinesis, which is consistent with previous studies showing its involvement in *C. elegans* embryo cytokinesis (Skop et al., 2001) and *Drosophila* cellularisation (Riggs et al., 2003). This important function of Rab11's in cytokinesis is conserved from worms to mammalian cells. Although the source of membrane material inserted for furrowing and midbody abscission in cell division still remains controversial, this study has showed clearly that Rab11 regulated RE at least partially contributes membrane material required for mammalian cell cytokinesis.

This thesis also indicated another GTPase, Arf6 playing a role in cytokinesis. Arf6 has been previously shown involved in animal cytokinesis in a previous report (Schweitzer and D'Souza-Schorey, 2002; Schweitzer and D'Souza-Schorey, 2005). The author showed that expression GTP bound mutant (Q67L) caused abnormal cytokinesis phenotype. Interestingly, in this study, the GDP form of Arf6 (T27N) instead of GTP-Arf6 (Q67L) impairs cytokinesis. This observation is somehow inconsistent with Schweitzer and

D'Souza-Schorey paper. However, considering GTPases activity is dependent on their GTP cycle, it is not surprising that interruption of this cycle by overexpression of the protein will interfere with its function. Similarly to Rab11, video microscopy indicated that Arf6 acts at the late stage of cytokinesis after furrow completion, which supports the notion that Rab11 and Arf6 act in the same mechanism. Although, a subtle difference is that cells disrupted with Arf6 seldom formed the midbody bridge, while in Rab11 cells this structure is more evident. This observation together with the Rab11 and Arf6 co-depletion data implicate that Arf6 might be also involved in earlier steps of cytokinesis, such as midbody formation and stabilisation, which will be interesting to further investigate. It was also shown that localisations at the midbody of both Rab11 and FIP4 were greatly attenuated or completely abolished due to overexpression of Arf6 T27N. Conversely, active form of Arf6 (Q67L) accumulates these two molecules to the central spindle, which implicates that Arf6 activity may be responsible for properly targeting Rab11 and FIP4 to the midbody through interaction with FIP4. Arf6 has been previously reported to interact with mammalian exocyst complex component, Sec10 (Prigent et al., 2003), which provide an intriguing hypothesis that Arf6 may facilitate Rab11 and FIP4 positive endosomes docking to the dividing site via interaction with exocyst for exocytosis of the vesicles. It was subsequently discovered that FIP3 and FIP4 can both bind to a component of exocyst, Exo70 (Fielding et al., 2005), which further supports this hypothesis.

A recent study discovered a number of proteins arrived at the midbody in particular order and leads to abscission (Gromley et al., 2005). The authors also suggested the model of secretory vesicle-mediated asymmetric abscission during cytokinesis (Figure 6.1). The arrived molecules, MKLP1, MacRacGAP, Centriolin, exocyst and the delivery of SNAREs prepare for the maturation timing for final abscission at the midbody ring site. Intriguingly, the addition of the secretory vesicles to the cleavage site is only from one daughter cell, the vesicles accumulated at the midbody ring and fuse subsequently which lead to abscission. The mechanism underlying this asymmetric membrane delivery is unclear. A study showing mother centriole from one of the daughter cells moving to the intercellular bridge late in cytokinesis, and leaving from the midbody initiate cytokinesis may implicate a role of centrioles in this process (Piel et al., 2001). It is not known whether the Rab11-regulated RE trafficking to the midbody is also asymmetric as the secretory vesicles or from both daughter cells. It will be very intriguing to address this question by using fluorescence labelled protein and real time imaging, which will provide more insight for analysing membrane trafficking from different routes during cytokinesis. Despite this point, findings in this thesis can reasonably fit in the midbody abscission model suggested by Gromley paper with the fact that Arf6 and FIP3/4 all localise to the midbody ring structure and bind

to exocyst components. They may create a platform for Rab11-mediated endosome targeting to the midbody body ring via interacting with exocyst components and SNAREs mediated fusion prompts abscission as described in Figure 6.3.

FIP3 and FIP4 have been identified as dual Rab and Arf interaction proteins by our group and others (Hickson et al., 2003; Shin et al., 2001). They were subsequently shown to interact with Rab11 and Arf5/6 simultaneously, and colocalise at the furrow/midbody with these GTPases (Fielding et al., 2005). Studies from our group suggested FIP3 and FIP4 may be recruited to the RE via interaction with Rab11, and targeted to the midbody by Arf6. RNAi of FIP3 and a mutant blocking the interaction with Rab11 both resulted in increased binucleate cells implying an functional role in cytokinesis associated with Rab11 (Wilson et al., 2005). However, some key questions remain to be investigated. What is the role of FIP4 in cell division? Why there are two close homologues, FIP3 and FIP4 in mammalian cells? What is the biological meaning of the preferential binding to their GTPases interaction partners? To answer these questions, RNAi was used to determine FIP4 function. Unfortunately, the knockdown was not successful with several attempts both by my colleagues and this study. An interesting phenotype was observed from video microscopy showing expression of GFP-FIP4 arrested cells before anaphase elongation. This is puzzling, considering FIP4's striking localisation to the central spindle and midbody and sequence similarity to FIP3. It would be more reasonable to expect FIP4 functions in the late stage of cytokinesis as FIP3 instead of early step like anaphase. However, it cannot be ruled out this arrest was caused by secondary effect due to over expression of GFP tagged protein in cells. This experiments need to be repeated to confirm this phenotype, cells with lower expression of GFP-FIP4.

The RE are known to mediate recycling of proteins and membrane material to PM, the cytokinesis defects caused by interference of Rab11, FIP3 and Arf6 probably are not merely due to the lack of membrane transport, but some essential proteins associated with these vesicles required for cytokinesis. This idea is backed up by the recent study of Rab35, which controls a fast recycling pathway and acts in midbody bridge stability and abscission by delivering of PIP2 and SEP2 to the midbody (Kouranti et al., 2006). Therefore, in future studies, it would be interesting to analyse the cargoes Rab11/FIPs/Arf6 vesicles could possibly transport to the furrow/midbody. Numerous molecules that have been established to be essential for cytokinesis have been added to the candidate list: Centriolin, syntaxin2, syntaxin4, SEP2, SEP9, Snapin, Rho, MKLP1 and exocyst. Several approaches have been considered to test this hypothesis. The most straightforward method is perturbing Rab11, FIP3/4 or Arf6 by treating the cells with RNAi or express mutant

proteins, then examine localisation of these tested proteins at the midbody by immunofluorescence. If there are some effects in these treated cells, purification of the midbodies can be carried out and proteomics can be performed to analyse the presence of the protein in question (Skop et al, 2004).

Having demonstrated Rab11's importance in cytokinesis, we wondered whether other widely expressed endosomal Rabs, notably Rab4, 5, 7, 8, 9, 21 and 22, also contribute to this process, because many of them have overlapping distribution in endocytic pathway. In this regard, recent data have argued that endocytosis from the PM into the furrow may also play a fundamental role in cytokinesis (Schweitzer et al., 2005). Endocytosis ceases during entry of cell in prophase and metaphase, but resumes during anaphase and may be involved in the selective traffic of vesicles from the poles of cells into the furrow/midbody region. In Figure 4.1, it was shown that other endosomal Rabs but not Rab11 are enriched at the two pole areas, which is consistent with the sites where endocytosis occurred during cell division. Surprisingly, disruption of these endosomal Rab using RNAi and GTP deficient mutants did not cause an obvious effect in cytokinesis. However, in contrast to Rab11 depleted cells undergoing furrow regression, Rab4 knock down led to delay of midbody abscission. Previous study observed that Rab11 RNAi resulted in an up-regulation of Rab4 expression (Wilson et al., 2005), suggesting that Rab4 mediated fast recycling trafficking may take part in sealing of the cytoplasmic bridge. This role may not be as central as Rab11. That may be why its absence only causes minor defect in final abscission.

During the course of this study, Rab35, a member of Rab family has been reported to regulate a distinct endocytic recycling pathway and essential for the midbody stability and abscission in both *Drosophila* and human cells (Kouranti et al., 2006). This work backed up the idea that Rab GTPases regulated membrane trafficking pathways (Rab11, Rab35 and Rab4) participate in the cytokinesis process, especially final abscission. Due to its importance, multiple pathways are involved to ensure a proper completion. According to the known data, Rab11 and Rab35 seem to play a major role since their interruption led to more severe defects, largely increased cell binucleation. In contrast, Rab4 may play a minor role in this event, though further experiments need to be carried out to verify this. In the future, it will be worthwhile trying to disrupt these Rabs simutanously to dissect the relationships between different pathways. Whether other members of Rab family also contribute to cytokinesis require further investigation. Considering the complexity of Rab family as well as their partial overlapping intracellular distributions, compensatory mechanism may take place when a single Rab is knocked down, hence it may be

challenging to observe evident phenotype as well as study the precise role of individual proteins.

The striking redistribution of FIP3 and FIP4 from centrosome to the midbody during mitosis raises questions on how their localisations are regulated. A possible candidate for this dynamic distribution is phosphorylation. Here, preliminary data showed localisation of FIP3 and FIP4 with Aurora B kinase at the central spindle and the midbody, furthermore, depletion of Aurora B blocks FIP3 and FIP4 goes to midbody. This observation implicated that the proper localisation of FIPs in mitosis maybe mediated by Aurora B. The idea is supported by the discovery of several phosphorylation consensus sites in these two molecules. Interestingly, FIP3 and FIP4 homologue Nuf in *Drosophila* are cell-cycle regulated, highly phosphorylated proteins required for cellularisation (Rothwell et al., 1998). Very recently, the Prekeris group has revealed that centralspindlin is required for Rab11 and FIP3 localisation to the midbody. Considering that Aurora B mediated phosphorylation of centralspindlin proper localisation and proper function (Minoshima et al., 2003), it is logical that Aurora B also affects FIP3 localisation in cytokinesis (Prekeris unpublished data). With all this information, we want to determine whether certain mitotic kinases like Aurora B have the ability to phosphorylate FIP3 and FIP4 *in vitro*. In order to do this, full-length FIP3 and FIP4 proteins were expressed in Sf9 cells using Bac-to-Bac baculovirus expression system. It is encouraging that both proteins were expressed by the baculovirus system and were detected on SDS-PAGE and following immunobloting. However, the difficulty is that many non-specific insect cell proteins are also eluted with the proteins of interest. Because it was reaching the end of my PhD study when this part of experiments was carried out, there was not enough time to obtain better results. In order to obtain purer and larger amount of proteins of interest, the baculovirus stocks have been sent to the technology facility in university of York to carry out large-scale protein production. Purified proteins will proceed to carry out the *in vitro* phosphorylation experiment. In the event that phosphorylation of either protein is verified, the phosphorylation sites can be mapped by generation of series of point mutations and truncations.

Cytokinesis is the last step before two individual daughter cells part ways, hence it can be considered as the checkpoint to end all checkpoints. For dividing cells, it is the last chance to divide everything appropriately, so it is an essential step for all organisms. Numerous studies have suggested solid tumours generally exhibit polyploidy and single chromosome abnormalities, which are likely resulted from failures in both mitosis and cytokinesis. A direct connection between cytokinesis failure and carcinogenesis is presented by Pellman

and colleagues, block of cytokinesis causes primary cells lacking p53 become much more carcinogenic in mice (Fujiwara et al., 2005). Thus cytokinesis is a valuable point of possible therapeutic intervention in cancer. A good example is Aurora kinase inhibitors, currently in clinical trials.

Recently, great strides have been made in dissecting the intriguing cytokinesis mechanism and more and more key regulators have been added to the "play list" of cytokinesis, as shown in Figure 6.2. Although it is far from a exhaustive list and not yet possible to synthesize the data from all diverse model system into a cohesive theory, continuing to identify novel molecules and discover pathways important underlying this process will help to broaden and deepen our understanding in this essential cellular event and provide more therapeutic targets for cytokinesis related disease.

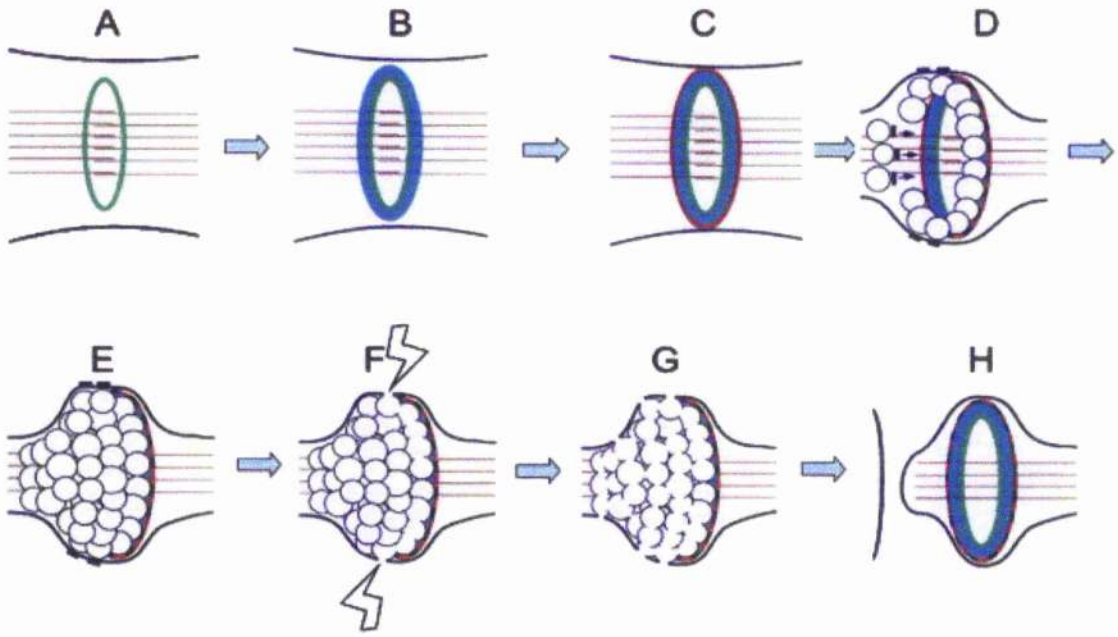

Figure 6.1 Model of secretory vesicle-mediated abscission during cytokinesis (Gromley et al, 2005)

(A) MKLP1 and MgcRacGAP (green) arrive at the midbody ring after cleavage furrow complete. **(B-C)** Centriolin (blue) moves to the ring and anchors Sec15 as well as other exocyst components, and snapin (red). **(D)** The secretory vesicles and v- and t-SNAREs (black) move to the midbody ring from one prospective daughter cell. **(E)** Vesicles pack asymmetrically at one side of the midbody ring. **(F-G)** Vesicles adjacent to the ring fuse with the PM facilitated by SNAREs and exocyst. **(H)** Abscission occurs at the site of membrane fusion, and the midbody is retained by the daughter cell opposite to the fusion site. The released midbody ring still contains multiple proteins present before and usually retains microtubule bundles.

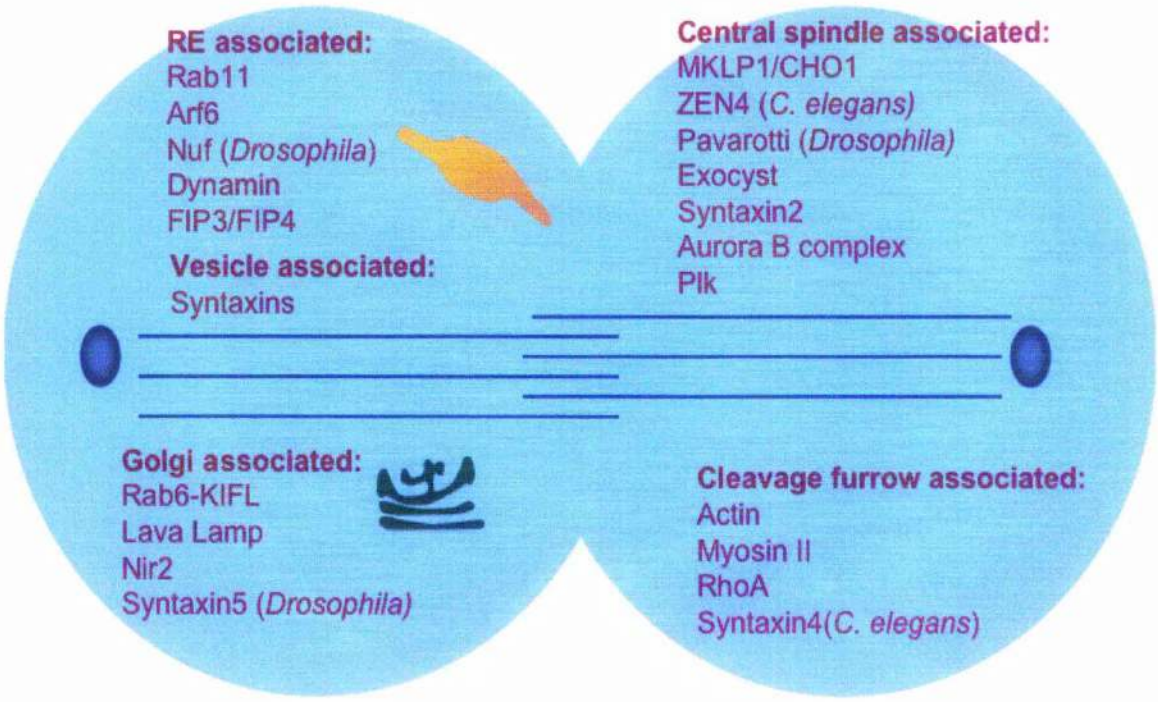

Figure 6.2 Essential regulators involved in animal cytokinesis

Studies from a variety of organisms have identified proteins within the secretary and endocytic pathways that are crucial for cytokinesis. Cleavage furrow ingresses driven by actin-myosin ring constriction and is regulated by numerous proteins. Vesicles contributing to this process may be derived from the Golgi or from intermediate trafficking organelles such as the RE by proteins found on these organelles. Membrane vesicles delivery to the midbody may be guided by the central spindle and associated proteins. SNARE that localise on the PM and vesicles prompt specific vesicle targeting and fusion at the furrow and midbody.

A

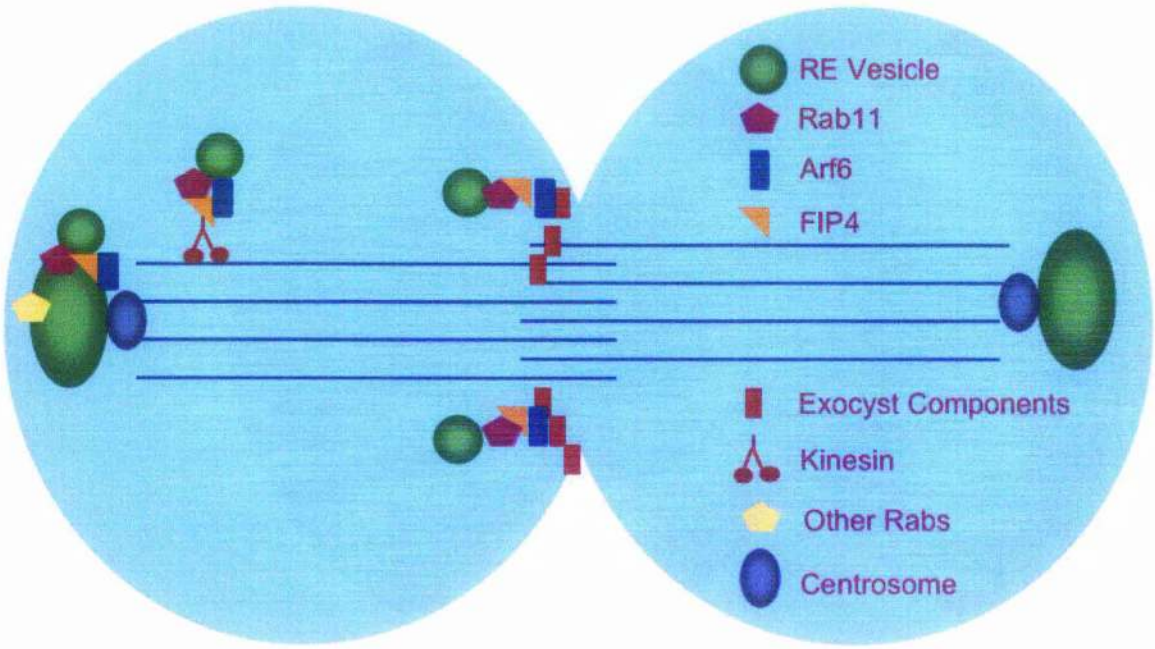
RE Vesicle
Rab11
Arf6
FIP4
Exocyst Components
Kinesin
Other Rabs
Centrosome

B

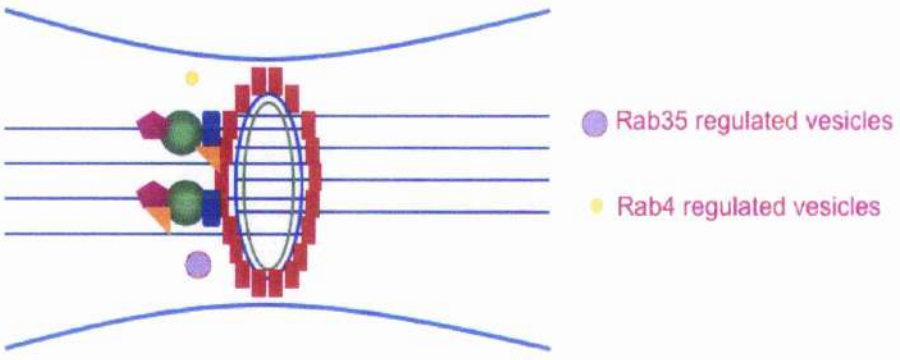
Rab35 regulated vesicles
Rab4 regulated vesicles

Figure 6.3 Model depicting membrane vesicles trafficking during cytokinesis

(A) A Cartoon of cell at telophase/cytokinesis. During this period, Rab11 positive endosomes localise to the pericentrosomal area. FIP3/4 is recruited to these compartments via the interaction between Rab11. "Arf6 endosome" may also collapse into this area. Other Rab proteins, such as Rab4 or Rab5 may regulate endocytosis in this region. Then Rab11 regulates the exit of vesicles trafficking from the recycling endosome, with FIP3/4 and possibly Arf6 presence. These vesicles then are loaded onto astral microtubules which leads towards the center of the cell, possibly through a association with a kinesin-like protein. Then they travel along the microtubules to the furrow/midbody area. When the Rab11/FIP3/4/Arf6 regulated vesicles arrive the proximity of the furrow during cytokineiss stage, Arf6 and FIP3/4 may interact with exocyst complex aligned on the midbody ring to allow the vesicle dock on the abscission site. These vesicles may contain SNARE proteins required for fusion events which create a membrane barrier between two daughter cells. Rab35 and Rab4 regulated vesicles may also contribute to the inserted membrane material to some extent. **(B)** The midbody abscission. As suggested by Gromley A. et al, MKLP1 and MgcRacGAP (green ring) arrive at midbody ring first, then Centriolin (blue ring) moves to the ring. These molecules anchor exocyst components (red) to the midbody ring structure. Interaction of Arf6 and FIP3/4 with the exocyst components may facilitate targeting the vesicles to the midbody ring for the final closure.

Reference

Adamo, J.E., G. Rossi, and P. Brennwald. 1999. The Rho GTPase Rho3 has a direct role in exocytosis that is distinct from its role in actin polarity. *Mol Biol Cell*. 10:4121-33.

Adams, R.R., M. Carmena, and W.C. Earnshaw. 2001a. Chromosomal passengers and the (aurora) ABCs of mitosis. *Trends Cell Biol*. 11:49-54.

Adams, R.R., H. Maiato, W.C. Earnshaw, and M. Carmena. 2001b. Essential roles of *Drosophila* inner centromere protein (INCENP) and aurora B in histone H3 phosphorylation, metaphase chromosome alignment, kinetochore disjunction, and chromosome segregation. *J Cell Biol*. 153:865-80.

Adams, R.R., A.A. Tavares, A. Salzberg, H.J. Bellen, and D.M. Glover. 1998. pavarotti encodes a kinesin-like protein required to organize the central spindle and contractile ring for cytokinesis. *Genes Dev*. 12:1483-94.

Adams, R.R., S.P. Wheatley, A.M. Gouldsworthy, S.E. Kandels-Lewis, M. Carmena, C. Smythe, D.L. Gerloff, and W.C. Earnshaw. 2000. INCENP binds the Aurora-related kinase AIRK2 and is required to target it to chromosomes, the central spindle and cleavage furrow. *Curr Biol*. 10:1075-8.

Allan, V.J., and T.A. Schroer. 1999. Membrane motors. *Curr Opin Cell Biol*. 11:476-82.

Alsop, G.B., and D. Zhang. 2003. Microtubules are the only structural constituent of the spindle apparatus required for induction of cell cleavage. *J Cell Biol*. 162:383-90.

Altan-Bonnet, N., R.D. Phair, R.S. Polishchuk, R. Weigert, and J. Lippincott-Schwartz. 2003. A role for Arf1 in mitotic Golgi disassembly, chromosome segregation, and cytokinesis. *Proc Natl Acad Sci U S A*. 100:13314-9.

Amano, M., M. Ito, K. Kimura, Y. Fukata, K. Chihara, T. Nakano, Y. Matsuura, and K. Kaibuchi. 1996. Phosphorylation and activation of myosin by Rho-associated kinase (Rho-kinase). *J Biol Chem*. 271:20246-9.

Anant, J.S., L. Desnoyers, M. Machius, B. Demeler, J.C. Hansen, K.D. Westover, J. Deisenhofer, and M.C. Seabra. 1998. Mechanism of Rab geranylgeranylation: formation of the catalytic ternary complex. *Biochemistry*. 37:12559-68.

Bailly, E., M. McCaffrey, N. Touchot, A. Zahraoui, B. Goud, and M. Bornens. 1991. Phosphorylation of two small GTP-binding proteins of the Rab family by p34cdc2. *Nature*. 350:715-8.

Barr, F.A. 2004. Golgi inheritance: shaken but not stirred. *J Cell Biol*. 164:955-8.

Barral, Y., V. Mermall, M.S. Mooseker, and M. Snyder. 2000. Compartmentalization of the cell cortex by septins is required for maintenance of cell polarity in yeast. *Mol Cell*. 5:841-51.

Beites, C.L., H. Xie, R. Bowser, and W.S. Trimble. 1999. The septin CDCrel-1 binds syntaxin and inhibits exocytosis. *Nat Neurosci*. 2:434-9.

Benli, M., F. Doring, D.G. Robinson, X. Yang, and D. Gallwitz. 1996. Two GTPase isoforms, Ypt31p and Ypt32p, are essential for Golgi function in yeast. *Embo J*. 15:6460-75.

Berlin, R.D., and J.M. Oliver. 1980. Surface functions during mitosis. II. Quantitation of pinocytosis and kinetic characterization of the mitotic cycle with a new fluorescence technique. *J Cell Biol*. 85:660-71.

Bischoff, J.R., L. Anderson, Y. Zhu, K. Mossie, L. Ng, B. Souza, B. Schryver, P. Flanagan, F. Clairvoyant, C. Ginther, C.S. Chan, M. Novotny, D.J. Slamon, and G.D. Plowman. 1998. A homologue of *Drosophila* aurora kinase is oncogenic and amplified in human colorectal cancers. *Embo J*. 17:3052-65.

Bluemink, J.G., and S.W. de Laat. 1973. New membrane formation during cytokinesis in normal and cytochalasin B-treated eggs of *Xenopus laevis*. I. Electron microscope observations. *J Cell Biol*. 59:89-108.

Boman, A.L., and R.A. Kahn. 1995. Arf proteins: the membrane traffic police? *Trends Biochem Sci*. 20:147-50.

Bottger, G., B. Nagelkerken, and P. van der Sluijs. 1996. Rab4 and Rab7 define distinct nonoverlapping endosomal compartments. *J Biol Chem.* 271:29191-7.

Brown, F.D., A.L. Rozelle, H.L. Yin, T. Balla, and J.G. Donaldson. 2001. Phosphatidylinositol 4,5-bisphosphate and Arf6-regulated membrane traffic. *J Cell Biol.* 154:1007-17.

Bucci, C., R.G. Parton, I.H. Mather, H. Stunnenberg, K. Simons, B. Hoflack, and M. Zerial. 1992. The small GTPase rab5 functions as a regulatory factor in the early endocytic pathway. *Cell.* 70:715-28.

Burd, C.G., T.I. Strochlic, and S.R. Gangi Setty. 2004. Arf-like GTPases: not so Arf-like after all. *Trends Cell Biol.* 14:687-94.

Burgess, R.W., D.L. Deitcher, and T.L. Schwarz. 1997. The synaptic protein syntaxin1 is required for cellularization of *Drosophila* embryos. *J Cell Biol.* 138:861-75.

Calhoun, B.C., L.A. Lapierre, C.S. Chew, and J.R. Goldenring. 1998. Rab11a redistributes to apical secretory canaliculus during stimulation of gastric parietal cells. *Am J Physiol.* 275:C163-70.

Canman, J.C., L.A. Cameron, P.S. Maddox, A. Straight, J.S. Tirnauer, T.J. Mitchison, G. Fang, T.M. Kapoor, and E.D. Salmon. 2003. Determining the position of the cell division plane. *Nature.* 424:1074-8.

Cantalupo, G., P. Alifano, V. Roberti, C.B. Bruni, and C. Bucci. 2001. Rab-interacting lysosomal protein (RILP): the Rab7 effector required for transport to lysosomes. *Embo J.* 20:683-93.

Caplen, N.J., S. Parrish, F. Imani, A. Fire, and R.A. Morgan. 2001. Specific inhibition of gene expression by small double-stranded RNAs in invertebrate and vertebrate systems. *Proc Natl Acad Sci U S A.* 98:9742-7.

Castillon, G.A., N.R. Adames, C.H. Rosello, H.S. Seidel, M.S. Longtine, J.A. Cooper, and R.A. Heil-Chapdelaine. 2003. Septins have a dual role in controlling mitotic exit in budding yeast. *Curr Biol.* 13:654-8.

Caumont, A.S., M.C. Galas, N. Vitale, D. Aunis, and M.F. Bader. 1998. Regulated exocytosis in chromaffin cells. Translocation of ARF6 stimulates a plasma membrane-associated phospholipase D. *J Biol Chem.* 273:1373-9.

Chavrier, P., and B. Goud. 1999. The role of ARF and Rab GTPases in membrane transport. *Curr Opin Cell Biol.* 11:466-75.

Chavrier, P., R.G. Parton, H.P. Hauri, K. Simons, and M. Zerial. 1990. Localization of low molecular weight GTP binding proteins to exocytic and endocytic compartments. *Cell.* 62:317-29.

Chavrier, P., P. van der Sluijs, Z. Mishal, B. Nagelkerken, and J.P. Gorvel. 1997. Early endosome membrane dynamics characterized by flow cytometry. *Cytometry.* 29:41-9.

Chen, W., Y. Feng, D. Chen, and A. Wandinger-Ness. 1998. Rab11 is required for trans-golgi network-to-plasma membrane transport and a preferential target for GDP dissociation inhibitor. *Mol Biol Cell.* 9:3241-57.

Cheng, K.W., J.P. Lahad, W.L. Kuo, A. Lapuk, K. Yamada, N. Auersperg, J. Liu, K. Smith-McCune, K.H. Lu, D. Fishman, J.W. Gray, and G.B. Mills. 2004. The RAB25 small GTPase determines aggressiveness of ovarian and breast cancers. *Nat Med.* 10:1251-6.

Christoforidis, S., H.M. McBride, R.D. Burgoyne, and M. Zerial. 1999. The Rab5 effector EEA1 is a core component of endosome docking. *Nature.* 397:621-5.

Conner, S.D., and G.M. Wessel. 1999. Syntaxin is required for cell division. *Mol Biol Cell.* 10:2735-43.

Cox, D., D.J. Lee, B.M. Dale, J. Calafat, and S. Greenberg. 2000. A Rab11-containing rapidly recycling compartment in macrophages that promotes phagocytosis. *Proc Natl Acad Sci U S A.* 97:680-5.

Danilchik, M.V., S.D. Bedrick, E.E. Brown, and K. Ray. 2003. Furrow microtubules and localized exocytosis in cleaving *Xenopus laevis* embryos. *J Cell Sci.* 116:273-83.

Daro, E., P. van der Sluijs, T. Galli, and I. Mellman. 1996. Rab4 and cellubrevin define different early endosome populations on the pathway of transferrin receptor recycling. *Proc Natl Acad Sci U S A*. 93:9559-64.

D'Avino, P.P., M.S. Savoian, L. Capalbo, and D.M. Glover. 2006. RacGAP50C is sufficient to signal cleavage furrow formation during cytokinesis. *J Cell Sci*. 119:4402-8.

Donaldson, J.G. 2002. Arf6 and its role in cytoskeletal modulation. *Methods Mol Biol*. 189:191-8.

Donaldson, J.G. 2003. Multiple roles for Arf6: sorting, structuring, and signaling at the plasma membrane. *J Biol Chem*. 278:41573-6.

Donaldson, J.G., and C.L. Jackson. 2000. Regulators and effectors of the ARF GTPases. *Curr Opin Cell Biol*. 12:475-82.

Dornan, S., A.P. Jackson, and N.J. Gay. 1997. Alpha-adaptin, a marker for endocytosis, is expressed in complex patterns during *Drosophila* development. *Mol Biol Cell*. 8:1391-403.

Drivas, G.T., A. Shih, E.E. Coutavas, P. D'Eustachio, and M.G. Rush. 1991. Identification and characterization of a human homolog of the *Schizosaccharomyces pombe* ras-like gene YPT-3. *Oncogene*. 6:3-9.

Dutertre, S., S. Descamps, and C. Prigent. 2002. On the role of aurora-A in centrosome function. *Oncogene*. 21:6175-83.

Echard, A., F. Jollivet, O. Martinez, J.J. Lacapere, A. Rousselet, I. Janoueix-Lerosey, and B. Goud. 1998. Interaction of a Golgi-associated kinesin-like protein with Rab6. *Science*. 279:580-5.

Elbashir, S.M., W. Lendeckel, and T. Tuschl. 2001. RNA interference is mediated by 21- and 22-nucleotide RNAs. *Genes Dev*. 15:188-200.

Ellgaard, L., and A. Helenius. 2001. ER quality control: towards an understanding at the molecular level. *Curr Opin Cell Biol*. 13:431-7.

Emoto, K., T. Kobayashi, A. Yamaji, H. Aizawa, I. Yahara, K. Inoue, and M. Umeda. 1996. Redistribution of phosphatidylethanolamine at the cleavage furrow of dividing cells during cytokinesis. *Proc Natl Acad Sci U S A*. 93:12867-72.

Emoto, K., and M. Umeda. 2001. Membrane lipid control of cytokinesis. *Cell Struct Funct*. 26:659-65.

Feng, B., H. Schwarz, and S. Jesuthasan. 2002. Furrow-specific endocytosis during cytokinesis of *zebrafish* blastomeres. *Exp Cell Res*. 279:14-20.

Feng, Y., B. Press, and A. Wandinger-Ness. 1995. Rab 7: an important regulator of late endocytic membrane traffic. *J Cell Biol*. 131:1435-52.

Field, C.M., and D. Kellogg. 1999. Septins: cytoskeletal polymers or signalling GTPases? *Trends Cell Biol*. 9:387-94.

Field, S.J., N. Madson, M.L. Kerr, K.A. Galbraith, C.E. Kennedy, M. Tahiliani, A. Wilkins, and L.C. Cantley. 2005. PtdIns(4,5)P2 functions at the cleavage furrow during cytokinesis. *Curr Biol*. 15:1407-12.

Fielding, A.B., E. Schonteich, J. Matheson, G. Wilson, X. Yu, G.R. Hickson, S. Srivastava, S.A. Baldwin, R. Prekeris, and G.W. Gould. 2005. Rab11-FIP3 and FIP4 interact with Arf6 and the exocyst to control membrane traffic in cytokinesis. *Embo J*. 24:3389-99.

Fielding, A.B. 2005. Rab11-FIP4, It's Small GTPase Binding Partners And Their Roles in Cytokinesis. PhD Thesis. Wellcome Laboratory of Cell Biology. University of Glasgow. Glasgow.

Finger, F.P., and J.G. White. 2002. Fusion and fission: membrane trafficking in animal cytokinesis. *Cell*. 108:727-30.

Fire, A., S. Xu, M.K. Montgomery, S.A. Kostas, S.E. Driver, and C.C. Mello. 1998. Potent and specific genetic interference by double-stranded RNA in *Caenorhabditis elegans*. *Nature*. 391:806-11.

Flemming, W. 1891. Arch-mikr. Anat. 37, 685-691.

Fujiwara, K., M.E. Porter, and T.D. Pollard. 1978. Alpha-actinin localization in the cleavage furrow during cytokinesis. *J Cell Biol.* 79:268-75.

Fujiwara, T., M. Bandi, M. Nitta, E.V. Ivanova, R.T. Bronson, and D. Pellman. 2005. Cytokinesis failure generating tetraploids promotes tumorigenesis in p53-null cells. *Nature.* 437:1043-7.

Garrett, M.D., J.E. Zahner, C.M. Cheney, and P.J. Novick. 1994. GDI1 encodes a GDP dissociation inhibitor that plays an essential role in the yeast secretory pathway. *Embo J.* 13:1718-28.

Glotzer, M. 2001. Animal cell cytokinesis. *Annu Rev Cell Dev Biol.* 17:351-86.

Glotzer, M. 2004. Cleavage furrow positioning. *J Cell Biol.* 164:347-51.

Goldenring, J.R., K.R. Shen, H.D. Vaughan, and I.M. Modlin. 1993. Identification of a small GTP-binding protein, Rab25, expressed in the gastrointestinal mucosa, kidney, and lung. *J Biol Chem.* 268:18419-22.

Gonzalez, C. 2003. Dispatch. Cell division: the place and time of cytokinesis. *Curr Biol.* 13:R363-5.

Gonzalez, L., Jr., and R.H. Scheller. 1999. Regulation of membrane trafficking: structural insights from a Rab/effector complex. *Cell.* 96:755-8.

Goody, R.S., A. Rak, and K. Alexandrov. 2005. The structural and mechanistic basis for recycling of Rab proteins between membrane compartments. *Cell Mol Life Sci.* 62:1657-70.

Gorbsky, G.J. 2004. Mitosis: MCAK under the aura of Aurora B. *Curr Biol.* 14:R346-8.

Goshima, G., and R.D. Vale. 2003. The roles of microtubule-based motor proteins in mitosis: comprehensive RNAi analysis in the *Drosophila* S2 cell line. *J Cell Biol.* 162:1003-16.

Gromley, A., C. Yeaman, J. Rosa, S. Redick, C.T. Chen, S. Mirabelle, M. Guha, J. Sillibourne, and S.J. Doxsey. 2005. Centriolin anchoring of exocyst and SNARE complexes at the midbody is required for secretory-vesicle-mediated abscission. *Cell.* 123:75-87.

Gruneberg, U., R. Neef, R. Honda, E.A. Nigg, and F.A. Barr. 2004. Relocation of Aurora B from centromeres to the central spindle at the metaphase to anaphase transition requires MKlp2. *J Cell Biol.* 166:167-72.

Guo, S., and K.J. Kemphues. 1995. par-1, a gene required for establishing polarity in C. elegans embryos, encodes a putative Ser/Thr kinase that is asymmetrically distributed. *Cell.* 81:611-20.

Guo, W., A. Grant, and P. Novick. 1999a. Exo84p is an exocyst protein essential for secretion. *J Biol Chem.* 274:23558-64.

Guo, W., D. Roth, C. Walch-Solimena, and P. Novick. 1999b. The exocyst is an effector for Sec4p, targeting secretory vesicles to sites of exocytosis. *Embo J.* 18:1071-80.

Guo, W., F. Tamanoi, and P. Novick. 2001. Spatial regulation of the exocyst complex by Rho1 GTPase. *Nat Cell Biol.* 3:353-60.

Guse, A., M. Mishima, and M. Glotzer. 2005. Phosphorylation of ZEN-4/MKLP1 by aurora B regulates completion of cytokinesis. *Curr Biol.* 15:778-86.

Hales, C.M., R. Griner, K.C. Hobdy-Henderson, M.C. Dorn, D. Hardy, R. Kumar, J. Navarre, E.K. Chan, L.A. Lapierre, and J.R. Goldenring. 2001. Identification and characterization of a family of Rab11-interacting proteins. *J Biol Chem.* 276:39067-75.

Hashimoto, S., Y. Onodera, A. Hashimoto, M. Tanaka, M. Hamaguchi, A. Yamada, and H. Sabe. 2004. Requirement for Arf6 in breast cancer invasive activities. *Proc Natl Acad Sci U S A.* 101:6647-52.

Hickson, G.R., A. Echard, and P.H. O'Farrell. 2006. Rho-kinase controls cell shape changes during cytokinesis. *Curr Biol.* 16:359-70.

Hickson, G.R., J. Matheson, B. Riggs, V.H. Maier, A.B. Fielding, R. Prekeris, W. Sullivan, F.A. Barr, and G.W. Gould. 2003. Arfophilins are dual Arf/Rab 11 binding proteins

that regulate recycling endosome distribution and are related to Drosophila nuclear fallout. *Mol Biol Cell*. 14:2908-20.

Hill, E., M. Clarke, and F.A. Barr. 2000. The Rab6-binding kinesin, Rab6-KIFL, is required for cytokinesis. *Embo J*. 19:5711-9.

Hirokawa, N. 1998. Kinesin and dynein superfamily proteins and the mechanism of organelle transport. *Science*. 279:519-26.

Honda, R., R. Korner, and E.A. Nigg. 2003. Exploring the functional interactions between Aurora B, INCENP, and survivin in mitosis. *Mol Biol Cell*. 14:3325-41.

Hsu, S.C., C.D. Hazuka, R. Roth, D.L. Foletti, J. Heuser, and R.H. Scheller. 1998. Subunit composition, protein interactions, and structures of the mammalian brain sec6/8 complex and septin filaments. *Neuron*. 20:1111-22.

Jackson, C.L., and J.E. Casanova. 2000. Turning on ARF: the Sec7 family of guanine-nucleotide-exchange factors. *Trends Cell Biol*. 10:60-7.

Jantsch-Plunger, V., and M. Glotzer. 1999. Depletion of syntaxins in the early *Caenorhabditis elegans* embryo reveals a role for membrane fusion events in cytokinesis. *Curr Biol*. 9:738-45.

Jantsch-Plunger, V., P. Gonczy, A. Romano, H. Schnabel, D. Hamill, R. Schnabel, A.A. Hyman, and M. Glotzer. 2000. CYK-4: A Rho family gtpase activating protein (GAP) required for central spindle formation and cytokinesis. *J Cell Biol*. 149:1391-404.

Kahn, R.A., J. Cherfils, M. Elias, R.C. Lovering, S. Munro, and A. Schurmann. 2006. Nomenclature for the human Arf family of GTP-binding proteins: ARF, ARL, and SAR proteins. *J Cell Biol*. 172:645-50.

Kahn, R.A., and A.G. Gilman. 1984. Purification of a protein cofactor required for ADP-ribosylation of the stimulatory regulatory component of adenylate cyclase by cholera toxin. *J Biol Chem*. 259:6228-34.

Kaitna, S., M. Mendoza, V. Jantsch-Plunger, and M. Glotzer. 2000. Incenp and an aurora-like kinase form a complex essential for chromosome segregation and efficient completion of cytokinesis. *Curr Biol*. 10:1172-81.

Kaitna, S., P. Pasierbek, M. Jantsch, J. Loidl, and M. Glotzer. 2002. The aurora B kinase AIR-2 regulates kinetochores during mitosis and is required for separation of homologous Chromosomes during meiosis. *Curr Biol*. 12:798-812.

Kato, M., T. Sasaki, T. Ohya, H. Nakanishi, H. Nishioka, M. Imamura, and Y. Takai. 1996. Physical and functional interaction of rabphilin-3A with alpha-actinin. *J Biol Chem*. 271:31775-8.

Kauppi, M., A. Simonsen, B. Bremnes, A. Vieira, J. Callaghan, H. Stenmark, and V.M. Olkkonen. 2002. The small GTPase Rab22 interacts with EEA1 and controls endosomal membrane trafficking. *J Cell Sci*. 115:899-911.

Kikuchi, A., T. Yamashita, M. Kawata, K. Yamamoto, K. Ikeda, T. Tanimoto, and Y. Takai. 1988. Purification and characterization of a novel GTP-binding protein with a molecular weight of 24,000 from bovine brain membranes. *J Biol Chem*. 263:2897-904.

Kimura, M., S. Kotani, T. Hattori, N. Sumi, T. Yoshioka, K. Todokoro, and Y. Okano. 1997. Cell cycle-dependent expression and spindle pole localization of a novel human protein kinase, Aik, related to Aurora of *Drosophila* and yeast Ipl1. *J Biol Chem*. 272:13766-71.

Kimura, M., Y. Matsuda, T. Yoshioka, and Y. Okano. 1999. Cell cycle-dependent expression and centrosome localization of a third human aurora/Ipl1-related protein kinase, AIK3. *J Biol Chem*. 274:7334-40.

Kinoshita, M., S. Kumar, A. Mizoguchi, C. Ide, A. Kinoshita, T. Haraguchi, Y. Hiraoka, and M. Noda. 1997. Nedd5, a mammalian septin, is a novel cytoskeletal component interacting with actin-based structures. *Genes Dev*. 11:1535-47.

Kishida, S., H. Shirataki, T. Sasaki, M. Kato, K. Kaibuchi, and Y. Takai. 1993. Rab3A GTPase-activating protein-inhibiting activity of Rabphilin-3A, a putative Rab3A target protein. *J Biol Chem.* 268:22259-61.

Komatsu, S., T. Yano, M. Shibata, R.A. Tuft, and M. Ikebe. 2000. Effects of the regulatory light chain phosphorylation of myosin II on mitosis and cytokinesis of mammalian cells. *J Biol Chem.* 275:34512-20.

Kosako, H., H. Goto, M. Yanagida, K. Matsuzawa, M. Fujita, Y. Tomono, T. Okigaki, H. Odai, K. Kaibuchi, and M. Inagaki. 1999. Specific accumulation of Rho-associated kinase at the cleavage furrow during cytokinesis: cleavage furrow-specific phosphorylation of intermediate filaments. *Oncogene.* 18:2783-8.

Kouranti, I., M. Sachse, N. Arouche, B. Goud, and A. Echard. 2006. Rab35 regulates an endocytic recycling pathway essential for the terminal steps of cytokinesis. *Curr Biol.* 16:1719-25.

Kufer, T.A., H.H. Sillje, R. Korner, O.J. Gruss, P. Meraldi, and E.A. Nigg. 2002. Human TPX2 is required for targeting Aurora-A kinase to the spindle. *J Cell Biol.* 158:617-23.

Kuge, O., C. Dascher, L. Orci, T. Rowe, M. Amherdt, H. Plutner, M. Ravazzola, G. Tanigawa, J.E. Rothman, and W.E. Balch. 1994. Sar1 promotes vesicle budding from the endoplasmic reticulum but not Golgi compartments. *J Cell Biol.* 125:51-65.

Kusch, J., A. Meyer, M.P. Snyder, and Y. Barral. 2002. Microtubule capture by the cleavage apparatus is required for proper spindle positioning in yeast. *Genes Dev.* 16:1627-39.

Lapierre, L.A., R. Kumar, C.M. Hales, J. Navarre, S.G. Bhartur, J.O. Burnette, D.W. Provance, Jr., J.A. Mercer, M. Bahler, and J.R. Goldenring. 2001. Myosin vb is associated with plasma membrane recycling systems. *Mol Biol Cell.* 12:1843-57.

Lauber, M.H., I. Waizenegger, T. Steinmann, H. Schwarz, U. Mayer, I. Hwang, W. Lukowitz, and G. Jurgens. 1997. The *Arabidopsis* KNOLLE protein is a cytokinesis-specific syntaxin. *J Cell Biol.* 139:1485-93.

Lazar, T., M. Gotte, and D. Gallwitz. 1997. Vesicular transport: how many Ypt/Rab-GTPases make a eukaryotic cell? *Trends Biochem Sci.* 22:468-72.

Lecuit, T., and E. Wieschaus. 2000. Polarized insertion of new membrane from a cytoplasmic reservoir during cleavage of the *Drosophila* embryo. *J Cell Biol.* 150:849-60.

Liang, J.O., and S. Kornfeld. 1997. Comparative activity of ADP-ribosylation factor family members in the early steps of coated vesicle formation on rat liver Golgi membranes. *J Biol Chem.* 272:4141-8.

Lindsay, A.J., A.G. Hendrick, G. Cantalupo, F. Senic-Matuglia, B. Goud, C. Bucci, and M.W. McCaffrey. 2002. Rab coupling protein (RCP), a novel Rab4 and Rab11 effector protein. *J Biol Chem.* 277:12190-9.

Litvak, V., R. Argov, N. Dahan, S. Ramachandran, R. Amarilio, A. Shainskaya, and S. Lev. 2004. Mitotic phosphorylation of the peripheral Golgi protein Nir2 by Cdk1 provides a docking mechanism for Plk1 and affects cytokinesis completion. *Mol Cell.* 14:319-30.

Liu, X., T. Zhou, R. Kuriyama, and R.L. Erikson. 2004. Molecular interactions of Polo-like-kinase 1 with the mitotic kinesin-like protein CHO1/MKLP-1. *J Cell Sci.* 117:3233-46.

Lombardi, D., T. Soldati, M.A. Riederer, Y. Goda, M. Zerial, and S.R. Pfeffer. 1993. Rab9 functions in transport between late endosomes and the trans Golgi network. *Embo J.* 12:677-82.

Low, S.H., X. Li, M. Miura, N. Kudo, B. Quinones, and T. Weimbs. 2003. Syntaxin 2 and endobrevin are required for the terminal step of cytokinesis in mammalian cells. *Dev Cell.* 4:753-9.

Mammoto, A., T. Ohtsuka, I. Hotta, T. Sasaki, and Y. Takai. 1999. Rab11BP/Rabphilin-11, a downstream target of rab11 small G protein implicated in vesicle recycling. *J Biol Chem.* 274:25517-24.

Martinez, O., and B. Goud. 1998. Rab proteins. *Biochim Biophys Acta.* 1404:101-12.

Matuliene, J., and R. Kuriyama. 2002. Kinesin-like protein CHO1 is required for the formation of midbody matrix and the completion of cytokinesis in mammalian cells. *Mol Biol Cell.* 13:1832-45.

McBride, H.M., V. Rybin, C. Murphy, A. Giner, R. Teasdale, and M. Zerial. 1999. Oligomeric complexes link Rab5 effectors with NSF and drive membrane fusion via interactions between EEA1 and syntaxin 13. *Cell.* 98:377-86.

McLauchlan, H., J. Newell, N. Morrice, A. Osborne, M. West, and E. Smythe. 1998. A novel role for Rab5-GDI in ligand sequestration into clathrin-coated pits. *Curr Biol.* 8:34-45.

Mesa, R., C. Salomon, M. Roggero, P.D. Stahl, and L.S. Mayorga. 2001. Rab22a affects the morphology and function of the endocytic pathway. *J Cell Sci.* 114:4041-9.

Miaczynska, M., and M. Zerial. 2002. Mosaic organization of the endocytic pathway. *Exp Cell Res.* 272:8-14.

Milburn, M.V., L. Tong, A.M. deVos, A. Brunger, Z. Yamaizumi, S. Nishimura, and S.H. Kim. 1990. Molecular switch for signal transduction: structural differences between active and inactive forms of protooncogenic ras proteins. *Science.* 247:939-45.

Millar, C.A., K.A. Powell, G.R. Hickson, M.F. Bader, and G.W. Gould. 1999. Evidence for a role for ADP-ribosylation factor 6 in insulin-stimulated glucose transporter-4 (GLUT4) trafficking in 3T3-L1 adipocytes. *J Biol Chem.* 274:17619-25.

Minoshima, Y., T. Kawashima, K. Hirose, Y. Tonozuka, A. Kawajiri, Y.C. Bao, X. Deng, M. Tatsuka, S. Narumiya, W.S. May, Jr., T. Nosaka, K. Semba, T. Inoue, T. Satoh, M. Inagaki, and T. Kitamura. 2003. Phosphorylation by aurora B converts MgcRacGAP to a RhoGAP during cytokinesis. *Dev Cell.* 4:549-60.

Mishima, M., S. Kaitna, and M. Glotzer. 2002. Central spindle assembly and cytokinesis require a kinesin-like protein/RhoGAP complex with microtubule bundling activity. *Dev Cell.* 2:41-54.

Mohrmann, K., L. Gerez, V. Oorschot, J. Klumperman, and P. van der Sluijs. 2002. Rab4 function in membrane recycling from early endosomes depends on a membrane to cytoplasm cycle. *J Biol Chem.* 277:32029-35.

Mohrmann, K., and P. van der Sluijs. 1999. Regulation of membrane transport through the endocytic pathway by rabGTPases. *Mol Membr Biol.* 16:81-7.

Moskalenko, S., D.O. Henry, C. Rosse, G. Mirey, J.H. Camonis, and M.A. White. 2002. The exocyst is a Ral effector complex. *Nat Cell Biol.* 4:66-72.

Moss, J., and M. Vaughan. 1998. Molecules in the ARF orbit. *J Biol Chem.* 273:21431-4.

Murata-Hori, M., K. Fumoto, Y. Fukuta, T. Iwasaki, A. Kikuchi, M. Tatsuka, and H. Hosoya. 2000. Myosin II regulatory light chain as a novel substrate for AIM-1, an aurora/Ipl1p-related kinase from rat. *J Biochem (Tokyo).* 128:903-7.

Napoli, C., C. Lemieux, and R. Jorgensen. 1990. Introduction of a Chimeric Chalcone Synthase Gene into Petunia Results in Reversible Co-Suppression of Homologous Genes in trans. *Plant Cell.* 2:279-289.

Neef, R., C. Preisinger, J. Sutcliffe, R. Kopajtich, E.A. Nigg, T.U. Mayer, and F.A. Barr. 2003. Phosphorylation of mitotic kinesin-like protein 2 by polo-like kinase 1 is required for cytokinesis. *J Cell Biol.* 162:863-75.

Ng, EL., Y. Wang, B.L. Tang. 2007. Rab22B's role in trans-Golgi network membrane dynamics. *Biochem Biophys Res Commun.* 28;361(3):751-7.

Nislow, C., V.A. Lombillo, R. Kuriyama, and J.R. McIntosh. 1992. A plus-end-directed motor enzyme that moves antiparallel microtubules in vitro localizes to the interzone of mitotic spindles. *Nature.* 359:543-7.

Novick, P., and W. Guo. 2002. Ras family therapy: Rab, Rho and Ral talk to the exocyst. *Trends Cell Biol.* 12:247-9.

Otegui, M.S., and L.A. Staehelin. 2004. Electron tomographic analysis of post-meiotic cytokinesis during pollen development in Arabidopsis thaliana. *Planta*. 218:501-15.

Palacios, F., L. Price, J. Schweitzer, J.G. Collard, and C. D'Souza-Schorey. 2001. An essential role for ARF6-regulated membrane traffic in adherens junction turnover and epithelial cell migration. *Embo J.* 20:4973-86.

Pelissier, A., J.P. Chauvin, and T. Lecuit. 2003. Trafficking through Rab11 endosomes is required for cellularization during *Drosophila* embryogenesis. *Curr Biol.* 13:1848-57.

Pellinen, T., A. Arjonen, K. Vuoriluoto, K. Kallio, J.A. Fransen, and J. Ivaska. 2006. Small GTPase Rab21 regulates cell adhesion and controls endosomal traffic of beta1-integrins. *J Cell Biol.* 173:767-80.

Pfeffer, S., and D. Aivazian. 2004. Targeting Rab GTPases to distinct membrane compartments. *Nat Rev Mol Cell Biol.* 5:886-96.

Piel, M., J. Nordberg, U. Euteneuer, and M. Bornens. 2001. Centrosome-dependent exit of cytokinesis in animal cells. *Science*. 291:1550-3.

Prekeris, R. 2003. Rabs, Rips, FIPs, and endocytic membrane traffic. *ScientificWorldJournal*. 3:870-80.

Prekeris, R., J.M. Davies, and R.H. Scheller. 2001. Identification of a novel Rab11/25 binding domain present in Eferin and Rip proteins. *J Biol Chem*. 276:38966-70.

Prigent, M., T. Dubois, G. Raposo, V. Derrien, D. Tenza, C. Rosse, J. Camonis, and P. Chavrier. 2003. ARF6 controls post-endocytic recycling through its downstream exocyst complex effector. *J Cell Biol.* 163:1111-21.

Radhakrishna, H., O. Al-Awar, Z. Khachikian, and J.G. Donaldson. 1999. ARF6 requirement for Rac ruffling suggests a role for membrane trafficking in cortical actin rearrangements. *J Cell Sci.* 112 (Pt 6):855-66.

Radhakrishna, H., and J.G. Donaldson. 1997. ADP-ribosylation factor 6 regulates a novel plasma membrane recycling pathway. *J Cell Biol.* 139:49-61.

Radhakrishna, H., R.D. Klausner, and J.G. Donaldson. 1996. Aluminum fluoride stimulates surface protrusions in cells overexpressing the ARF6 GTPase. *J Cell Biol.* 134:935-47.

Raich, W.B., A.N. Moran, J.H. Rothman, and J. Hardin. 1998. Cytokinesis and midzone microtubule organization in *Caenorhabditis elegans* require the kinesin-like protein ZEN-4. *Mol Biol Cell.* 9:2037-49.

Ren, M., G. Xu, J. Zeng, C. De Lemos-Chiarandini, M. Adesnik, and D.D. Sabatini. 1998. Hydrolysis of GTP on rab11 is required for the direct delivery of transferrin from the pericentriolar recycling compartment to the cell surface but not from sorting endosomes. *Proc Natl Acad Sci U S A.* 95:6187-92.

Ridley, A.J., and A. Hall. 1992. The small GTP-binding protein rho regulates the assembly of focal adhesions and actin stress fibers in response to growth factors. *Cell.* 70:389-99.

Riggs, B., W. Rothwell, S. Mische, G.R. Hickson, J. Matheson, T.S. Hays, G.W. Gould, and W. Sullivan. 2003. Actin cytoskeleton remodeling during early *Drosophila* furrow formation requires recycling endosomal components Nuclear-fallout and Rab11. *J Cell Biol.* 163:143-54.

Robinson, N.G., L. Guo, J. Imai, E.A. Toh, Y. Matsui, and F. Tamanoi. 1999. Rho3 of *Saccharomyces cerevisiae*, which regulates the actin cytoskeleton and exocytosis, is a GTPase which interacts with Myo2 and Exo70. *Mol Cell Biol.* 19:3580-7.

Romano, N., and G. Macino. 1992. Quelling: transient inactivation of gene expression in Neurospora crassa by transformation with homologous sequences. *Mol Microbiol.* 6:3343-53.

Rothman, J.E. 1994. Intracellular membrane fusion. *Adv Second Messenger Phosphoprotein Res.* 29:81-96.

Rothwell, W.F., P. Fogarty, C.M. Field, and W. Sullivan. 1998. Nuclear-fallout, a *Drosophila* protein that cycles from the cytoplasm to the centrosomes, regulates cortical microfilament organization. *Development*. 125:1295-303.

Rybin, V., O. Ullrich, M. Rubino, K. Alexandrov, I. Simon, M.C. Seabra, R. Goody, and M. Zerial. 1996. GTPase activity of Rab5 acts as a timer for endocytic membrane fusion. *Nature*. 383:266-9.

Sabe, H. 2003. Requirement for Arf6 in cell adhesion, migration, and cancer cell invasion. *J Biochem (Tokyo)*. 134:485-9.

Santy, L.C., S.R. Frank, and J.E. Casanova. 2001. Expression and analysis of ARNO and ARNO mutants and their effects on ADP-ribosylation factor (ARF)-mediated actin cytoskeletal rearrangements. *Methods Enzymol*. 329:256-64.

Satterwhite, L.L., M.J. Lohka, K.L. Wilson, T.Y. Scherson, L.J. Cisek, J.L. Corden, and T.D. Pollard. 1992. Phosphorylation of myosin-II regulatory light chain by cyclin-p34cdc2: a mechanism for the timing of cytokinesis. *J Cell Biol*. 118:595-605.

Schafer, D.A., C. D'Souza-Schorey, and J.A. Cooper. 2000. Actin assembly at membranes controlled by ARF6. *Traffic*. 1:892-903.

Schiavo, G., C.C. Shone, M.K. Bennett, R.H. Scheller, and C. Montecucco. 1995. Botulinum neurotoxin type C cleaves a single Lys-Ala bond within the carboxyl-terminal region of syntaxins. *J Biol Chem*. 270:10566-70.

Schlichting, I., S.C. Almo, G. Rapp, K. Wilson, K. Petratos, A. Lentfer, A. Wittinghofer, W. Kabsch, E.F. Pai, G.A. Petsko, and et al. 1990. Time-resolved X-ray crystallographic study of the conformational change in Ha-Ras p21 protein on GTP hydrolysis. *Nature*. 345:309-15.

Schlierf, B., G.H. Fey, J. Hauber, G.M. Hocke, and O. Rosorius. 2000. Rab11b is essential for recycling of transferrin to the plasma membrane. *Exp Cell Res*. 259:257-65.

Schweitzer, J.K., E.E. Burke, H.V. Goodson, and C. D'Souza-Schorey. 2005. Endocytosis resumes during late mitosis and is required for cytokinesis. *J Biol Chem*. 280:41628-35.

Schweitzer, J.K., and C. D'Souza-Schorey. 2002. Localization and activation of the ARF6 GTPase during cleavage furrow ingression and cytokinesis. *J Biol Chem*. 277:27210-6.

Schweitzer, J.K., and C. D'Souza-Schorey. 2005. A requirement for ARF6 during the completion of cytokinesis. *Exp Cell Res*. 311:74-83.

Severson, A.F., D.R. Hamill, J.C. Carter, J. Schumacher, and B. Bowerman. 2000. The aurora-related kinase AIR-2 recruits ZEN-4/CeMKLP1 to the mitotic spindle at metaphase and is required for cytokinesis. *Curr Biol*. 10:1162-71.

Shapiro, A.D., and S.R. Pfeffer. 1995. Quantitative analysis of the interactions between prenyl Rab9, GDP dissociation inhibitor-alpha, and guanine nucleotides. *J Biol Chem*. 270:11085-90.

Sheff, D.R., E.A. Daro, M. Hull, and I. Mellman. 1999. The receptor recycling pathway contains two distinct populations of early endosomes with different sorting functions. *J Cell Biol*. 145:123-39.

Shin, O.H., A.D. Couvillon, and J.H. Exton. 2001. Arfophilin is a common target of both class II and class III ADP-ribosylation factors. *Biochemistry*. 40:10846-52.

Shin, O.H., and J.H. Exton. 2001. Differential binding of arfaptin 2/POR1 to ADP-ribosylation factors and Rac1. *Biochem Biophys Res Commun*. 285:1267-73.

Shin, O.H., A.H. Ross, I. Mihai, and J.H. Exton. 1999. Identification of arfophilin, a target protein for GTP-bound class II ADP-ribosylation factors. *J Biol Chem*. 274:36609-15.

Shuster, C.B., and D.R. Burgess. 1999. Parameters that specify the timing of cytokinesis. *J Cell Biol*. 146:981-92.

Shuster, C.B., and D.R. Burgess. 2002. Targeted new membrane addition in the cleavage furrow is a late, separate event in cytokinesis. *Proc Natl Acad Sci U S A*. 99:3633-8.

Simpson, J.C., G. Griffiths, M. Wessling-Resnick, J.A. Fransen, H. Bennett, and A.T. Jones. 2004. A role for the small GTPase Rab21 in the early endocytic pathway. *J Cell Sci.* 117:6297-311.

Sisson, J.C., C. Field, R. Ventura, A. Royou, and W. Sullivan. 2000. Lava lamp, a novel peripheral golgi protein, is required for *Drosophila melanogaster* cellularization. *J Cell Biol.* 151:905-18.

Skop, A.R., D. Bergmann, W.A. Mohler, and J.G. White. 2001. Completion of cytokinesis in *C. elegans* requires a brefeldin A-sensitive membrane accumulation at the cleavage furrow apex. *Curr Biol.* 11:735-46.

Skop, A.R., H. Liu, J. Yates, 3rd, B.J. Meyer, and R. Heald. 2004. Dissection of the mammalian midbody proteome reveals conserved cytokinesis mechanisms. *Science.* 305:61-6.

Somers, W.G., and R. Saint. 2003. A RhoGEF and Rho family GTPase-activating protein complex links the contractile ring to cortical microtubules at the onset of cytokinesis. *Dev Cell.* 4:29-39.

Somsel Rodman, J., and A. Wandinger-Ness. 2000. Rab GTPases coordinate endocytosis. *J Cell Sci.* 113 Pt 2:183-92.

Song, J., Z. Khachikian, H. Radhakrishna, and J.G. Donaldson. 1998. Localization of endogenous ARF6 to sites of cortical actin rearrangement and involvement of ARF6 in cell spreading. *J Cell Sci.* 111 (Pt 15):2257-67.

Sonnichsen, B., S. De Renzis, E. Nielsen, J. Rietdorf, and M. Zerial. 2000. Distinct membrane domains on endosomes in the recycling pathway visualized by multicolor imaging of Rab4, Rab5, and Rab11. *J Cell Biol.* 149:901-14.

Spiliotis, E.T., and W.J. Nelson. 2006. Here come the septins: novel polymers that coordinate intracellular functions and organization. *J Cell Sci.* 119:4-10.

Stenmark, H., and V.M. Olkkonen. 2001. The Rab GTPase family. *Genome Biol.* 2:REVIEWS3007.

Stenmark, H., R.G. Parton, O. Steele-Mortimer, A. Lutcke, J. Gruenberg, and M. Zerial. 1994. Inhibition of rab5 GTPase activity stimulates membrane fusion in endocytosis. *Embo J.* 13:1287-96.

Straight, A.F., A. Cheung, J. Limouze, I. Chen, N.J. Westwood, J.R. Sellers, and T.J. Mitchison. 2003. Dissecting temporal and spatial control of cytokinesis with a myosin II Inhibitor. *Science.* 299:1743-7.

Strickland, L.I., and D.R. Burgess. 2004. Pathways for membrane trafficking during cytokinesis. *Trends Cell Biol.* 14:115-8.

Stroupe, C., and A.T. Brunger. 2000. Crystal structures of a Rab protein in its inactive and active conformations. *J Mol Biol.* 304:585-98.

Surka, M.C., C.W. Tsang, and W.S. Trimble. 2002. The mammalian septin MSF localizes with microtubules and is required for completion of cytokinesis. *Mol Biol Cell.* 13:3532-45.

Tamkun, J.W., R.A. Kahn, M. Kissinger, B.J. Brizuela, C. Rulka, M.P. Scott, and J.A. Kennison. 1991. The arflike gene encodes an essential GTP-binding protein in *Drosophila*. *Proc Natl Acad Sci U S A.* 88:3120-4.

TerBush, D.R., T. Maurice, D. Roth, and P. Novick. 1996. The Exocyst is a multiprotein complex required for exocytosis in *Saccharomyces cerevisiae*. *Embo J.* 15:6483-94.

Thompson, H.M., A.R. Skop, U. Euteneuer, B.J. Meyer, and M.A. McNiven. 2002. The large GTPase dynamin associates with the spindle midzone and is required for cytokinesis. *Curr Biol.* 12:2111-7.

Tisdale, E.J., J.R. Bourne, R. Khosravi-Far, C.J. Der, and W.E. Balch. 1992. GTP-binding mutants of rab1 and rab2 are potent inhibitors of vesicular transport from the endoplasmic reticulum to the Golgi complex. *J Cell Biol.* 119:749-61.

Tseng, T.C., S.H. Chen, Y.P. Hsu, and T.K. Tang. 1998. Protein kinase profile of sperm and eggs: cloning and characterization of two novel testis-specific protein kinases

(AIE1, AIE2) related to yeast and fly chromosome segregation regulators. *DNA Cell Biol.* 17:823-33.

Ui-Tei, K., S. Zenno, Y. Miyata, and K. Saigo. 2000. Sensitive assay of RNA interference in *Drosophila* and Chinese hamster cultured cells using firefly luciferase gene as target. *FEBS Lett.* 479:79-82.

Ullrich, O., S. Reinsch, S. Urbe, M. Zerial, and R.G. Parton. 1996. Rab11 regulates recycling through the pericentriolar recycling endosome. *J Cell Biol.* 135:913-24.

Urbe, S., L.A. Huber, M. Zerial, S.A. Tooze, and R.G. Parton. 1993. Rab11, a small GTPase associated with both constitutive and regulated secretory pathways in PC12 cells. *FEBS Lett.* 334:175-82.

van der Sluijs, P., M. Hull, L.A. Huber, P. Male, B. Goud, and I. Mellman. 1992a. Reversible phosphorylation--dephosphorylation determines the localization of rab4 during the cell cycle. *Embo J.* 11:4379-89.

van der Sluijs, P., M. Hull, P. Webster, P. Male, B. Goud, and I. Mellman. 1992b. The small GTP-binding protein rab4 controls an early sorting event on the endocytic pathway. *Cell.* 70:729-40.

Vaughn, J.L., R.H. Goodwin, G.J. Tompkins, and P. McCawley. 1977. The establishment of two cell lines from the insect *Spodoptera frugiperda* (Lepidoptera; Noctuidae). *In Vitro.* 13:213-7.

Verbrugghe, K.J., and J.G. White. 2004. SPD-1 is required for the formation of the spindle midzone but is not essential for the completion of cytokinesis in *C. elegans* embryos. *Curr Biol.* 14:1755-60.

Walch-Solimena, C., J. Blasi, L. Edelmann, E.R. Chapman, G.F. von Mollard, and R. Jahn. 1995. The t-SNAREs syntaxin 1 and SNAP-25 are present on organelles that participate in synaptic vesicle recycling. *J Cell Biol.* 128:637-45.

Walworth, N.C., P. Brennwald, A.K. Kabcenell, M. Garrett, and P. Novick. 1992. Hydrolysis of GTP by Sec4 protein plays an important role in vesicular transport and is stimulated by a GTPase-activating protein in *Saccharomyces cerevisiae*. *Mol Cell Biol.* 12:2017-28.

Wang, H., X. Tang, J. Liu, S. Trautmann, D. Balasundaram, D. McCollum, and M.K. Balasubramanian. 2002. The multiprotein exocyst complex is essential for cell separation in *Schizosaccharomyces pombe*. *Mol Biol Cell.* 13:515-29.

Wang, X., R. Kumar, J. Navarre, J.E. Casanova, and J.R. Goldenring. 2000. Regulation of vesicle trafficking in madin-darby canine kidney cells by Rab11a and Rab25. *J Biol Chem.* 275:29138-46.

Warren, G., J. Davoust, and A. Cockcroft. 1984. Recycling of transferrin receptors in A431 cells is inhibited during mitosis. *Embo J.* 3:2217-25.

Weigert, R., A.C. Yeung, J. Li, and J.G. Donaldson. 2004. Rab22a regulates the recycling of membrane proteins internalized independently of clathrin. *Mol Biol Cell.* 15:3758-70.

Wilcke, M., L. Johannes, T. Galli, V. Mayau, B. Goud, and J. Salamero. 2000. Rab11 regulates the compartmentalization of early endosomes required for efficient transport from early endosomes to the trans-golgi network. *J Cell Biol.* 151:1207-20.

Wilson, G.M., A.B. Fielding, G.C. Simon, X. Yu, P.D. Andrews, R.S. Hames, A.M. Frey, A.A. Peden, G.W. Gould, and R. Prekeris. 2005. The FIP3-Rab11 protein complex regulates recycling endosome targeting to the cleavage furrow during late cytokinesis. *Mol Biol Cell.* 16:849-60.

Xie, H., M. Surka, J. Howard, and W.S. Trimble. 1999. Characterization of the mammalian septin H5: distinct patterns of cytoskeletal and membrane association from other septin proteins. *Cell Motil Cytoskeleton.* 43:52-62.

Xue, Y., F. Zhou, M. Zhu, K. Ahmed, G. Chen, and X. Yao. 2005. GPS: a comprehensive www server for phosphorylation sites prediction. *Nucleic Acids Res.* 33:W184-7.

Yamakita, Y., S. Yamashiro, and F. Matsumura. 1994. In vivo phosphorylation of regulatory light chain of myosin II during mitosis of cultured cells. *J Cell Biol.* 124:129-37.

Yin, H.L., and P.A. Janmey. 2003. Phosphoinositide regulation of the actin cytoskeleton. *Annu Rev Physiol.* 65:761-89.

Zerial, M., and H. McBride. 2001. Rab proteins as membrane organizers. *Nat Rev Mol Cell Biol.* 2:107-17.

Zhang, Q., D. Cox, C.C. Tseng, J.G. Donaldson, and S. Greenberg. 1998. A requirement for ARF6 in Fcgamma receptor-mediated phagocytosis in macrophages. *J Biol Chem.* 273:19977-81.

Zhou, F.F., Y. Xue, G.L. Chen, and X. Yao. 2004. GPS: a novel group-based phosphorylation predicting and scoring method. *Biochem Biophys Res Commun.* 325:1443-8.